Characterising the Protective Bioactivity of Macroalgal Polyphenols

A study on neuroprotection, epithelial barrier function, ACE-2 expression and activity

PhD thesis

To obtain the degree of Doctor of Philosophy (PhD) in Medicine at the University of Adelaide

By

Srijan Shrestha, B. Pharm, M.Sc.

Supervisors

Dr. Scott Smid

Prof. Wei Zhang

June 2022

Adelaide, Australia

Table of Contents

Abstract iv

Declaration vi

Dedication vii

Acknowledgment viii

Publications arising from this thesis x

Chapter 1: General introduction and literature review 1

Phlorotannins: a review on biosynthesis, chemistry and bioactivity 6

Food Bioscience., 2021, 39, 100832; DOI: 10.1016/j.fbio.2020.100832 6

Appendix A: Supplementary Material 45

Chapter 2. *Ecklonia radiata* extract containing eckol protects neuronal cells against $A\beta_{1-42}$ evoked toxicity and reduces aggregate density 57

Food & Function., 2020, 11, 6509-6516; DOI: 10.1039/D0FO01438A 57

Appendix A: Supplementary Material 79

Chapter 3: A phlorotannin isolated from *Ecklonia radiata,* Dibenzodioxin-fucodiphloroethol, inhibits neurotoxicity and aggregation of β-amyloid 86

Phytomedicine Plus., 2021, 1, 100125; DOI: 10.1016/j.phyplu.2021.100125 86

Appendix A: Supplementary Material 112

Chapter 4: Neuroprotective activity of macroalgal fucofuroeckols against amyloid β peptide-induced cell death and oxidative stress 119

International Journal of Food Science and Technology., 2022; DOI: 10.1111/ijfs.15753 119

Chapter 5: Protective effects of phlorotannins on cytokine-induced intestinal epithelial barrier damage 145

Chapter 6: Macroalgal phlorotannins decrease both basal and cytokine-induced angiotensin converting enzyme 2 (ACE-2) expression in human intestinal and respiratory epithelial cells 163

Chapter 7: Conclusion 188

Abstract

Phlorotannins are novel polyphenolic compounds mostly found in brown seaweed and are comprised of variable polymeric chains of phloroglucinol residues (1,3,5-trihydroxybenzene). Biochemical and cell-based assays and some preclinical and clinical studies have highlighted a potential multi-faceted bioactivity of phlorotannins. This thesis aimed at characterizing neuroprotective and epithelial protective bioactivity via cell and enzyme-based assays along with transmission electron microscopy (TEM) and molecular docking of various phlorotannins isolated and identified from the South Australian seaweed *Ecklonia radiata* using a range of analytical techniques.

Firstly, *Ecklonia radiata* from South Australian coastal regions was collected and its ethanolic extract and solvent-soluble fractions evaluated for neuroprotective activity against the toxic amyloid β protein ($A\beta_{1\text{-}42}$) in neuronal PC-12 cells. The ethyl acetate fraction (EA) comprising 62% phlorotannins demonstrated the most efficacious neuroprotective activity, inhibiting neurotoxicity at all $A\beta_{1\text{-}42}$ concentrations and was associated with Aβ anti-aggregatory properties. Various phlorotannins were tentatively identified via ion mobility mass spectrometry and HPLC quadrupole-time-of flight mass spectroscopy. Two compounds were isolated, purified and identified via high-performance centrifugal partition chromatography (HPCPC) combined with size exclusion chromatography. Nuclear magnetic resonance (NMR) and mass spectroscopy enabled us to identify the major phlorotannins as eckol and dibenzodioxin-fucodiphloroethol (DFD). DFD significantly reduced cell viability in response to $A\beta_{1\text{-}42}$ and significantly reduced $A\beta_{1\text{–}42}$ aggregation, while molecular docking studies revealed DFD binding to key $A\beta_{1\text{-}42}$ residues associated with fibrillisation propensity. DFD also showed moderate cholinesterase inhibitory activity and was also able to significantly scavenge reactive oxygen species (ROS) in PC-12 cells.

In addition, eckol, dieckol, phlorofucofuroeckol-A (PFFA) and 974-A previously identified in the *E. radiata* extract significantly scavenged ROS. However, only PFFA and 974-A protected neuronal PC-12 cells against oxidative stress-evoked neurotoxicity, increasing cell viability significantly in response to both cytosolic (H_2O_2) and lipid peroxidation-evoked (*t*-BHP) cell stress and Aβ exposure.

Next, the effect of eckol, dieckol, PFFA and 974-A on cytokine-evoked trans-epithelial electrical resistance (TEER) reductions in Caco-2 intestinal epithelial monolayers as a measure of paracellular permeability and epithelial barrier integrity was investigated. Significant improvements in epithelial barrier function occurred at 48 h with eckol, dieckol, and PFFA but not 974-A, indicating a broader capacity of the phlorotannins to support intestinal epithelial barrier function against detrimental proinflammatory cytokines.

The effects of these phlorotannins on modulating angiotensin converting enzyme 2 (ACE-2) expression and activity in human epithelial cells (A549 and Caco-2) were also investigated for potential COVID-19 prophylaxis and treatment. Eckol and dieckol had negligible influence on either basal or cytokine-induced ACE-2 expression in Caco-2 cell line, however both significantly reduced cytokine-induced expression of ACE-2 isoform A in A549 cells. PFFA and 974-A significantly reduced ACE-2 expression and downregulated both major ACE-2 isoforms under basal and cytokine-induced conditions, except for isoform B in PFFA-treated A549 cells. Altered expression profiles were accompanied by substantial inhibition of cytokine-augmented ACE-2 enzymatic activity in PFFA and 974-A- treated cells.

This thesis demonstrated the widespread biological activity of phlorotannins applied towards neurodegenerative, intestinal and potentially infectious diseases. These findings may inform their further development as nutraceuticals or pharmaceuticals for human health.

Declaration

I certify that this work contains no material which has been accepted for the award of any other degree or diploma in my name in any university or other tertiary institution and, to the best of my knowledge and belief, contains no material previously published or written by another person, except where due reference has been made in the text. In addition, I certify that no part of this work will, in the future, be used in a submission in my name for any other degree or diploma in any university or other tertiary institution without the prior approval of the University of Adelaide and where applicable, any partner institution responsible for the joint award of this degree.

The author acknowledges that copyright of published works contained within this thesis resides with the copyright holder(s) of those works.

I give permission for the digital version of my thesis to be made available on the web, via the University's digital research repository, the Library Search and also through web search engines, unless permission has been granted by the University to restrict access for a period of time.

I acknowledge the support I have received for my research through the provision of an Australian Government Research Training Program Scholarship.

Srijan Shrestha Date: 21/05/2021

Dedication

This work is dedicated to my father, Tara Prasad Newar, my mother, Fathina Shrestha, for paving my way into this and showing me the right direction when I was lost and my beloved wife, Sneha Shrestha for supporting me into every decision and the rest of my family for their support and input into my life.

Acknowledgment

I would like to acknowledge all the individuals who have contributed to the completion of my PhD directly or indirectly.

First and foremost, I want to express my heartfelt thanks to Dr. Scott Smid, my Principal supervisor, and Professor Wei Zhang, my co-supervisor, for their unwavering support, expert guidance, and overall scientific counsel that helped me complete my PhD projects successfully. I am grateful for your unwavering support and advice in all aspects of my work.

Dear Scott, I cannot thank you enough for welcoming me to your research group and making me comfortable throughout the process. I genuinely enjoyed the freedom of working independently. I will always remember the knowledge you have shared and the career guidance you offered me. Moreover, I am incredibly grateful that you have provided me with all the available opportunities to collaborate with the other research groups. I would want to express my gratitude to Dr. Tara Pukala, Dr. Martin Johnston, and Dr. Alexander Jacob Begbie for their support and insight on my project.

I would like to express my sincere thanks to Dr. Ian Musgrave, Dr. Abdallah Salem, Kushari Burns, Dr. Adarsha Gupta, Dr. Chris Franco, and Peng Su, who have all been helpful. I would like to thank Dylan Marsh and John Staton Laws III for their support and encouragement. Their unwavering support aided me in navigating the ups and downs of this trip. My sincere appreciation goes to my mentor Kaylee Azzopardi for opening my eyes to new stages of opportunity and strength.

It is a privilege for me to thank my prior supervisor, Dr. Jae Sue Choi (Pukyong National University; South Korea) and Dr. Pradeep Poudel, for introducing me to the research pathway.

I would also like to acknowledge the University of Adelaide for the scholarship support through the Australian Research Training program (RTP). It is a great privilege to study at the University of Adelaide.

Sneha, my amazing wife, deserves special thanks and admiration. You have always been my best buddy, always standing by my side no matter what. Thank you for looking after me and bearing with me. My father and mother deserve special appreciation for their unwavering love and support. Finally, thank you God for taking care of me.

Publications arising from this thesis

1. **Shrestha, S**., Choi, J.S., Zhang W., Smid, S.D. (2022) Neuroprotective activity of macroalgal fucofuroeckols against amyloid β peptide-induced cell death and oxidative stress. International Journal of Food Science & Technology. DOI: 10.1111/ijfs.15753.
2. **Shrestha, S**., Johnston, M. R., Zhang, W., Smid, S. D. (2021) A phlorotannin isolated from *Ecklonia radiata*, Dibenzodioxin-fucodiphloroethol, inhibits neurotoxicity and aggregation of β-amyloid. Phytomedicine Plus, 1(4), 100125.
3. **Shrestha, S**., W. Zhang, Smid, S.D. (2020) Phlorotannins: A review on biosynthesis, chemistry and bioactivity. Food Bioscience, 100832.
4. **Shrestha, S**., Zhang, W., Begbie, A. J., Pukala, T. L., Smid, S. D. (2020). *Ecklonia radiata* extract containing eckol protects neuronal cells against $A\beta_{1-42}$ evoked toxicity and reduces aggregate density. Food & Function, 11, 6509-6516.

Presentation

1. A phlorotannin isolated from *Ecklonia radiata*, Dibenzodioxin-fucodiphloroethol, inhibits neurotoxicity and aggregation of β-amyloid. PHYSIOMAR 2021 (Virtual oral presentation, New Zealand)

Chapter 1: General introduction and literature review

Ecklonia radiata (C. Ag.) J. Agardh (Phaeophyceae) is a small kelp found abundantly in the warm-temperate parts of southern South Africa, Australia and New Zealand and the most abundant brown seaweed species in South Australia. Extensive research has been previously performed on chemical profiling and biological activity of *Ecklonia* species, however there are very few studies regarding *Ecklonia radiata* and none relating to the bioactive chemical constituents of this particular species. Therefore, further investigation of *E. radiata* was warranted to characterise the antioxidant, neuroprotective, anti-inflammatory, and immunomodulatory properties ascribed to specific chemical constituents, in particular the novel phlorotannins as the predominant polyphenols occurring in brown seaweeds.

Chapter 1 provides an overview of the various classes of phlorotannins with their characteristic structure and their documented biological activities to date. Phlorotannins are comprised of diverse polymeric chains of phloroglucinol residues (1,3,5-trihydroxybenzene) connected via a variety of C–C and/or C–O–C couplings, and a library (^{1}H and ^{13}C) of reported phlorotannins was presented to assist with further identification for future research. While bioactivity and prospective use as nutraceuticals and supplements have been assigned to a variety of phlorotannins, including trials of phlorotannin-rich extracts used as nutritional supplements in livestock feed to improve growth and condition, use of phlorotannins in human health settings has yet to be extensively investigated. This overview of phlorotannin bioactivity in experimental therapeutic settings sets the background for the subsequent aims of the studies presented in this thesis.

In Chapter 2, neuroprotective activity against the toxic Alzheimer's disease-related amyloid β protein ($A\beta_{1–42}$) of an ethanol extract of *E. radiata* were compared with various additional solvent-solubilised fractions in a neuronal PC-12 cell line. The ethyl acetate fraction comprising 62%

phlorotannins demonstrated the most efficacious neuroprotective activity, inhibiting neurotoxicity at all $A\beta_{1–42}$ concentrations. The major phlorotannins in the extract were tentatively identified after profiling of phlorotannin in *E. radiata* using ion mobility mass spectrometry and HPLC quadrupole-time-of-flight mass spectrometry. Furthermore, high performance centrifugal partition chromatography was used to isolate the major compound, eckol, identified by NMR spectroscopy.

Chapter 3 explored the isolation, characterization and identification of the phlorotannin dibenzodioxin-fucodiphloroethol (DFD) from *E. radiata* using high performance counter-current chromatography (HPCCC) combined with size exclusion chromatography, nuclear magnetic resonance (NMR) including ^{1}H and ^{13}C and 2D COZY, HSQC, HMBC (broad and band selective) and NOESY along with mass spectrometry. DFD significantly protected PC-12 neuronal cells against $A\beta_{1-42}$ and reduced aggregation of $A\beta_{1–42}$ as evidenced by transmission electron microscopy, while molecular docking studies revealed DFD binding to key $A\beta_{1–42}$ residues associated with fibrillisation propensity. DFD demonstrated moderate cholinesterase inhibitory activity, sharing similar interacting binding residues to donepezil in the crystallized structure, and was also able to significantly scavenge ROS in PC-12 cells.

Chapter 4 explored the bioactivity of different phlorotannins previously identified in the *E. radiata* extract. Eckol, dieckol, phlorofucofuroeckol-A (PFFA) and 974-A were assessed for their ability to protect neuronal PC-12 cells against the toxic effects of H_2O_2, lipid peroxidation via tert-butyl hydroperoxide (*t*-BHP) and $A\beta_{1-42}$. All compounds significantly scavenged reactive oxygen species (ROS). However, only PFFA and 974-A protected PC-12 cells from oxidative stress-evoked neurotoxicity, providing significant increases in cell viability in response to both cytosolic (H_2O_2) and lipid peroxidation-evoked (*t*-BHP) cell stress. Our results indicate that while all phlorotannins assessed exhibited ROS scavenging activity, only fucofuroeckol-type phlorotannins

such as PFFA and 974-A afforded broader neuroprotective activity in response to both oxidative stress and amyloid β exposure. The additional amyloid-protective capacity of fucofuroeckols revealed the potential importance of the benzofuran moiety in neuroprotection.

Increased intestinal permeability, systemic inflammation and gut dysbiosis have been linked to a facilitation of conditions conducive to the development of Alzheimer's disease (AD) pathologies and cognitive impairment via neuronal, immunological, endocrine, and metabolic pathways. Sodium oligomannate derived from brown seaweed has recently been approved for the treatment for Alzheimer's disease in China, whereby improvements in intestinal function are believed to be the underlying mechanism behind its clinical benefit. In Chapter 5, we explored the innate intestinal immune bioactivity of phlorotannins via their influence on cytokine-evoked barrier function impairment in intestinal Caco-2 monolayers, using epithelial paracellular permeability measurements. Significant improvements in epithelial barrier function at 48 h occurred with all phlorotannins except 974-A. This indicated a broader capacity of the phlorotannins to support intestinal epithelial barrier function against deleterious proinflammatory cytokines. All phlorotannins were also found to be excellent scavengers of lipid peroxidation-generated free radicals in Caco-2 cells as indicated by the DCFDA assay, which may be linked to the general improvement in epithelial barrier function.

Chapter 6 explored the effects of four phlorotannins on modulating angiotensin converting enzyme 2 (ACE-2) expression and activity in human lung-derived epithelial cells (A549) and human intestinal epithelial cells (Caco-2), for potential COVID-19 prophylaxis and treatment. ACE-2 is a key conduit for infection by the novel coronavirus SARS-CoV-2, so modulating expression of this epithelial marker may be a useful infection mitigation strategy. ACE-2 levels in both cell lines were increased when incubated with proinflammatory cytokines TNF-α and IL-1β. The

phlorotannins eckol and dieckol had negligible influence on either basal or cytokine-induced ACE-2 expression, however both significantly reduced cytokine-induced expression of the ACE-2 isoform A in A549 cells. The fucofuroeckols, PFFA and 974-A significantly reduced ACE-2 expression and downregulated both major ACE-2 isoforms under both basal and cytokine-induced conditions, with the exception of isoform B in PFFA-treated A549 cells. Furthermore, PFFA and 974-A significantly inhibited cytokine-stimulated increases in ACE-2 enzymatic activity. These findings demonstrated not only the augmented expression of functional ACE-2 under pro-inflammatory signalling conditions, but also an important potential application of selected phlorotannins in the downregulation of constitutive and cytokine-induced ACE-2 expression and activity.

Statement of Authorship

Title of Paper	Phlorotannins: A review on biosynthesis, chemistry and bioactivity
Publication Status	☑ Published ☐ Accepted for Publication ☐ Submitted for Publication ☐ Unpublished and Unsubmitted work written in manuscript style
Publication Details	Shrestha, S., W. Zhang, Smid, S.D. (2020) Phlorotannins: A review on biosynthesis, chemistry and bioactivity. Food Bioscience, 100832.

Principal Author

Name of Principal Author (Candidate)	Srijan Shrestha		
Contribution to the Paper	Conceived the research concept and design, performed the literature review, made an interpretation of the results, and prepared the first draft of the manuscript, revised after reviewer's comment, and finalized.		
Overall percentage (%)	80%		
Certification:	This paper reports on original research I conducted during the period of my Higher Degree by Research candidature and is not subject to any obligations or contractual agreements with a third party that would constrain its inclusion in this thesis. I am the primary author of this paper.		
Signature		Date	17/05/2022

Co-Author Contributions

By signing the Statement of Authorship, each author certifies that:

i. the candidate's stated contribution to the publication is accurate (as detailed above);

ii. permission is granted for the candidate in include the publication in the thesis; and

iii. the sum of all co-author contributions is equal to 100% less the candidate's stated contribution.

Name of Co-Author	Dr. Wei Zhang		
Contribution to the Paper	Data interpretation and drafting of the manuscript.		
Signature		Date	31/05/2022

Name of Co-Author	Dr. Scott Smid		
Contribution to the Paper	Searching, identification and critical review of the literature data interpretation, drafting of the manuscript and overall responsibility for the study.		
Signature		Date	21-06-22

Please cut and paste additional co-author panels here as required.

Phlorotannins: a review on biosynthesis, chemistry and bioactivity

Shrestha S[1], Zhang W[2,3] and Smid SD[1]

[1]Discipline of Pharmacology, Adelaide Medical School, Faculty of Health Sciences, The University of Adelaide, South Australia, Australia;

[2]Centre for Marine Bioproducts Development (CMBD), and [3]Medical Biotechnology, College of Medicine and Public Health, Flinders University, Adelaide, South Australia, Australia;

Food Bioscience., 2021, 39, 100832; DOI: 10.1016/j.fbio.2020.100832

Abstract

Phlorotannins are polyphenolic compounds mostly found in brown seaweed and are comprised of polymeric chains of phloroglucinol residues (1,3,5-trihydroxybenzene) connected via C-C and/or C-O-C couplings. Due to the presence of highly complex polymeric mixtures of structural and conformational isomers of phlorotannins and the absence of available commercial phlorotannin standards, accurate chemical identification from extracts using MS/MS is difficult. Therefore, the optimal approach for identification of specific phlorotannins includes both NMR (1D and 2D) analysis coupled with HRMS. Herein, a library (^{1}H and ^{13}C) of the reported phlorotannins has been generated to assist with further identification. Additionally, a range of phlorotannins have been ascribed bioactivity and potential use as nutraceuticals and supplements, including trials of phlorotannin-rich extracts used as nutritional supplements in livestock feed to improve overall growth and condition. Bioactivity studies have identified neuroprotective, antidiabetic, anticancer, antioxidant, anti-inflammatory, antimicrobial and microbiome-beneficial properties, highlighting a multi-faceted potential of phlorotannins. Overall, the majority of such findings have been generated via biochemical and cell-based assays, with only a limited number of in vivo animal experiments conducted. Further preclinical and clinical studies will be required to comprehensively investigate bioavailability, efficacy and safety of phlorotannins, to further define the potential of these unique brown algal polyphenols in animal and human health.

Keywords: Marine algae, Brown seaweed, Polyphenols, Phlorotannins

1. Introduction

Phlorotannins are a unique set of polymers synthesized by brown algae (*Phaeophyta*), which are structurally analogous to tannins from terrestrial plants. Phlorotannins are highly hydrophilic in nature, with molecular weights ranging from 126 Da to 650 kDa (Gümüş Yılmaz et al., 2019). They are comprised of polymeric chains of base phloroglucinol (1,3,5-trihydroxybenzene) residues connected via C-C and/or C-O-C couplings. The exact biological roles of phlorotannins in seaweeds have not been fully elucidated. However, they are believed to play an important role in cell wall structure, UV protection and as a possible defense mechanism against marine herbivory (Koivikko et al., 2005).

Phlorotannins are produced by polymerization of phloroglucinol in various combinations. The biosynthetic pathways of the phlorotannins have not been fully elucidated. However, it is believed to occur via condensation of acetate and malonate units via the shikimate or phenylpropanoid pathway (Figure 1). Two acetyl-CoA molecules in the presence of carbon dioxide are converted to malonyl-CoA. The process is catalyzed by type III polyketide synthase and the resultant chain undergoes cyclization and tautomerisation to form phloroglucinol (Meslet-Cladière et al., 2013). The phloroglucinol moiety connects via C-C and/or C-O-C couplings and are classed according to their inter-phloroglucinol linkages (Gümüş Yılmaz et al., 2019). Structural and conformational isomers are common in the case of phlorotannins, due to the binding of monomers at different positions of the phloroglucinol ring. Due to their structural diversity, the phlorotannins are classified as fucols (phenyl bond), phloroethols (ether bond), fucophloroethols (ether and phenyl bonds), eckols, fuhalols, and carmalols (Isaza Martínez & Torres Castañeda, 2013). Fucols include phlorotannins with inter-phloroglucinol links in meta-position e.g. tetrafucol A, tetrafucol B and heptafucol as shown in Figure 2. In the case of phloroethols, phloroglucinol residues are

interconnected via ether bonds in the ortho-, meta- or para-position e.g., triphlorethol A, tetraphlorethol C and tetraphlorethol B (Figure 3). Fuhalols and eckols contain an additional hydroxyl group on the terminal monomer unit as shown in Figure 4 (e.g. trifuhalol A, bifuhalol and trifuhalol B). Eckols are characterized by the presence of 1,4-dibenzodioxin in their structure, as exemplified by eckol, dieckol and 2-phloroeckol (Figure 5). Carmalols are a unique set of phlorethols with different substitution patterns along with hydroxyl groups when compared to eckols, such as diphloroethohydroxycarmalol (shown in Figure 8). The fucophloroethols are formed by the combination of ether and phenyl bonds as seen in fucophlorethol B, fucophlorethol A, and fucodiphlorethol B (Figure 8). Furthermore, heterocyclic fucophloroeckols include compounds such as 6,6'-biekol, 8,8'-bieckol, and eckmaxol (Figure 6) and fucofuroeckols include 974-A, phlorofucofureoeckol B, and phlorofucofuroeckol (Figure 7) (Isaza Martínez & Torres Castañeda, 2013).

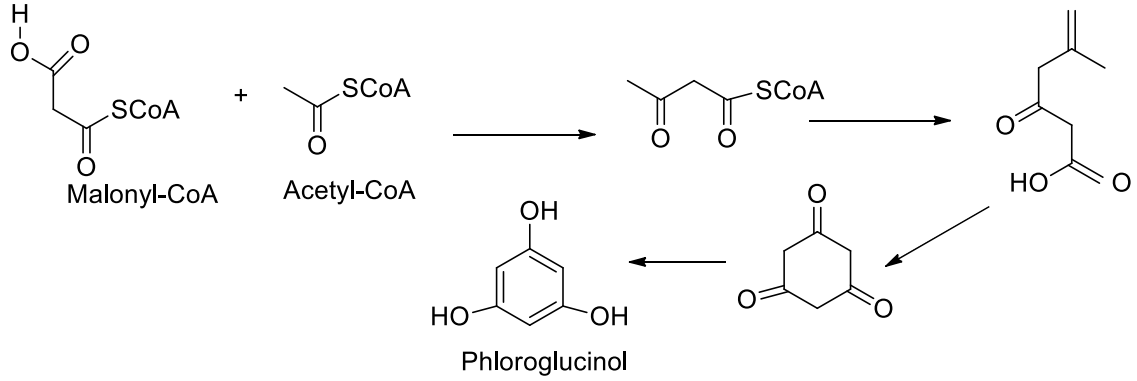

Figure 1. Biosynthesis of phloroglucinol

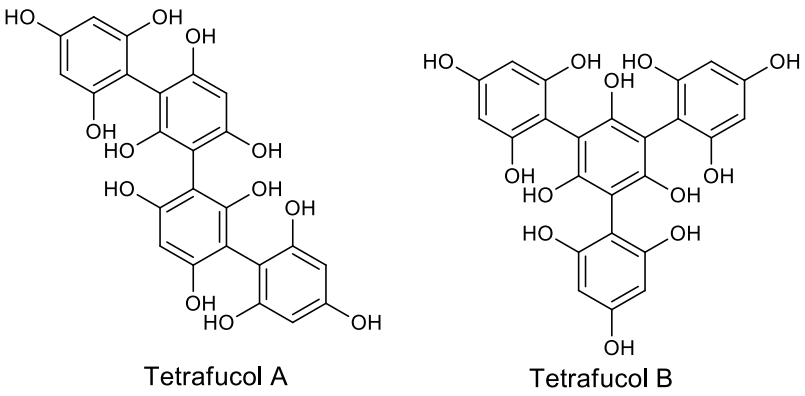

Figure 2. Structure of fucols

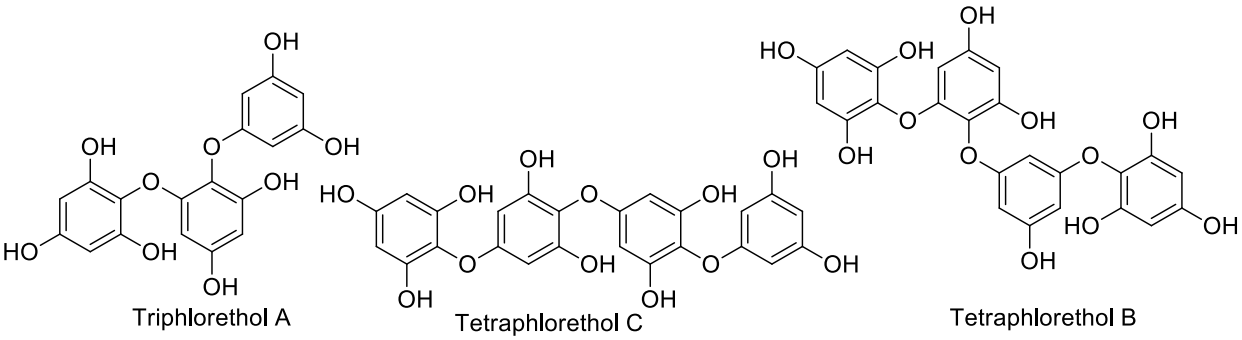

Figure 3. Structure of phlorethols

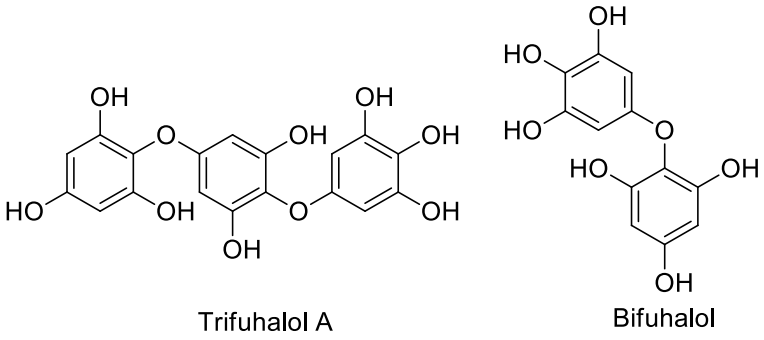

Figure 4. Structure of fuhalols

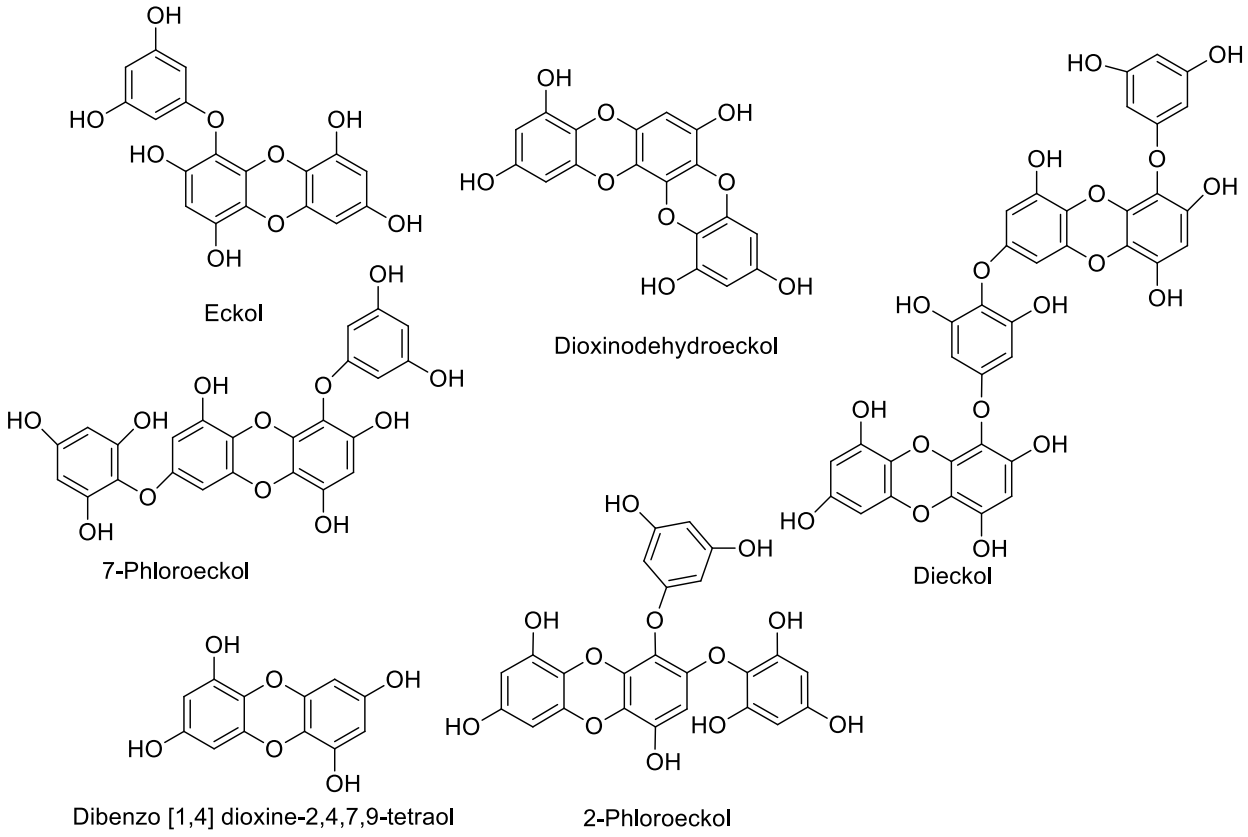

Figure 5. Structure of eckols

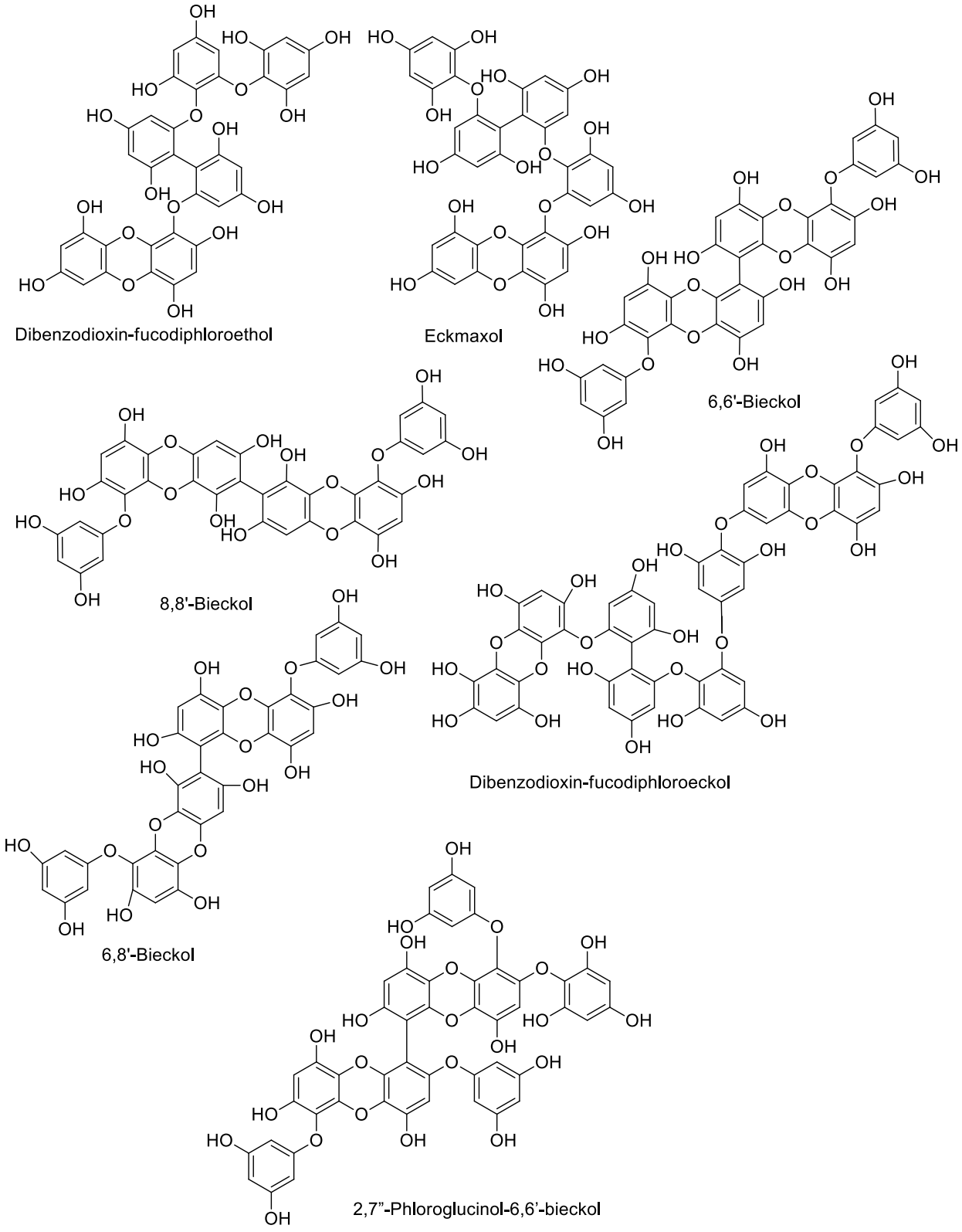

Figure 6. Structure of fucophloroeckols

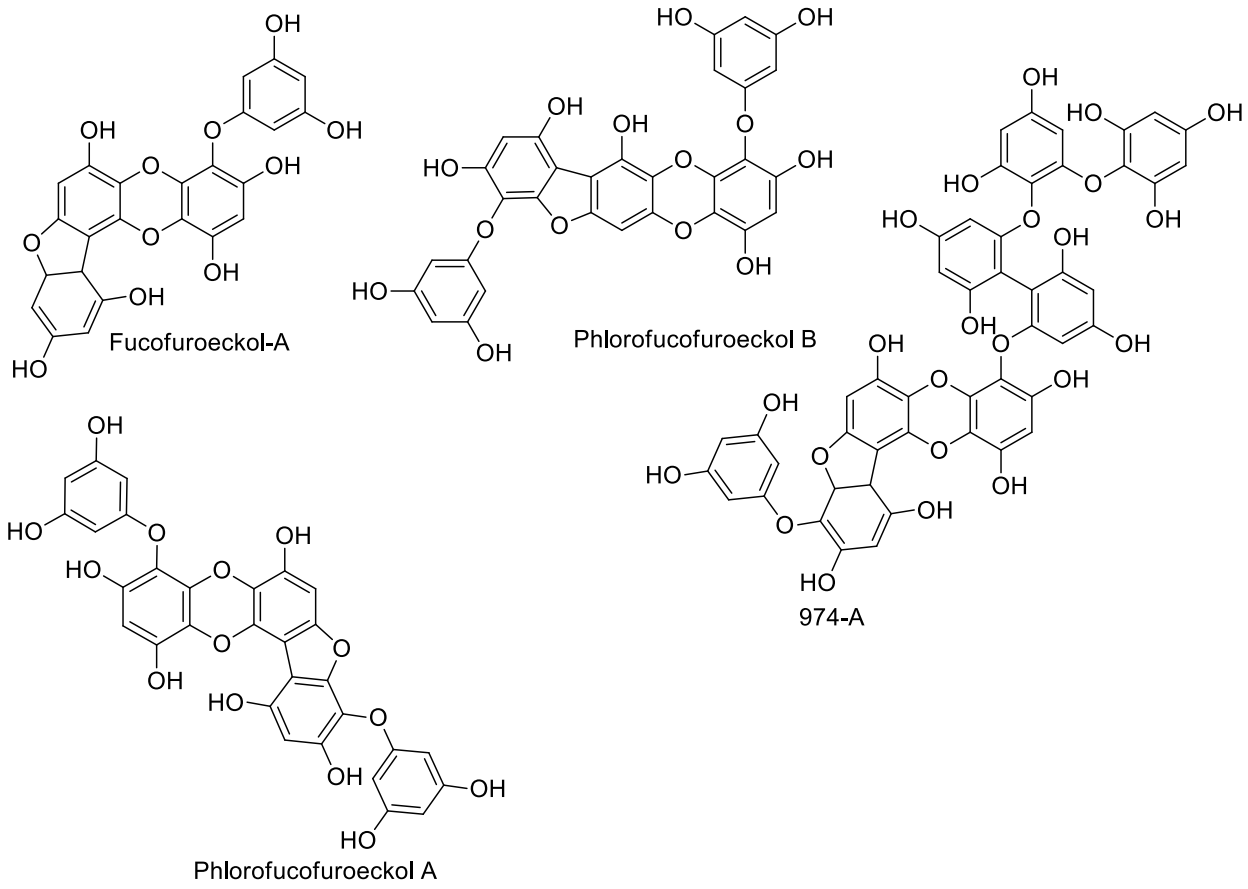

Figure 7. Structure of fucofuroeckols

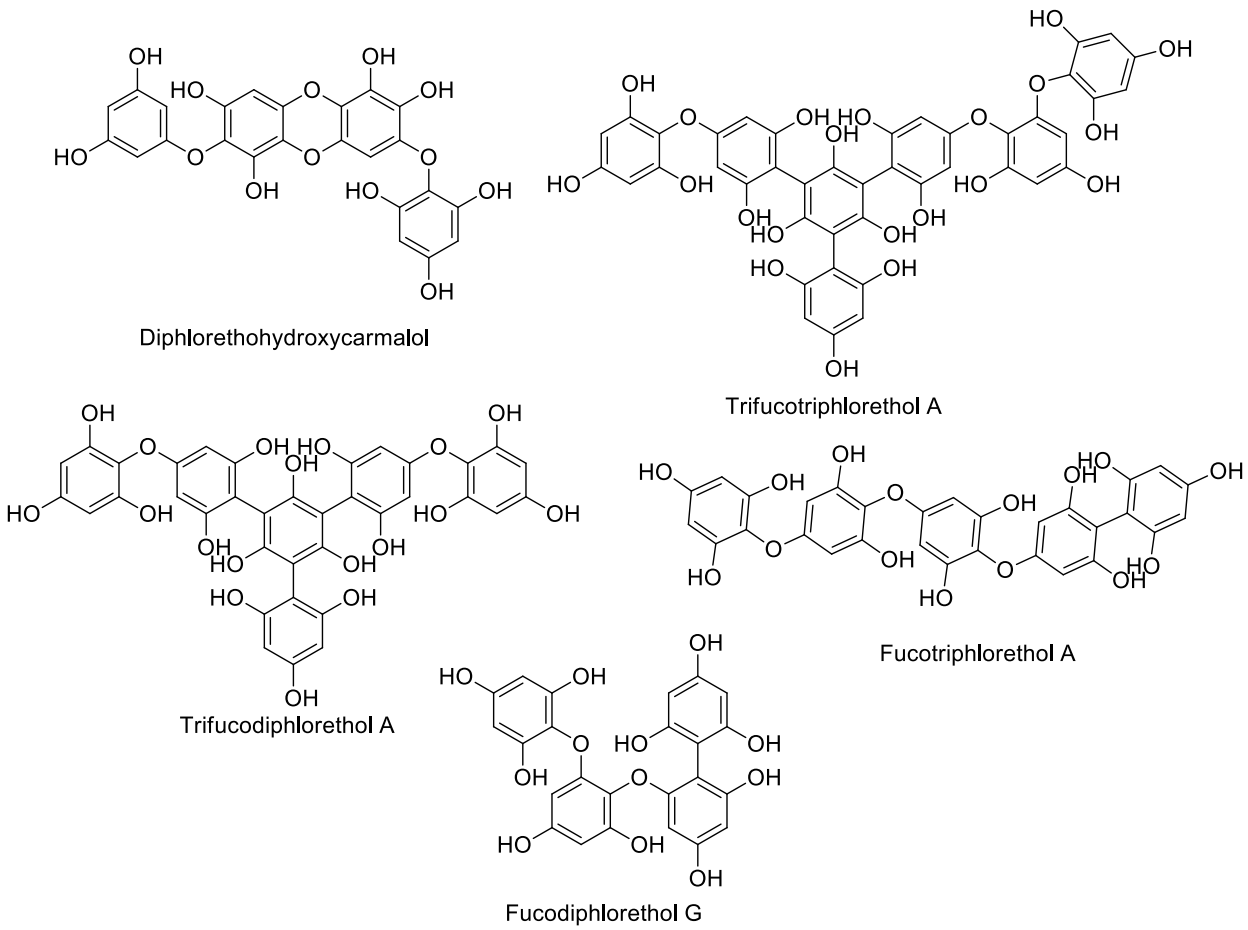

Figure 8. Structure of carmalols and fucophlorethols

2. Quantitative and qualitative analysis of phlorotannins

The most common assays used to determine the total phlorotannin content of algal extracts are based on the use of Folin-Ciocalteu and 2,4-dimethoxybenzaldehyde (DMBA) reagents. The Folin-Ciocalteu assay is based on the transfer of electrons from phenolic compounds to phosphomolybdic/phosphotungstic acid complexes in alkaline conditions (Wang et al., 2012). The movement of electrons results in a color change detected at 760 nm. This assay lacks sensitivity and accuracy, where several other molecules like sugars, proteins, and thiols present in the extract may interact and confer a false positive result (Ford et al., 2019). DMBA interacts with 1,3- and 1,3,5-trihydroxybenzenes, resulting in color change which can be detected at 510 nm. This assay

is considered more specific for the detection of phlorotannin content. However, 2-,4- or 6-OH substituted phlorotannins and branched phlorotannins with aryl linkages may not react with DMBA, resulting in the underestimation of total phlorotannin content (Ford et al., 2019). In both assays, quantification is performed via a calibration curve using phloroglucinol as a standard and expressed in phloroglucinol equivalents (PGE).

3. Phlorotannin profiling in brown algal extracts

Due to the presence of highly complex polymeric mixtures of structural and conformational isomers of phlorotannins, accurate identification from an extract can be difficult to perform. Various attempts have been made to tentatively characterize the phlorotannins present in seaweed extracts via MS/MS coupled with HPLC (Cho et al., 2019; Ferreres et al., 2012; Li et al., 2017; Lopes et al., 2018; Shrestha et al., 2020). Previously, we were able to identify the major phlorotannins from *E. radiata* via ion mobility mass spectrometry and HPLC quadrupole-time-of flight mass spectroscopy (Shrestha et al., 2020). The majority of phlorotannins were identified as eckol-type, which is a characteristic of *Ecklonia* species. Recently, Cho *et al*. (2019) used HPLC-q TOFMS to identify eighteen phlorotannins from *E. cava*. They were also able to identify and isolate two novel phlorotannins. Ferreres *et al.* (2012) characterized phlorotannins from four brown seaweeds (*Cystoseira nodicaulis, Cystoseira tamariscifolia, Cystoseira usneoides*, and *Fucus spiralis*) by HPLC-DAD-ESI-MS. They were able to tentatively identify 22 different phlorotannins belonging to eckol and fucophloroethol-type classes (Ferreres et al., 2012). Another research group proposed an accurate method for profiling phlorotannins from *Fucus vesiculosus* based on their degree of polymerization (Steevensz et al., 2012). They used ultra high-pressure liquid chromatography (UHPLC) operating in hydrophilic interaction liquid chromatography (HILIC) mode combined with high-resolution mass spectrometry (HRMS). Using this method,

they were able to detect moderate molecular weight phlorotannins ranging from 3 to 49 kDa. Li *et al.* (2017) and also identified various phlorotannins based on their degree of polymerization and types using MS/MS data (Li et al., 2017). The author concluded that isolation and further purification is required to identify the exact structure of candidate phlorotannins, followed by NMR (1D and 2D) analysis coupled with HRMS (Li et al., 2017).

Ford *et al.* (2019) insisted that the best approach would be the identification of these phlorotannins via NMR, then linking these structures to HPLC conditions (solvents) along with retention time and UV spectral data (Ford et al., 2019). In an attempt to prepare the library of phlorotannins via NMR (^{1}H and ^{13}C) data, some of the reported data are summarized in the supplementary file (S1).

4. Bioactivity of Phlorotannins

Phlorotannins have been variably ascribed a range of biological activities, including antioxidant (Sathya et al., 2017), anti-diabetic (Kang et al., 2010), anti-cancer (Ahn et al., 2015), antiviral (Cho et al., 2019), antimicrobial (Eom et al., 2012), anti-inflammatory (Barbosa et al., 2019) and neuroprotective activity (Lee et al., 2019), demonstrating promising potential in commercial applications in areas such as food, nutraceutical and pharmaceutical applications. Aside from their recognized scavenging role for reactive oxygen species (ROS), phlorotannins confer this activity at a number of cellular and molecular targets, including enzymes, membrane proteins and pro-inflammatory signaling cascades, some of which are described below.

4.1. Antioxidant activity

Numerous endogenous and exogenous factors are responsible for the production of reactive oxygen and nitrogen species, and imbalances between these species and antioxidant defenses result in oxidative stress. This contributes towards a host of various pathological sequelae including DNA damage, atherosclerosis, inflammation, oncogenesis, insulin resistance, muscular dystrophy

and neurodegeneration, among others (Liguori et al., 2018). Typically, natural antioxidants from terrestrial sources have traditionally been considered as able to mitigate oxidative stress through their multitude of constituent radical scavenging polyphenols (Pérez-Jiménez et al., 2010), but the sheer diversity of compounds also suggests additional operant protective actions such as hormesis (Franco et al., 2019). As the marine equivalent of these terrestrial polyphenols, phlorotannins are electron-rich compounds prone to entering into efficient electron donation reactions. These produce phenoxyl radical species as intermediates, stabilized by resonance delocalization in the presence of oxidizing agents (Wijesekara et al., 2010). Select phlorotannins with their ROS scavenging EC_{50} values are listed in Table 1. Among the various phlorotannins, 974-A and 974-B, diphlorethohydroxycarmalol, dieckol and eckstolonol have demonstrated potent diphenyl-1-picrylhydrazyl (DPPH) scavenging activity, with EC_{50} values of 0.86, 3.4, 6.2, 8.8 and 10.0 µM, respectively (Choi et al., 2015; Heo et al., 2008; Kang et al., 2004; Kim et al., 2009; Kwon et al., 2013; Lee et al., 2012; Sugiura et al., 2008; Yotsu-Yamashita et al., 2013). Recently, several dieckol derivatives were produced, where the hydroxyl group (5-O position) of dieckol was replaced with five substituents (methyl, benzyl, methoxymethyl, 3-hydroxypropyl, and 3-(ethoxycarbonyl)propyl) under S_N2 reactions (nucleophilic substitution reaction) (Kim et al., 2020). The authors demonstrated that a 6-O-(ethoxycarbonyl) propyl-substituted dieckol derivative demonstrated enhanced antioxidant activity (DPPH, ABTS, and FRAP) compared to dieckol. In a recent paper, Bogolitsyn *et al*. (2019) discussed the relationship between the radical scavenging activity properties of polymolecular phlorotannins (Bogolitsyn et al., 2019). The authors demonstrated that the highest antioxidant activity was observed for the phlorotannin fraction with a molecular weight in the range of 8-18 kDa, with higher molecular weights demonstrating decreased activity. The authors argued that this may be due to the mutual shielding

of the reducing centers of phlorotannins by the formation of hydrogen bonds (Bogolitsyn et al., 2019).

At a cellular level, several phlorotannins have been reported to have protective effects against oxidative stress-evoked cell damage (Kang et al., 2005). Eckol, triphlorethol-A and phloroglucinol have been reported to have protective effects in H_2O_2-induced cell damage in Chinese hamster lung fibroblasts (V79-4) by enhancing cellular antioxidant activity (Kang et al., 2005a; Kang et al., 2006; Kang et al., 2005b). Eckol reduced H_2O_2-induced, serum starvation and radiation-evoked cell death in V79-4 fibroblast cells via increased phosphorylation of extracellular signal-regulated kinase and NF-κB (Kang et al., 2005). Furthermore, eckol also protected cells by activating Nrf-2 mediated heme oxygenase-1 (plays an important role in cytoprotection against oxidative stress) induction via ERK and PI3K/Akt signaling (Kim et al., 2010). Additionally, it protected the human hepatocyte-derived Chang liver cell line against H_2O_2-induced mitochondrial dysfunction (Kim et al., 2014). Eckol was able to decrease mitochondrial reactive oxygen species and high intracellular Ca^{2+} levels, recover ATP levels and succinate dehydrogenase activity. Eckol also increased the expression of manganese superoxide dismutase by activating AMPK/ forkhead box O3a (Kim et al., 2014). Triphlorethol-A and phloroglucinol isolated from *E. cava* were able to protect and reduce apoptosis induced by H_2O_2 in V79-4 cells via activation of ERK protein and stimulation of cellular antioxidant enzymes, including superoxide dismutase (SOD), catalase (CAT) and glutathione peroxidase (GPx) (Kang et al., 2005; Kang et al., 2006). Lee *et al*. (2018) recently reported the antioxidant property of eckol and dieckol in a human keratinocyte cell line (HaCaT) exposed to PM10 (airborne particulate matter with a diameter of <10 μM) (Lee et al.,2018). Both compounds rescued cells, attenuated cellular lipid peroxidation and decreased the

expression of inflammatory cytokines such as TNF-α, IL-1β, IL-6 and IL-8 at both the mRNA and protein levels.

Table 1. Antioxidant activity of phlorotannins

Phlorotannins	EC_{50} (μM)		References
	DPPH	Total ROS	
Eckol	96.00	4.04	(Kang et al., 2004; Sugiura et al., 2008)
Dieckol	6.20	12.68	(Kang et al., 2004; Kim et al., 2009;m Kwon et al., 2013)
Dioxinodehydroeckol (Eckstolonol)	8.80	12.17	(Kang et al., 2004; Kim et al., 2009)
974-A	10.00	-	(Yotsu Yamashita et al., 2013)
2-Phloroeckol	35.20	-	(Lee et al., 2012)
974-B	0.86	6.45	(Choi et al., 2015)
6,6′-Bieckol	126.00	-	(Sugiura et al., 2008)
8,8′-Bieckol	59.00	-	(Sugiura et al., 2008)
Phlorofucofuroeckol A	60.00	3.80	(Kang et al., 2004; Kwon et al., 2013; Sugiura et al., 2008)
Phlorofucofuroeckol B	81.00	-	(Sugiura et al., 2008)
6,8′-Bieckol	59.00	-	(Sugiura et al., 2008)
Diphlorethohydroxycarmalol	3.41	-	(Heo et al., 2008)

4.2. Anti-inflammatory properties of phlorotannins

Inflammation is a host defense mechanism to harmful stimuli involving a cascade of events. Macrophages play a key role in the overall inflammatory chain, leading to the production of pro-inflammatory cytokines such as interleukin (IL)-1β, IL-6, tumor necrosis factor (TNF)-α and inflammatory mediators such as nitric oxide (NO) and prostaglandin E_2 (PGE_2). Overproduction of these components is associated with various diseases including atherosclerosis, arthritis, and cancer (Barbosa et al., 2019). Various reports on the anti-inflammatory and protective effects of phlorotannins are documented using RAW 264.7 macrophages induced by lipopolysaccharide (bacterial endotoxin). Phlorotannins were reported to inhibit the LPS-induced production of NO and PGE_2 via downregulation of NO synthase and COX-2 expression in LPS-induced RAW 264.7 murine macrophages (Barbosa et al., 2019; Jung et al., 2013; Yang et al., 2014; Yang et al., 2012). Furthermore, they reduced pro-inflammatory cytokine levels (IL-1β, IL-6, TNF-α), inhibited inflammatory mediators (iNOS and COX-2), transcriptional factors (NF-κB, nuclear translocation of p50 and p65 subunits and AP-1) and activated Akt and p38 MAPK signaling pathways (Lee et al., 2012).

4.3. Antimicrobial and Antiviral activity

The presence of bacteria with increasing multidrug-resistance to existing antibiotics is a major problem globally, with an urgent need for new antibacterial agents (Eom et al., 2012). Antibacterial properties of phlorotannins have been demonstrated, manifest through inhibition of oxidative phosphorylation, alteration of microbial cell permeability, loss of internal macromolecules and their ability to bind with bacterial proteins to elicit cell death (Shannon & Abu-Ghannam, 2016). It has been shown that the phenolic aromatic rings and hydroxyl groups of phlorotannins commonly bind to bacterial proteins by hydrophobic and hydrogen bonding interactions

respectively (Shannon & Abu-Ghannam, 2016). In a recent study, low molecular weight phlorotannins from *Sargassum thunbergii* damaged bacterial cell membranes and elicited cell death in *Vibrio parahaemolyticus*, a marine bacterium associated with human infection causing severe abdominal pain and diarrhea (Wei et al., 2016).

Lee *et al.* (2014) assessed different solvent-soluble fractions and phlorotannins (eckol, dieckol, fucofuroeckol-A, 7-phloroeckol, dioxinodehydroeckol, and phlorofucofuroeckol-A) from *Eisenia bicyclis* against *Propionibacterium*-related acne and *Listeria monocytogenes*, a foodborne pathogen responsible for listeriosis, meningitis and encephalitis (Lee et al., 2014). Among the tested phlorotannins, fucofuroeckol-A exhibited the strongest activity against *Propionibacterium*-related acne (MIC; 32 μg/mL) and *Listeria monocytogenes* (MIC; 16-32 μg/mL). The compound also demonstrated significant synergism with streptomycin against aminoglycoside-resistant strains (Kim et al., 2018; Lee et al., 2014). The potent activity of dieckol and phlorofucofuroeckol-A against *P. acnes* was also reported by Choi *et al*. (2014) (Choi et al., 2014). Both compounds demonstrated significant antibacterial activity, with a MIC of 39 μg/mL. Additionally, these compounds demonstrated significant activity against methicillin-resistant *Staphylococcus aureus* (MRSA), with phlorofucofuroeckol-A being the strongest inhibitor (MIC; 32 μg/mL) while further demonstrating synergistic effects with ampicillin, penicillin, and oxacillin (Eom et al., 2013). In other studies, phlorotannins were tested for antifungal activity against *Candida albicans.* Interestingly, fucofuroeckol-A not only exhibited potent antifungal activity but also restored the effect of fluconazole against fluconazole-resistant *C. albicans* in combination (Kim et al., 2018). Phlorofucofuroeckol-A was also tested for an antimicrobial effect against MRSA, significantly suppressing the expression of methicillin resistance-associated genes (mecI, mecR1, and mecA) and the production of penicillin-binding protein PBP2a in a concentration-dependent manner (Eom

et al., 2014). Furthermore, the bactericidal activity of the phlorotannins eckol, phlorofucofuroeckol A, dieckol, and 8,8′-bieckol were evaluated against food-borne pathogenic bacteria, MRSA and *Streptococcus pyogenes* (Nagayama et al., 2002). Dieckol and 8,8′-bieckol significantly inhibited *Campylobacter jejuni*, with MBC values of 0.03 μmol/mL (Nagayama et al., 2002). Eckol was also shown to demonstrate strong antibacterial activity against MRSA and *Salmonella* spp. and exhibited synergistic activity with ampicillin (Choi et al., 2010). Dieckol was reported to have antibacterial activity against methicillin-susceptible *S. aureus* (MSSA) and MRSA strains, with a MIC in the range of 32 to 64 μg/mL. In addition, it was found to reverse the ampicillin and penicillin resistance of MRSA (Lee et al., 2008).

There are various reports regarding the antiviral properties of phlorotannins. Park *et al.* (2013) tested nine phlorotannins (phloroglucinol, triphlorethol A, eckol, dioxinodehydroeckol, 2-phloroeckol, 7-phloroeckol, fucodiphloroethol G, dieckol and phlorofucofuroeckol A) against SARS-CoV $3CL^{pro}$ (Park et al., 2013). All phlorotannins demonstrated moderate inhibitory activity, with dieckol the most active phlorotannin with an IC_{50} value of 2.7 μM (Park et al., 2013). Furthermore, these phlorotannins exerted potent activity against porcine epidemic diarrhea virus (PEDV), blocking the binding of viral spike protein to sialic acid by hemagglutination inhibition and inhibiting viral replication (Kwon et al., 2013). Additional studies have shown that dieckol and phlorofucofuroeckol A exhibited strong antiviral activity against murine norovirus in RAW 264.7 cells, with an EC_{50} of 0.9 μM (Eom et al., 2015). Phlorofucofuroeckol A also demonstrated strong antiviral activity against influenza viruses H1N1 (A/PR/8/34) and H9N2 (A/chicken/Korea/01210/2001) by decreasing neuraminidase protein expression in viral-infected Madin–Darby canine kidney cells (Cho et al., 2019). Furthermore, 8,8′-bieckol, 8,4‴-dieckol and 6,6′-bieckol have been reported to have anti-HIV activity via inhibition of HIV-1 reverse

transcriptase/ protease, inhibition of HIV-1 induced syncytia formation, lytic effects and/or viral p24 antigen production (Ahn et al., 2004; Artan et al., 2008).

4.4. Anti-diabetic activity

Type 2 diabetes mellitus is characterized by defects in insulin secretion and response which can lead to hyperglycemia, neuropathies and vasculopathies. Enzymic pathways that have prompted interest as targets in the management of diabetes are PTP1B, a negative regulator of insulin signaling that plays a key role in developing insulin resistance and α-glucosidase, an enzyme involved in digestion and absorption of carbohydrate (Moon et al., 2011). Phlorotannins have been reported to have strong inhibitory effects against PTP1B and α-glucosidase, as shown in Table 2. Among the reported phlorotannins, dieckol and phlorofucofuroeckol A demonstrated strong inhibition in both enzyme assay systems (Heo et al., 2009; Lee et al., 2009; Moon et al., 2011).

Roy *et al.* (2011) investigated the bioactivity of a commercially available phlorotannin-rich extract from *Ascophyllum nodosum* and *Fucus vesiculosus* towards inhibiting carbohydrate digestive enzymes *in vitro* (α-amylase activity and α-glucosidase activity) and *in vivo* in male Wistar rats (Roy et al., 2011). Their results suggested that the extract inhibited both enzymes in a concentration-dependent manner, notably α-amylase (IC_{50}; 2.8 μg/mL) and α-glucosidase (IC_{50}; 5.0 μg/mL). Furthermore, the extract decreased the normal increase in postprandial blood glucose after a meal by 90% and consecutively reduced peak insulin secretion by 40% (Roy et al., 2011). Another study demonstrated that dieckol and diphlorethohydroxycarmalol significantly inhibited α-glucosidase and α-amylase and suppressed postprandial blood glucose elevations in streptozotocin-induced diabetic mice (Heo et al., 2009; Lee et al., 2010). Similar results were obtained with 2,7″-phloroglucinol, 6,6′-bieckol and phlorofucofuroeckol A in diabetic mice (Lee et al., 2017; You et al., 2015). Additionally, dieckol significantly lowered blood glucose,

glycosylated hemoglobin and plasma insulin levels in male C57BL/KsJ-db/db mice compared with controls (Kang et al., 2013; Lee et al., 2012). Antioxidant enzymes such as superoxide dismutase, catalase, glutathione peroxidase and hepatic glucose-regulating enzyme activities were elevated, while glucose-6-phosphatase and phosphoenolpyruvate carboxykinase activities were lowered. The authors suggested that the anti-diabetic activity of the dieckol-rich extract and dieckol itself was due to improved glucose and lipid metabolism and antioxidant enzyme expression (Kang et al., 2013; Lee, Min, et al., 2012). The anti-diabetic activity of dieckol was further confirmed in an alloxan-induced hyperglycemic zebrafish model by Kim *et al*. (2016), where dieckol was able to reduce glucose-6-phosphate and phosphoenolpyruvate carboxykinase and increase phosphorylation of protein kinase B (Akt) in muscle tissue (Kim et al., 2016). Furthermore, octaphlorethol A was able to increase glucose uptake in differentiated L6 rat myoblast cells in a concentration-dependent manner via protein kinase B (Akt) and AMP-activated protein kinase (AMPK) activation (Lee et al., 2012).

Table 2. Inhibitory activities of phlorotannins against PTP1B and α-glucosidase

Phlorotannins	IC_{50} (μM)		References
	PTP1B	α-glucosidase	
Eckol	2.64	22.78	(Moon et al., 2011)
Dieckol	1.18	1.61	(Moon et al., 2011)
Dioxinodehydroeckol (Eckstolonol)	29.97	34.60	(Moon et al., 2011)
7-Phloroeckol	2.09	6.13	(Moon et al., 2011)
6,6′-Bieckol	-	22.22	(Lee et al., 2009)
Phlorofucofuroeckol A	0.56	1.37	(Moon et al., 2011)
Diphlorethohydroxycarmalol	-	160.00	(Heo et al., 2009)
Fucodiphloroethol G	-	19.52	(Lee et al., 2009)

4.5. Neuroprotective activity

With an increase in life expectancy, the increasing prevalence of neurodegenerative diseases including Alzheimer's disease (AD), Parkinson's disease, Huntington's disease, amyotrophic lateral sclerosis, frontotemporal and other forms of dementia represent a collective major global health burden. These are diverse in etiology and cause memory and cognitive decline in addition to variably eliciting dysfunction of movement, speech, swallowing and breathing (Gitler et al., 2017).

The key cholinesterase enzymes, acetylcholinesterase (AChE) and butyrylcholinesterase (BChE), play an important role in cholinergic transmission in the brain by way of the hydrolysis of the neurotransmitter acetylcholine (ACh), whereby loss of ACh signaling in the brain is correlated with the increased severity of AD (Roseiro et al., 2012). Evidence suggests that AChE and BChE significantly regulate the concentration of ACh in the brain, and inhibition of these enzymes is used therapeutically in the symptomatic treatment of AD (Colovic et al., 2013); this includes natural products such as galantamine, an alkaloid from *Galanthus* spp. now used clinically (Colovic et al., 2013). Additionally, β-secretase 1 (BACE1) catalyzes the rate-limiting step in the production of amyloid β, which results in amyloid plaque formation in Alzheimer's disease. Various phlorotannins have been tested for their ability to inhibit these target enzymes, with inhibitory activity listed in Table 3 (Choi et al., 2015; Jung et al., 2010; Kannan et al., 2013; Lee & Jun, 2019; Lee & Byun, 2018; Yoon et al., 2008; Yoon et al., 2009). Among the isolated phlorotannins, 974-B has been reported to have the most potent inhibitory activity against AChE and BChE, with IC_{50} values of 1.95 and 3.26 μM respectively (Choi et al., 2015). Furthermore, Lee *et al.* (2019) reported the AChE inhibitory activity of eckol, dieckol, and 8,8′-bieckol, with IC_{50} values of 10.03, 5.69, and 4.59 μM, respectively. Furthermore, these compounds were also

shown to be active in BACE1 inhibitory assays. Among these compounds, 8,8′-bieckol demonstrated significant inhibition against BACE1, with an IC_{50} value of 1.62 μM (Lee & Jun, 2019). Furthermore, Um *et al.* (2018) reported that a phlorotannin-rich extract from *Ishige foliace* reduced acetylcholinesterase activity in the brain and prevented the scopolamine-induced memory impairment in mice via oxidative scavenging and activation of the ERK-CREB-BDNF pathway (Um et al., 2018).

Table 3. Reports on AChE, BChE, and BACE1 inhibitory activity of phlorotannins.

Phlorotannins	IC_{50} (μM)			References
	AChE	BChE	BACE1	
Eckol	20.56	> 500	7.67	(Lee & Jun, 2019; Yoon et al., 2008)
Dieckol	5.69	> 500	2.34	(Lee & Jun, 2019)
Dioxinodehydroeckol (Eckstolonol)	42.66	230.27	5.35	(Jung et al., 2010; Yoon et al., 2008)
Dibenzo [1,4]dioxine-2,4,7,9-tetraol	84.48	-	-	(Kannan et al., 2013)
Phlorofucofuroeckol A	4.80	136.71	2.13	(Jung et al., 2010; Yoon et al., 2008)
2-Phloroeckol	38.13	>500	-	(Yoon et al., 2008)
7-Phloroeckol	21.11	> 500	8.59	(Jung et al., 2010; Yoon et al., 2008)
974-B	1.95	3.26	-	(Choi et al., 2015)
8,8′-Bieckol	4.59	10.90	1.62	(Choi et al., 2015; Lee & Jun, 2019)
Triphlorethol A	>500	>500	11.68	(Jung et al., 2010; Yoon et al., 2008)
6,6′-Bieckol	44.50	27.40	-	(Choi et al., 2015)
Diphlorethohydroxycarmalol	>200	110.83	-	(Yoon et al., 2009)

Fucofuroeckol B	-	-	16.1	(Lee & Byun, 2018)

In addition, phlorotannins and phlorotannin-rich extracts have been reported to protect various neuronal cell lines against neurotoxic amyloid β ($A\beta_{1-42}$). The excessive accumulation of amyloid β has been characterized as a major pathological hallmark of AD. Recently, we demonstrated that the ethyl acetate (phlorotannin-rich) fraction from *Ecklonia radiata* protected neuronal PC-12 cells against $A\beta_{1-42}$ (Shrestha et al., 2020). Furthermore, Ahn *et al.* (2012) reported that the phlorotannins eckol, phlorofucofuroeckol A, dieckol and 7-phloroeckol isolated from *Eisenia bicyclis* significantly reduced Aβ-induced cell death in PC-12 cells and inhibited both ROS generation and calcium release (Ahn et al., 2012). In addition, Lee *et al.* (2019) reported that eckol, dieckol and 8,8′-bieckol from *Ecklonia cava* also protected PC-12 cells against $A\beta_{25-35}$-induced cytotoxicity and apoptosis (Lee et al., 2019). These phlorotannins inhibited TNF-α, IL-β and PGE_2 production and downregulated the pro-inflammatory enzymes iNOS and COX-2 (Lee et al., 2019). Among the phlorotannins investigated, dieckol was reported to have superior effects via suppression of p38, ERK and JNK (Lee et al., 2019). In addition, dieckol has been reported to suppress LPS-induced production of NO and PGE_2, downregulate the expression of iNOS and COX-2 and significantly reduce the generation of proinflammatory cytokines IL-1β and TNF-α in LPS-stimulated murine BV2 microglial cells, via suppression of the NF-κB and p38 MAPK signaling pathway (Jung et al., 2009). Similarly, a novel phlorotannin, eckmaxol was reported to prevent Aβ oligomer-induced neurotoxicity in neuronal SH-SY5Y cells via a direct action on GSK-3β (Wang et al., 2018). Kang *et al.* (2012) reported that phloroglucinol, eckol, triphlorethol A, eckstolonol and dieckol significantly protected murine hippocampal HT22 cells against H_2O_2-induced oxidative stress via inhibition of reactive oxygen species. Overall, phlorotannins were

found to have neuroprotective activity via various modes of action, as evidenced by their ability to inhibit AChE, BChE and BACE1 and regulate the signaling pathways linked to neuroinflammation, oxidative stress and neuronal cell death (Barbosa et al., 2020).

4.6. Anti-cancer activity

There is evidence that oxidative stress and inflammation are associated with the development of cancer via fostering genomic lesions, tumor initiation, promotion and progression (Rakoff-Nahoum, 2006). In addition to antioxidant activity, it has been suggested that phlorotannins may inhibit the formation of mitotic spindles in cancer cells by preventing microtubule formation, decreasing angiogenesis, cell adhesion and invasion (Mansur et al., 2020). Dioxinodehydroeckol isolated from *E. cava* exerted significant inhibition of proliferation and apoptosis in a concentration-dependent manner in MCF-7 human cancer cells via a NF-κB dependent pathway. This phlorotannin also induced an increase in caspase-3 and -9 activity and increased DNA repair enzyme poly-(ADP-ribose) polymerase (PARP) cleavage (Kong et al., 2009). Dieckol has been reported to have inhibitory activity against MCF-7 cells, downregulating the expression of migration-related genes such as matrix metalloprotease (MMP)-9 and vascular endothelial growth factor (VEGF), while also increasing the expression of tissue inhibitor of metalloproteinase (TIMP)-1 and TIMP-2 (Kim et al., 2015). Dieckol also induced apoptosis and suppressed tumor growth in SKOV3 ovarian cancer cells and human breast cancer cell lines SK-BR-3 and MCF-7 (Ahn et al., 2015; You et al., 2018). It also triggered the activation of caspase-3, -8 and -9, and inhibited the activity of AKT and p38 signaling in SKOV3 ovarian cancer cells (Ahn et al., 2015). Additionally, it significantly inhibited the invasive and migratory properties in a non-small-cell lung cancer cell line (A549), induced apoptosis via inhibition of Pi3K/AKT/mTOR signaling and activated the tumor suppressor protein E-cadherin (Wang et al., 2019). Phlorotannins also inhibited

hypoxia-induced epithelial mesenchymal transition in HT29 human colorectal cancer cells, via regulating the levels of cellular ROS and downregulating HIF1α protein expression (Jeong et al., 2016). Furthermore, dieckol and phlorofucofuroeckol-A inhibited the LPS-induced MCF-7 breast cancer cell line invasion through the downregulation of Toll-like receptor-4, NF-κB promoter-driven transcriptional activity and the matrix metalloproteinase-9 (TLR-4-NF-κB-MMP-9) signaling axis (Lee et al., 2020). Dieckol also suppressed the migration and invasion of HT1080 human fibrosarcoma cells via downregulating focal adhesion kinase pathway (FAK) signaling, through scavenging intracellular ROS and inhibiting the expression of MMP-2 and -9 in a concentration-dependent manner (Park & Jeon, 2012; Zhang et al., 2011). In addition, eckol and 7-phloroeckol were examined for their cytotoxicity in different cancer cell lines. Among them, eckol exhibited the highest activity against HeLa cells, H157 and MCF7 cell lines (Park & Jeon, 2012; Zhang et al., 2011). Eckol also demonstrated anti-tumor activity in sarcoma 180 xenograft bearing mice, via stimulating phagocytes, $CD11c^{+}$-dendritic cells, tumor-specific Th1 and cytotoxic T lymphocyte responses (Zhang et al., 2019). Kim *et al.* (2015) and Hyun *et al.* (2011) reported that phloroglucinol and eckol suppressed the migratory and invasive properties of breast cancer cell lines MDA-MB231 and BT549, via inhibition of PI3K/AKT and rat sarcoma RAS/RAF-1/ERK signaling pathways. It also suppressed the metastatic ability of MDA-MB231 breast cancer cells to the lungs and extended the survival time of mice (Hyun et al., 2011; Kim et al., 2015).

5. Phlorotannins as supplements in animal feed

Livestock is kept in high concentrations in commercial farms to maximize economic returns, thereby increasing the risk and impacts of disease outbreaks. Widespread antibiotic use in feedstocks for prophylaxis and mitigation of infection risk and growth promotion is recognized as

a leading contributor to antimicrobial resistance in animals and humans (O'Neill, 2015). As alternatives or adjunctive agents to antibiotics, phlorotannin-rich brown seaweed extract and phlorotannins have been reported to have antibacterial activity against various foodborne pathogens including *Listeria monocytogenes*, *Escherichia coli* O157, *Salmonella agona*, *Streptococcus suis*, *Staphylococcus aureus*, *Streptococcus pyogenes* and *Vibrio parahaemolyticus* (Ford et al., 2020; Kim et al., 2018; Nagayama et al., 2002). Animal trials have demonstrated that when *Sargassum fusiforme* and *Ecklonia cava* were used as dietary supplements in juvenile olive flounder (*Paralichthys olivaceus*), survival rates were significantly higher after challenge with *Edwardsiella tarda*, a bacteria capable of eliciting gastrointestinal infection in humans (Kim et al., 2014). In livestock animals, a study performed by Katayama *et al.* (2011) on swine demonstrated an increase in salivary IgA and IgG production in the seaweed-treated (Algiflora-3; Shinkyo Sangyo Co., Yamaguchi, Japan) group compared to controls (Katayama et al., 2011).

In addition, seaweed is also rich in polysaccharides, xanthophylls, fucoidan, vitamins A, B, C, D, and E, and minerals including calcium, phosphorous, and sodium (Rajauria, 2015). The protein content of some seaweeds is comparable with that of soybeans and they also contain polyunsaturated omega-3 and omega 6 fatty acids (Rajauria, 2015). The nutritional benefits of seaweed were demonstrated by Hwang *et al.* (2014), who used Hanwoo steers (Korean native cattle) to evaluate the effect of a 2% *Undaria pinnatifida* by-product in their feed (Hwang et al., 2014). The study concluded that the supplement significantly improved growth, immunity, and fatty acid profile while decreasing cholesterol content in the beef. In another study, the brown seaweed extract from *Laminaria* spp. was fed to pigs from gestation and/or postweaning, where pigs weaned on seaweed extract had a significantly higher average daily weight gain and enhanced overall growth performance (Draper et al., 2016). Turner *et al.* (2002) also demonstrated the

beneficial effects of dietary *Ascophyllum nodosum* on young pig growth performance (Turner et al., 2002). Furthermore, the effect of commercially available seaweed extract (OceanFeed Swine^{TM}; mixture of brown, red and green seaweeds) on body weight, average daily weight gain and feed efficiency was evaluated in fattening pigs of terminal lines (Satessa et al., 2020). The author concluded that consumption of the seaweed extract increased slaughter weight, reduced *E. coli* and increased *Lactobacillus spp levels*. Inclusion of seaweed extract containing laminarin and fucoidan derived from *Laminaria spp.* increased digestive function, reduced fecal *E. coli* and improved the immune response in newly weaned pigs (O'Doherty et al., 2010). This seaweed extract also has been reported to improve rumen fermentation and digestion in steers and the quality of milk in lactating cows (Bendary et al., 2013; Ead et al., 2011). Additionally, the brown seaweed extract (*Ascophyllum nodosum*) supplement has been reported to have a positive impact on small ruminants via altered immunity and gastrointestinal microbial function, offering improved disease resistance while maintaining the texture and shelf life of meat (Kannan et al., 2019). Further studies are required to elucidate the component bioactivity of algal extracts, especially of phlorotannins from brown seaweed extracts used as supplements in domestic livestock feeds.

6. Conclusions

Overall, phlorotannins are complex polymeric structures optimally identified via NMR (1D and 2D) analysis coupled with HRMS. Linking these structures to HPLC conditions (solvents) along with retention time and UV spectral data facilitate accurate identification of phlorotannins without the requirement to isolate individual constituents via various column chromatography techniques. Preliminary evidence suggests that phlorotannins are bioactive in areas related to anti-inflammatory and neuroprotective actions, but that they also have beneficial metabolic benefits

related to glucose homeostasis and gut health, with an influence of the microbiome likely to contribute in-part to the latter benefit. Additional *in vivo* studies are required to confirm their bioavailability, efficacy and safety for nutraceutical applications in animal and human health, whereby brown algal-sourced phlorotannins may be an accessible and cost-effective active ingredient.

7. Conflicts of interest

The authors confirm that they have no conflicts of interest with respect to the work described in this manuscript.

8. Acknowledgments

Srijan Shrestha is supported by the Australian Government Research Training Program (RTP) Scholarship. Wei Zhang acknowledges the support of ARC Industry Transformation and Training Centre for Green Chemistry in Manufacturing, Qingdao Gather Great Ocean Algae Industry Group Co, Ltd, and Australian Kelp Products Pty Ltd.

References

Ahn, B. R., Moon, H. E., Kim, H. R., Jung, H. A., & Choi, J. S. (2012). Neuroprotective effect of edible brown alga *Eisenia bicyclis* on amyloid beta peptide-induced toxicity in PC12 cells. *Archives of Pharmacal Research, 35*(11), 1989-1998.

Ahn, J. H., Yang, Y. I., Lee, K. T., & Choi, J. H. (2015). Dieckol, isolated from the edible brown algae *Ecklonia cava*, induces apoptosis of ovarian cancer cells and inhibits tumor xenograft growth. *Journal of Cancer Research and Clinical Oncology, 141*(2), 255-268.

Ahn, M. J., Yoon, K. D., Min, S. Y., Lee, J. S., Kim, J. H., Kim, T. G., et al. (2004). Inhibition of HIV-1 reverse transcriptase and protease by phlorotannins from the brown alga *Ecklonia cava*. *Biological and Pharmaceutical Bulletin, 27*(4), 544-547.

Artan, M., Li, Y., Karadeniz, F., Lee, S. H., Kim, M. M., & Kim, S. K. (2008). Anti-HIV-1 activity of phloroglucinol derivative, 6, 6′-bieckol, from *Ecklonia cava*. *Bioorganic & Medicinal Chemistry, 16*(17), 7921-7926.

Barbosa, M., Lopes, G., Andrade, P. B., & Valentão, P. (2019). Bioprospecting of brown seaweeds for biotechnological applications: Phlorotannin actions in inflammation and allergy network. *Trends in Food Science & Technology, 86*, 153-171.

Barbosa, M., Valentão, P., Ferreres, F., Gil-Izquierdo, Á., & Andrade, P. B. (2020). In vitro multifunctionality of phlorotannin extracts from edible *Fucus* species on targets underpinning neurodegeneration. *Food Chemistry*, 127456.

Bendary, M., Bassiouni, M., Ali, M., Gaafar, H., & Shamas, A. S. (2013). Effect of premix and seaweed additives on productive performance of lactating friesian cows. *International Research Journal of Agricultural Science and Soil Science, 3*, 174-181.

Bogolitsyn, K., Druzhinina, A., Kaplitsin, P., Ovchinnikov, D., Parshina, A., & Kuznetsova, M. (2019). Relationship between radical scavenging activity and polymolecular properties of brown algae polyphenols. *Chemical Papers*, 1-9.

Cho, H. M., Doan, T. P., Ha, T. K. Q., Kim, H. W., Lee, B. W., Pham, H. T. T., et al. (2019). Dereplication by high-performance liquid chromatography (HPLC) with quadrupole-time-of-flight mass spectroscopy (qTOF-MS) and antiviral activities of phlorotannins from *Ecklonia cava*. *Marine Drugs, 17*(3), 149.

Choi, B. W., Lee, H. S., Shin, H. C., & Lee, B. H. (2015). Multifunctional activity of polyphenolic compounds associated with a potential for Alzheimer's disease therapy from *Ecklonia cava*. *Phytotherapy Research, 29*(4), 549-553.

Choi, J. G., Kang, O. H., Brice, O. O., Lee, Y. S., Chae, H. S., Oh, Y. C., et al. (2010). Antibacterial activity of *Ecklonia cava* against methicillin-resistant *Staphylococcus aureus* and *Salmonella spp*. *Foodborne Pathogens and Disease, 7*(4), 435-441.

Choi, J. S., Haulader, S., Karki, S., Jung, H. J., Kim, H. R., & Jung, H. A. (2015). Acetyl- and butyryl-cholinesterase inhibitory activities of the edible brown alga *Eisenia bicyclis*. *Archives of Pharmacal Research, 38*(8), 1477-1487.

Choi, J. S., Lee, K., Lee, B. B., Kim, Y. C., Kim, Y. D., Hong, Y. K., et al. (2014). Antibacterial activity of the phlorotannins dieckol and phlorofucofuroeckol-A from *Ecklonia cava* against *Propionibacterium acnes*. *Botanical Sciences, 92*(3), 425-431.

Colovic, M. B., Krstic, D. Z., Lazarevic-Pasti, T. D., Bondzic, A. M., & Vasic, V. M. (2013). Acetylcholinesterase inhibitors: pharmacology and toxicology. *Current Neuropharmacology, 11*(3), 315-335.

Draper, J., Walsh, A., McDonnell, M., & O'Doherty, J. (2016). Maternally offered seaweed extracts improves the performance and health status of the postweaned pig. *Journal of Animal Science, 94*(suppl_3), 391-394.

Ead, H., Maklad, E. H., El-Shinnawy, M., Hamza, A. S., & Ibrahim, K. (2011). Effects of seaweed supplementation to dairy friesian cows, rations on: 2-milk yield, blood parameters and feed efficiency. *Journal of Animal and Poultry Production, 2*(7), 231-242.

Eom, S. H., Kim, D. H., Lee, S. H., Yoon, N. Y., Kim, J. H., Kim, T. H., et al. (2013). In vitro antibacterial activity and synergistic antibiotic effects of phlorotannins isolated from *Eisenia bicyclis* against methicillin-resistant *Staphylococcus aureus*. *Phytotherapy Research, 27*(8), 1260-1264.

Eom, S. H., Kim, Y. M., & Kim, S. K. (2012). Antimicrobial effect of phlorotannins from marine brown algae. *Food and Chemical Toxicology, 50*(9), 3251-3255.

Eom, S. H., Lee, D. S., Jung, Y. J., Park, J. H., Choi, J. I., Yim, M. J., et al. (2014). The mechanism of antibacterial activity of phlorofucofuroeckol-A against methicillin-resistant *Staphylococcus aureus*. *Applied Microbiology and Biotechnology, 98*(23), 9795-9804.

Eom, S. H., Moon, S. Y., Lee, D. S., Kim, H. J., Park, K., Lee, E. W., et al. (2015). In vitro antiviral activity of dieckol and phlorofucofuroeckol-A isolated from edible brown alga *Eisenia bicyclis* against murine norovirus. *Algae, 30*(3), 241.

Ferreres, F., Lopes, G., Gil-Izquierdo, A., Andrade, P. B., Sousa, C., Mouga, T., et al. (2012). Phlorotannin extracts from *Fucales* characterized by HPLC-DAD-ESI-MSn: approaches to hyaluronidase inhibitory capacity and antioxidant properties. *Marine Drugs, 10*(12), 2766-2781.

Ford, L., Stratakos, A. C., Theodoridou, K., Dick, J. T. A., Sheldrake, G. N., Linton, M., et al. (2020). Polyphenols from brown seaweeds as a potential antimicrobial agent in animal feeds. *ACS Omega, 5*(16), 9093-9103.

Ford, L., Theodoridou, K., Sheldrake, G. N., & Walsh, P. J. (2019). A critical review of analytical methods used for the chemical characterisation and quantification of phlorotannin compounds in brown seaweeds. *Phytochemical Analysis, 30*(6), 587-599.

Franco, R., Navarro, G., & Martínez-Pinilla, E. (2019). Hormetic and mitochondria-related mechanisms of antioxidant action of phytochemicals. *Antioxidants, 8*(9), 373.

Gitler, A. D., Dhillon, P., & Shorter, J. (2017). Neurodegenerative disease: models, mechanisms, and a new hope. *Disease Models & Mechanisms, 10*(5), 499-502.

Gümüş Yılmaz, G., Gómez Pinchetti, J. L., Cifuentes, A., Herrero, M., & Ibáñez, E. (2019). Comparison of extraction techniques and surfactants for the isolation of total polyphenols and phlorotannins from the brown algae *Lobophora variegata*. *Analytical Letters*, 1-17.

Heo, S. J., Hwang, J. Y., Choi, J. I., Han, J. S., Kim, H. J., & Jeon, Y. J. (2009). Diphlorethohydroxycarmalol isolated from *Ishige okamurae*, a brown algae, a potent α-glucosidase and α-amylase inhibitor, alleviates postprandial hyperglycemia in diabetic mice. *European Journal of Pharmacology, 615*(1-3), 252-256.

Heo, S. J., Kim, J. P., Jung, W. K., Lee, N. H., Kang, H. S., Jun, E. M., et al. (2008). Identification of chemical structure and free radical scavenging activity of diphlorethohydroxycarmalol isolated from a brown alga, *Ishige okamurae*. *Journal of Microbiology and Biotechnology, 18*(4), 676-681.

Hwang, J. A., Islam, M. M., Ahmed, S. T., Mun, H. S., Kim, G. M., Kim, Y. J., et al. (2014). Seamustard (*Undaria pinnatifida*) improves growth, immunity, fatty acid profile and

reduces cholesterol in Hanwoo Steers. *Asian-Australasian Journal of Animal Sciences, 27*(8), 1114-1123.

Hyun, K. H., Yoon, C. H., Kim, R. K., Lim, E. J., An, S., Park, M. J., et al. (2011). Eckol suppresses maintenance of stemness and malignancies in glioma stem-like cells. *Toxicology and Applied Pharmacology, 254*(1), 32-40.

Isaza Martínez, J. H., & Torres Castañeda, H. G. (2013). Preparation and chromatographic analysis of phlorotannins. *Journal of Chromatographic Science, 51*(8), 825-838.

Jeong, S. H., Jeon, Y. J., & Park, S. J. (2016). Inhibitory effects of dieckol on hypoxia-induced epithelial-mesenchymal transition of HT29 human colorectal cancer cells. *Molecular Medicine Reports, 14*(6), 5148-5154.

Jung, H. A., Jin, S. E., Ahn, B. R., Lee, C. M., & Choi, J. S. (2013). Anti-inflammatory activity of edible brown alga *Eisenia bicyclis* and its constituents fucosterol and phlorotannins in LPS-stimulated RAW264. 7 macrophages. *Food and Chemical Toxicology, 59*, 199-206.

Jung, H. A., Oh, S. H., & Choi, J. S. (2010). Molecular docking studies of phlorotannins from *Eisenia bicyclis* with BACE1 inhibitory activity. *Bioorganic & Medicinal Chemistry Letters, 20*(11), 3211-3215.

Jung, W. K., Heo, S. J., Jeon, Y. J., Lee, C. M., Park, Y. M., Byun, H. G., et al. (2009). Inhibitory effects and molecular mechanism of dieckol isolated from marine brown alga on COX-2 and iNOS in microglial cells. *Journal of Agricultural and Food Chemistry, 57*(10), 4439-4446.

Kang, C., Jin, Y. B., Lee, H., Cha, M., Sohn, E.T., Moon, J., et al. (2010). Brown alga *Ecklonia cava* attenuates type 1 diabetes by activating AMPK and Akt signaling pathways. *Food and Chemical Toxicology, 48*(2), 509-516.

Kang, H. S., Chung, H. Y., Kim, J. Y., Son, B. W., Jung, H. A., & Choi, J. S. (2004). Inhibitory phlorotannins from the edible brown alga *Ecklonia stolonifera* on total reactive oxygen species (ROS) generation. *Archives of Pharmacal Research, 27*(2), 194-198.

Kang, K. A., Lee, K. H., Chae, S., Koh, Y. S., Yoo, B.-S., Kim, J. H., et al. (2005a). Triphlorethol-A from *Ecklonia cava* protects V79-4 lung fibroblast against hydrogen peroxide induced cell damage. *Free Radical Research, 39*(8), 883-892.

Kang, K. A., Lee, K. H., Chae, S., Zhang, R., Jung, M. S., Ham, Y. M., et al. (2006). Cytoprotective effect of phloroglucinol on oxidative stress induced cell damage via catalase activation. *Journal of cellular biochemistry, 97*(3), 609-620.

Kang, K. A., Lee, K. H., Chae, S., Zhang, R., Jung, M. S., Lee, Y., et al. (2005b). Eckol isolated from *Ecklonia cava* attenuates oxidative stress induced cell damage in lung fibroblast cells. *FEBS letters, 579*(28), 6295-6304.

Kang, M. C., Wijesinghe, W., Lee, S. H., Kang, S. M., Ko, S. C., Yang, X., et al. (2013). Dieckol isolated from brown seaweed *Ecklonia cava* attenuates type II diabetes in db/db mouse model. *Food and chemical toxicology, 53*, 294-298.

Kang, S. M., Cha, S. H., Ko, J. Y., Kang, M. C., Kim, D., Heo, S. J., et al. (2012). Neuroprotective effects of phlorotannins isolated from a brown alga, *Ecklonia cava*, against H_2O_2-induced oxidative stress in murine hippocampal HT22 cells. *Environmental toxicology and pharmacology, 34*(1), 96-105.

Kannan, G., Terrill, T. H., Kouakou, B., & Lee, J. H. (2019). Dietary brown seaweed extract supplementation in small ruminants. In N. Joshee, S. A. Dhekney & P. Parajuli (Eds.), *Medicinal Plants: From Farm to Pharmacy* (pp. 291-312). Cham: Springer International Publishing.

Kannan, R. R., Aderogba, M. A., Ndhlala, A. R., Stirk, W. A., & Van Staden, J. (2013). Acetylcholinesterase inhibitory activity of phlorotannins isolated from the brown alga, *Ecklonia maxima* (Osbeck) Papenfuss. *Food research international, 54*(1), 1250-1254.

Katayama, M., Fukuda, T., Okamura, T., Suzuki, E., Tamura, K., Shimizu, Y., et al. (2011). Effect of dietary addition of seaweed and licorice on the immune performance of pigs. *Animal science journal, 82*(2), 274-281.

Kim, A. D., Kang, K. A., Piao, M. J., Kim, K. C., Zheng, J., Yao, C. W., et al. (2014). Cytoprotective effect of Eckol against oxidative stress-induced mitochondrial dysfunction: Involvement of the Foxo3a/Ampk pathway. *Journal of Cellular Biochemistry, 115*(8), 1403-1411.

Kim, A. R., Shin, T. S., Lee, M. S., Park, J. Y., Park, K. E., Yoon, N. Y., et al. (2009). Isolation and identification of phlorotannins from *Ecklonia stolonifera* with antioxidant and anti-inflammatory properties. *Journal of Agricultural and Food Chemistry, 57*(9), 3483-3489.

Kim, E. A., Lee, S. H., Lee, J. H., Kang, N., Oh, J. Y., Ahn, G., et al. (2016). A marine algal polyphenol, dieckol, attenuates blood glucose levels by Akt pathway in alloxan induced hyperglycemia zebrafish model. *RSC Advances*, *6*(82), 78570-78575.

Kim, E. K., Tang, Y., Kim, Y. S., Hwang, J. W., Choi, E. J., Lee, J. H., et al. (2015). First evidence that *Ecklonia cava*-derived dieckol attenuates MCF-7 human breast carcinoma cell migration. *Marine Drugs, 13*(4), 1785-1797.

Kim, H. J., Dasagrandhi, C., Kim, S. H., Kim, B. G., Eom, S. H., & Kim, Y. M. (2018). In vitro antibacterial activity of phlorotannins from edible brown algae, *Eisenia bicyclis* against streptomycin-resistant *Listeria monocytogenes*. *Indian Journal of Microbiology, 58*(1), 105-108.

Kim, K. C., Kang, K. A., Zhang, R., Piao, M. J., Kim, G. Y., Kang, M. Y., et al. (2010). Up-regulation of Nrf2-mediated heme oxygenase-1 expression by eckol, a phlorotannin compound, through activation of Erk and PI3K/Akt. *The International Journal of Biochemistry & Cell Biology, 42*(2), 297-305.

Kim, K. H., Yu, D., Eom, S. H., Kim, H. J., Kim, D. H., Song, H. S., et al. (2018). Fucofuroeckol-A from edible marine alga *Eisenia bicyclis* to restore antifungal activity of fluconazole against fluconazole-resistant *Candida albicans*. *Journal of Applied Phycology, 30*(1), 605-609.

Kim, K. W., Kim, S. S., Khosravi, S., Rahimnejad, S., & Lee, K. J. (2014). Evaluation of *Sargassum fusiforme* and *Ecklonia cava* as dietary additives for olive flounder (*Paralichthys olivaceus*). *Turkish Journal of Fisheries and Aquatic Sciences 14*, 321-330.

Kim, R. K., Suh, Y., Yoo, K. C., Cui, Y. H., Hwang, E., Kim, H. J., et al. (2015). Phloroglucinol suppresses metastatic ability of breast cancer cells by inhibition of epithelial-mesenchymal cell transition. *Cancer Science, 106*(1), 94-101.

Kim, Y., Shin, J., Kang, S. M., Song, J., Shin, H. C., Keum, Y. S., et al. (2020). Highly regioselective preparation and characterization of new 6-O-substituted dieckol derivatives. *Journal of Industrial and Engineering Chemistry*.

Koivikko, R., Loponen, J., Honkanen, T., & Jormalainen, V. (2005). Contents of soluble, cell-wall-bound and exuded phlorotannins in the brown alga *Fucus vesiculosus*, with implications on their ecological functions. *Journal of Chemical Ecology, 31*(1), 195-212.

Kong, C. S., Kim, J. A., Yoon, N. Y., & Kim, S. K. (2009). Induction of apoptosis by phloroglucinol derivative from *Ecklonia cava* in MCF-7 human breast cancer cells. *Food and Chemical Toxicology, 47*(7), 1653-1658.

Kwon, H. J., Ryu, Y. B., Kim, Y. M., Song, N., Kim, C. Y., Rho, M. C., et al. (2013). In vitro antiviral activity of phlorotannins isolated from *Ecklonia cava* against porcine epidemic diarrhea coronavirus infection and hemagglutination. *Bioorganic & Medicinal Chemistry, 21*(15), 4706-4713.

Kwon, T. H., Kim, T. W., Kim, C. G., & Park, N. H. (2013). Antioxidant activity of various solvent fractions from edible brown alga, *Eisenia bicyclis* and its active compounds. *Journal of Food Science, 78*(5), C679-C684.

Lee, D. S., Kang, M. S., Hwang, H. J., Eom, S. H., Yang, J. Y., Lee, M. S., et al. (2008). Synergistic effect between dieckol from *Ecklonia stolonifera* and β-lactams against methicillin-resistant *Staphylococcus aureus*. *Biotechnology and Bioprocess Engineering, 13*(6), 758-764.

Lee, H. A., Lee, J. H., & Han, J. S. (2017). A phlorotannin constituent of *Ecklonia cava* alleviates postprandial hyperglycemia in diabetic mice. *Pharmaceutical Biology, 55*(1), 1149-1154.

Lee, J., & Jun, M. (2019). Dual BACE1 and cholinesterase inhibitory effects of phlorotannins from *Ecklonia cava*—An in vitro and in silico study. *Marine Drugs, 17*(2), 91.

Lee, J. H., Eom, S. H., Lee, E. H., Jung, Y. J., Kim, H. J., Jo, M. R., et al. (2014). In vitro antibacterial and synergistic effect of phlorotannins isolated from edible brown seaweed *Eisenia bicyclis* against acne-related bacteria. *Algae, 29*(1), 47.

Lee, J. K., & Byun, H.-G. (2018). A novel BACE inhibitor isolated from *Eisenia bicyclis* exhibits neuroprotective activity against β-amyloid toxicity. *Fisheries and Aquatic Sciences, 21*(1), 38.

Lee, J. W., Seok, J. K., & Boo, Y. C. (2018). *Ecklonia cava* extract and dieckol attenuate cellular lipid peroxidation in keratinocytes exposed to PM10. *Evidence-Based Complementary and Alternative Medicine, 2018*.

Lee, M. S., Kwon, M. S., Choi, J. W., Shin, T., No, H. K., Choi, J. S., et al. (2012). Anti-inflammatory activities of an ethanol extract of *Ecklonia stolonifera* in lipopolysaccharide-stimulated RAW 264.7 murine macrophage cells. *Journal of Agricultural and Food Chemistry, 60*(36), 9120-9129.

Lee, M. S., Shin, T., Utsuki, T., Choi, J. S., Byun, D. S., & Kim, H. R. (2012). Isolation and identification of phlorotannins from *Ecklonia stolonifera* with antioxidant and hepatoprotective properties in tacrine-treated HepG2 cells. *Journal of Agricultural and Food Chemistry, 60*(21), 5340-5349.

Lee, S., Youn, K., Kim, D., Ahn, M. R., Yoon, E., Kim, O. Y., et al. (2019). Anti-neuroinflammatory property of phlorotannins from *Ecklonia cava* on $A\beta_{25-35}$-induced damage in PC12 cells. *Marine Drugs, 17*(1), 7.

Lee, S. H., Kang, S. M., Ko, S. C., Lee, D. H., & Jeon, Y. J. (2012). Octaphlorethol A, a novel phenolic compound isolated from a brown alga, *Ishige foliacea*, increases glucose transporter 4-mediated glucose uptake in skeletal muscle cells. *Biochemical and Biophysical Research Communications, 420*(3), 576-581.

Lee, S. H., Karadeniz, F., Kim, M. M., & Kim, S. K. (2009). α-Glucosidase and α-amylase inhibitory activities of phloroglucinal derivatives from edible marine brown alga, *Ecklonia cava*. *Journal of the Science of Food And Agriculture, 89*(9), 1552-1558.

Lee, S. H., Min, K. H., Han, J. S., Lee, D. H., Park, D. B., Jung, W. K., et al. (2012). Effects of brown alga, *Ecklonia cava* on glucose and lipid metabolism in C57BL/KsJ-db/db mice, a model of type 2 diabetes mellitus. *Food and Chemical Toxicology, 50*(3-4), 575-582.

Lee, S. H., Park, M. H., Heo, S. J., Kang, S. M., Ko, S. C., Han, J. S., et al. (2010). Dieckol isolated from *Ecklonia cava* inhibits α-glucosidase and α-amylase in vitro and alleviates postprandial hyperglycemia in streptozotocin-induced diabetic mice. *Food and Chemical Toxicology, 48*(10), 2633-2637.

Lee, Y. J., Park, J. H., Park, S. A., Joo, N. R., Lee, B. H., Lee, K. B., et al. (2020). Dieckol or phlorofucofuroeckol extracted from *Ecklonia cava* suppresses lipopolysaccharide-mediated human breast cancer cell migration and invasion. *Journal of Applied Phycology, 32*(1), 631-640.

Li, Y., Fu, X., Duan, D., Liu, X., Xu, J., & Gao, X. (2017). Extraction and identification of phlorotannins from the brown alga, *Sargassum fusiforme* (Harvey) Setchell. *Marine Drugs, 15*(2), 49.

Liguori, I., Russo, G., Curcio, F., Bulli, G., Aran, L., Della-Morte, D., et al. (2018). Oxidative stress, aging, and diseases. *Clinical Interventions in Aging, 13*, 757.

Lopes, G., Barbosa, M., Vallejo, F., Gil-Izquierdo, Á., Andrade, P. B., Valentão, P., et al. (2018). Profiling phlorotannins from *Fucus* spp. of the Northern Portuguese coastline: Chemical approach by HPLC-DAD-ESI/MSn and UPLC-ESI-QTOF/MS. *Algal Research, 29*, 113-120.

Mansur, A. A., Brown, M. T., & Billington, R. A. (2020). The cytotoxic activity of extracts of the brown alga *Cystoseira tamariscifolia* (Hudson) Papenfuss, against cancer cell lines changes seasonally. *Journal of Applied Phycology*.

Meslet-Cladière, L., Delage, L., Leroux, C. J.-J., Goulitquer, S., Leblanc, C., Creis, E., et al. (2013). Structure/function analysis of a type III polyketide synthase in the brown alga *Ectocarpus siliculosus* reveals a biochemical pathway in phlorotannin monomer biosynthesis. *The Plant Cell, 25*(8), 3089-3103.

Moon, H. E., Islam, M. N., Ahn, B. R., Chowdhury, S. S., Sohn, H. S., Jung, H. A., et al. (2011). Protein tyrosine phosphatase 1B and α-glucosidase inhibitory phlorotannins from edible brown algae, *Ecklonia stolonifera* and *Eisenia bicyclis*. *Bioscience, Biotechnology, and Biochemistry, 75*(8), 1472-1480.

Nagayama, K., Iwamura, Y., Shibata, T., Hirayama, I., & Nakamura, T. (2002). Bactericidal activity of phlorotannins from the brown alga *Ecklonia kurome*. *Journal of Antimicrobial Chemotherapy, 50*(6), 889-893.

O'Doherty, J., Dillon, S., Figat, S., Callan, J., & Sweeney, T. (2010). The effects of lactose inclusion and seaweed extract derived from *Laminaria spp*. on performance, digestibility of diet components and microbial populations in newly weaned pigs. *Animal Feed Science and Technology, 157*(3-4), 173-180.

O'Neill, J. (2015). *Antimicrobials in agriculture and the environment: reducing unnecessary use and waste*.

Park, J. Y., Kim, J. H., Kwon, J. M., Kwon, H. J., Jeong, H. J., Kim, Y. M., et al. (2013). Dieckol, a SARS-CoV 3CLpro inhibitor, isolated from the edible brown algae *Ecklonia cava*. *Bioorganic & Medicinal Chemistry, 21*(13), 3730.

Park, S. J., & Jeon, Y. J. (2012). Dieckol from *Ecklonia cava* suppresses the migration and invasion of HT1080 cells by inhibiting the focal adhesion kinase pathway downstream of Rac1-ROS signaling. *Molecules and Cells, 33*(2), 141-149.

Pérez-Jiménez, J., Neveu, V., Vos, F., & Scalbert, A. (2010). Identification of the 100 richest dietary sources of polyphenols: an application of the Phenol-Explorer database. *European Journal of Clinical Nutrition, 64*(3), S112-S120.

Rajauria, G. (2015). Chapter 15 - Seaweeds: a sustainable feed source for livestock and aquaculture. In B. K. Tiwari & D. J. Troy (Eds.), *Seaweed Sustainability* (pp. 389-420). San Diego: Academic Press.

Rakoff-Nahoum, S. (2006). Why cancer and inflammation? *The Yale journal of biology and medicine, 79*(3-4), 123-130.

Roseiro, L. B., Rauter, A. P., & Serralheiro, M. L. M. (2012). Polyphenols as acetylcholinesterase inhibitors: structural specificity and impact on human disease. *Nutrition and Aging, 1*(2), 99-111.

Roy, M. C., Anguenot, R., Fillion, C., Beaulieu, M., Bérubé, J., & Richard, D. (2011). Effect of a commercially-available algal phlorotannins extract on digestive enzymes and carbohydrate absorption in vivo. *Food Research International, 44*(9), 3026-3029.

Satessa, G. D., Kjeldsen, N. J., Mansouryar, M., Hansen, H. H., Bache, J. K., & Nielsen, M. O. (2020). Effects of alternative feed additives to medicinal zinc oxide on productivity, diarrhoea incidence and gut development in weaned piglets. *Animal, 14*(8), 1638-1646.

Sathya, R., Kanaga, N., Sankar, P., & Jeeva, S. (2017). Antioxidant properties of phlorotannins from brown seaweed *Cystoseira trinodis* (Forsskål) C. Agardh. *Arabian Journal of Chemistry, 10*, S2608-S2614.

Shannon, E., & Abu-Ghannam, N. (2016). Antibacterial derivatives of marine algae: An overview of pharmacological mechanisms and applications. *Marine Drugs, 14*(4), 81.

Shrestha, S., Zhang, W., Begbie, A. J., Pukala, T. L., & Smid, S. D. (2020). *Ecklonia radiata* extract containing eckol protects neuronal cells against $A\beta_{1-42}$ evoked toxicity and reduces aggregate density. *Food & Function, 11*(7), 6509-6516.

Steevensz, A. J., MacKinnon, S. L., Hankinson, R., Craft, C., Connan, S., Stengel, D. B., et al. (2012). Profiling phlorotannins in brown macroalgae by liquid chromatography–high resolution mass spectrometry. *Phytochemical Analysis, 23*(5), 547-553.

Sugiura, Y., Matsuda, K., Yamada, Y., Imai, K., Kakinuma, M., & Amano, H. (2008). Radical scavenging and hyaluronidase inhibitory activities of phlorotannins from the edible brown alga *Eisenia arborea*. *Food Science and Technology Research, 14*(6), 595-595.

Turner, J., Dritz, S., Higgins, J., & Minton, J. (2002). Effects of *Ascophyllum nodosum* extract on growth performance and immune function of young pigs challenged with *Salmonella typhimurium*. *Journal of Animal Science, 80*(7), 1947-1953.

Um, M. Y., Lim, D. W., Son, H. J., Cho, S., & Lee, C. (2018). Phlorotannin-rich fraction from *Ishige foliacea* brown seaweed prevents the scopolamine-induced memory impairment via regulation of ERK-CREB-BDNF pathway. *Journal of Functional Foods, 40*, 110-116.

Wang, C. H., Li, X. F., Jin, L. F., Zhao, Y., Zhu, G. J., & Shen, W. Z. (2019). Dieckol inhibits non-small–cell lung cancer cell proliferation and migration by regulating the PI3K/AKT signaling pathway. *Journal of Biochemical and Molecular Toxicology, 33*(8), e22346.

Wang, J., Zheng, J., Huang, C., Zhao, J., Lin, J., Zhou, X., et al. (2018). Eckmaxol, a phlorotannin extracted from *Ecklonia maxima*, produces anti-beta-amyloid oligomer neuroprotective effects possibly via directly acting on glycogen synthase kinase 3beta. *ACS Chemical Neuroscience, 9*(6), 1349-1356.

Wang, T., Jónsdóttir, R. s., Liu, H., Gu, L., Kristinsson, H. G., Raghavan, S., et al. (2012). Antioxidant capacities of phlorotannins extracted from the brown algae *Fucus vesiculosus*. *Journal of Agricultural and Food Chemistry, 60*(23), 5874-5883.

Wei, Y., Liu, Q., Xu, C., Yu, J., Zhao, L., & Guo, Q. (2016). Damage to the membrane permeability and cell death of Vibrio parahaemolyticus caused by phlorotannins with low molecular weight from *Sargassum thunbergii*. *Journal of Aquatic Food Product Technology, 25*(3), 323-333.

Wijesekara, I., Yoon, N. Y., & Kim, S. K. (2010). Phlorotannins from *Ecklonia cava* (Phaeophyceae): Biological activities and potential health benefits. *Biofactors, 36*(6), 408-414.

Yang, Y. I., Jung, S. H., Lee, K. T., & Choi, J. H. (2014). 8, 8′-Bieckol, isolated from edible brown algae, exerts its anti-inflammatory effects through inhibition of NF-κB signaling and ROS production in LPS-stimulated macrophages. *International Immunopharmacology, 23*(2), 460-468.

Yang, Y. I., Shin, H. C., Kim, S. H., Park, W. Y., Lee, K. T., & Choi, J. H. (2012). 6, 6′-Bieckol, isolated from marine alga *Ecklonia cava*, suppressed LPS-induced nitric oxide and PGE2 production and inflammatory cytokine expression in macrophages: The inhibition of NFκB. *International Immunopharmacology, 12*(3), 510-517.

Yoon, N. Y., Chung, H. Y., Kim, H. R., & Choi, J. E. (2008). Acetyl-and butyrylcholinesterase inhibitory activities of sterols and phlorotannins from *Ecklonia stolonifera*. *Fisheries Science, 74*(1), 200-207.

Yoon, N. Y., Lee, S.-H., & Kim, S.-K. (2009). Phlorotannins from *Ishige okamurae* and their acetyl-and butyrylcholinesterase inhibitory effects. *Journal of Functional Foods, 1*(4), 331-335.

Yotsu Yamashita, M., Kondo, S., Segawa, S., Lin, Y. C., Toyohara, H., Ito, H., et al. (2013). Isolation and structural determination of two novel phlorotannins from the brown alga *Ecklonia kurome* Okamura, and their radical scavenging activities. *Marine Drugs, 11*(1), 165-183.

You, H.-N., Lee, H.-A., Park, M.-H., Lee, J.-H., & Han, J.-S. (2015). Phlorofucofuroeckol A isolated from *Ecklonia cava* alleviates postprandial hyperglycemia in diabetic mice. *European Journal of Pharmacology, 752*, 92-96.

You, S. H., Kim, J. S., & Kim, Y. S. (2018). Apoptosis and cell cycle arrest in two human breast cancer cell lines by dieckol isolated from *Ecklonia cava*. *Journal of Breast Disease, 6*(2), 39-45.

Zhang, C., Li, Y., Qian, Z. J., Lee, S. H., Li, Y. X., & Kim, S. k. (2011). Dieckol from *Ecklonia cava* regulates invasion of human fibrosarcoma cells and modulates MMP-2 and MMP-9 expression via NF-κB pathway. *Evidence-based Complementary and Alternative Medicine, 2011*.

Zhang, M. Y., Guo, J., Hu, X. M., Zhao, S. Q., Li, S. I., & Wang, J. (2019). An in vivo anti-tumor effect of eckol from marine brown algae by improving the immune response. *Food & Function, 10*(7), 4361-4371.

Appendix A: Supplementary Material

S1. Summary of NMR data of reported phlorotannins:

1. Phloroglucinol (Pale brown powder; $C_{22}H_{14}O_{11}$)

   ^{1}H NMR (90 MHz, CD_3OD): δ 5.82 (3H, br s, H-2, H-4, H-6); ^{13}C NMR (360 MHz, CD_3OD): δ 86.1 (C-2, C-4, C-6), 150.4 (C-1, C-3, C-5) (Hattori et al., 1988).

2. Eckol (Light brown powder; $C_{18}H_{12}O_9$)

   ^{1}H NMR (DMSO-*d*$_6$, 600 MHz): δ 9.48 (1H, s, OH-9), 9.42 (1H, s, OH-4), 9.15 (2H, s, OH-2, OH-7), 9.12 (2H, s, OH-3', OH-5'), 6.14 (1H, s, H-3), 5.96 (1H, d, *J* = 2.7 Hz, H-8), 5.80 (1H, t, *J* = 1.9 Hz, H-4'), 5.79 (1H, d, *J* = 2.7 Hz, H-6), 5.72 (2H, d, *J* = 2.1 Hz, H-2', H-6'); ^{13}C NMR (DMSO-*d*$_6$ 150, MHz): δ 123.1 (C-1), 145.9 (C-2), 98.1 (C-3), 141.8 (C-4), 122.2 (C-4a), 142.5 (5a), 93.7 (C-6), 152.9 (C-7), 98.4 (C-8), 146.0 (C-9), 122.6 (9a), 137.1 (10a), 160.3 (C-1'), 93.6 (C-2', C-6'), 158.7 (C-3', C-5'), 96.1 (C-4') (Okada, Ishimaru, Suzuki, & Okuyama, 2004).

3. Dieckol (Brown powder; $C_{36}H_{22}O_{18}$)

   ^{1}H NMR (DMSO-*d*$_6$, 300 MHz): δ 6.16 (1H, s, H-1''), 6.14 (1H, s, H-3), 6.01 (1H, d, *J* = 2.2 Hz, H-8), 6.99 (1H, d, *J* = 2.2 Hz, H-8''), 5.94 (1H, s, H-2''', H-6'''), 5.82 (1H, br d, *J* = 2.7 Hz, H-6), 5.81 (1H, br d, *J* = 2.8 Hz, H-6''), 5.79 (1H, H-4'), 5.71 (1H, br d, H-2', H-6'); ^{13}C NMR (DMSO-*d*$_6$, 75 MHz): δ 160.3 (C-1'), 158.8 (C-2', C-5'), 155.9 (C-1'''), 154.2 (C-7), 153.1 (C-7''), 151.2 (C-3''', C-5'''), 146.1 (C-2), 146.1 (C- 9''), 146.0 (C-9), 145.9 (C-2''), 142.6 (C-5a''), 142.4 (C-5a), 142.0 (C-4''), 141.9 (C-4), 137.2 (C-10a), 137.0 (C-10a''), 124.2 (C-1''), 124.0 (C-9a), 123.2 (C-4a'') 123.1 (C-4), 122.5 (C-9a''), 122.2 (C-1''), 122.1 (C-1) (Cho et al., 2019).

4. Phlorofucofuroeckol A (Brown powder; $C_{30}H_{18}O_{14}$)

   ^{1}H NMR (DMSO-*d*$_6$, 300 MHz): δ 6.72 (1H, s, H-13), 6.43 (1H, s, H-9), 6.30 (1H, s, H-3), 5.83 (2H, br t, *J* = 1.6 Hz, H-4', H-4''), 5.76 (2H, d, *J* = 2.0 Hz, H-2', H-6'), 5.72 (2H, d, *J* = 2.0 Hz, H-2', H-6'); ^{13}C NMR (DMSO-*d*$_6$, 75 MHz): δ 160.2 (C-1'), 160.0 (C-1''), 159.0 (C-3'', C-5''), 158.9 (C-3', C-5'), 150.8 (C-12a), 150.4 (C-10), 149.5 (C-11a), 147.0 (C-2), 146.5 (C-8), 144.8 (C-14), 142.1 (C-4), 136.8 (C-15a), 134.0 (C-5a), 126.3 (C-14a), 122.5

(C-1), 122.4 (C-4a), 120.1 (C-11), 103.4 (C-7), 103.2 (C-6), 99.1 (C-9), 98.3 (C-3), 96.3 (C-4, C-4''), 94.8 (C-13), 93.7 (C-2', C-6'), 93.5 (C-2'', C-6'') (Cho et al., 2019).

5. Dibenzo [1,4]dioxine-2,4,7,9-tetraol (Brown powder; $C_{12}H_7O_6$)

   ^{1}H NMR (DMSO-*d*$_6$, 300 MHz): δ 5.96 (2H, d, *J* = 2.7 Hz, H-3, H-8), 5.78 (2H, d, *J* = 2.7 Hz, H-1, H-6); ^{13}C-NMR (DMSO-*d*$_6$, 75 MHz): δ 152.8 (C-2, C-7), 145.8 (C-4, C-9), 42.8 (C-5a, C-10), 122.9 (C-4a C-9a), 98.3 (C-3, C-8), 93.9 (C-1, C-6) (Cho et al., 2019).

6. Dioxinodehydroeckol (Brown powder; $C_{18}H_9O_9$)

   ^{1}H NMR (DMSO-*d*$_6$, 300 MHz): δ 6.10 (1H, s, H-7), 6.05 (1H, d, *J* = 2.7 Hz, H-2), 6.02 (1H, d, *J* = 2.7 Hz, H-10), 5.84 (1H, d, J = 2.7 Hz, H-4), 5.82 (1H, d, *J* = 2.7 Hz, H-12); ^{13}C NMR (DMSO-*d*$_6$, 75 MHz): δ 153.3 (C-3), 153.0 (C-11), 146.1 (C-1), 145.9 (C-9), 142.0 (C-4a), 141.7 (C-12a), 140.1 (C-6), 137.1 (C-7a), 131.5 (C-13b), 122.6 (C-8), 122.5 (C-13a), 122.2 (C-14a), 98.8 (C-2, C-10), 97.9 (C-7), 93.9 (C-4, C-12) (Cho et al., 2019).

7. Fucofuroeckol A (Brown powder; $C_{24}H_{13}O_{11}$)

   ^{1}H NMR (DMSO-*d*$_6$, 400 MHz) : δ 10.05 (1H, s, OH-14), 9.88 (1H, s, OH-4), 9.76 (1H, s, OH-10), 9.44 (1H, s, OH-2), 9.18 (2H, s, OH-3′, 5′), 8.22 (1H, s, OH-8), 6.71 (1H, s, H-13), 6.47 (1H, d, *J* = 1.1 Hz, H-11), 6.29 (1H, s, H-3), 6.25 (1H, d, *J* = 1.5 Hz, H-9), 5.83 (1H, s, H-4′), 5.76 (2H, d, *J* = 1.5 Hz, H-2′, 6′); ^{13}C NMR (DMSO-*d*$_6$, 100 MHz): δ 160.7 (C-1′), 158.8 (C-3′, 5′), 158.3 (C-11a), 157.6 (C-10), 150.5 (C-12a), 150.2 (C-8), 146.9 (C-2), 144.4 (C-14), 142.0 (C-4), 136.8 (C-15a), 133.6 (C-5a), 126.1 (C-14a), 122.6 (C-4a), 122.4 (C-1), 103.1 (C-6), 102.4 (C-7), 98.2 (C-3), 98.0 (C-9), 96.3 (C-4′), 94.6 (C-13), 93.7 (C-2′, 6′), 90.5 (C-11) (Lee et al., 2016).

8. 974-A (Brown powder; $C_{48}H_{29}O_{23}$)

   ^{1}H NMR (DMSO-*d*$_6$, 300 MHz): δ 6.15 (1H, d, *J* = 2.1 Hz, H-4'), 6.01 (1H, d, *J* = 2.1 Hz, H-6'), 6.26 (1H, s, H-3), 6.72 (1H, s, H-6), 6.44 (1H, s, H-10), 6.73 (2H, d, *J* = 1.8 Hz, H-2'', H-6''), 5.83 (1H, dt, *J* = 1.8, 2.1 Hz, H-4''), 6.11 (1H, d, *J* = 1.2 Hz, H4'''), 5.75 (1H, d, *J* = 1.5 Hz, H-6'''), 5.86 (2H, s, H-3'''', H-5'''') ; ^{13}C-NMR (DMSO-*d*$_6$, 75 MHz): δ 157.9 (C-1'), 120.1 (C-2'), 157.7 (C-3'), 99.2 (C-4'), 158.8 (C-5'), 95.9 (C-6'), 136.9 (C-1), 146.6 (C-2), 103.4 (C-3), 146.1 (C-4), 141.9 (C-4a), 142.4 (C-15a), 145.9 (C-5a), 92.7 (C-6),

153.1 (C-6a), 123.5 (C-13), 144.7 (C-14), 142.0 (C-14a), 150.1 (C-7a), 126.4 (C-8), 150.4 (C-9), 103.3 (C-10), 149.6 (C-11), 122.9 (C-12), 160.3 (C-1"), 96.5 (C-2", C-6"), 160.0 (C-3", C-5"), 98.4 (C-4"), 158.1 (C-1'"), 122.1 (C-2'"), 157.8 (C-3'"), 100.7 (C-4'"), 159.0 (C-5'"), 94.9 (C-6'"), 137.1 (C-1'""), 151.3 (C-2'""), 97.5 (C-3'""), 155.8 (C-4'""), 93.6 (C-5'""), 154.7 (C-6'""), 133.9 (C-1'""'), 150.9 (C-2'""', C-6'""'), 96.9 (C-3'""', C-5'""'), 154.8 (C-4'""') (Cho et al., 2019).

9. 974-B (Light brown powder; $C_{48}H_{29}O_{23}$)

^{1}H NMR (DMSO-*d*$_6$, 600 MHz): δ 6.20 (1H, d, *J* = 2.05 Hz, H-4'), 6.15 (1H, d, *J* = 2.05 Hz, H-6'), 6.17 (1H, s, H-3), 6.69 (1H, s, H-6), 6.38 (1H, s, H-10), 5.87 (2H, d, *J* = 2.06 Hz, H-2", H-6"), 5.91 (1H, t, *J* = 2.05 Hz, H-4"), 6.22 (1H, d, *J* = 2.06 Hz, H-4'"), 5.89 (1H, d, *J* = 2.05 Hz, H-6'"), 6.05 (1H, d, *J* = 2.64 Hz, H-3'""), 5.75 (1H, d, *J* = 2.64 Hz, H-5'""), 6.00 (2H, s, H-3'""', H-5'""') ; ^{13}C-NMR (DMSO-*d*$_6$, 150 MHz): δ 159.0 (C-1'), 102.5 (C-2'), 156.9 (C-3'), 98.4 (C-4'), 159.6 (C-5'), 95.2 (C-6'), 124.0 (C-1), 147.0 (C-2), 99.6 (C-3), 143.9 (C-4), 125.3 (C-4a), 138.0 (C-15a), 142.9 (C-5a), 92.7 (C-6), 152.7 (C-6a), 109.9 (C-13), 138.3 (C-14), 127.4 (C-14a), 150.9 (C-7a), 122.1 (C-8), 151.6 (C-9), 99.5 (C-10), 148.4 (C-11), 106.4 (C-12), 161.9 (C-1"), 95.3 (C-2", C-6"), 160.2 (C-3", C-5"), 97.6 (C-4"), 159.2 (C-1'"), 102.7 (C-2'"), 157.5 (C-3'"), 98.6 (C-4'"), 159.7 (C-5'"), 94.2 (C-6'"), 124.7 (C-1'""), 152.2 (C-2'""), 97.6 (C-3'""), 156.6 (C-4'""), 94.2 (C-5'""), 153.8 (C-6'""), 124.0 (C-1'""'), 152.2 (C-2'""', C-6'""'), 96.5 (C-3'""', C-5'""'), 156.5 (C-4'""') (Yamashita et al., 2013).

10. 7-Phloroeckol (Brown powder; $C_{24}H_{15}O_{12}$)

^{1}H NMR (DMSO-*d*$_6$, 300 MHz): δ 6.14 (s, H-3), 6.00 (1H, d, *J* = 2.9 Hz, H-8), 5.77 (1H, d, *J* = 2.9 Hz, H-6), 5.80 (1H, d, *J* = 1.9 Hz, H-4'), 5.86 (1H, d, *J* = 2.4 Hz, H-2', H-6'); ^{13}C NMR (DMSO-*d*$_6$, 75 MHz): δ 122.2 (C-1), 146.0 (C-2), 98.4 (C-3), 141.9 (C-4), 123.2 (C-4a), 142.9 (C-5a), 93.4 (C-6), 154.6 (C-7), 98.1 (C-8), 146.1 (C-9), 124.0 (C-9a), 137.1 (C-10a), 160.3 (C-1'), 93.6 (C-2'), 159.0 (C-3'), 96.3 (C-4'), 159.0 (C-5'), 93.7 (C-6'), 122.9 (C-1"), 151.3 (C-2"), 94.9 (C-3"), 154.9 (C-4"), 94.9 (C-5"), 151.3 (C-6") (Cho et al., 2019).

11. 6,6'-Bieckol (Brown powder; $C_{36}H_{21}O_{18}$)

^{1}H NMR (DMSO-*d*$_6$, 300 MHz): δ 6.09 (s, H-3), 6.04 (1H, s, H-8), 5.80 (1H, d, *J* = 1.8 Hz, H-4'), 5.74 (1H, d, *J* = 2.1 Hz, H-2', H-6'); ^{13}C NMR (DMSO-*d*$_6$, 75 MHz): δ 160.5 (C-1'),

158.9 (C-3', C-5), 151.3 (C-7), 145.4 (C-2), 144.5 (C-9), 141.9 (C-4), 141.4 (C-5a), 137.2. (C-10), 123.6 (C-1), 122.7 (C-9a), 122.0 (C-4a), 99.7 (C-6), 97.8 (C-8), 97.8 (C-3), 96.2 (C-4'), 93.7 (C-2', C-6') (Cho et al., 2019).

12. Dibenzodioxin-fucodiphloroethol (Brown powder; $C_{36}H_{23}O_{18}$)

^{1}H NMR (DMSO-d_6, 800 MHz): δ 9.19 (1H, brs, OH-6''), 9.11 (1H, brs, OH-7), 9.05 (1H, brs, OH-6'''), 8.98 (2H, brs, OH-4''', OH-6'''), 8.89 (1H, brs, OH-4''''), 8.88 (1H, brs, OH-4''), 6.12 (2H, s, H-3, H-5''), 6.09 (1H, brs, H-6'), 5.99 (1H, d, J = 1.5 Hz, H-2'), 5.97 (1H, d, J = 2.7 Hz), 5.89 (1H, d, J = 2.7 Hz, H-5'''), 5.86 (2H, s, H-3'''', H-5''''), 5.81 (1H, d, J = 2.7 Hz, H-6), 5.70 (1H, d, J = 1.5 Hz, H-3''), 5.54 (1H, d, J = 2.7 Hz, H-3'''); ^{13}C NMR (DMSO-d_6, 200 MHz): δ 122.6 (C-1), 144.7 (C-2), 98.1 (C-3), 142.2 (C-4), 123.3 (C-4a), 137.2 (C-10a), 142.4 (C-5a), 93.7 (C-6), 153.1 (C-7), 98.5 (C-8), 146.1 (C-9), 122.6 (C-9a), 157.9 (C-1'), 94.7 (C-2'), 157.7 (C-3'), 100.7 (C-4'), 158.1 (C-5'), 96.8 (C-6'), 101.4 (C-1''), 155.7 (C-2''), 93.8 (C-3''), 157.7 (C-4'', C-6''), 97.3 (C-5''), 123.5 (C-1'''), 150.0 (C-2'''), 92.7 (C-3'''), 153.1 (C-4'''), 95.8 (C-5'''), 154.7 (C-6'''), 122.1 (C-1''''), 151.2 (C-2'''', C-6''''), 94.9 (C-3'''', C-5''''), 154.7 (C-4'''') (Cho et al., 2019).

13. Dibenzodioxin-fucodiphloroeckol (Brown powder; $C_{54}H_{33}O_{27}$)

^{1}H NMR (DMSO-d_6, 850 MHz): δ 5.74 (2H, d, J = 1.8 Hz, H-2', H-6'), 5.81 (1H, brt, H-4'), 5.92 (1H, s, H-3), 5.88 (1H, d, J = 2.2 Hz, H-6), 6.01 (1H, d , J = 2.2 Hz, H-8), 5.87 (2H, s, H-3'', H-5''), 5.55 (1H, d, J = 2.4 Hz, H-3'''), 5.89 (1H, d, J = 2.4 Hz, H-5'''), 5.71 (1H, brs, H-3''''), 6.14 (1H, brs, H-5''''), 6.00 (1H, brs, H-3''''''), 6.11 (1H, brs, H-5''''''), 6.21 (1H, s, H-5'''''), 6.14 (1H, s, H-4'''''''); ^{13}C NMR (DMSO-d_6, 212.5 MHz) : δ 160.1 (C-1'), 158.9 (C-3', C-5'), 157.9 (C-2''''), 157.8 (C-4''''), 157.8 (C-4''''''), 155.7 (C-6''''), 154.8 (C-6'''), 154.7 (C-4''), 153.2 (C-7), 153.1 (C-4'''), 151.3 (C-2'', C-6''), 150.1 (C-2'''), 146.2 (C-9), 145.9 (C-6'''''), 145.8 (C-2), 143.1 (C-4), 142.6 (C-4'''''), 142.3 (C-5a), 137.2 (C-10a), 136.7 (C-2'''''), 123.8 (C-4a), 123.7 (C-1), 123.5 (C-1'''), 122.9 (C-3'''''), 122.5 (C-9a), 122.1 (C-1''), 121.4 (C-1'''''), 101.5 (C-1''''), 100.7 (C-1''''''), 98.7 (C-8), 98.4 (C-5'''''), 98.3 (C-4'''''), 97.5 (C-5''''), 96.8 (C-5''''''), 96.4 (C-4'), 95.9 (C-5'''), 95.8 (C-3), 94.9 (C-3'', C-5''), 94.9 (C-3''''), 93.9 (C-6), 93.7 (C-2', C-6'), 93.5 (C-3''''), 92.7 (C-3''') (Cho et al., 2019).

14. Eckmaxol (Brown powder; $C_{36}H_{24}O_{18}$)

^{1}H NMR ($CDOD_3$, 500 MHz): δ 6.11 (1H, d, J = 2.4 Hz, H-3), 5.86 (1H, d, J = 2.4 Hz, H-5), 6.20 (1H, s, H-10), 6.01 (1H, d, J = 2.4 Hz, H-14), 5.94 (1H, d, J = 2.4 Hz, H-16), 5.93 (1H, d, J = 2.4 Hz, H-20), 6.32 (1H, d, J = 2.4 Hz, H-22), 6.20 (1H, d, J = 2.0 Hz, H-27), 6.28 (1H, d, J = 2.0 Hz, H-29), 6.03 (1H, s, H-33), 6.03 (1H, s, H-35); ^{13}C NMR ($CDOD_3$, 125 MHz): δ 159.3 (C-28), 159.2 (C-21), 158.7 (C-15), 158.5 (C-30), 157.1 (C-19), 156.4 (C-4), 156.1 (C-26, C-34), 154.4 (C-6), 153.4 (C-13), 151.6 (C-32, C-36), 151.3 (C-2), 146.7 (C-17), 146.3 (C-11), 143.5 (C-9), 143.3 (C-23), 137.7 (C-8), 124.8 (C-1), 124.7 (C-12), 124.0 (C-31), 123.8 (C-18), 123.5 (C-7), 102.0 (C-24), 101.8 (C-25), 99.3 (C-14), 98.9 (C-10), 98.7 (C-22), 98.3 (C-29), 97.6 (C-3), 96.1 (C-33, C-35), 95.2 (C-16, C-27), 94.7 (C-5), 94.2 (C-20) (Zhou, Yi, Ding, He, & Yan, 2019).

15. Diphlorethohydroxycarmalol ($C_{24}H_{16}O_{13}$)

^{1}H NMR (DMSO-d_6, 500 MHz): δ 6.06 (1H, s, H-6), 5.87 (2H, s, H-3', H-5'), 5.78 (1H, t, J = 2.0 Hz, H-4''), 5.69 (1H, s, H-4), 5.67 (2H, d, J = 2.0 Hz, H-2'', H-6''); ^{13}C NMR (DMSO-d_6, 125 MHz): δ 160.1 (C-1''), 158.9 (C-3'', C-5''), 154.9 (C-4'), 151.3 (C-2', C-6'), 146.0 (C-5a), 143.0 (C-4a), 139.6 (C-6), 138.8 (C-7), 135.1 (C-1), 133.8 (C-3), 130.7 (C-10a), 126.4 (C-9a), 125.5 (C-2), 124.1 (C-8), 122.9 (C-1'), 96.1 (C-4''), 95.0 (C-3', C-5'), 94.3 (C-9), 93.7 (C-2'', C-6''), 92.4 (C-4) (Heo et al., 2008).

16. 8,8′-bieckol ($C_{36}H_{12}O_{18}$)

^{1}H NMR (DMSO-d_6, 400 MHz): δ 6.17 (1H, s, H-3), 5.97 (1H, s, H-6), 5.75 (1H, d, J = 2.1 Hz, H-2', H-6'), 5.81 (1H, t, J = 2.1 Hz, H-4'); ^{13}C NMR (DMSO-d_6, 100 MHz): δ 160.5 (C-1'), 158.8 (C-3', C-5'), 151.8 (C-7), 146.2 (C-2), 144.6 (C-9), 141.9 (C-4), 141.5(C-5a), 137.3 (C-10a), 123.5 (C-1), 123.3 (C-9a), 122.7 (C-4a), 104.5 (C-8), 98.4 (C-3), 96.5(C-4'), 94.1 (C-2', C-6'), 94.0 (C-6) (Fukuyama et al., 1989).

17. 6,8′-bieckol ($C_{36}H_{12}O_{18}$))

^{1}H NMR (DMSO-d_6, 500 MHz): δ 6.02 (H-3), 6.15 (H-8), 6.06 (H-3'), 5.94 (H-6'), 5.71 (H-2'', H-6''), 5.78 (H-4''), 5.74 (H-2''', H-6'''), 5.78 (H-4'''); ^{13}C NMR (DMSO-d_6, 125 MHz): δ 160.4(C-1''), 160.4 (C-1'''), 158.7 (C-3'',C- 5''), 158.7 (C-3''', C-5'''), 151.5 (C-7), 151.5 (C-7'), 145.8 (C-2), 145.4 (C-2'), 144.8 (C-9), 144.3 (C-9'), 141.9 (C-4), 141.8 (C-4'), 141.6 (C-5a), 140.9 (C-5a'), 137.3 (C-10a), 137.2 (C-10a'), 123.6 (C-1), 123.4 (C-1'),

123 (C-9a), 122.9 (C-9a'), 122.4 (C-4a), 122 (C-4a'), 104.5(C-8'), 99.5 (C-6), 98.2 (C-8), 97.9 (C-3), 97.9 (C-3'), 96.3 (C-4"), 96.2 (C-4'"), 93.9 (C-2'", C-6'"), 93.7 (C-2", C-6"), 93.6 (C-6') (Sugiura et al., 2007).

18. Phlorofucofuroeckol B (Brown yellow oil; $C_{30}H_{18}O_{14}$)

^{1}H NMR (DMSO-d_6, 400 MHz): δ 6.19 (H-3), 6.75 (H-6), 6.48 (H-10), 5.76 (H-2′), 5.82 (H-4′), 5.76 (6′), 5.71 (H-2″), 5.82 (H-4″), 5.71 (6″); ^{13}C NMR (100 MHz, DMSO-d_6): δ 122.2 (C-1), 146.3 (C-2), 98.6 (C-3), 142.0 (C-4), 123.0 (C-4a), 141.4 (C-5a), 91.5 (C-6), 150.3 (C-6a), 149.2 (C-7a), 120.4 (C-8), 150.4 (C-9), 98.6 (C-10), 145.5 (C-11), 104.9 (C-12), 108.0 (C-13), 137.2 (C-14), 125.8 (C-14a), 136.7 (C-15a), 160.3 (C-1′), 93.7 (C-2′), 93.7 (6′), 158.9 (C-3′), 96.5 (C-4′), 158.9 (5′), 159.9 (C-1″), 93.5 (C-2″), 159.0 (C-3″), 96.3 (C-4″), 159.0 (5″), 93.5 (6″) (Sugiura et al., 2007).

19. Fucodiphloroethol G (Off-white powder; $C_{24}H_{18}O_{12}$)

^{1}H NMR (DMSO-d_6, 400 MHz): δ 5.83 (1H, d, J = 2.8 Hz, H-3), 5.52 (1H, d, J = 2.8 Hz, H-5), 5.84 (2H, br s, H-3′, H-5′), 5.98 (1H, d, J = 2.3 Hz, H-4″), 5.85 (1H, d, J = 2.3 Hz, H-6″), 5.90 (2H, br s, H-3‴, H-5‴), 9.11 (3H, s, OH-2, OH-2′, OH- 6′), 8.99 (1H, s, OH-4), 8.93 (2H, s, OH-4, 6‴), 8.95 (2H, s, OH-3″, OH-5″), 8.57 (1H, s, OH-2‴), 8.47 (1H, s, OH-4‴); ^{13}C NMR (DMSO-d_6, 100 MHz): δ 157.8 (C-5″), 157.2 (C-3″, C-4‴), 157.1 (C-2‴, C-6‴), 156.5 (C-1″), 154.6 (C-4′), 154.5 (C-2), 153 (C-4), 151.1 (C-2′, C-6′), 150.3 (C-6), 123.3 (C-1), 121.9 (C-1′), 101.6 (C-2″), 101.0 (C-1‴), 96.8 (C-4″), 95.7 (C-3), 94.7 (C-3′, C-5′, C-3‴, C-5‴), 93.3 (C-6″), 92.3 (C-5) (Li, Lee, Le, Kim, & Kim, 2008).

20. 2-Phloroeckol ($C_{24}H_{16}O_{12}$)

^{1}H NMR (DMSO-d_6, 400 MHz): δ 5.80 (H-3), 5.82 (H-6), 5.96 (H-8), 5.86 (H-2′), 5.84 (H-4′), 5.86 (6′), 5.84 (H-3″), 5.84 (5″); ^{13}C NMR (DMSO-d_6, 100 MHz): δ 123.0 (C-1), 148.1 (C-2), 96.4 (C-3), 142.0 (C-4), 124.7 (C-4a), 142.9 (C-5a), 94.3 (C-6), 153.5 (C-7), 99.1 (C-8), 146.5 (C-9), 123.0 (9a), 137.5 (C-10a), 160.7 (C-1′), 94.5 (C-2′), 159.2 (C-3′), 96.8 (C-4′), 159.2 (C-5′), 94.5 (C-6′), 122.4 (C-1″), 151.6 (C-2″), 95.3 (C-3″), 155.1 (C-4″), 95.3 (5″), 151.6 (6″) (Lee et al., 2012) .

21. Trifuhalol A ($C_{18}H_{14}O_{10}$)

^{1}H NMR (CD_3OD, 600 MHz): δ 5.89 (2H, d, J = 2.6 Hz), 5.90 (2H, s), 5.92 (2H, s); ^{13}C NMR (CD_3OD, 150 MHz): δ 95.54 (2C, CH), 95.54 (2C, CH), 98.11 (2C, CH), 125.13 (1C, C), 125.78 (1C, C), 147.99 (1C, C), 152.48 (2C, C), 152.62 (2C, C), 152.71 (2C, C), 158.77 (1C, C), 158.78 (1C, C), 160.75 (1C, C) (Phasanasophon & Kim, 2018).

22. Trifucodiphlorethol A (Brown solid; $C_{36}H_{26}O_{18}$)

^{1}H NMR (MeOD, 300 MHz): δ 6.03 (2H, s, H-2, H-6), 6.11 (4H, s, H-15, H-17), 6.01 (4H, s, H-21, H-23); ^{13}C NMR (MeOD, 75 MHz): δ 160.1 (C-1), 162.1 (C-16), 158.7 (C-14, C-18), 158.4 (C-3, C-5), 158.3 (C-8, C-12), 158.1 (C-10), 156.3 (C-22), 152.3 (C-20, C-24), 124.8 (C-19), 101.2 (C-13), 99.7 (C-4), 99.4 (C-7), 99.4 (C-9, C-11), 96.3 (C-21, C-23), 95.8 (C-2, C-6), 95.4 (C-15, C-17) (Parys et al., 2010).

23. Trifucotriphlorethol A (Brown solid; $C_{42}H_{30}O_{21}$)

^{1}H NMR (MeOD, 300 MHz): δ 6.02 (2H, s, H-2, H-6), 6.25 (2H, s, H-15, H-17), 5.80 (1H, d, J = 2.5 Hz, H-21), 6.11 (1H, d, J = 2.5 Hz, H-23), 5.95 (2H, s, H-27, H-29), 6.11 (2H, s, H-33, H-35), 5.99 (2H, s, H-39, H-41); ^{13}C NMR (MeOD, 75 MHz): δ 160.0 (C-1), 162.2(C-16), 162.1 (C-34), 158.8 (C-32, C-36), 158.7(C-3, C-5), 158.4 (C-8, C-12), 158.3 (C-14, C-18), 158 (C-10), 156.4 (C-28), 156.3 (C-40), 156.2 (C-22), 154.0 (C-20), 152.5 (C-24), 152.3 (C-38, C-42), 152.2 (C-26, C-30), 125.4 (C-19), 124.8 (C-37), 124.7 (C-25), 101.4 (C-31), 101.1 (C-13), 99.9 (C-4), 99.4 (C-7), 99.4 (C-9, C-11), 97.9 (C-23), 96.3 (C-27, C-29), 96.2 (C-39, C-41), 95.8 (C-2, C-6), 95.8 (C-15, C-17), 95.4 (C-33, C-35), 94.9 (C-21) (Parys et al., 2010).

24. Fucotriphlorethol A (Brown solid; $C_{30}H_{22}O_{15}$)

^{1}H NMR (MeOD, 300 MHz): δ 6.11 (2H, s, H-2, H-6), 6.01 (2H, s, H-9, H-11), 6.11 (2H, s, H-15, H-17), 6.09 (2H, s, H-21, H-23), 5.99 (2H, s, H-27, H-29); ^{13}C NMR (MeOD, 75 MHz): δ 161.3 (C-1), 159.5 (C-10), 158.6 (C-3, C-5), 158.2 (C-8, C-12), 158.0 (C-22), 157.8 (C-16), 156.3 (C-28), 152.5 (C-26, C-30), 152.3 (C-20, C-24), 152.2 (C-14, C-18), 126.1 (C-13), 126.1 (C-19), 124.9 (C-25), 102.1 (C-4), 100.5 (C-7), 96.2 (C-9, C-11), 96.2 (C-27, C-29), 96.0 (C-2, C-6, C-21, C-23), 95.5 (C-15, C-17) (Parys et al., 2010).

25. 2,7″-Phloroglucinol-6,6′-bieckol

^{1}H NMR (DMSO-d_6, 500 MHz): δ 5.57 (1H, s, H-3), 5.89 (1H, s, H-8), 5.74 (1H, m, H-2′), 5.84 (1H, m, H-4′), 5.74 (1H, m, H-6′), 6.25 (1H, s, H-3″), 6.14 (1H, m, H-8″), 5.84 (1H, m, H-2‴), 6.52 (1H, s, H-2⁗), 6.14 (1H, m, H-4⁗), 6.44 (1H, m, H-6⁗), 6.77 (1H, s, H-3⁗′), 6.72 (1H, s, H-5⁗′), 8.93 (1H, s, OH-4, OH-7), 9.19 (1H, s, OH-3′, OH-5′, OH-2″), 9.04 (1H, s, OH-4″), 8.26 (1H, s, OH-9″), 9.94 (1H, OH-3‴), 8.59 (1H, s, OH-5‴), 9.88 (1H, s , OH-3⁗′), 9.86 (1H, s, OH-5⁗′), 9.25 (1H, s, OH-2⁗′), 9.75 (1H, s, OH-4⁗′), 9.21 (1H, s, OH-6⁗′); ^{13}C NMR (DMSO-d_6, 125 MHz): δ 162 (C-1′), 160.5 (C-5′), 160.3(C-3′), 159.8 (C-1⁗′), 159.7 (C-1‴), 159.3 (C-3‴, C-3⁗′, C-2⁗′), 159.2 (C-5⁗′), 157.1 (C-5‴), 156.8 (C-4⁗′), 152.8 (C-6⁗′), 152.4 (C-9), 152.2 (C-7), 151.8 (C-9″), 147.2 (C-5a, C-2″), 147.2 (C-5a″), 144.1 (C-4″, C-7″, C-10a″), 143.0 (C-2), 137.2 (C-9a″), 137.1 (C-10a), 127.6 (C-1, C-9a), 125.6 (C-4a), 124.3 (C-1″, C-4a″),122.5 (C-1⁗′), 110.0 (C-6″), 106.5 (C-6), 101.5 (C-8″), 99.9 (C-5⁗′), 99.8 (C-3⁗′), 98.8 (C-6′), 98.7 (C-2′), 97.9 (C-6⁗′), 97.8 (C-2⁗′), 96.7 (C-2‴, C-6‴), 95.5 (C-8, C-4′, C-4‴), 95.2 (C-4⁗′), 94.5(C-3″), 93.0 (C-3) (Kang, Heo, Kim, Lee, & Jeon, 2012).

References

Cho, H. M., Doan, T. P., Ha, T. K. Q., Kim, H. W., Lee, B. W., Pham, H. T. T., et al. (2019). Dereplication by high-performance liquid chromatography (HPLC) with quadrupole-time-of-flight mass spectroscopy (qTOF-MS) and antiviral activities of phlorotannins from *Ecklonia cava*. *Marine Drugs, 17*(3), 149.

Fukuyama, Y., Kodama, M., Miura, I., Kinzyo, Z., Mori, H., Nakayama, Y., et al. (1989). Anti-plasmin Inhibitor. V.: Structures of novel dimeric eckols isolated from the brown alga *Ecklonia kurome* Okamura. *Chemical and Pharmaceutical Bulletin, 37*(9), 2438-2440.

Hattori, M., Shu, Y.Z., El-Sedawy, A. I., Namba, T., Kobashi, K., & Tomimori, T. (1988). Metabolism of homoorientin by human intestinal bacteria. *Journal of Natural Products, 51*(5), 874-878.

Heo, S. J., Kim, J. P., Jung, W. K., Lee, N. H., Kang, H. S., Jun, E. M., et al. (2008). Identification of chemical structure and free radical scavenging activity of diphlorethohydroxycarmalol isolated from a brown alga, *Ishige okamurae*. *Journal of Microbiology And Biotechnology, 18*(4), 676-681.

Kang, S.M., Heo, S.J., Kim, K.N., Lee, S.H., & Jeon, Y.J. (2012). Isolation and identification of new compound, 2, 7 ″-phloroglucinol-6, 6′-bieckol from brown algae, *Ecklonia cava* and its antioxidant effect. *Journal of Functional Foods, 4*(1), 158-166.

Lee, M. S., Shin, T., Utsuki, T., Choi, J. S., Byun, D. S., & Kim, H. R. (2012). Isolation and identification of phlorotannins from *Ecklonia stolonifera* with antioxidant and hepatoprotective properties in tacrine-treated HepG2 cells. *Journal of Agricultural and Food Chemistry, 60*(21), 5340-5349.

Lee, S.H., Eom, S.H., Yoon, N.Y., Kim, M.M., Li, Y.X., Ha, S. K., et al. (2016). Fucofuroeckol-A from *Eisenia bicyclis* inhibits inflammation in lipopolysaccharide-induced mouse macrophages via downregulation of the MAPK/NF-κB Signaling Pathway. *Journal of Chemistry, 2016*.

Li, Y., Lee, S.H., Le, Q.T., Kim, M.M., & Kim, S.K. (2008). Anti-allergic effects of phlorotannins on histamine release via binding inhibition between IgE and FcεRI. *Journal of Agricultural and Food Chemistry, 56*(24), 12073-12080.

Okada, Y., Ishimaru, A., Suzuki, R., & Okuyama, T. (2004). A new phloroglucinol derivative from the brown alga *Eisenia bicyclis*: potential for the effective treatment of diabetic complications. *Journal of natural products*, *67*(1), 103-105.

Parys, S., Kehraus, S., Krick, A., Glombitza, K.W., Carmeli, S., Klimo, K., et al. (2010). In vitro chemopreventive potential of fucophlorethols from the brown alga *Fucus vesiculosus* L. by anti-oxidant activity and inhibition of selected cytochrome P450 enzymes. *Phytochemistry*, *71*(2-3), 221-229.

Phasanasophon, K., & Kim, S. M. (2018). Antioxidant and cosmeceutical activities of *Agarum cribrosum* phlorotannin extracted by ultrasound treatment. *Natural Product Communications*, *13*(5), 565-570.

Sugiura, Y., Matsuda, K., Yamada, Y., Nishikawa, M., Shioya, K., Katsuzaki, H., et al. (2007). Anti-allergic phlorotannins from the edible brown alga, *Eisenia arborea*. *Food Science and Technology Research*, *13*(1), 54-60.

Yotsu Yamashita, M., Kondo, S., Segawa, S., Lin, Y. C., Toyohara, H., Ito, H., et al. (2013). Isolation and structural determination of two novel phlorotannins from the brown alga *Ecklonia kurome* Okamura, and their radical scavenging activities. *Marine Drugs*, *11*(1), 165-183.

Zhou, X., Yi, M., Ding, L., He, S., & Yan, X. (2019). Isolation and purification of a neuroprotective phlorotannin from the marine algae *Ecklonia maxima* by size exclusion and high-speed counter-current chromatography. *Marine Drugs*, *17*(4), 212.

Statement of Authorship

Title of Paper	*Ecklonia radiata* extract containing eckol protects neuronal cells against $A\beta_{1-42}$ evoked toxicity and reduces aggregate density
Publication Status	☑ Published ☐ Accepted for Publication ☐ Submitted for Publication ☐ Unpublished and Unsubmitted work written in manuscript style
Publication Details	Shrestha, S., Zhang, W., Begbie, A. J., Pukala, T. L., Smid, S. D. (2020). *Ecklonia radiata* extract containing eckol protects neuronal cells against $A\beta_{1-42}$ evoked toxicity and reduces aggregate density. Food & Function, 11, 6509-6516.

Principal Author

Name of Principal Author (Candidate)	Srijan Shrestha		
Contribution to the Paper	Conceptualization, Investigation, Formal analysis, Data curation, Methodology, Writing- original draft.		
Overall percentage (%)	70%		
Certification:	This paper reports on original research I conducted during the period of my Higher Degree by Research candidature and is not subject to any obligations or contractual agreements with a third party that would constrain its inclusion in this thesis. I am the primary author of this paper.		
Signature		Date	17/05/2022

Co-Author Contributions

By signing the Statement of Authorship, each author certifies that:

i. the candidate's stated contribution to the publication is accurate (as detailed above);

ii. permission is granted for the candidate in include the publication in the thesis; and

iii. the sum of all co-author contributions is equal to 100% less the candidate's stated contribution.

Name of Co-Author	Dr. Alexander Begbie		
Contribution to the Paper	Data Curation, Methodology, software		
Signature		Date	01/06/2022

Name of Co-Author	Dr. Tara L Pukala		
Contribution to the Paper	Data interpretation, Writing-review and editing, software		
Signature		Date	27/05/2022

Name of Co-Author	Dr. Wei Zhang		
Contribution to the Paper	Conceptualization, Resources, Methodology, Supervision, Writing-review, and editing		
Signature		Date	31/05/2022

Name of Co-Author	Dr. Scott Smid
Contribution to the Paper	Conceptualization, Funding acquisition, Formal analysis, Resources, Supervision, Writing-review, and editing.

Signature			Date	21-6-22

Chapter 2. *Ecklonia radiata* extract containing eckol protects neuronal cells against $A\beta_{1–42}$ evoked toxicity and reduces aggregate density

Srijan Shrestha,[a] Wei Zhang,[b,c] Alexander J. Begbie,[d] Tara L. Pukala,[d] and Scott D. Smid[a]

[a.]Discipline of Pharmacology, Adelaide Medical School, Faculty of Health Sciences, The University of Adelaide, Adelaide, South Australia, Australia;

[b.]Centre for Marine Bioproducts Development (CMBD), and [c.]Medical Biotechnology, College of Medicine and Public Health, Flinders University, GPO Box 2100, Adelaide 5001, South Australia, Australia; Medical Biotechnology, College of Medicine and Public Health, Flinders University, GPO Box 2100, Adelaide 5001, South Australia, Australia;

[d.]Discipline of Chemistry, Faculty of Sciences, The University of Adelaide, Adelaide, South Australia, Australia;

Food & Function., 2020, 11, 6509-6516; DOI: 10.1039/D0FO01438A

Abstract

Brown seaweed (Phaeophyceae) polyphenolics such as phlorotannins are ascribed various biological activities, including neuroprotection. Of these seaweeds, *Ecklonia radiata* (*E. radiata*) is found abundantly along South Australian coastal regions; however it has not been explored for various biological activities relative to any component phlorotannins previously ascribed neuroprotective capacity. In the present study, we evaluated neuroprotective activity against the neurotoxic amyloid β protein ($A\beta_{1\text{-}42}$) of an ethanol extract of *E. radiata* compared with various additional solvent-solubilised fractions in a neuronal PC-12 cell line. The ethyl acetate fraction comprising 62% phlorotannins demonstrated the most efficacious neuroprotective activity, inhibiting neurotoxicity at all $A\beta_{1\text{-}42}$ concentrations. In addition, this fraction demonstrated a significant reduction in Aβ aggregate density but did not alter overall aggregate morphology. Centrifugal partitioning chromatography was used to isolate the major component, eckol, in high yield and liquid chromatography-mass spectrometry was used to characterize the major components of the ethyl acetate fraction. Our results demonstrate that the prevalence of eckol-type phlorotannins are associated with neuroprotective bioactivity of *E. radiata*, suggestive of potential nutraceutical and biopharmaceutical uses of this brown seaweed phlorotannin in dementia treatment.

Introduction

Alzheimer's disease (AD) is the most prominent neurodegenerative disease contributing to dementia in the ageing population, which is characterized by progressive memory loss and cognitive decline. Accumulation of extracellular amyloid beta (Aβ) plaques in the brain and intracellular neurofibrillary tangles are the pathological hallmarks of AD.[1] Aβ plaques, soluble Aβ oligomers and protofibrillar forms interfere with normal neuronal cell function by disrupting synaptic signaling at neural junctions, with their accumulation leading to neuronal toxicity. Therefore, studies have been directed towards the Aβ peptides as a potential target for AD.[2] In particular, small molecule compounds that can disrupt the aggregatory properties or rescue neuronal cells from Aβ toxicity are considered as potential disease-modifying therapeutics.

A wide range of naturally-occurring polyphenolic compounds (e.g. epigallocatechin gallate, curcumin, resveratrol and flavonoids) have shown anti-Aβ aggregation properties via increasing the stability of amyloid peptide in the native state, inhibiting the formation of toxic oligomers, disassembling toxic Aβ species and inhibiting toxic Aβ oligomers interacting with cell membranes.[3, 4] Sodium oligomannate (GV-971) from brown algae has been identified as a potential drug for the treatment of AD[5], being recently approved by China's National Medical Product Administration (NMPA). This underscores the important role of bioprospecting and natural product-derived small molecules in providing potential breakthrough medicines for conditions such as AD, which have proven refractory to new drug development for nearly two decades.[5]

Ecklonia radiata (C. Ag.) J. Agardh (Phaeophyceae) is a small kelp found abundantly in the warm-temperate parts of southern South Africa, Australia and New Zealand[6] and the most abundant seaweed species in South Australia.[7] In relation to neuroprotective components, *Ecklonia* extract

and its components, especially phlorotannins, were reported to have antioxidant, anti-inflammatory, anti-cholinesterase, anti-BACE1 and anti-Aβ aggregatory properties.[8-16] Extensive research has been previously performed on the chemical profiling and biological activity of *Ecklonia* species. However, there are very few studies regarding *Ecklonia radiata* and none relating to the chemical constituents of this particular species.[17-19] A recent study demonstrated the neuroprotective activity of *Ecklonia radiata* without identifying chemical components attributable to neuroprotection, although specific neuroprotective and anti-Aβ aggregatory properties have been previously ascribed to the phlorotannin-rich extracts predominant in *Ecklonia*.[11, 20] Therefore, further investigation on *E. radiata* was warranted to correlate neuroprotective bioactivity ascribed to any specific constituents, where previously bioactivity was defined only on a predominant compound class based within extract fractions.[21] In this study, we investigated the effects of an ethanolic extract and other solvent soluble fractions of *Ecklonia radiata* on neuroprotection against $A\beta_{1-42}$ toxicity in semi-differentiated PC-12 cells, including anti-aggregation properties against $A\beta_{1-42,}$ and identified major phlorotannins in the extracts associated with neuroprotection via high performance centrifugal partitioning chromatography (HPCPC) and LC-MS/MS.

Materials and methods

Reagent and chemicals

Human amyloid beta protein ($A\beta_{1-42}$) was obtained from rPeptide (Bogart, Georgia, USA). 3-(4,5-dimethylthiazol-2-yl)-2,5-diphenyltetrazolium bromide (MTT, 97.5%), Roswell Park Memorial Institute 1640 (RPMI) media, trypan blue, DMSO, non-essential amino acids (NEAA), penicillin/streptomycin, trypsin EDTA, foetal bovine serum (FBS), phosphate buffered saline (PBS) and phloroglucinol were purchased from Sigma-Aldrich (NSW, Australia). DMSO-d6 was obtained from Cambridge Isotope Laboratories Inc (D99.9%, MA, USA).

Plant material

Brown seaweed (*Ecklonia radiata*) was identified by the State Herbarium of South Australia and was collected from freshly deposited beach-cast seaweed in Rivoli bay, Beachport, South Australia in March 2019. It was rinsed with fresh water and dried in oven at 50 ˚C for 24 hours, blended (Blendtec, Orem, UT, USA) and sieved (< 0.5 mm) to maintain consistent particle size.

Extraction and fractionation of extract

The powdered sample (900 g) was extracted with 80% ethanol (24 h × 3 times) at room temperature. The supernatant was filtered (Whatman 1) and concentrated *in vacuo* at 40 °C before final freeze drying (Ex = 177.91 g). The extract was re-suspended in water and defatted with hexane. The resultant solution was fractionated with ethyl acetate and butanol to provide an ethyl acetate soluble fraction (EA = 8.9 g), butanol soluble fraction (B = 22.4 g) and water residue (H = 50.1 g), respectively (Supplement, Figure 1) All final drying was performed using a freeze dryer (VirTis benchtop SP Industries Inc, USA).

Preparation and separation using high performance centrifugal partition chromatography (HPCPC)

The HPCPC experiment was performed by using a biphasic system comprising of *n*-hexane/ethyl acetate/methanol/water (2:8:2:8, v/v/v/v). The two phases were mixed vigorously then equilibrated and finally separated at room temperature. The upper organic phase was used as a stationary phase while the lower aqueous phase was employed as the mobile phase.

The HPCPC column was filled with organic stationary phase and rotated at 800 rpm, then the mobile aqueous phase was pumped into the column in the descending mode at a flow rate of 2 mL/min. Hydrodynamic equilibrium was maintained initially (mobile phase emerged from column) before the injection. The powdered ethyl acetate fraction (500 mg) was dissolved in 6 mL

(1:1, v/v) biphasic system and injected through the injection valve. UV detection was set at 290 nm and fractions collected by automatic fraction collector (each 6mL). The final sample was recovered by changing the mode from descending to ascending following the reverse solvent system. NMR spectra of the pure compound were collected at 600 MHz (^{1}H) and 150 MHz (^{13}C) on Bruker Avance III NMR Spectrometer. Chemical shift is reported in ppm and coupling constants in Hz.

Ion mobility mass spectrometry (IMMS) and HPLC quadrupole-time-of flight mass spectroscopy (HPLC-qTOF-MS) analysis of extract

Ion mobility mass spectra were acquired for separated fractions using an Agilent 6560 Ion Mobility Q-TOF mass spectrometer (California, USA). Mass spectra were collected in offline negative ion mode using nanoESI from platinum-coated borosilicate capillaries prepared in-house. Typical instrument parameters included a capillary voltage of 1700 V, fragmentor voltage of 50 V, gas temperature of 75 °C, gas flow of 1.5 L/min, trap fill time of 10,000 μs, and trap release time of 2000 μs.

An Agilent Infinity 1290 II (California, USA) LC system was used for HPLC-qTOF-MS. Sample was separated on a Phenomenex Jupiter C18 column, 50 x 2.0 mm 5 uM, 300 Å, fitted with a peptide map guard column, 2.1 x 5 mm 2.7 uM (Phenomenex, CA, USA) using a elution gradient as specified by Lopes *et al*.[22] The ionization conditions were adjusted to 350 °C and 3.5 kV for capillary temperature and voltage, respectively. The nebulizer pressure and flow rate of nitrogen were 65.0 psi and 11 L/min, respectively. Collision-induced fragmentation experiments were performed using helium as the collision gas, with voltage ramping at 5 V intervals. Mass spectrometry data were acquired in the negative ionization mode. Mass spectra were analyzed

using Agilent Masshunter Qualitative Analysis B.06.00 and ion mobility spectra using Agilent Masshunter IM-MS Browser.

Total phlorotannin content

The total phlorotannin content of the samples was quantified according to a previous method.[23] Briefly, 0.1 mL of sample or standard was added to 0.5 mL Folin-Ciocalteu reagent (10 % w/v). After 5 minutes, 0.4 mL of sodium carbonate was added and the absorbance measured at 725 nm after 1 hour of incubation in the dark at room temperature. The calibration curve was prepared by using a range of known concentrations (0-100μM) of phloroglucinol. The TPC was expressed as a phloroglucinol equivalents (PGE).

Preparation of $A\beta_{1-42}$

Native, non-fibrillar $A\beta_{1-42}$ was prepared by dissolving dry $A\beta_{1-42}$ in DMSO to yield a protein concentration of 3.8 mM. Sterile PBS was added to prepare a final concentration of 100 μM. $A\beta_{1-42}$ was dispensed into aliquots and immediately frozen at -70 °C until required.

Cell culture

Rat pheochromocytoma PC-12 (Ordway) cells displaying a semi-differentiated neuronal phenotype with neuronal projections were maintained in RPMI-1640 media with 10% (v/v), foetal bovine serum (FBS), 1% (v/v) penicillin/streptomycin and 1% (v/v) non-essential amino acids. The cells were incubated at 37°C with 5 % CO_2. Cells were seeded in a 96 well plate at 2×10^4 cells per well.

Neuronal cell viability assay

The measurement of the neuronal cell viability was performed using the MTT assay of mitochondrial activity and was performed as described previously.[24] To assess potential

cytotoxicity of the *E. radiata* extract and fractions, cells were seeded at 2×10^4 cells per well in 100 µL media into 96 well tissue culture plates. PC-12 cells were treated with each of these fractions at a final concentration up to 100 µg/mL then incubated for 24 hours at 37°C. In order to determine the neuroprotective activity of extracts, PC-12 cells were pre-treated with 100 µg/mL extract for 15 min prior to incubation with $A\beta_{1–42}$ (0-1 µM) for 48 h at 37°C. MTT absorbance was measured at 570 nm.

Transmission electron microscopy of $A\beta_{1–42}$ morphology

The impact of the EA fraction of *E. radiata* on $A\beta_{1–42}$ aggregate morphology was visualized by transmission electron microscopy as described previously.[25] $A\beta_{1–42}$ (10 µM) was incubated alone or with 100 µg/mL EA for 48 h at 37 °C. From the mixture, 5 µL was placed on a 200 mesh formvar carbon coated copper electron microscopy grid (Proscitech, Kirwan, QLD, Australia). The excess sample was blotted off using filter paper and 10 µL of contrast dye (2 % uranyl acetate) added to the grid. The excess dye was blotted off and grids loaded and visualized using a FEI Technai G2 Spirit Transmission Electron Microscope (FEI, Milton, QLD, Australia). Manual scanning was undertaken for $A\beta_{1–42}$ proteins at a magnification of 34,000-92,000× and representative images were taken.

Statistical analysis

All MTT assays of cell viability were performed in quadruplicate and an average viability value recorded from at least 3-4 independent experiments. MTT results were analyzed via a two-way analysis of variance (ANOVA) with a Bonferroni's *post hoc* test used to determine the significance level ($p<0.05$). Data analysis and production of graphs was performed in GraphPad Prism 8 (GraphPad Software, San Diego, USA).

Results and Discussion

Yield and total phlorotannin content (TPC) of ethanol extract and solvent soluble fractions

The yields and total phlorotannin content of the 80% ethanol extract and solvent soluble fractions are shown in Table 1. The yield of ethanol extract was 19.76%. Among the solvent partitioning fractions, the water fraction exhibited the highest yield (28.16%). Phlorotannins are typically stored in cell organelles which form complexes with water soluble polysaccharides in marine plants, so higher concentrations of ethanol are required for optimum extraction.[26]

The total phlorotannin content (TPC) was evaluated using Folin-Ciocalteu reagent. TPC was recorded as phloroglucinol equivalent milligram per sample gram (PGE mg/g). The ethanol extract of *E. radiata* exhibited a TPC of 127.48 PGE mg/g (12.7%). Amongst the solvent soluble fractions, ethyl acetate showed the highest TPC (619.13 PGE mg/g). Our result vary from that obtained by Charoensiddhi *et al*. [21] where the TPC of crude extract fraction and phlorotannin-enriched fraction of *E. radiata* was reported to be 4.6 and 13.4 g PGE/100g dry fraction, respectively.[21] This might be due to seasonal variations in phlorotannin expression and differences in extraction methods.[27]

Table 1. Yield and total phlorotannin content of ethanol extract and solvent-partitioned fractions from *E. radiata.*

Samples	Yield (%)	PGE mg/g Sample ± SD
Ethanol extract	19.76	127.48 ± 0.011
Ethyl acetate fraction	5.00	619.13 ± 0.009
Butanol Fraction	12.59	64.52 ± 0.005
Water fraction	28.16	51.90 ± 0.005

Yield is expressed as wt/wt of dried seaweed and yield of solvent-partitioned fractions as % of total ethanol extract. PGE = phoroglucinol equivalent

Impact of E. radiata extract and solvent soluble fractions on PC-12 neuronal cell viability

Ecklonia radiata extracts exhibited no intrinsic neurotoxicity to PC-12 cells up to 100 µg/mL (Fig. 1) and this concentration was used for further analysis of bioactivity. Incubation of PC-12 cells with $A\beta_{1-42}$ (0.05-1 µM) over 48 h demonstrated a concentration-dependent decrease in cell viability up to 79% at 1 µM $A\beta_{1-42}$ (Fig. 2). All three extracts demonstrated protection against Aβ-evoked PC-12 neuronal cell toxicity. The ethanol extract increased cell viability to >89 % compared to control group (79%), which is concordant with a previous study.[20] Importantly, the EA fraction demonstrated the most significant protective activity across all Aβ concentrations, increasing cell viability to more than 100% versus control at low concentrations of Aβ (Fig. 2), indicating a potential proliferative or stimulating effect of EA on mitochondrial activity. Overall, the EA extract afforded PC-12 cells significant protection against neurotoxicity over most Aβ concentrations. The result was consistent with other neuroprotective studies generally, where EA demonstrated superior activity among the other fractions in different seaweeds.[12, 28, 29] Previously, Ahn *et al.* demonstrated that EA fraction of *Eisenia bicyclis* significantly increased cell viability to 104.30% upon treatment with $A\beta_{25-35}$ (2.5 µM) in the PC-12 cell line and also significantly reduced Aβ induced ROS generation.[12] Further, Kang *et al.* reported that ethanolic extract of *Ecklonia cava* significantly decreased the concentration of $A\beta_{1-40}$ and $A\beta_{1-42}$ in the culture media of HEK293 APP Swedish stable cells via inhibition of amyloid precursor protein processing.[30, 31] In addition, among the solvent soluble fractions butanol fraction effectively reduced Aβ secretion from HEK293 cells, inhibited Aβ oligomerization and fibril formation, and protected primary corticol neurons from Aβ-induced cell death.[30] The author mentioned that the EA fraction of *E. cava* showed severe cytotoxicity at Aβ-lowering concentration (15 and 50 µg/ml) which may be

due to the variation in the chemical compounds between the species as demonstrated by MS/MS data.

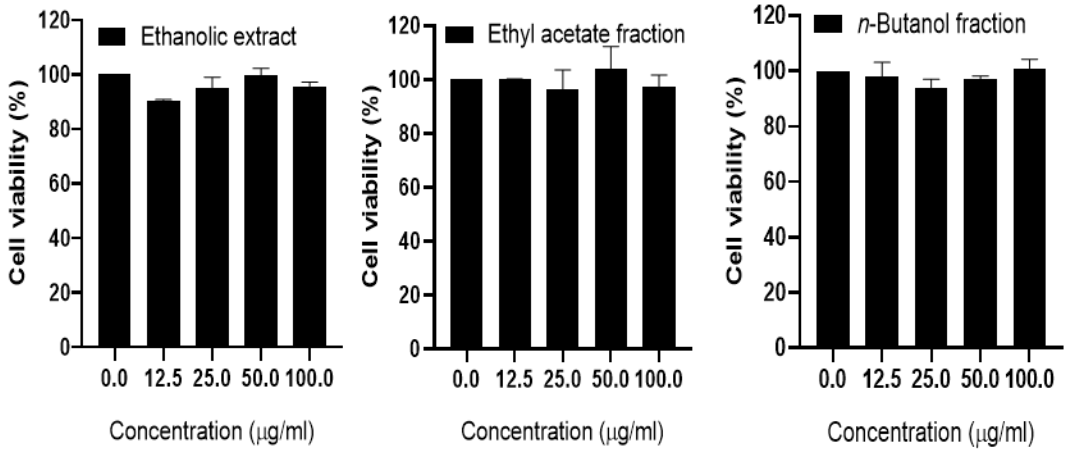

Figure 1. Neuronal PC-12 cell viability in response to increasing concentrations of *Ecklonia radiata* ethanolic extract and solvent soluble ethyl acetate and *n*-butanol fractions. None of the fractions elicited toxicity up to 100 µg/mL(n=3).

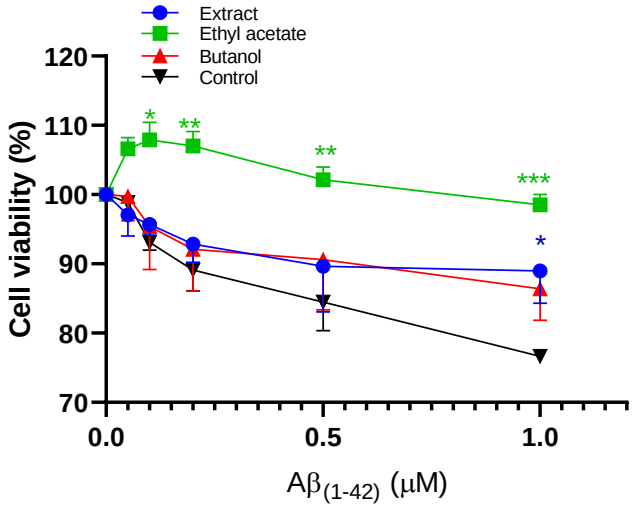

Figure 2. MTT assay of neuronal PC-12 cell viability in response to 48hrs incubation with $A\beta_{1\text{-}42}$ (0-1µM), alone and in the presence of different solvent soluble fractions of *Ecklonia radiata* extract (100 µg/mL). The ethyl acetate soluble fraction provided significant neuroprotection against $A\beta_{1\text{-}42}$ toxicity across all concentrations. ***$p < 0.001$, **$p < 0.01$, *$p < 0.05$ vs control (n=4).

Effect of *Ecklonia radiata* extracts on Aβ$_{1–42}$ fibrillisation and aggregate formation

In order to visualize Aβ aggregates and fibrils and investigate the effects of EA on Aβ morphology, transmission electron microscopy (TEM) analysis was performed. TEM demonstrated that in the presence of EA, the prevalence and the density of Aβ$_{1-42}$ aggregates was found to be reduced as compared with the control after 48 h incubation as shown in Figure 3. These results are supported by previous structural and fibrillisation kinetic studies demonstrating direct anti-aggregative effects of phlorotannin-rich *Ecklonia* extracts on amyloid β.[20, 30]

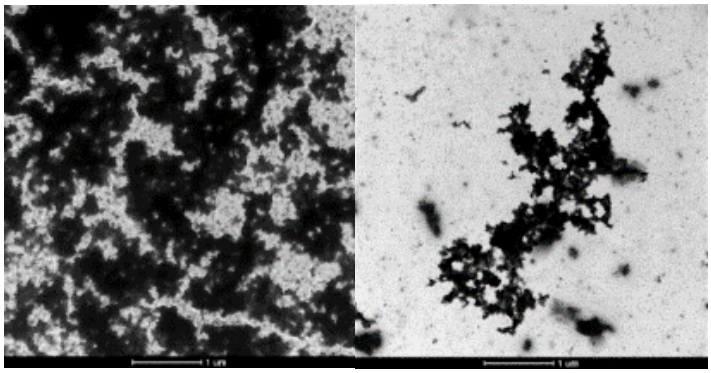

Aβ$_{1-42}$ (10 μM) **Aβ$_{1-42}$ (10 μM) + ethyl acetate fraction (100 μg/mL)**

Figure 3. TEM micrographs showing representative effects of *Ecklonia radiata* EA fraction on reducing the density and prevalence of aggregates after 48 h incubation.

Isolation of major phlorotannin: eckol

Following the bioactivity assay, the active ethyl acetate fraction was subjected to centrifugal partition chromatography (CPC), a separation technique based on the difference in the distribution of analytes in two immiscible liquid phases. It is widely used in the field of natural chemistry due to various advantages including high capacity, low solvent consumption and flexible elution modes.[32] We used a "generally useful estimate of solvent systems" (GUESS) method in order to determine the most suitable solvent system for our study.[33] Various ratios of hexane: ethyl acetate: methanol: water (HEMW) were used, with a HEMW (2:8:2:8) achieving an optimal P value of

1.48, which was between the desired range of 0.4 and 2.5. Thus, preparative CPC was operated in the descending mode, with the upper organic phase acting as the stationary phase and lower aqueous phase as mobile phase. The fractions were pooled to give four sub-fractions based on TLC analysis. A pure compound (30 mg) was obtained from the EA-3 subfraction and 1D and 2D NMR used to demonstrate spectral data consistent with the identification of the compound as eckol (Figure S2; supporting information).[34]

Profiling of phlorotannin in *E. radiata* via ion mobility mass spectrometry and HPLC quadrupole-time-of flight mass spectroscopy

Structural characterization of the phlorotannins is onerous due to the occurrence of highly complex polymeric mixtures of structural and conformational isomers, while no reference phlorotannins are commercially available. Here we first combined ion mobility mass spectrometry (IMMS) and high performance liquid chromatography quadrupole-time-of flight mass spectroscopy (HPLC-qTOF-MS) in order to characterize the major phlorotannins present in the EA fraction. The extracted ion chromatograms (EIC) of deprotonated molecular ions ($[M-H]^-$) from the major phlorotannins identified in the literature (phloroglucinol, eckol, dieckol, bieckol, fucophloroethol, phlorofucofuroeckol, and phloroeckol) were selected for this study.[35-38]

Table 2. Identification of major eckol-type phlorotannins from the ethyl acetate (EA) fraction of *E. radiata* by HPLC-qTOF-MS and IMMS in negative mode.

Peak	R_T (min)	$[M-H]^-$ (m/z)	HPLC-qTOF MS/MS	Tentative assignment
			MS^2	
1	6.39	371	371, 246, 217, 149, 124	Eckol
2	10.15	743	743, 601, 443, 353, 265, 231, 139, 125	Dibenzodioxin-fucodiphloroethol, Eckmaxol

3	11.62	741	741, 502, 478, 336, 231, 161	Dieckol, Bieckol
4	1.05	497	497, 374, 328, 292, 242, 163, 147, 135	Fucodiphloroethol G,
5	6.96	495	495, 345, 270, 231, 204, 177, 135	Phloroeckol
6	1.16	373	373, 343, 283, 247, 183, 126	Fucophloroethol A, Triphloroethol-A
7	12.44	601	601, 520, 383, 327, 243, 202, 188	Phlorofucofuroeckol A, Phlorofucofuroeckol B
8	12.79	477	477, 465, 377, 293, 248, 194	Fucofuroeckol A

[a]Main observed fragments. Other ions were evident but were not included for brevity

Tentative identification of the phlorotannins was achieved by comparison with previously reported compounds in *Ecklonia* genus.[35-38] The major molecular ions were selected via IMMS based on their drift time.[39] IMMS is a powerful technique which has a capacity to detect and resolve all species present in the solution, including the transiently stable and isobaric species. It separates ions based on the rate at which they migrate through a neutral carrier gas under the influence of an external field.[40] IMMS data demonstrated the presence of various isomers as indicated by features with the same *m/z* value but differing in drift time. Sample was then subjected to HPLC-qTOF-MS in order to identify the major phlorotannins through fragmentation analysis. The structure of the compounds detected in the spectra and identified tentatively are shown in Table 2 and Figure 4. According to spectral data, major compounds detected were identified as eckol-type phlorotannins which contain at least the 1, 4-dibenzodioxin fragment in their structure, a common feature of *Ecklonia* genus. The fragment peaks that were observed in the MS/MS patterns of these compounds revealed the successive loss of phloroglucinol (*m/z* 126), pentahydroxyl dibenzodioxin (*m/z* 263) and eckol (*m/z* 371) as suggested by Cho et al.[35] $[M-H]^-$ ions corresponding to the trimer

(*m/z* 371) was identified as eckol. The fragments at *m/z* 246, 262, and 231 were detected due to the loss of one O-phloroglucinol, phloroglucinol and phloroglucinol with water, respectively, along with the NMR of the isolated compound (Figure S2; supporting information). Previously, Cho *et al.* and Wang *et al.* isolated compounds (Eckmaxol and Dibenzodioxin-fucodiphloroethol) corresponding to the $[M-H]^-$ *m/z* 743.[35, 36] The major fragments include *m/z* 601, 371, and 248. This might be due to the loss of one, three, and four phloroglucinol units, respectively.

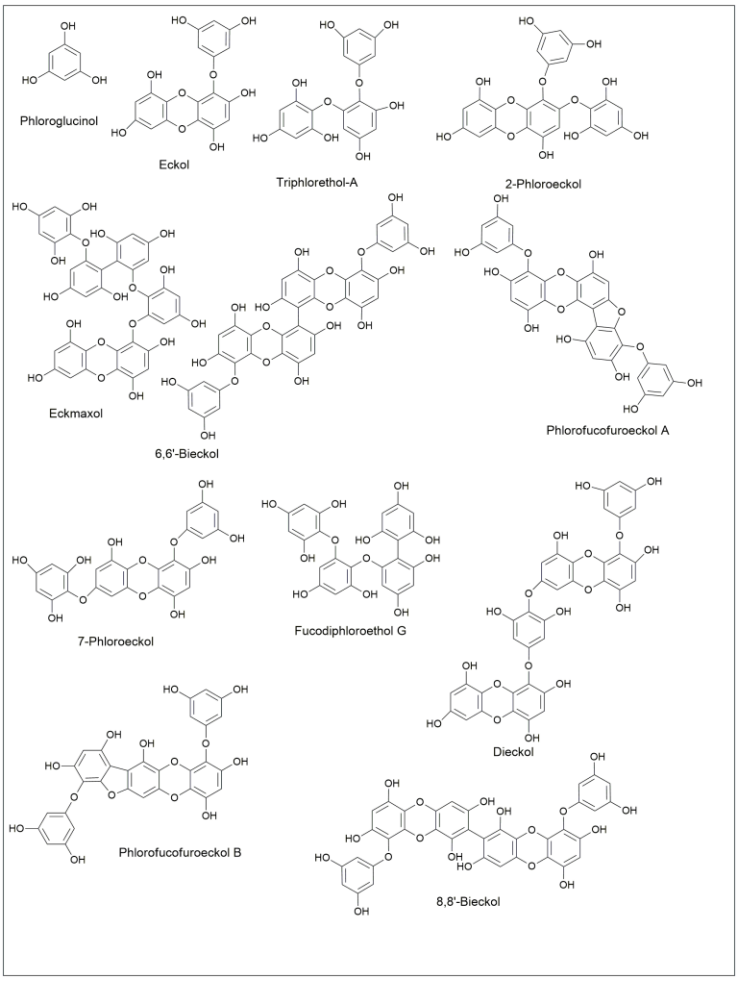

Figure 4. Structure of phlorotannins tentatively identified via HPLC-qTOF-MS in *Ecklonia radiata.*

Other compounds that belong to the fucophlorethol groups (m/z 373 and 497) were also detected in our spectra. The product ions resultant from cross-ring cleavages were detected from the loss of one or more phloroglucinol units, O-phloroglucinol (140/142) and its fuhalol derivatives and /or resorcinol (108/110), indicative of ether bond cleavages. Since these compounds possess C-O-C (as phloroethols) and C-C (as fucols) linkage in their structure, accurate identification of higher molecular weight compounds are very difficult via LC-MS.[41] Furthermore, unique fragments detected at m/z 477 and 383 due to the loss of one and two units of phloroglucinol respectively from m/z 601, indicated the presence of both the dibenzo-1,4-dioxin and dibenzofuran elements. Thus, the detected compound was predicted to be Phlorofucofuroeckol A or Phlorofucofuroeckol B. Some of the proposed fragmentation patterns of the compounds tentatively identified in EA are shown in Figure S8 (supporting information). Furthermore, as ion abundance from eckol was much more intense and has large contribution towards TIC, eckol was considered the major component in the EA fraction as evident from the TIC and EIC (Figure S9; supporting information).

Previously, several attempts were made to characterize phlorotannins from brown macroalgae, with most characterized as phlorotannins based on the degree and type of polymerization.[22, 35, 37, 42-44] Herein, we attempted to characterize the major components of the active ethyl acetate fraction, in order to predict the probable compounds responsible for the neuroprotective bioactivity. This includes the phlorotannins eckol, dieckol, 8,8'-bieckol and phlorofucofuroeckol, which were previously reported to have neuroprotective activity in PC-12 cells.[11, 12, 45] Recently, Lee *et al*. compared the anti-neuroinflammatory properties of phlorotannins and reported the pronounced activity of dieckol, amongst others.[11] Collectively, our results and previous studies attest to the bioactivity of phlorotannins towards the neuroprotective activity of the ethyl acetate fraction of *Ecklonia* and other brown algal species.

To our knowledge, this is the first study characterizing the major components from *E. radiata* via LC-MS. Thus, similar to other *Ecklonia* species (*E. brevipes*, *E. cava*, *E. stolonifera*, *E. muratii*, and *E. maxima*), *E. radiata* also contains eckols (1, 4-dibenzodioxins) as the major component phlorotannin. However, further extensive isolation and identification as well as further defined activity-guided fractionation is needed to definitively confirm the role of individual components to neuroprotection.

Conclusions

The neuroprotective potential of *E. radiata* ethanolic extract and solvent-soluble fractions against toxicity from $A\beta_{1\text{-}42}$ was investigated in neuronal PC-12 cells. The ethyl acetate fraction (EA) proved to be most efficacious and this fraction contained the highest total phlorotannin content. Neuroprotection was associated with a reduction in both the prevalence and density of amyloid $\beta_{(1\text{-}42)}$ aggregates. Analysis of EA via CPC enabled the isolation of the major phlorotannin, eckol, while MS/MS analysis of EA demonstrated the presence of eckol as the predominant constituent and therefore a likely candidate responsible for bioactivity in this extract. Collectively, our results support *E. radiata* as a promising natural brown algal source for therapeutic neuroprotective phlorotannins. However, further in-depth studies are required to identify other novel compounds associated with this particular *Ecklonia* species as indicated by MS/MS analysis.

Conflicts of interest

There are no conflicts to declare.

Acknowledgements

The authors would like to thank Peng Su and Prof. Martin Johnston from Flinders University for assisting in extraction and NMR analysis.

References

1. C. M. Huber, C. Yee, T. May, A. Dhanala and C. S. Mitchell, Cognitive decline in preclinical Alzheimer's disease: amyloid-beta versus tauopathy, *J. Alzheimer's Dis.*, 2018, **61**, 265-281.
2. X. Du, X. Wang and M. Geng, Alzheimer's disease hypothesis and related therapies, *Transl. Neurodegener.*, 2018, **7**, 2.
3. S. Das and S. D. Smid, in *Bioactive Nutraceuticals and Dietary Supplements in Neurological and Brain Disease*, Elsevier, 2015, pp. 73-76.
4. X.-L. Bu, P. P. Rao and Y.-J. Wang, Anti-amyloid aggregation activity of natural compounds: implications for Alzheimer's drug discovery, *Mol. Neurobiol.*, 2016, **53**, 3565-3575.
5. X. Wang, G. Sun, T. Feng, J. Zhang, X. Huang, T. Wang, Z. Xie, X. Chu, J. Yang and H. Wang, Sodium oligomannate therapeutically remodels gut microbiota and suppresses gut bacterial amino acids-shaped neuroinflammation to inhibit Alzheimer's disease progression, *Cell Res.*, 2019, **29**, 787-803.
6. S. Charoensiddhi, C. Franco, P. Su and W. Zhang, Improved antioxidant activities of brown seaweed *Ecklonia radiata* extracts prepared by microwave-assisted enzymatic extraction, *J. Appl. Phycol.*, 2015, **27**, 2049-2058.
7. K. H. Wiltshire, F. Gurgel and M. R. Deveney, Feasibility Study for Integrated Multitrophic Aquaculture in Southern Australia: Report to the Fisheries Research & Development Corporation, SARDI Aquatic Sciences, 2015.
8. A.-R. Kim, B. Lee, E.-J. Joung, W.-G. Gwon, T. Utsuki, N.-G. Kim and H.-R. Kim, 6, 6′-Bieckol suppresses inflammatory responses by down-regulating nuclear factor-κB activation via Akt, JNK, and p38 MAPK in LPS-stimulated microglial cells, *Immunopharmacol. Immunotoxicol.*, 2016, **38**, 244-252.
9. Y. Li, Z.-J. Qian, B. Ryu, S.-H. Lee, M.-M. Kim and S.-K. Kim, Chemical components and its antioxidant properties in vitro: an edible marine brown alga, *Ecklonia cava*, *Arch. Pharmacal Res.*, 2009, **17**, 1963-1973.
10. J. S. Choi, S. Haulader, S. Karki, H. J. Jung, H. R. Kim and H. A. Jung, Acetyl- and butyryl-cholinesterase inhibitory activities of the edible brown alga *Eisenia bicyclis*, *Bioorg. Med. Chem.*, 2015, **38**, 1477-1487.

11. S. Lee, K. Youn, D. Kim, M.-R. Ahn, E. Yoon, O.-Y. Kim and M. Jun, Anti-Neuroinflammatory property of phlorotannins from *Ecklonia cava* on $A\beta_{25-35}$-induced damage in PC12 cells, *Mar. Drugs*, 2019, **17**, 7.
12. B. R. Ahn, H. E. Moon, H. R. Kim, H. A. Jung and J. S. Choi, Neuroprotective effect of edible brown alga *Eisenia bicyclis* on amyloid beta peptide-induced toxicity in PC12 cells, *Arch. Pharmacal Res.*, 2012, **35**, 1989-1998.
13. R. Pangestuti and S.-K. Kim, Neuroprotective effects of marine algae, *Mar. Drugs*, 2011, **9**, 803-818.
14. J.-S. Choi, H.-J. Bae, S.-J. Kim and I. S. Choi, In vitro antibacterial and anti-inflammatory properties of seaweed extracts against acne inducing bacteria, *Propionibacterium acnes*, , *J. Environ. Biol.*, 2011, **32**, 313.
15. M. Artan, Y. Li, F. Karadeniz, S.-H. Lee, M.-M. Kim and S.-K. Kim, Anti-HIV-1 activity of phloroglucinol derivative, 6, 6′-bieckol, from *Ecklonia cava*, *Bioorg. Med. Chem.*, 2008, **16**, 7921-7926.
16. Q.-T. Le, Y. Li, Z.-J. Qian, M.-M. Kim and S.-K. Kim, Inhibitory effects of polyphenols isolated from marine alga *Ecklonia cava* on histamine release, *Process Biochem.*, 2009, **44**, 168-176.
17. J. Edmonds and K. Francesconi, Arseno-sugars from brown kelp (*Ecklonia radiata*) as intermediates in cycling of arsenic in a marine ecosystem, *Nature*, 1981, **289**, 602.
18. J. S. Edmonds and K. A. Francesconi, Arsenic-containing ribofuranosides: isolation from brown kelp *Ecklonia radiata* and nuclear magnetic resonance spectra, *J. Chem. Soc., Perkin Trans.1*, 1983, 2375-2382.
19. S. Charoensiddhi, A. J. Lorbeer, J. Lahnstein, V. Bulone, C. M. Franco and W. Zhang, Enzyme-assisted extraction of carbohydrates from the brown alga *Ecklonia radiata*: Effect of enzyme type, pH and buffer on sugar yield and molecular weight profiles, *Process Biochem.*, 2016, **51**, 1503-1510.
20. M. Alghazwi, S. Charoensiddhi, S. Smid and W. Zhang, Impact of *Ecklonia radiata* extracts on the neuroprotective activities against amyloid beta (Aβ1-42) toxicity and aggregation, *J. Funct. Foods*, 2020, **68**, 103893.

21. S. Charoensiddhi, M. A. Conlon, M. S. Vuaran, C. M. Franco and W. Zhang, Polysaccharide and phlorotannin-enriched extracts of the brown seaweed *Ecklonia radiata* influence human gut microbiota and fermentation in vitro, *J. Appl. Phycol.*, 2017, **29**, 2407-2416.
22. G. Lopes, M. Barbosa, F. Vallejo, Á. Gil-Izquierdo, P. B. Andrade, P. Valentão, D. M. Pereira and F. Ferreres, Profiling phlorotannins from Fucus spp. of the Northern Portuguese coastline: Chemical approach by HPLC-DAD-ESI/MSn and UPLC-ESI-QTOF/MS, *Algal Res.*, 2018, **29**, 113-120.
23. T. Wang, R. s. Jónsdóttir, H. Liu, L. Gu, H. G. Kristinsson, S. Raghavan and G. n. Ólafsdóttir, Antioxidant capacities of phlorotannins extracted from the brown algae *Fucus vesiculosus*, *J. Agric. Food Chem.*, 2012, **60**, 5874-5883.
24. C. Eggers, M. Fujitani, R. Kato and S. Smid, Novel cannabis flavonoid, cannflavin A displays both a hormetic and neuroprotective profile against amyloid β-mediated neurotoxicity in PC12 cells: Comparison with geranylated flavonoids, mimulone and diplacone, *Biochem. Pharmacol*, 2019, **169**, 113609.
25. D. T. Marsh, S. Das, J. Ridell and S. D. Smid, Structure-activity relationships for flavone interactions with amyloid β reveal a novel anti-aggregatory and neuroprotective effect of 2′, 3′, 4′-trihydroxyflavone (2-D08), *Bioorg. Med. Chem.*, 2017, **25**, 3827-3834.
26. M. Yoon, J.-S. Kim, M. Y. Um, H. Yang, J. Kim, Y. T. Kim, C. Lee, S.-B. Kim, S. Kwon and S. Cho, Extraction optimization for phlorotannin recovery from the edible brown seaweed *Ecklonia cava*, *J. Aquat. Food Prod. Technol.*, 2017, **26**, 801-810.
27. S. M. Kim, S. W. Kang, J.-S. Jeon, Y.-J. Jung, W.-R. Kim, C. Y. Kim and B.-H. Um, Determination of major phlorotannins in Eisenia bicyclis using hydrophilic interaction chromatography: seasonal variation and extraction characteristics, *Food Chem.*, 2013, **138**, 2399-2406.
28. A. R. Kim, T. S. Shin, M. S. Lee, J. Y. Park, K. E. Park, N. Y. Yoon, J. S. Kim, J. S. Choi, B. C. Jang, D. S. Byun, N. K. Park and H. R. Kim, Isolation and identification of phlorotannins from *Ecklonia stolonifera* with antioxidant and anti-inflammatory properties, *J. Agric. Food Chem.*, 2009, **57**, 3483-3489.
29. M.-S. Lee, T. Shin, T. Utsuki, J.-S. Choi, D.-S. Byun and H.-R. Kim, Isolation and identification of phlorotannins from *Ecklonia stolonifera* with antioxidant and

hepatoprotective properties in tacrine-treated HepG2 cells, *J. Agric. Food Chem.*, 2012, **60**, 5340-5349.

30. I. J. Kang, Y. E. Jeon, X. F. Yin, J. S. Nam, S. G. You, M. S. Hong, B. G. Jang and M. J. Kim, Butanol extract of *Ecklonia cava* prevents production and aggregation of beta-amyloid, and reduces beta-amyloid mediated neuronal death, *Food Chem. Toxicol.*, 2011, **49**, 2252-2259.
31. I.-J. Kang, B. G. Jang, S. In, B. Choi, M. Kim and M.-J. Kim, Phlorotannin-rich *Ecklonia cava* reduces the production of beta-amyloid by modulating alpha-and gamma-secretase expression and activity, *Neurotoxicology*, 2013, **34**, 16-24.
32. X.-Y. Huang, D. Pei, J.-F. Liu and D.-L. Di, A review on chiral separation by counter-current chromatography: development, applications and future outlook, *J. Chromatogr., A*, 2018, **1531**, 1-12.
33. J. Brent Friesen and G. F. Pauli, GUESS—a generally useful estimate of solvent systems for CCC, *J. Liq. Chromatogr. Relat. Technol.*, 2005, **28**, 2777-2806.
34. Y. Okada, A. Ishimaru, R. Suzuki and T. Okuyama, A new phloroglucinol derivative from the brown alga *Eisenia bicyclis*: potential for the effective treatment of diabetic complications, *J. Nat. Prod.*, 2004, **67**, 103-105.
35. H. M. Cho, T. P. Doan, T. K. Q. Ha, H. W. Kim, B. W. Lee, H. T. T. Pham, T. O. Cho and W. K. Oh, Dereplication by High-Performance Liquid Chromatography (HPLC) with Quadrupole-Time-of-Flight Mass Spectroscopy (qTOF-MS) and Antiviral Activities of Phlorotannins from *Ecklonia cava*, *Mar. Drugs*, 2019, **17**, 149.
36. J. Wang, J. Zheng, C. Huang, J. Zhao, J. Lin, X. Zhou, C. B. Naman, N. Wang, W. H. Gerwick, Q. Wang, X. Yan, W. Cui and S. He, Eckmaxol, a phlorotannin extracted from *Ecklonia maxima*, produces anti-beta-amyloid oligomer neuroprotective effects possibly via directly acting on glycogen synthase kinase 3beta, *ACS Chem. Neurosci.*, 2018, **9**, 1349-1356.
37. J. H. Isaza Martínez and H. G. Torres Castañeda, Preparation and chromatographic analysis of phlorotannins, *J. Chromatogr. Sci.*, 2013, **51**, 825-838.
38. C. S. Myung, H. C. Shin, H. Y. Bao, S. J. Yeo, B. H. Lee and J. S. Kang, Improvement of memory by dieckol and phlorofucofuroeckol in ethanol-treated mice: possible involvement of the inhibition of acetylcholinesterase, *Arch. Pharmacal Res.*, 2005, **28**, 691-698.

39. F. Lanucara, S. W. Holman, C. J. Gray and C. E. Eyers, The power of ion mobility-mass spectrometry for structural characterization and the study of conformational dynamics, *Nat. Chem.*, 2014, **6**, 281.
40. D. M. Williams and T. L. Pukala, Novel insights into protein misfolding diseases revealed by ion mobility-mass spectrometry, *Mass Spectrom. Rev.*, 2013, **32**, 169-187.
41. M. D. Catarino, A. Silva, N. Mateus and S. M. Cardoso, Optimization of phlorotannins extraction from *Fucus vesiculosus* and evaluation of their potential to prevent metabolic disorders, *Mar. Drugs*, 2019, **17**, 162.
42. F. Ferreres, G. Lopes, A. Gil-Izquierdo, P. B. Andrade, C. Sousa, T. Mouga and P. Valentao, Phlorotannin extracts from fucales characterized by HPLC-DAD-ESI-MSn: approaches to hyaluronidase inhibitory capacity and antioxidant properties, *Mar. Drugs*, 2012, **10**, 2766-2781.
43. C. Olate-Gallegos, A. Barriga, C. Vergara, C. Fredes, P. García, B. Giménez and P. Robert, Identification of polyphenols from chilean brown seaweeds extracts by LC-DAD-ESI-MS/MS, *J. Aquat. Food Prod. Technol.*, 2019, **28**, 375-391.
44. Y. Li, X. Fu, D. Duan, X. Liu, J. Xu and X. Gao, Extraction and identification of phlorotannins from the brown alga, *Sargassum fusiforme* (Harvey) Setchell, *Mar. Drugs*, 2017, **15**, 49.
45. J.-J. Kim, Y.-J. Kang, S.-A. Shin, D.-H. Bak, J. W. Lee, K. B. Lee, Y. C. Yoo, D.-K. Kim, B. H. Lee and D. W. Kim, Phlorofucofuroeckol improves glutamate-induced neurotoxicity through modulation of oxidative stress-mediated mitochondrial dysfunction in PC12 cells, *PloS one*, 2016, **11**, e0163433.

Appendix A: Supplementary Material

Figure S1. Fractionation scheme

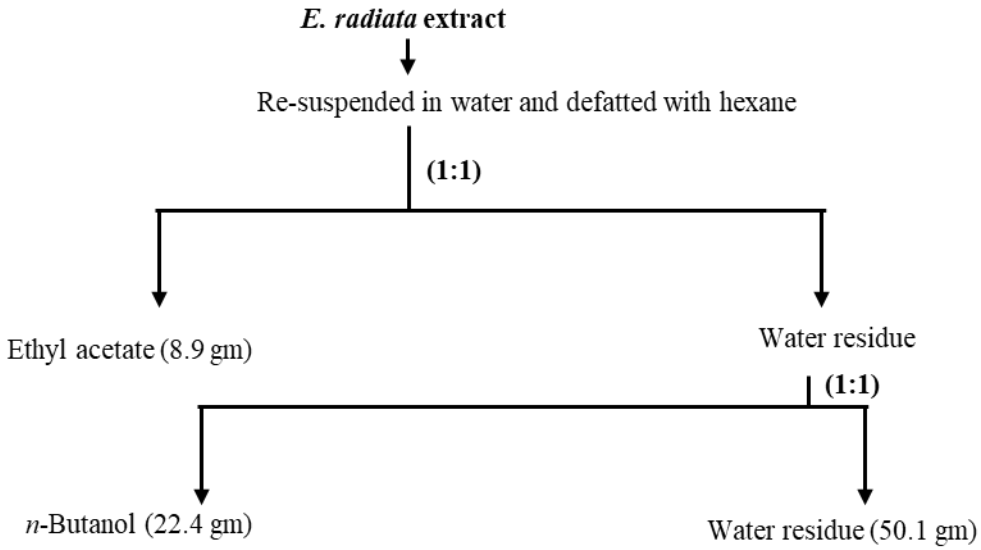

Figure S2. Structure and NMR data of eckol

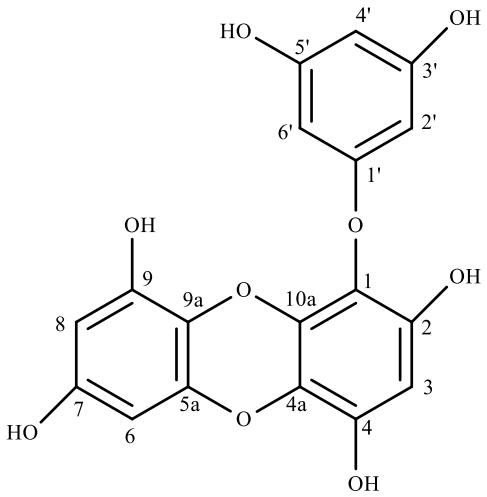

^{1}H NMR (DMSO-d_6, 600 MHz) δ 9.48 (1H, s, OH-9), 9.42 (1H, s, OH-4), 9.15 (2H, s, OH-2,7), 9.12 (2H, s, OH-3', -5'), 6.14 (1H, s, H-3), 5.96 (1H, d, J = 2.7 Hz, H-8), 5.80 (1H, t, J = 1.9 Hz, H-4'), 5.79 (1H, d, J = 2.7 Hz, H-6), 5.72 (2H, d, J = 2.1 Hz, H-2', -6');

^{13}C NMR (150 MHz, DMSO-d_6) 123.1 (C-1), 145.9 (C-2), 98.1 (C-3), 141.8 (C-4), 122.2 (C-4a), 142.5 (5a), 93.7 (C-6), 152.9 (C-7), 98.4 (C-8), 146.0 (C-9), 122.6 (9a), 137.1 (10a), 160.3 (C-1'), 93.6 (C-2'6'), 158.7 (C-3'5'), 96.1 (C-4')

Figure S3. HPLC analysis of eckol

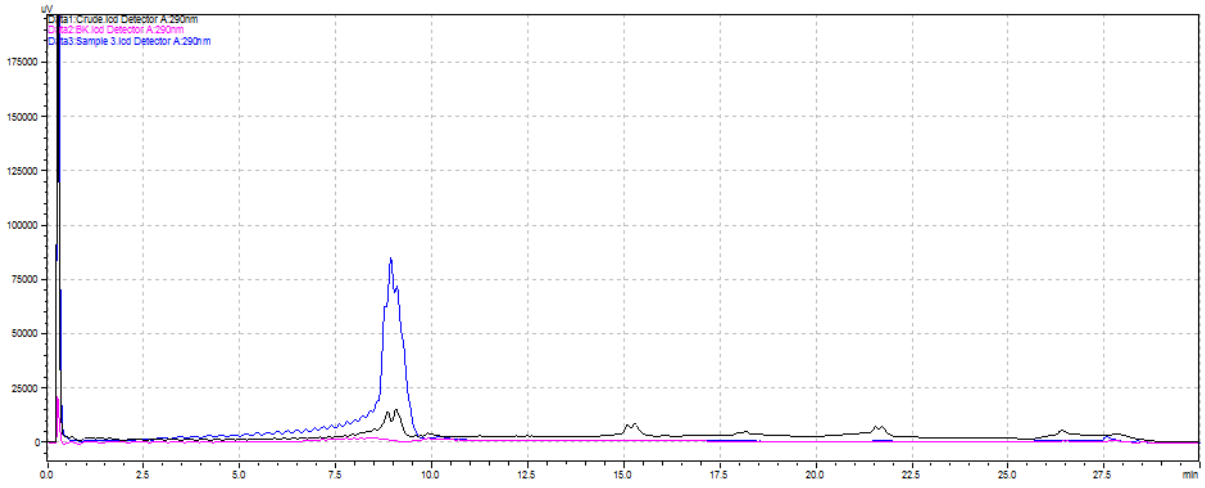

Figure S4. ^{13}C-NMR spectra of eckol

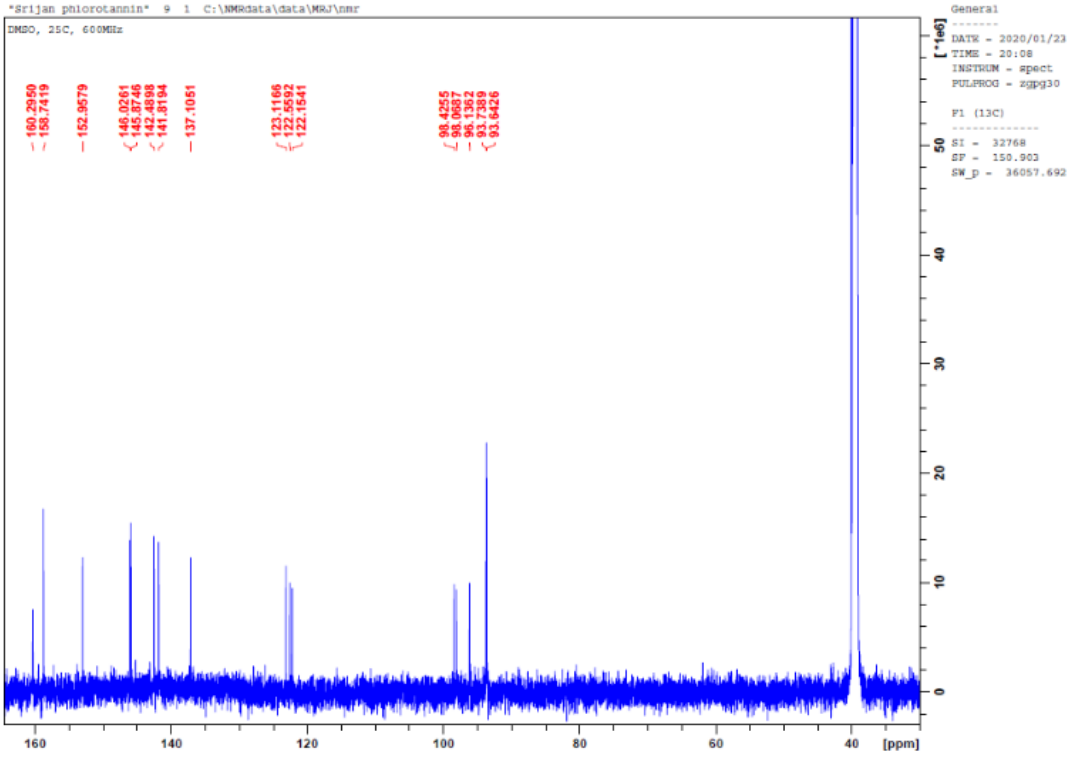

Figure S5. ^{13}C-NMR spectra of eckol

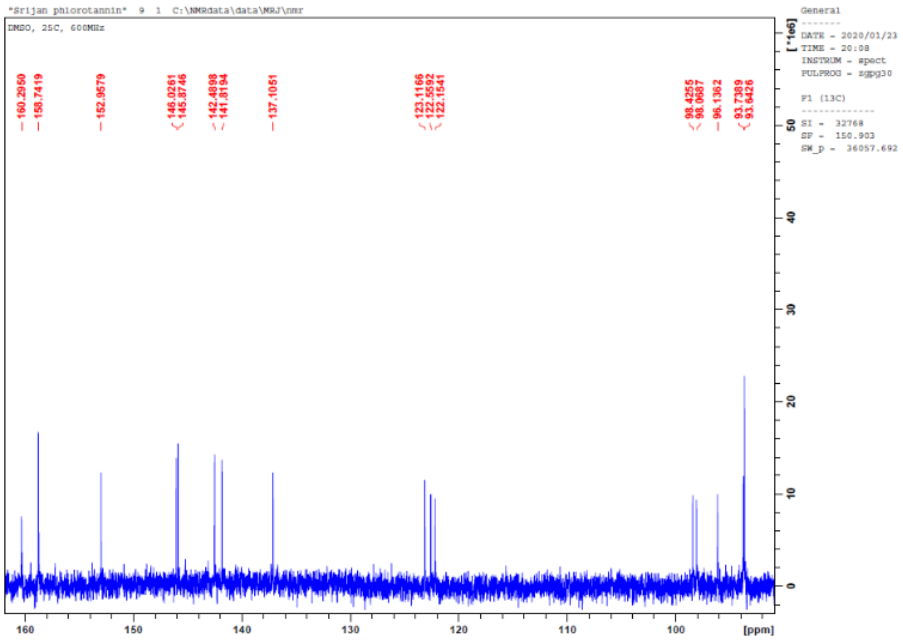

Figure S6. ^{1}H-NMR spectra of eckol

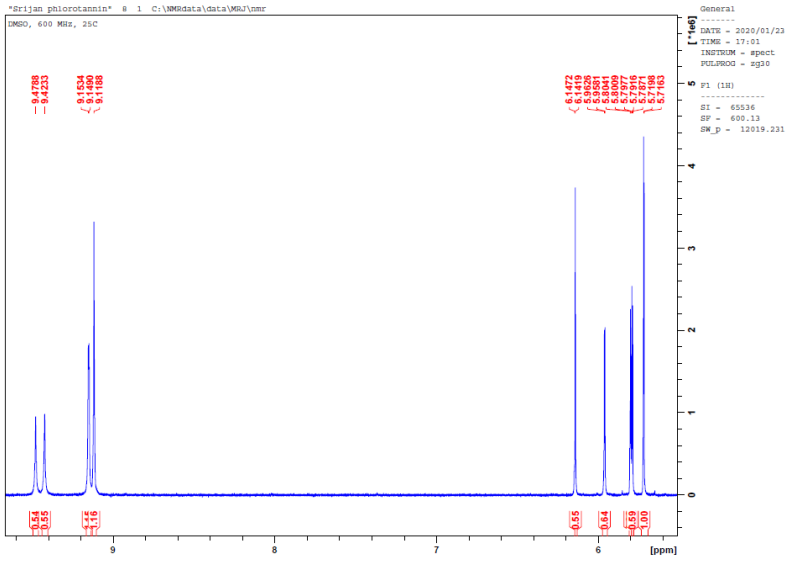

Figure S7. COSY of Eckol

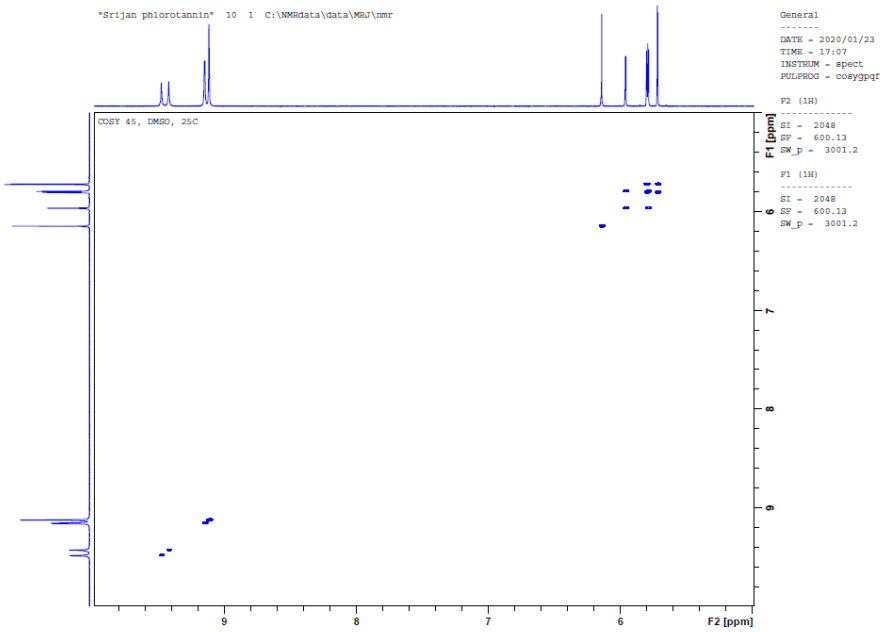

Figure S8. Proposed fragmentation pattern of the structures tentatively identified in EA fraction

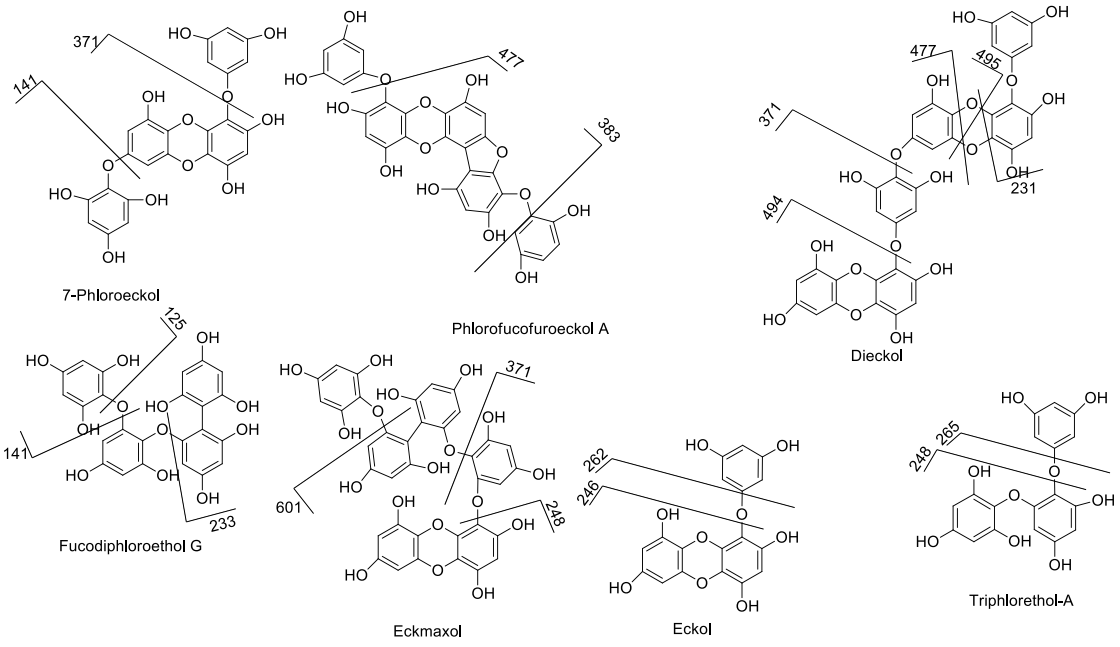

Figure S9. (A) Extracted Ion Chromatograms (EIC) of EA fraction obtained by molecular features in Agilent Masshunter. [M-H]- (m/z): 1, 371; 2, 743; 3, 741; 4, 497; 5, 495; 6, 373; 7, 601; 8, 477. (B) Total ion chromatogram (TIC) and EIC of EA fraction. The x-axis represents retention time (min), and the y-axis represents signal intensity.

A

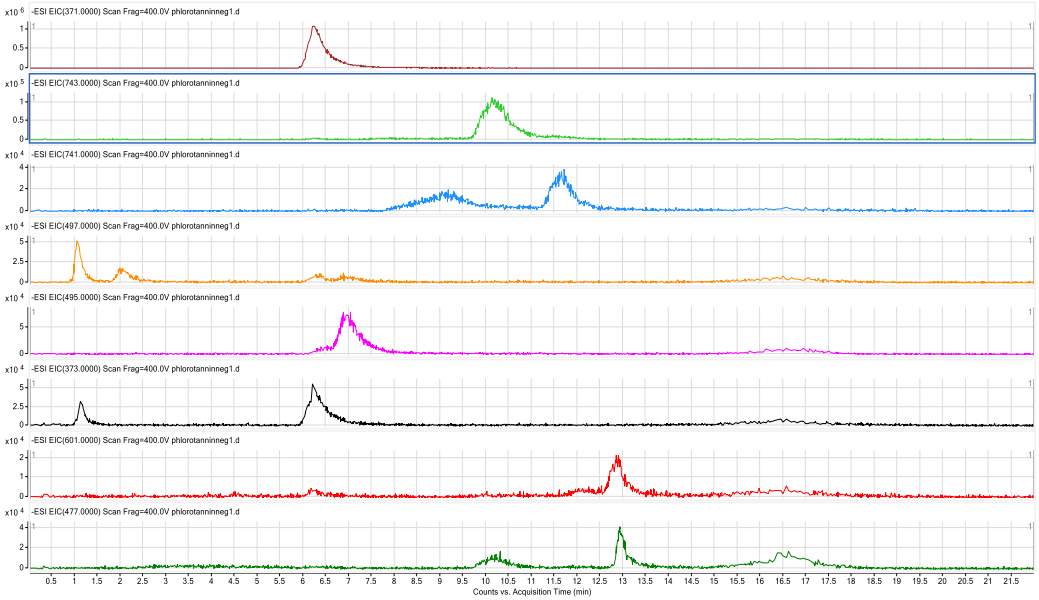

B

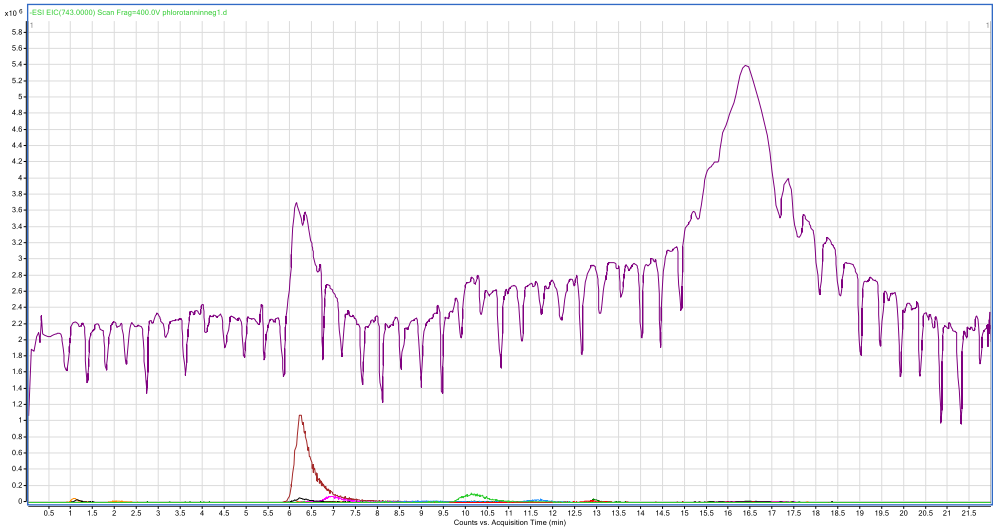

Statement of Authorship

Title of Paper	A phlorotannin isolated from *Ecklonia radiata*, Dibenzodioxin-fucodiphloroethol, inhibits neurotoxicity and aggregation of β-amyloid
Publication Status	☑ Published ☐ Accepted for Publication ☐ Submitted for Publication ☐ Unpublished and Unsubmitted work written in manuscript style
Publication Details	Shrestha, S., Johnston, M. R., Zhang, W., Smid, S. D. (2021) A phlorotannin isolated from *Ecklonia radiata*, Dibenzodioxin-fucodiphloroethol, inhibits neurotoxicity and aggregation of β-amyloid. Phytomedicine Plus, 1(4), 100125.

Principal Author

Name of Principal Author (Candidate)	Srijan Shrestha		
Contribution to the Paper	Conceptualization, Investigation, Formal analysis, Data curation, Methodology, Software, Writing- original draft.		
Overall percentage (%)	80%		
Certification:	This paper reports on original research I conducted during the period of my Higher Degree by Research candidature and is not subject to any obligations or contractual agreements with a third party that would constrain its inclusion in this thesis. I am the primary author of this paper.		
Signature		Date	17/05/2022

Co-Author Contributions

By signing the Statement of Authorship, each author certifies that:

i. the candidate's stated contribution to the publication is accurate (as detailed above);

ii. permission is granted for the candidate in include the publication in the thesis; and

iii. the sum of all co-author contributions is equal to 100% less the candidate's stated contribution.

Name of Co-Author	Dr. Martin Johnston		
Contribution to the Paper	Resources, Investigation, Data Curation, Software		
Signature		Date	27/05/22

Name of Co-Author	Dr. Wei Zhang		
Contribution to the Paper	Conceptualization, Resources, Methodology, Supervision, Writing-review, and editing		
Signature		Date	31/05/2022

Name of Co-Author	Dr. Scott Smid		
Contribution to the Paper	Conceptualization, Funding acquisition, Formal analysis, Resources, Supervision, Writing-review, and editing.		
Signature		Date	21-6-22

Chapter 3: A phlorotannin isolated from *Ecklonia radiata*, Dibenzodioxin-fucodiphloroethol, inhibits neurotoxicity and aggregation of β-amyloid

Srijan Shrestha [a], Martin R. Johnston [b], Wei Zhang [c,d], Scott D. Smid [a*]

[a] Discipline of Pharmacology, School of Biomedicine, Faculty of Health Sciences, The University of Adelaide, Adelaide, South Australia, Australia;

[b] Flinders Institute for Nanoscale Science and Technology, College of Science and Engineering, Flinders University, Adelaide, South Australia, Australia

[c] Centre for Marine Bioproducts Development (CMBD), and [d] Dept. of Medical Biotechnology, College of Medicine and Public Health, Flinders University, Adelaide, South Australia, Australia

Phytomedicine Plus., 2021, 1, 100125; DOI: 10.1016/j.phyplu.2021.100125

Abstract

Background: The polyphenolic phlorotannins derived from brown macroalgae consist of complex polymers of phloroglucinol residues with diverse structures ascribed pleiotropic bioactivity.

Purpose: This study aimed to isolate and purify the phlorotannins from *Ecklonia radiata* and to investigate their neuroprotective activity in PC-12 cells.

Methods: This study used high performance counter-current chromatography (HPCCC) combined with size exclusion chromatography to isolate and purify a phlorotannin from the marine brown algae *Ecklonia radiata*. Nuclear magnetic resonance (NMR) including 1H and 13C and 2D COSY, HSQC, HMBC (broad and band selective), and NOESY along with mass spectroscopy enabled us to identify the phlorotannin as dibenzodioxin-fucodiphloroethol (DFD). The compound was subsequently investigated for protective bioactivity against the neurotoxic β-amyloid protein $A\beta_{1-42}$, and intracellular reactive oxygen species (ROS) scavenging activity in PC-12 cells along with molecular modelling studies to identify direct interaction properties with $A\beta_{1-42}$ protein.

Results: DFD was nontoxic up to 50μM in the neuronal PC-12 cell line and significantly prevented loss of cell viability in response to $A\beta_{1-42}$ (0-1.5μM). Furthermore, it significantly reduced the aggregation of $A\beta_{1–42}$ as evidenced by transmission electron microscopy, while molecular docking studies revealed DFD binding to key $A\beta_{1-42}$ residues associated with fibrillisation propensity. Additionally, DFD demonstrated moderate cholinesterase inhibitory activity (IC_{50} value of 41μM), sharing similar interacting binding residues to donepezil in the crystallized structure, and was also able to significantly scavenge ROS in PC-12 cells.

Conclusions: Collectively, DFD possesses neuroprotective actions mitigating several mechanisms ascribed to amyloid β neurotoxicity, making this macroalgal phlorotannin an excellent candidate for further studies targeting neurodegenerative pathways in Alzheimer's disease.

Keywords: Dibenzodioxin-fucodiphloroethol, phlorotannin, *Ecklonia radiata*, neuroprotection, HPCCC, β amyloid

Introduction

Ecklonia radiata is a marine brown alga found in coastal waters of South Africa, Australia, and New Zealand. In Australia, *E. radiata* is distributed from coastal regions of Kalbarri and Abrolhos Island in Western Australia, South Australia, Tasmania to Caloundra in Queensland (Rothman et al., 2015). While other *Ecklonia* species e.g. *E. stolonifera*, *E. cava*, *E. maxima*, and *E. kurome* have been characterized for constituent phlorotannins, *E. radiata* has been less well characterized in this regard. Phlorotannins are a unique set of polyphenols specially synthesized by brown algae (*Phaeophyta*) and commonly identified from *Ecklonia* species. Such compounds include eckol, dieckol, 2-phloroeckol, 7-phloroeckol, dibenzo [1,4] dioxine-2,4,7,9-tetrol, 6,6′-bieckol, 8,8′-bieckol, 974-A, 974-B, phlorofucofureoeckol A and phlorofucofureoeckol B (Kang et al., 2005; Kannan et al., 2013; Lee et al., 2010; Shrestha et al., 2020; Shrestha et al., 2021; Yoon et al., 2008; Yotsu Yamashita et al., 2013). This large class of marine-derived polyphenolic compounds has been studied for a range of biological activities including antioxidant, antidiabetic, anticancer, antiviral, antimicrobial, anti-inflammatory, and neuroprotective activity as described in our previous review (Shrestha et al., 2021).

Previously we reported the neuroprotective potential of an extract and its solvent-soluble fractions, along with tentative phlorotannins identified from *E. radiata* (Shrestha et al., 2020). Further analytical identification of constituent bioactive phlorotannins is limited however, due to the complex structural and conformational nature of phlorotannins, while their isolation via traditional chromatography is time consuming and provides low yields (Lee et al., 2014).

High performance counter current chromatography (HPCCC) is a separation technique based on the difference in the distribution of analytes in two immiscible liquid phases (Berthod and Faure, 2015). It has various advantages over traditional chromatographic techniques including high capacity, low solvent consumption, high yield, flexible-elution modes, and scalability.

In the present study, we isolated a phlorotannin from *E. radiata* using HPCCC combined with size exclusion chromatography for the first time from this species. The phlorotannin was analyzed by nuclear magnetic resonance (NMR) and mass spectrometry and was identified as dibenzodioxin-fucodiphloroethol (DFD) (Figure 1). Subsequently, the neuroprotective activity of this compound was evaluated in an *in vitro* neuronal PC-12 cell line against the hallmark neurotoxic protein found in Alzheimer's disease, amyloid β (Aβ), demonstrating the isolation and identification of this constituent neuroprotective phlorotannin.

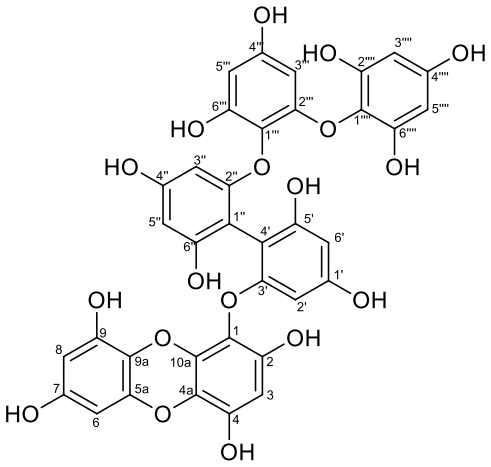

Fig. 1. Structure of dibenzodioxin-fucodiphloroethol.

Materials and methods

Plant material

Brown seaweed (*Ecklonia radiata*) was obtained from freshly deposited beach-cast seaweed in Rivoli Bay, Beachport, South Australia as previously described (Shrestha et al., 2020) and was authenticated by the State Herbarium of South Australia.

Extraction and fractionation of the extract

Seaweed kelp was rinsed with freshwater and dried in the oven at 50 ˚C for 24 hours, blended (Blendtec, Orem, UT, USA) and sieved (< 0.5 mm) to maintain consistent particle size. Extraction and fractionation of the extract were performed as previously described (Shrestha et al., 2020). Briefly, 900 g of powdered sample was extracted with 80 % ethanol at room temperature. The supernatant was filtered, concentrated, and dried completely. The powdered extract was resuspended in water and then defatted and fractioned with ethyl acetate and butanol. The ethyl acetate soluble fraction had a yield of 8.9 gm.

Preparation of two-phase solvent system

The two-phase solvent system comprising of *n*-hexane/ethyl acetate/methanol/water (2:8:2:8, v/v/v/v) was used for the HPCCC. The required volume of solvents was mixed vigorously in a separating funnel and allowed to equilibrate at room temperature. When the two separate layers were visible, the lower aqueous phase was removed and used as a mobile phase while the upper organic phase was used as a stationary phase.

HPCCC separation procedure

HPCCC separation was performed as described previously (Shrestha et al., 2020). Briefly, the HPCCC column was filled with the organic stationary phase and rotated at 800 rpm; the mobile aqueous phase was pumped into the column in the descending mode at the flow rate of 2 ml/min until the hydrodynamic equilibrium was maintained. 500 mg of the sample was dissolved in 6 ml of the biphasic system and injected through the injection valve. The effluent was monitored by UV at 290 nm and 6ml fractions were collected in a fraction collector.

Analytical procedure

HR-ESI-MS spectra were obtained in positive mode on Waters Synapt HDMS. External mass calibration was performed via injection of Sodium formate with a capillary voltage 3.5 kV, mass range 100-1000 m/z, source temperature 80 ℃, desolvation temperature 150 ℃ capillary voltage 3.5kV, desolvation gas flow rate 500 L/hr, sampling cone 40 V and extraction cone 4 V.

NMR spectra were recorded on either a Bruker Avance III 600 or 400 MHz NMR spectrometer using DMSO-d_6 as a solvent at 25 and 26˚C respectively. 1D and 2D spectra were recorded using standard Bruker pulse programs for HSQC, HMBC, and NOESY (evolution time 600us). Band selective HMBC were recorded using phase sensitive CT-HMBC with Chirp selective pulses and a two pass filter to remove one-bond coupling.

Chemical shifts were recorded in ppm and coupling constants (*J* values) recorded in Hz. Peaks were designated as m (multiplet), d (doublet), s (singlet), bs (broad singlet), and vbs (very broad singlet). Molecular modeling of the structure of DFD was undertaken via Spartan 16 version 2.07 software (Wavefunction, Inc. Irvine, CA).

TLC was performed with precoated Merck Kiesel gel 60 F_{254} plates. Spots were visualized by spraying with 25% H_2SO_4 followed by heating. All solvents used for HPCCC were of analytical grade (ChemSupply, Australia).

Dibenzodioxin-fucodiphloroethol (DFD) properties:

Dark brown powder; ^{1}H NMR (DMSO-d_6, 600 MHz) δ 10.01 (1H, vbs, OH-6"), 9.46 (1H, s, OH-4), 9.36 (1H, vbs, OH-9), 9.21 (1H, bs, OH-4"), 9.16 (1H, s, OH-7), 9.14 (1H, bs, OH-1'), 9.07 (2H, bs, OH-2"", OH-6""), 8.99 (1H, s, OH-4'"), 8.90 (s, 1H, OH-4""), 8.85 (1H, vbs, OH-2), 8.65

(1H, vbs, OH-6'''), 6.12 (2H, m, OH-3, OH-5''), 6.09 (1H, bs, OH-6'), 5.99 (1H, d, *J* = 1.5 Hz, OH-2'), 5.95 (1H, d, *J* = 2.5 Hz, OH-8), 5.88 (1H, d, *J* = 2.8, OH-5'''), 5.84 (2H, s, OH-3'''', OH-5''''), 5.81 (1H, d, *J* = 2.5 Hz, OH-6), 5.70 (1H, d, *J* = 1.5 Hz, OH-3''), 5.52 (1H, d, *J* = 2.8, OH-3'''); ^{13}C NMR (DMSO-*d*$_6$,150 MHz): δ 158.03, 157.81, 157.73, 157.69, 154.66, 154.61, 153.06, 151.19, 150.00, 146.01, 142.39, 142.18, 123.49, 123.25, 122.63, 122.58, 122.08, 98.48, 98.06, 97.29, 96.74, 95.79, 94.84, 94.71, 93.70, 93.35, 92.65. Peaks at 101.4, 137.2, 144.7 and 155.7 reported in the literature ^{13}C spectrum for DFD were not observed in our spectrum due to inadequate S/N. However, all of these carbon signals were observed to correlate with various protons in band selective HMBC experiments. HR-MS (ESI) showed a peak at 767.0883 consistent with the calculated value for $C_{36}H_{24}O_{18}$.Na (767.0860). These were in agreement with the values reported from the recent isolation of DFD from *Ecklonia cava* (Cho et al., 2019).

Neuronal cell culture and Aβ$_{1-42}$ preparation

Rat pheochromocytoma PC-12 (Ordway) cells displaying a semi-differentiated neuronal phenotype with neuronal projections were used for viability measurements. Native non-fibrillized amyloid β (Aβ$_{1-42}$) was obtained from rPeptide (Bogart, Georgia, USA) and prepared as described previously (Shrestha et al., 2020). PC-12 cells were maintained in RPMI-1640 media with 10% (v/v), foetal bovine serum (FBS), 1% (v/v) penicillin/streptomycin and 1% (v/v) non-essential amino acids and incubated at 37 °C with 5% CO_2.

Treatment and cell viability measurements

Cells were seeded in a 96 well plate at 2×10^4 cells per well and incubated for 24 h before treatment. The effect of DFD on PC-12 cells was tested by prior incubation (0-50 μM for 48 h) to determine any intrinsic toxicity in separate experiments. Thereafter, cells were pretreated with a non-toxic concentration (50 μM) of DFD for 15 min prior to treatment with non-fibrillized Aβ$_{1-42}$ (0 -1.5 μM)

and incubated for 48 h. Cell viability was measured via MTT assay at 570 nm using a Synergy MX microplate reader (Bio-Tek, Bedfordshire, UK).

Transmission electron microscopy of $A\beta_{1–42}$ fibril and aggregate morphology

$A\beta_{1-42}$ (10 µM) was incubated alone or with 50 µM of DFD for 48 h at 37 °C. The interaction between $A\beta_{1–42}$ aggregation and DFD was then visualized using an FEI Technai G2 Spirit Transmission Electron Microscope (FEI, Milton, QLD, Australia) as previously described (Shrestha et al., 2020).

Acetylcholinesterase inhibitory assay of DFD

Acetylcholinesterase (AChE) inhibitory assay of DFD was performed as mentioned previously (Shrestha et al., 2018). Electric eel AChE, acetylthiocholine iodide, 5,5′-dithiobis-(2-nitrobenzoic acid) (DTNB), and berberine were purchased from Sigma-Aldrich (Sydney, Australia). Briefly, the assay was performed in 96 well plates and all dilutions were prepared in sodium phosphate buffer (pH 8.0) with less than 0.1% DMSO in the final concentration. Absorbance was measured at 412 nm in a BioTek Synergy Mx microplate reader (BioTek, Vermont, USA). Berberine was used as a positive control. The percentage of inhibition was obtained by the following equation:

$$\%\ Inhibition = \left(1 - \frac{As}{Ac}\right) \times 100$$

As = Absorbance of sample

Ac = Absorbance of control

Molecular modeling studies of DFD with $A\beta_{1-42}$ and acetylcholinesterase

The 3D structure of DFD was optimized by Spartan 16 version 2.07 software (Wavefunction, Inc. Irvine, CA) and was docked with the $A\beta_{1-42}$ monomer (PDB ID: 1IYT) and pentamer (PDB ID: 2BEG) using CLC Drug Discovery Workbench (v2.4.1) as described previously (Marsh et al.,

2017; Marsh and Smid, 2020). The 3D X-ray crystal structure of AChE complexed with donepezil was retrieved from Protein Data Bank (PDB ID: 4EY7) and unwanted chains and water molecules were removed using CLC Drug Discovery Workbench (v2.4.1). The binding pockets of AChE were determined and the binding site was established centered around donepezil and defined to enclose residues located within 13 Å as mentioned previously (Cheung et al., 2012; Jang et al., 2018; Shrestha et al., 2018). The protocol was validated by re-docking the co-crystal ligands donepezil with co-crystal protein structure 4EY7. Finally, DFD was docked with the catalytic and peripheral pocket of AChE. The results were exported and visualized via Discovery Studio 2021 Client (Accelrys, San Diego, USA).

Measurement of intracellular ROS levels

The level of intracellular ROS was determined by using DCFDA / H2DCFDA - Cellular ROS Assay Kit (Abcam; Australia) according to the manufacturer's instructions. Briefly, PC-12 cells were stained with DCFDA (20 µM) for 30 min at 37°C in the dark. Cells were then washed with PBS and pretreated with DFD (50 µM) in phenol red-free media followed by treatment with t-BHP (50 µM) and incubated for 4 hours at 37°C in the dark. Fluorescence intensity was subsequently measured with excitation/emission wavelengths at 485 nm / 535 nm in a BioTek Synergy Mx microplate reader (BioTek, Vermont, USA).

Statistical analysis

All cell experiments were carried out in quadruplicate and average viability values were recorded from at least three independent experiments. Data obtained from the MTT assay and ROS were analyzed via two-way analysis of variance (ANOVA) with a Bonferroni's post hoc test used to determine the significance level ($p < 0.05$). Acetylcholinesterase activity was analyzed via one-

way ANOVA with a Dunnett's post-hoc test. Data analysis and graphs were performed in GraphPad Prism 8 (GraphPad Software, San Diego, USA).

Results and discussion

Selection of the high-performance counter current chromatography two-phase system

HPCCC is a liquid-liquid separation technique based on the difference in the distribution of analytes in two immiscible liquid phases in both stationary and mobile phases. Selecting a suitable solvent system is the first and most important step in the isolation of natural products via HPCCC. A generally useful estimate of the solvent systems (GUESS) method was used to determine the most suitable solvent system for our study (Brent Friesen and Pauli, 2005). GUESS method has been established as a simple, reproducible, and efficient method for natural product purification necessary for drug discovery, bioassay-guided fractionation, and metabolome analysis (Brent Friesen and Pauli, 2005). The method relies on the elucidation of a "sweet spot" where the partition coefficient (P) values are between 0.4 and 2.5 and can be correlated with R*f* values between 0.29 and 0.71 (optimal value 0.5) (Brent Friesen and Pauli, 2005; Liu et al., 2015). Herein, the TLC-based GUESS method was used for the selection of a two-phase solvent system. Briefly, the TLC of the sample was compared with eckol, dieckol, phlorofucofuroeckol-A, and phloroglucinol with various ratios of chloroform, methanol, and water. The mixture with an R*f* value of 0.5 was chosen that corresponds to the HEMW mixture +6 (2:8:2:8) suggested by Friesen and Pauli (Brent Friesen and Pauli, 2005).

Phlorotannin separation

The ethyl acetate soluble fraction (500 mg) was completely dissolved in a 6 ml (1:1) biphasic system. The sample was then injected and different flow rates and rotation speeds were evaluated and optimized. The flow rate of 2ml/min and rotation speed of 800 rpm was ideal for separation.

HPCCC was performed in the descending mode with the upper organic phase acting as the stationary phase and the lower aqueous phase as the mobile phase. Altogether, 100 tubes of 6 ml volume were each collected via a fraction collector and then combined to F1 to F5 according to their TLC pattern. DFD was found in the F4 fraction (176 mg), which was purified using Sephadex LH-20 column chromatography. Methanol was used as a mobile phase to obtain pure DFD (6.9 mg). Recently, Zhou et al. (2019) used similar techniques for the isolation of a similarly sized 6-phloroglucinol residue phlorotannin, eckmaxol from *Ecklonia maxima* (Zhou et al., 2019).

Structure elucidation

DFD was obtained as a dark brown powder and its structure was identified by a combination of 1D and 2D NMR spectra including 1D ^{1}H and ^{13}C and 2D COSY, HSQC, HMBC (broad and band selective), and NOESY (Figure 2 and ESI material).

The ^{1}H NMR spectrum (DMSO) revealed 11 signals in the 8.6-10 ppm region that corresponded to hydroxy proton resonances, some of which were considerably broadened (see ESI). The aromatic proton resonances were centered around the 5.8 ppm region and consisted of a series of doublets, one singlet (5.86 ppm) and a multiplet in which two resonances were overlapping (6.10 ppm). Analysis of coupling constants and coupling networks (COSY) allowed the identification of protons on the same aromatic ring (Figure 2). NOESY spectra allowed the adjacent hydroxyl proton resonances to be identified and linked with each aromatic ring. Our assignment of several of the hydroxyl proton resonances (see ESI) differed from that reported for DFD recently isolated from *Ecklonia cava* by Cho et al. (Cho et al., 2019).

The ^{13}C resonances were grouped into three chemical shift regions. The phenolic substituted carbon atoms (140-160 ppm), ether ring carbon atoms (120-125ppm), and finally non-oxygenated aromatic carbon atoms (90-100ppm). In comparison to literature spectral data of DFD, four

resonances were not evident in our 1D ^{13}C spectrum due to lower signal-to-noise compared with the literature spectrum (Cho et al., 2019). However, correlations to these peaks were evident in the HMBC spectra, allowing us to be confident of their presence within the molecule. Using a combination of HSQC and HMBC the various ^{13}C resonances were assigned. Some ^{13}C resonances were assigned by comparison with the literature (Cho et al., 2019) and these are color coded on the structure of DFD in Figure 2.

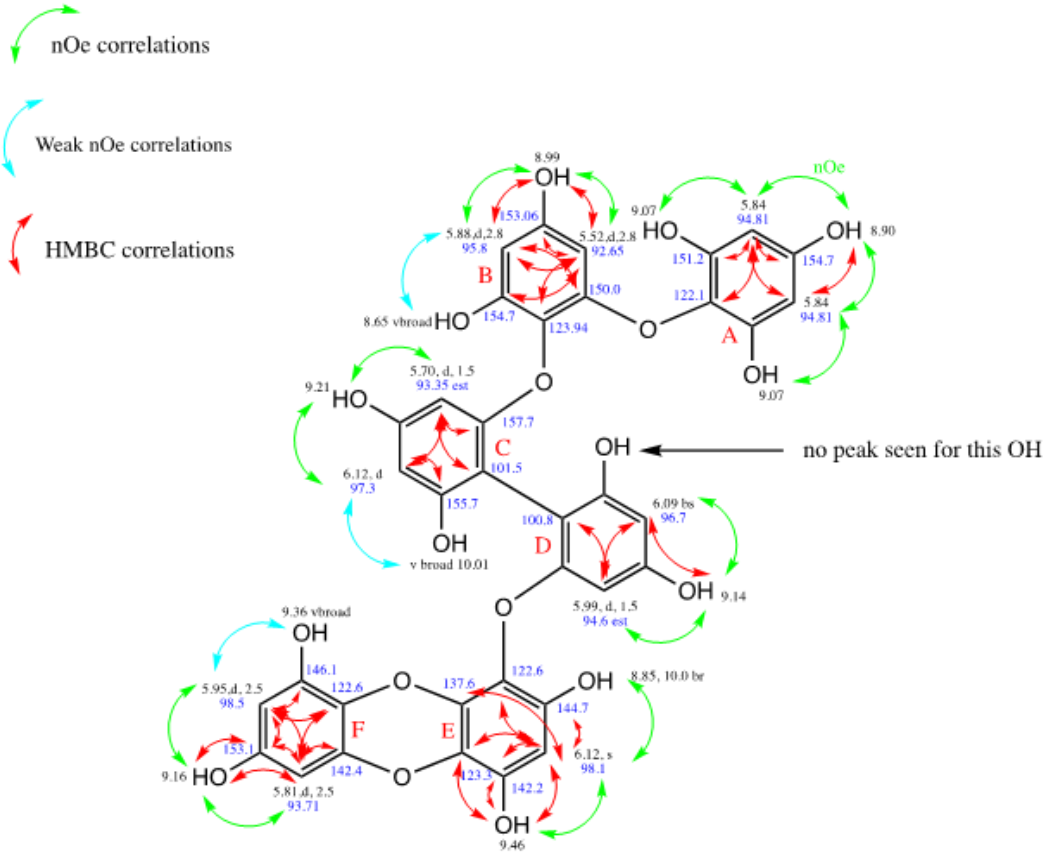

Fig. 2. Key NOE and HMBC correlations of DFD.

Molecular modeling of the structure of DFD was also undertaken via Spartan 16 version 2.07 software to gain an understanding of the overall conformation of DFD. A conformational analysis using MM2 was subsequently refined with the lowest 22 energy structures recalculated using *ab initio* methods (6-31G*). These results showed 16 conformations of DFD all lie within 4 kJ/mol of each other and hence the molecule may adopt a range of conformations at room temperature.

The sample was analyzed by ESI-HRMS, which showed a peak at 767.0883 consistent with the calculated value for $C_{36}H_{24}O_{18}$.Na (767.0860). Confirmatory MS was performed using ESI-MS. The isolated DFD compound was determined to be high purity by ^{1}H-NMR (see ESI S1) with minor impurity peaks evident in the aliphatic region of the spectrum.

Neuroprotective activity of DFD against Aβ$_{1-42}$

Treatment of PC-12 cells with DFD (0-50μM) did not elicit toxicity as shown in Figure 3A. Therefore, 50 μM DFD was used for subsequent neuroprotection experiments. Aβ$_{1-42}$ demonstrated a concentration-dependent loss of PC-12 cell viability after 48 h of incubation (Figure 3B), with neuronal cell viability decreased to 74.6 % at 1.5 μM Aβ$_{1-42}$ versus control (Figure 3B). When PC-12 cells were pretreated with 50 μM of DFD followed by Aβ$_{1-42}$ treatment, the phlorotannin significantly rescued cell viability at 1.0 and 1.5 μM Aβ$_{1-42}$ concentrations (Figure 3B). These results with DFD are generally consistent with the capacity of selected phlorotannins to rescue neuronal cell lines affected by amyloid β exposure (Ahn et al., 2012; Lee et al., 2019). Phlorotannins have also previously been shown to inhibit intracellular ROS generation and calcium release in a concentration-dependent manner arising from amyloid β exposure (Ahn et al., 2012). Furthermore, these compounds have also been reported to have anti-apoptotic and anti-inflammatory effects against amyloid β induced damage in PC-12 cells by suppressing intracellular oxidative stress, mitochondrial dysfunction, and activation of caspases, in addition to downregulating proinflammatory enzymes via negative regulation of the NF-κB pathway (Lee et al., 2019).

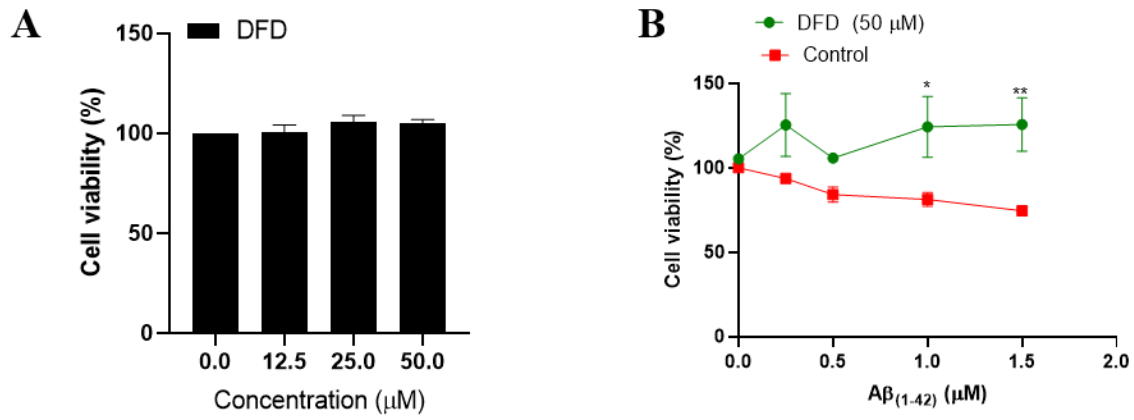

Fig. 3. Neuroprotective activity of DFD in $A\beta_{1–42}$ stimulated PC-12 cells. (A) DFD did not exert any intrinsic cytotoxicity in PC-12 cells up to 50 μM. (B) Prevention of $A\beta_{1–42}$ induced cell death by DFD. The cells were pretreated with 50 μM of DFD for 15 min prior to exposure with $A\beta_{1–42}$ (0–1.5 μM) for 48 h. ** $p < 0.01$, * $p < 0.05$ vs control (n = 3).

Transmission electron microscopy: $A\beta_{1–42}$ aggregation is inhibited by DFD

Transmission electron microscopic examination of the morphology of $A\beta_{1–42}$ aggregates incubated with or without DFD (50 μM) is shown in Figure 4. It can be clearly seen that DFD significantly reduced the aggregation of $A\beta_{1–42}$ (Figure 4). Negligible areas of dense staining were found when $A\beta_{1–42}$ protein was incubated with DFD for 48 hours, indicating its anti-aggregatory properties. These results suggest that part of the neuroprotective activity of DFD may be attributable to inhibition of aggregation of $A\beta_{1–42}$. Similar results were found when the phlorotannin-rich extract (ethyl acetate soluble fraction) from *E. radiata* was incubated with $A\beta_{1–42}$ previously, where neuroprotection was associated with a reduced prevalence and density of $A\beta_{1–42}$ aggregates (Shrestha et al., 2020). DFD may therefore contribute to this effect.

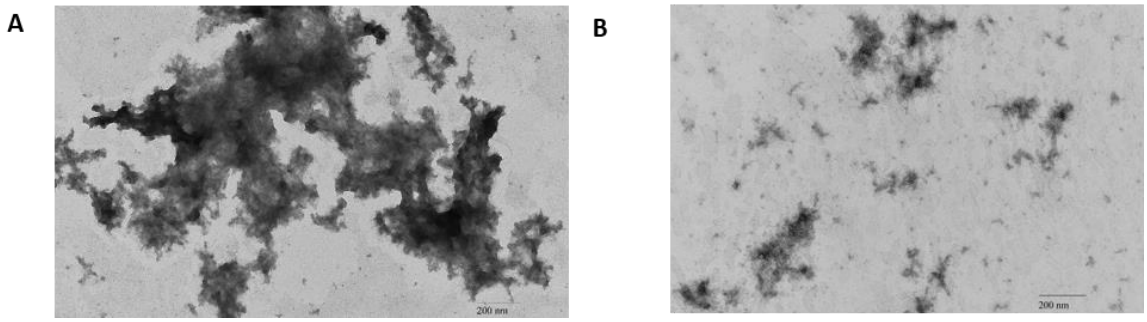

Fig. 4. Representative images of Aβ1–42 fibril and aggregate formation, (A) alone and (B) following 48 h incubation with DFD (50 µM). Prior DFD incubation clearly inhibited aggregation density.

Molecular modeling of DFD with $A\beta_{1\text{-}42}$

The neurotoxicity of the Aβ is linked with the formation of the β-sheet structure believed to promote it (Broersen et al., 2010). Thus, molecules with the ability to inhibit the formation of β-sheets are known to inhibit the aggregation and neurotoxicity associated with it (Harvey et al., 2011). Since DFD significantly reduced the aggregation of $A\beta_{1–42}$ in vitro, *in silico* studies were performed to understand the binding modes with $A\beta_{1–42}$. Docking results for DFD with $A\beta_{1\text{-}42}$ monomer (PDB: 1IYT) are summarized in Table 1. DFD bound towards the centre and displayed a strong affinity for the monomer (PDB: 1IYT) with a docking score of -43.28, forming two hydrogen bonds with HIS14 and GLU11 as shown in Figure 5 (A and B) and Table 1. The compound demonstrated a steric interaction score and hydrogen bond score of -32.92 and -8.75, respectively. The hydroxyl group of ring C and D were involved in the hydrogen bond interaction with the HIS14 and GLU11, respectively. Additionally, GLN15, LEU17, PHE19, GLU22 were noted to be involved in the van der Waals interactions. The dibenzo-*p*-dioxin skeleton of the compound showed π-π stacked hydrophobic interaction with HIS14 while ring A and C were involved in π-alkyl interactions with VAL18.

Table 1. Docking profiles of DFD with the $A\beta_{1-42}$ monomer (PDB: 1IYT) and pentamer (PDB: 2BEG).

Aβ protein	Docking score	Steric interaction score	Hydrogen bond score	H-bond forming residues	Van der Waals residues	Others	
						π-π stacked	π-Alkyl
1IYT	-43.28	-32.92	-8.75	HIS14, GLU11	GLN15, LEU17, PHE19, GLU22	HIS14	VAL18
2BEG	-64.01	-62.26	-12.64	Chain A: PHE19, ALA21	Chain A: LEU17, GLU22, VAL36, GLY37, GLY38, VAL39; Chain B: VAL36, GLY38	Chain A: PHE20	Chain A: VAL18, VAL40; Chain B: VAL40

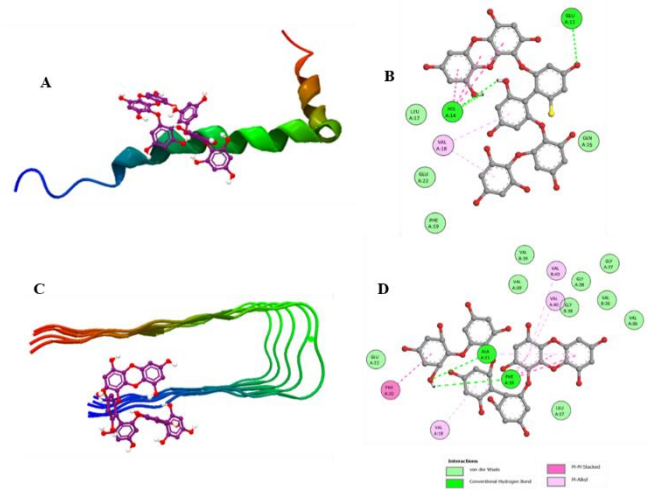

Fig. 5. Docking positions for DFD with $A\beta_{1-42}$ monomer (PDB: 1IYT) (A and B) and pentamer (PDB: 2BEG) (C and D).

Docking results for DFD with Aβ pentamer (PDB: 2BEG) are summarized in Table 1. 2BEG is a fibril structure that comprises five aligned Aβ monomers (chains A, B, C, D, and E) side by side to form β-sheets each consisting of 17-42 residues (Lührs et al., 2005). As shown in Figure 5(C and D), DFD bound towards chain A and interacted with the amino acid residues of both chains A and B with a docking score of -64.01. Two hydrogen bond interactions were observed between the hydroxyl group of ring A with PHE19 and ALA21 of chain A with a hydrogen bond score of -12.64. Furthermore, a high degree of steric interaction was observed with a score of -62.26. The compound also interacted with amino acid residues LEU17, GLU22, VAL36, GLY37, GLY38, and VAL39 of chain A and VAL36 and GLY38 of chain B via Van der Waals interactions.

Furthermore, ring B and the dibenzo-*p*-dioxin skeleton of the compound were found to interact via π-π stacked hydrophobic interactions with PHE20 and PHE19 of chain A, respectively. Additionally, ring C interacted with VAL18 (chain A) and ring E and F of the dibenzo-*p*-dioxin skeleton interacted with VAL40 (chain A and B) and ALA21, respectively via π-alkyl interaction.

Previously, the ^{16}KLVFFA^{21} segment of the protein has been identified as a key segment for nucleation and fibrillisation, which forms extended β-strands and stacks repetitively to form the Aβ core (Landau et al., 2011; Lu et al., 2019). In addition, the C-terminal segment ^{37}GGVVIA^{42} was reported to have an essential role in fibril formation (Landau et al., 2011; Lu et al., 2019). Furthermore, polyphenols interacting with HIS13, HIS14, and PHE19 to ALA21 were linked to the inhibition of Aβ nucleation and elongation (Hanaki et al., 2016). The interaction of DFD to these residues (Figure 5 and Table 1) might have potentially hindered the formation of a stable fibril structure, thus preventing aggregation.

Acetylcholinesterase (AChE) inhibitory activity of DFD

Alzheimer's Disease (AD) is accompanied by a loss of the neurotransmitter acetylcholine in areas associated with working memory such as the hippocampus, which facilitates cognitive decline (Francis et al., 1999; Haake et al., 2020). Thus, inhibition of AChE, which catalyzes the breakdown of acetylcholine is an established symptomatic therapy (Francis et al., 1999), with donepezil, galantamine, and rivastigmine all approved for the treatment of mild to moderate AD (Piton et al., 2018). In order to assess the potential multimodal bioactivity of DFD, it was assessed for its ability to inhibit AChE.

Table 2. Acetylcholinesterase inhibitory activity of DFD with positive control berberine

Compounds	IC_{50} ± SD (μM)
Dibenzodioxin-fucodiphloroethol (DFD)	41.09 ± 7.06***
Berberine	0.91 ± 0.001***

All values are shown as mean ± standard deviation. *** $p < 0.001$ vs control (n = 3).
DFD demonstrated a moderate and concentration-dependent inhibition of acetylcholinesterase activity, with an IC_{50} of 41.09 ± 7.06 μM (Table 2). Berberine was approximately 45 times more potent than DFD at inhibiting AChE as a positive control (Table 2).

Molecular docking simulation of DFD with AChE

The proposed binding modes of DFD and donepezil with AChE (PDB: 4EY7) are illustrated in Figure 6 and Table 3. It can be clearly seen that the orientation of the ligand (DFD) resembles that of donepezil, sharing similar interacting binding residues in the crystallized structure. As seen in Figure 6 and Table 3, DFD formed three hydrogen bonds with the protein and had a docking score of -43.48. In addition, the steric interaction score and hydrogen bond score were found to be -34.67 and -19.96, respectively. The hydroxyl group of ring A and ring F formed two hydrogen bonds (one each) with ALA204 and ARG296, respectively. The oxygen atom connecting the ring D and ring E formed the additional hydrogen bond with TYR124. The compound also interacted with TYR72, ASP74, TRP86, GLY120, GLY121, GLY122, TYR133, SER293, Val294, PHE297, TYR337, VAL340, GLY448, and ILE451 residues via Van der Waals interactions. Additionally, the docking results also exposed π-π stacking, where all aromatic rings of DFD interacted with the active site and formed π-π stacking with TYR124, TRP286, PHE338, TYR341, TRP236, and

HIS447 amino acid residues. In addition, π-alkyl interactions were observed between ring A and GLY122, which plays an important role in the stabilization of the inhibitor at the active site.

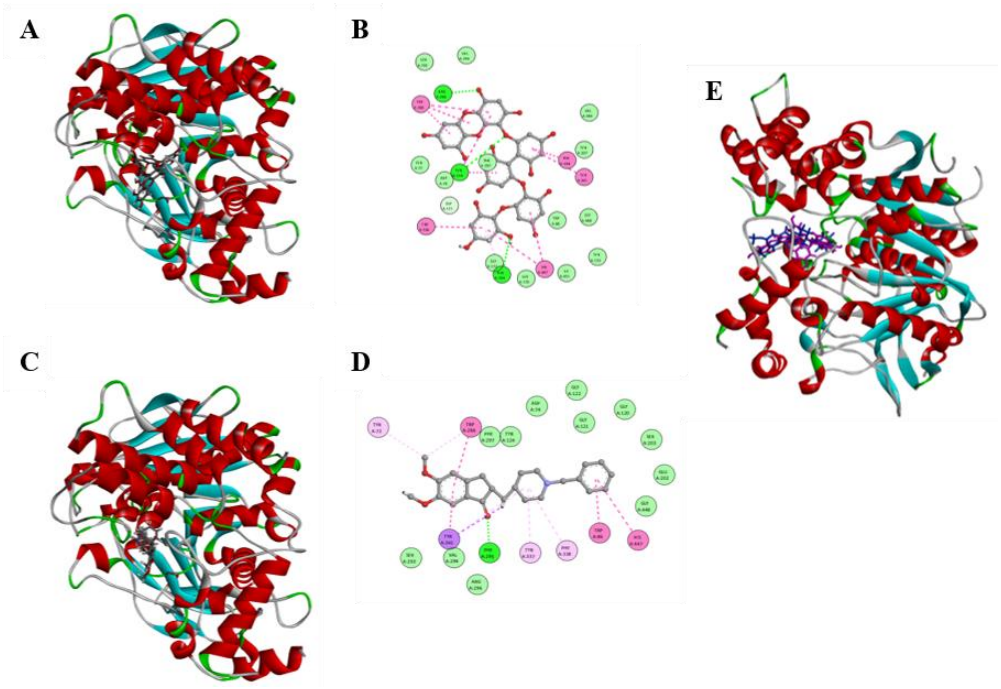

Fig. 6. Docking positions for DFD (A) and donepezil (C) with AChE (PDB: 4EY7). 2D diagram of DFD (B) and donepezil (C) interaction with AChE. Binding mode of DFD (pink) and donepezil (blue) in the catalytic and peripheral pocket of 4EY7 (E).

Table 3. Docking profiles of DFD with the AChE (PDB: 4EY7).

Samples	Docking score	Steric interaction score	Hydrogen bond score	H-bond forming residues	Van der Waals forming residues	Others		
						π-π stacked	π-Alkyl	π-Sigma
DFD	-43.48	-34.67	-19.96	TYR124, ALA204, ARG296	TYR72, ASP74, TRP86, GLY120, GLY121, GLY122, TYR133, SER293, Val294, PHE297, TYR337, VAL340, GLY448, ILE451	TYR124, TRP286, PHE338, TYR341, TRP236, HIS447	GLY122	-
Donepezil	-100.97	-102.01	-2.00	PHE295	ASP74, GLY120, GLY121, GLY122, TYR124, GLU202, SER203, SER293, VAL294, ARG296, PHE297, GLY448,	TRP86, TRP286, HIS447	TYR72, TYR337, PHE338	TYR341

Measurement of intracellular reactive oxygen species levels

Intracellular reactive oxygen species (ROS) levels in PC-12 cells were analyzed by the DCFDA fluorescence assay. 2,7-dichlorodihydro-fluorescein diacetate is deacetylated by cellular esterases to a non-fluorescent compound, which is later oxidized by ROS into 2,7-dichlorofluorescein (highly fluorescent) and can be detected by fluorescence spectroscopy (Eruslanov and Kusmartsev, 2010). As shown in Figure 7, t-BHP at a concentration of 50 µM significantly stimulated reactive oxygen species (ROS) generation in PC-12 cells. It increased ROS levels more than two-fold compared with the control group. However, upon pretreatment with 50 µM DFD, ROS levels were significantly attenuated (** $p < 0.01$). This data suggests that DFD may lessen neurotoxicity by reducing ROS impact in neuronal cell lines. Previously, other phlorotannins were also reported to have significantly scavenged intracellular ROS levels and provided protective effects in various cell lines and a zebrafish model (Kang et al., 2005; Kim et al., 2015; Lee et al., 2019).

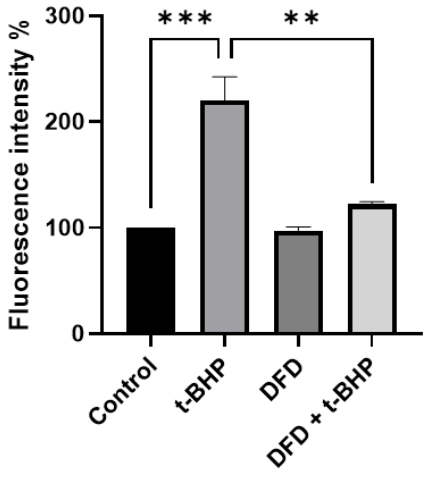

Fig. 7. The ROS scavenging effect of DFD (50 µM) in *t*-BHP (50 µM) incubated PC-12 cells. *** $p < 0.001$ vs control; ** $p < 0.01$ vs *t*-BHP (n = 3).

As with many polyphenols including phlorotannins, DFD ideally should possess adequate bioavailability and cross the blood brain barrier to achieve therapeutic concentrations affording direct neuroprotection. However, comprehensive information on the central nervous system

penetrance of phlorotannins is currently lacking. Fluorone-labelled dieckol derivatives were previously shown to have accessed the central nervous system following intravenous administration (Kwak et al., 2015), while another study indicated that brain access of orally administered eckstolonol was likely via effects on $GABA_A$ receptor activity (Cho et al., 2014). Additionally, recent evidence points to the potential efficacy of polyphenols via indirect actions on the gut microbiome, where a phlorotannin extract afforded behavioral and cognitive benefits in rats associated with marked improvements in gut dysbiosis (Donoso et al., 2020). In further support of the potential importance of the microbiota-gut-brain axis, clinical benefits on cognitive and memory functions of oligomannate derived from *Ecklonia kurome* leading to its recent approval as a dementia medication in China have been largely attributed to positive effects on the gut microbiome (Wang et al., 2019).

Conclusions

Overall, use of HPCCC for the isolation and purification of dibenzodioxin-fucodiphloroethol (DFD) from *E. radiata* enabled sufficient yield of this phlorotannin to conduct a panel of in vitro bioactivity assessments related to neuroprotection. In doing so we were able to demonstrate the neuroprotective activity of DFD against $A\beta_{1–42}$ protein, reducing its propensity for its aggregation while additionally demonstrating acetylcholinesterase inhibition and significant intracellular ROS-scavenging activity. These results highlight the multifaceted neuroprotective roles of this phlorotannin against molecular and cellular neurotoxic pathways attributed to amyloid β neurotoxicity in Alzheimer's disease.

Notes

There are no conflicts to declare.

ACKNOWLEDGEMENTS

Srijan Shrestha is supported by Australian Government Research Training Program (RTP) Scholarship. Wei Zhang acknowledges the support of ARC Industry Transformation and Training Centre for Green Chemistry in Manufacturing, Qingdao Gather Great Ocean Algae Industry Group Co, Ltd and Australian Kelp Products Pty Ltd.

References

Ahn, B.R., Moon, H.E., Kim, H.R., Jung, H.A., Choi, J.S., 2012. Neuroprotective effect of edible brown alga *Eisenia bicyclis* on amyloid beta peptide-induced toxicity in PC12 cells. Arch Pharm Res 35, 1989-1998.

Berthod, A., Faure, K., 2015. Separations with a liquid stationary phase: countercurrent chromatography or centrifugal partition chromatography. Analytical Separation Science, 1177-1206.

Brent Friesen, J., Pauli, G.F., 2005. GUESS—a generally useful estimate of solvent systems for CCC. J. Liq. Chrom. Relat. Tech. 28, 2777-2806.

Broersen, K., Rousseau, F., Schymkowitz, J., 2010. The culprit behind amyloid beta peptide related neurotoxicity in Alzheimer's disease: oligomer size or conformation? Alzheimers. Res. Ther. 2, 12.

Cheung, J., Rudolph, M.J., Burshteyn, F., Cassidy, M.S., Gary, E.N., Love, J., Franklin, M.C., Height, J.J., 2012. Structures of human acetylcholinesterase in complex with pharmacologically important ligands. J. Med. Chem. 55, 10282-10286.

Cho, H.M., Doan, T.P., Ha, T.K.Q., Kim, H.W., Lee, B.W., Pham, H.T.T., Cho, T.O., Oh, W.K., 2019. Dereplication by high-performance liquid chromatography (HPLC) with quadrupole-time-of-flight mass spectroscopy (qTOF-MS) and antiviral activities of phlorotannins from *Ecklonia cava*. Mar. Drugs 17, 149.

Cho, S., Yoon, M., Pae, A.N., Jin, Y.-H., Cho, N.-C., Takata, Y., Urade, Y., Kim, S., Kim, J.S., Yang, H., Kim, J., Kim, J., Han, J.K., Shimizu, M., Huang, Z.L., 2014. Marine polyphenol phlorotannins promote non-rapid eye movement sleep in mice via the benzodiazepine site of the GABAA receptor. Psychopharmacology 231, 2825-2837.

Donoso, F., Egerton, S., Bastiaanssen, T.F.S., Fitzgerald, P., Gite, S., Fouhy, F., Ross, R.P., Stanton, C., Dinan, T.G., Cryan, J.F., 2020. Polyphenols selectively reverse early-life stress-induced behavioural, neurochemical and microbiota changes in the rat. Psychoneuroendocrinology 116, 104673.

Eruslanov, E., Kusmartsev, S., 2010. Identification of ROS Using Oxidized DCFDA and Flow-Cytometry, in: Armstrong, D. (Ed.), Advanced Protocols in Oxidative Stress II. Humana Press, Totowa, NJ, pp. 57-72.

Francis, P.T., Palmer, A.M., Snape, M., Wilcock, G.K., 1999. The cholinergic hypothesis of Alzheimer's disease: a review of progress. J. Neurol. Neurosurg. Psychiatry 66, 137-147.

Haake, A., Nguyen, K., Friedman, L., Chakkamparambil, B., Grossberg, G.T., 2020. An update on the utility and safety of cholinesterase inhibitors for the treatment of Alzheimer's disease. Expert Opin. Drug Saf. 19, 147-157.

Hanaki, M., Murakami, K., Akagi, K., Irie, K., 2016. Structural insights into mechanisms for inhibiting amyloid β42 aggregation by non-catechol-type flavonoids. Bioorg. Med. Chem. 24, 304-313.

Harvey, B.S., Musgrave, I.F., Ohlsson, K.S., Fransson, Å., Smid, S.D., 2011. The green tea polyphenol (−)-epigallocatechin-3-gallate inhibits amyloid-β evoked fibril formation and neuronal cell death in vitro. Food Chem. 129, 1729-1736.

Jang, C., Yadav, D.K., Subedi, L., Venkatesan, R., Venkanna, A., Afzal, S., Lee, E.H., Yoo, J., Ji, E.H., Kim, S.Y., Kim, M.H., 2018. Identification of novel acetylcholinesterase inhibitors designed by pharmacophore-based virtual screening, molecular docking and bioassay. Sci. Rep. 8, 14921.

Kang, K.A., Lee, K.H., Chae, S., Zhang, R., Jung, M.S., Lee, Y., Kim, S.Y., Kim, H.S., Joo, H.G., Park, J.W., 2005. Eckol isolated from *Ecklonia cava* attenuates oxidative stress induced cell damage in lung fibroblast cells. FEBS letters 579, 6295-6304.

Kannan, R.R., Aderogba, M.A., Ndhlala, A.R., Stirk, W.A., Van Staden, J., 2013. Acetylcholinesterase inhibitory activity of phlorotannins isolated from the brown alga, *Ecklonia maxima* (Osbeck) *Papenfuss*. Food Res. Int. 54, 1250-1254.

Kim, E.A., Kang, M.C., Lee, J.H., Kang, N., Lee, W., Oh, J.Y., Yang, H.W., Lee, J.S., Jeon, Y.J., 2015. Protective effect of marine brown algal polyphenols against oxidative stressed zebrafish with high glucose. RSC Adv. 5, 25738-25746.

Kwak, J.H., Yang, Z., Yoon, B., He, Y., Uhm, S., Shin, H.C., Lee, B.H., Yoo, Y.C., Lee, K.B., Han, S.Y., Kim, J.S., 2015. Blood-brain barrier-permeable fluorone-labeled dieckols acting as neuronal ER stress signaling inhibitors. Biomaterials 61, 52-60.

Landau, M., Sawaya, M.R., Faull, K.F., Laganowsky, A., Jiang, L., Sievers, S.A., Liu, J., Barrio, J.R., Eisenberg, D., 2011. Towards a pharmacophore for amyloid. PLoS Biol. 9, e1001080.

Lee, J.H., Ko, J.Y., Oh, J.Y., Kim, C.Y., Lee, H.J., Kim, J., Jeon, Y.J., 2014. Preparative isolation and purification of phlorotannins from *Ecklonia cava* using centrifugal partition chromatography by one-step. Food Chem. 158, 433-437.

Lee, S., Youn, K., Kim, D., Ahn, M.R., Yoon, E., Kim, O.Y., Jun, M., 2019. Anti-neuroinflammatory property of phlorotannins from *Ecklonia cava* on $A\beta_{25-35}$-induced damage in PC-12 cells. Mar. Drugs 17, 7.

Lee, S.H., Park, M.H., Heo, S.J., Kang, S.M., Ko, S.C., Han, J.S., Jeon, Y.J., 2010. Dieckol isolated from *Ecklonia cava* inhibits α-glucosidase and α-amylase in vitro and alleviates postprandial hyperglycemia in streptozotocin-induced diabetic mice. Food Chem. Toxicol. 48, 2633-2637.

Liu, Y., Friesen, J.B., McAlpine, J.B., Pauli, G.F., 2015. Solvent system selection strategies in countercurrent separation. Planta Med. 81, 1582-1591.

Lu, J., Cao, Q., Wang, C., Zheng, J., Luo, F., Xie, J., Li, Y., Ma, X., He, L., Eisenberg, D., Nowick, J., Jiang, L., Li, D., 2019. Structure-based peptide inhibitor design of amyloid-β aggregation. Front. Mol. Neurosci. 12, 54.

Lührs, T., Ritter, C., Adrian, M., Riek-Loher, D., Bohrmann, B., Döbeli, H., Schubert, D., Riek, R., 2005. 3D structure of Alzheimer's amyloid-β(1–42) fibrils. Proc. Nat. Acad. Sc. U. S. 102, 17342-17347.

Marsh, D.T., Das, S., Ridell, J., Smid, S.D., 2017. Structure-activity relationships for flavone interactions with amyloid β reveal a novel anti-aggregatory and neuroprotective effect of 2′, 3′, 4′-trihydroxyflavone (2-D08). Bioorg. Med. Chem. 25, 3827-3834.

Marsh, D.T., Smid, S.D., 2020. Cannabis phytochemicals: A review of phytocannabinoid chemistry and bioactivity as neuroprotective agents. Aust. J. Chem. 74, 338-404.

Piton, M., Hirtz, C., Desmetz, C., Milhau, J., Lajoix, A.D., Bennys, K., Lehmann, S., Gabelle, A., 2018. Alzheimer's disease: Advances in drug development. J J. Alzheimer's Dis. 65, 3-13.

Rothman, M.D., Mattio, L., Wernberg, T., Anderson, R.J., Uwai, S., Mohring, M.B., Bolton, J.J., 2015. A molecular investigation of the genus *Ecklonia* (Phaeophyceae, Laminariales) with special focus on the Southern Hemisphere. J. Phycol. 51, 236-246.

Shrestha, S., Seong, S.H., Paudel, P., Jung, H.A., Choi, J.S., 2018. Structure related inhibition of enzyme systems in cholinesterases and BACE1 in vitro by naturally occurring naphthopyrone and its glycosides isolated from *Cassia obtusifolia*. Molecules 23, 69.

Shrestha, S., Zhang, W., Begbie, A.J., Pukala, T.L., Smid, S.D., 2020. *Ecklonia radiata* extract containing eckol protects neuronal cells against $A\beta_{(1-42)}$ evoked toxicity and reduces aggregate density. Food Funct. 11, 6509-6516.

Shrestha, S., Zhang, W., Smid, S., 2021. Phlorotannins: a review on biosynthesis, chemistry and bioactivity. Food Biosci. 39, 100832.

Wang, X., Sun, G., Feng, T., Zhang, J., Huang, X., Wang, T., Xie, Z., Chu, X., Yang, J., Wang, H., Chang, S., Gong, Y., Ruan, L., Zhang, G., Yan, S., Lian, W., Du, C., Yang, D., Zhang, Q., Lin, F., Liu, J., Zhang, H., Ge, C., Xiao, S., Ding, J., Geng, M., 2019. Sodium oligomannate therapeutically remodels gut microbiota and suppresses gut bacterial amino acids-shaped neuroinflammation to inhibit Alzheimer's disease progression. Cell Res. 29, 787-803.

Yoon, N.Y., Chung, H.Y., Kim, H.R., Choi, J.E., 2008. Acetyl-and butyrylcholinesterase inhibitory activities of sterols and phlorotannins from *Ecklonia stolonifera*. Fish. Sci. 74, 200.

Yotsu Yamashita, M., Kondo, S., Segawa, S., Lin, Y.C., Toyohara, H., Ito, H., Konoki, K., Cho, Y., Uchida, T., 2013. Isolation and structural determination of two novel phlorotannins from the brown alga *Ecklonia kurome* Okamura, and their radical scavenging activities. Mar. Drugs 11, 165-183.

Zhou, X., Yi, M., Ding, L., He, S., Yan, X., 2019. Isolation and purification of a neuroprotective phlorotannin from the marine algae *Ecklonia maxima* by size exclusion and high-speed counter-current chromatography. Mar. Drugs 17, 212.

Appendix A: Supplementary Material

Figure S1. ^{1}H-NMR spectra of dibenzodioxin-fucodiphloroethol

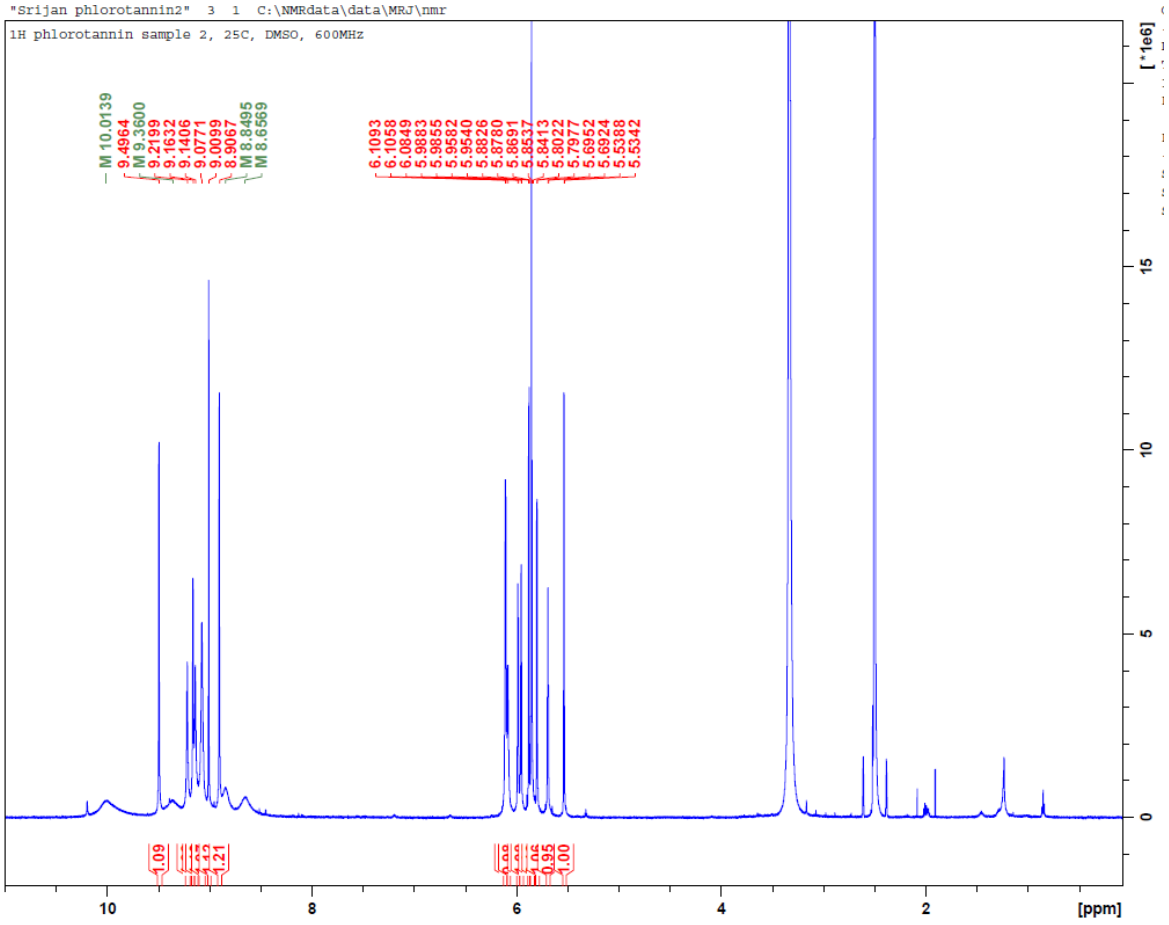

Figure S2. ^{13}C-NMR spectra of dibenzodioxin-fucodiphloroethol

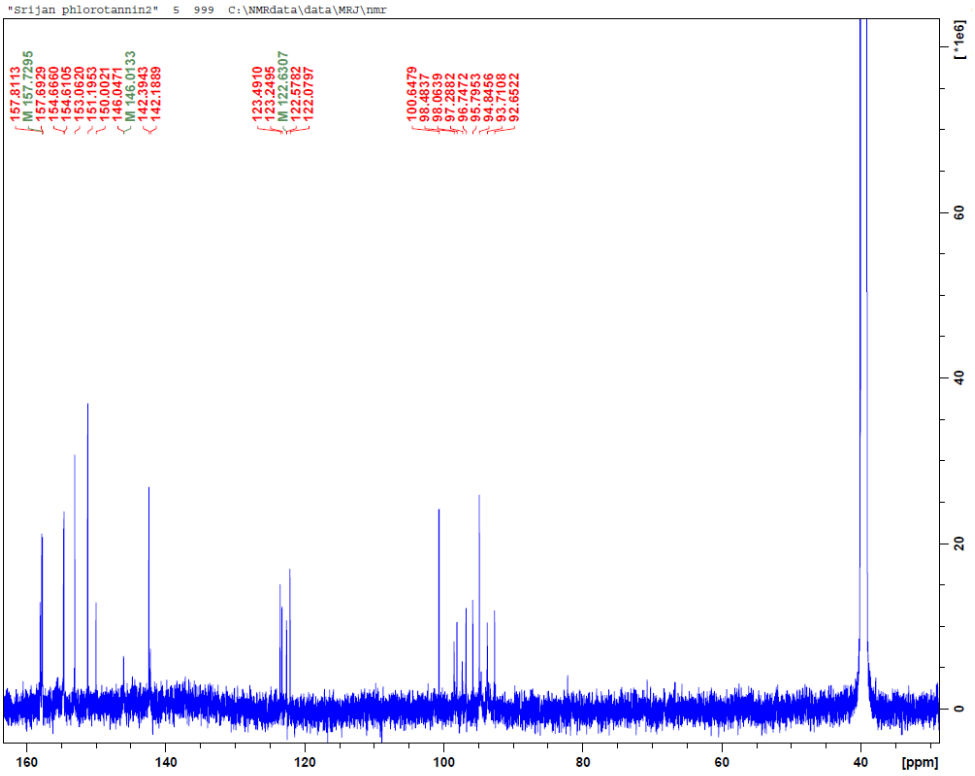

Figure S3. COSY of dibenzodioxin-fucodiphloroethol

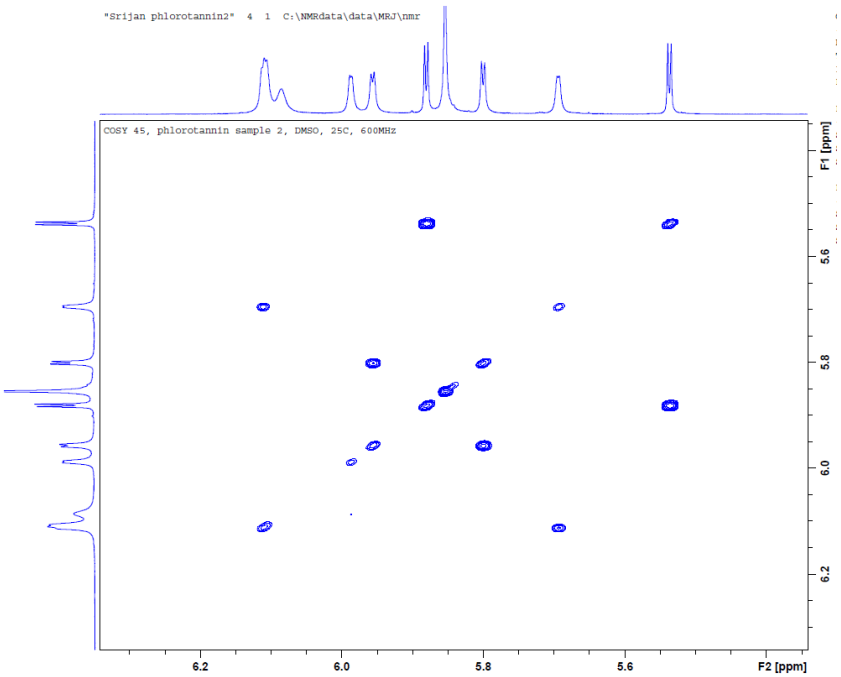

Figure S4. HSQC of dibenzodioxin-fucodiphloroethol

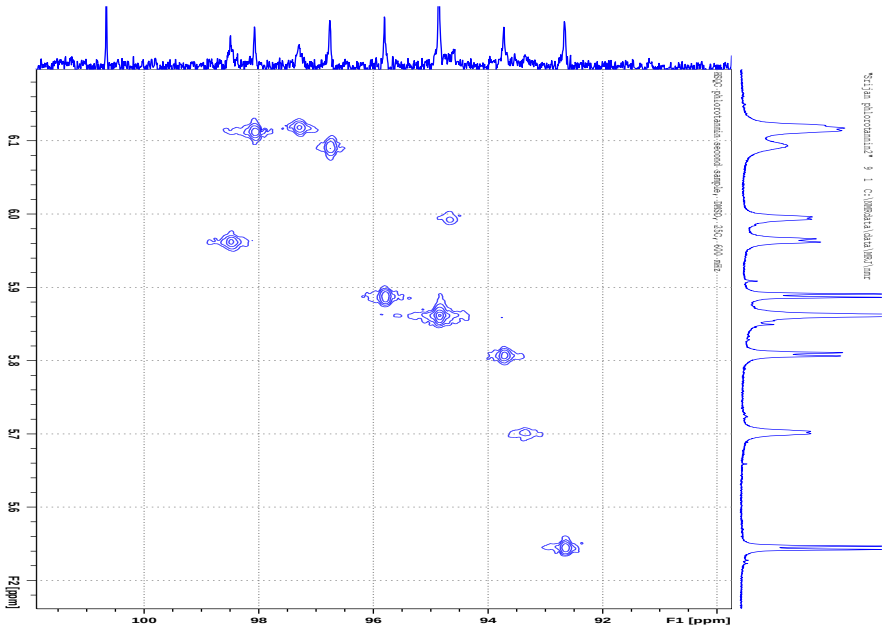

Figure S5. HMBC of dibenzodioxin-fucodiphloroethol

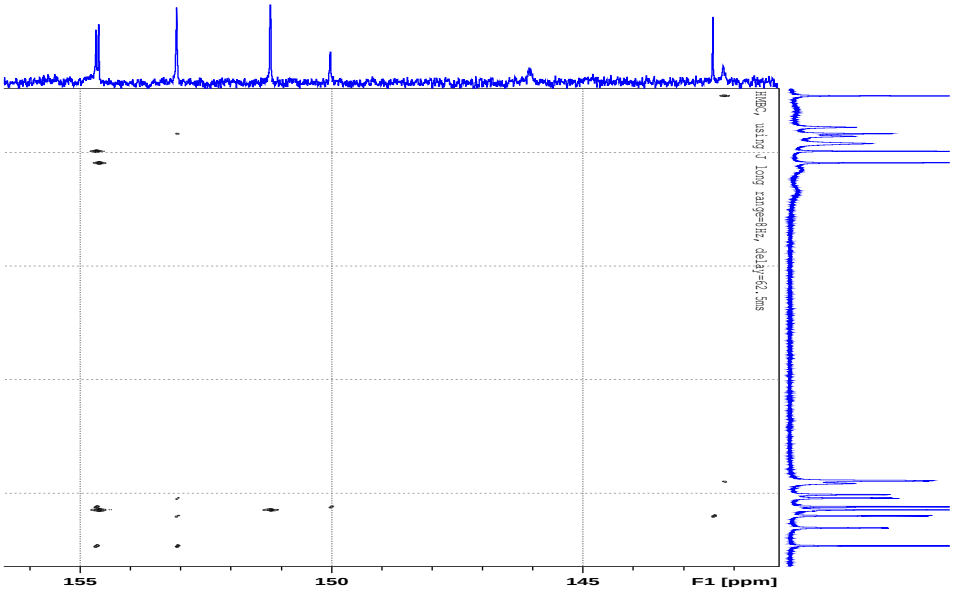

Figure S6. HMBC of dibenzodioxin-fucodiphloroethol

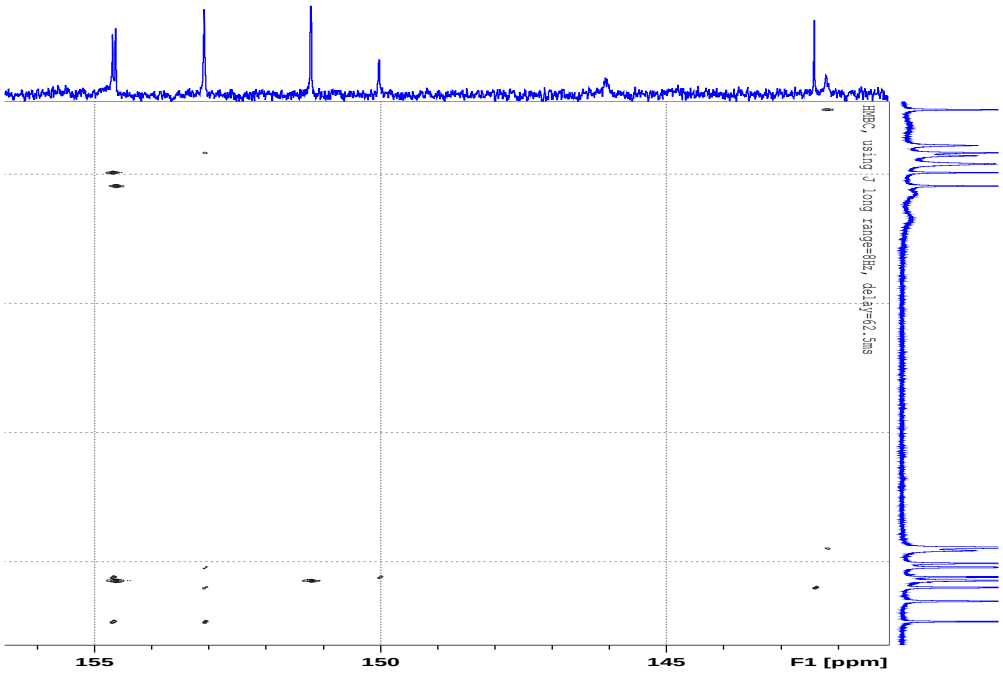

Figure S7. HMBC of dibenzodioxin-fucodiphloroethol

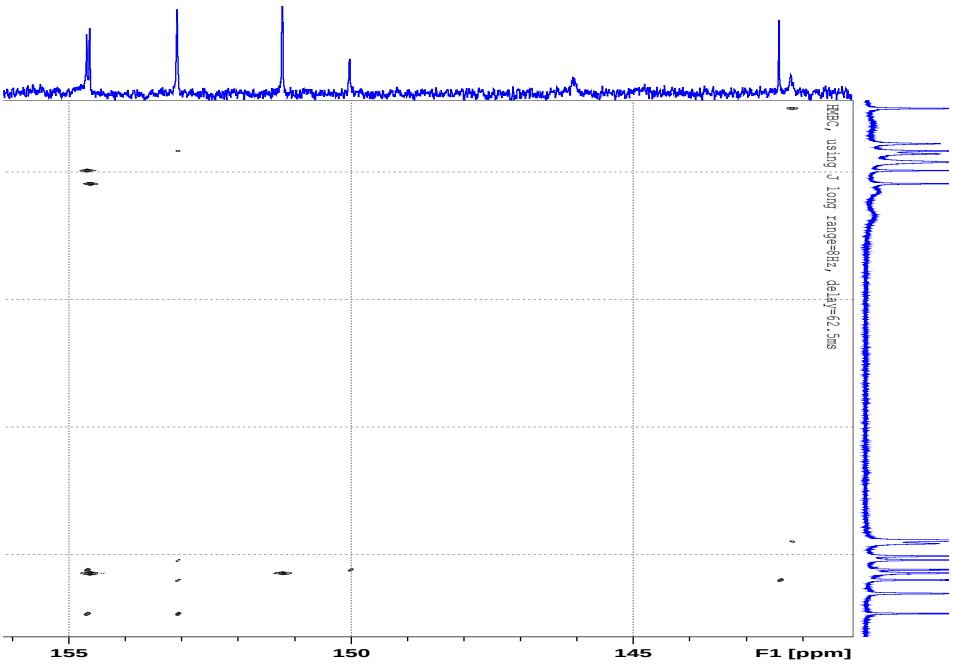

Figure S8. NOESY of dibenzodioxin-fucodiphloroethol

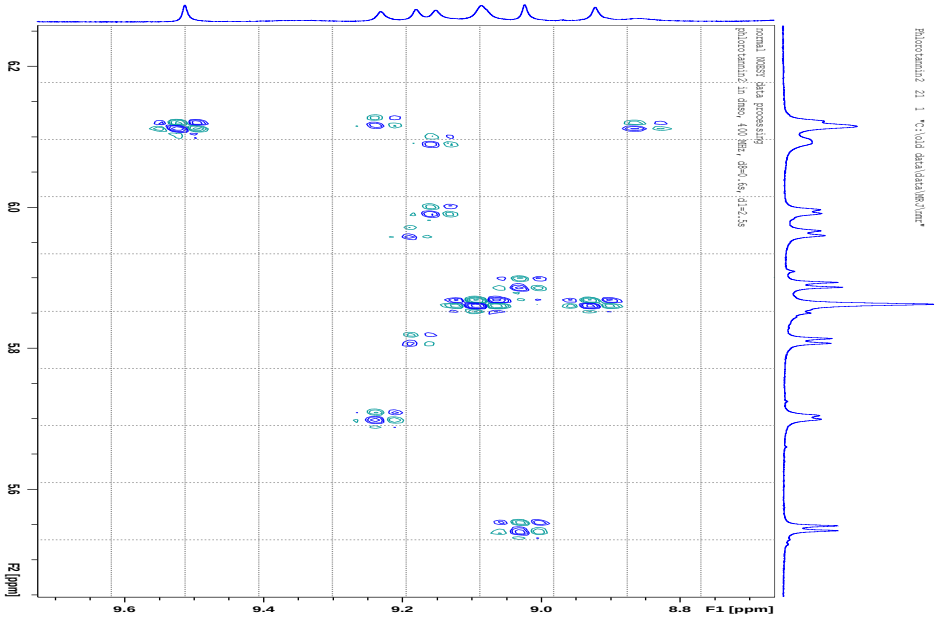

Figure S9. NOESY of dibenzodioxin-fucodiphloroethol with EM filter in processing showing NOE to broad proton signals

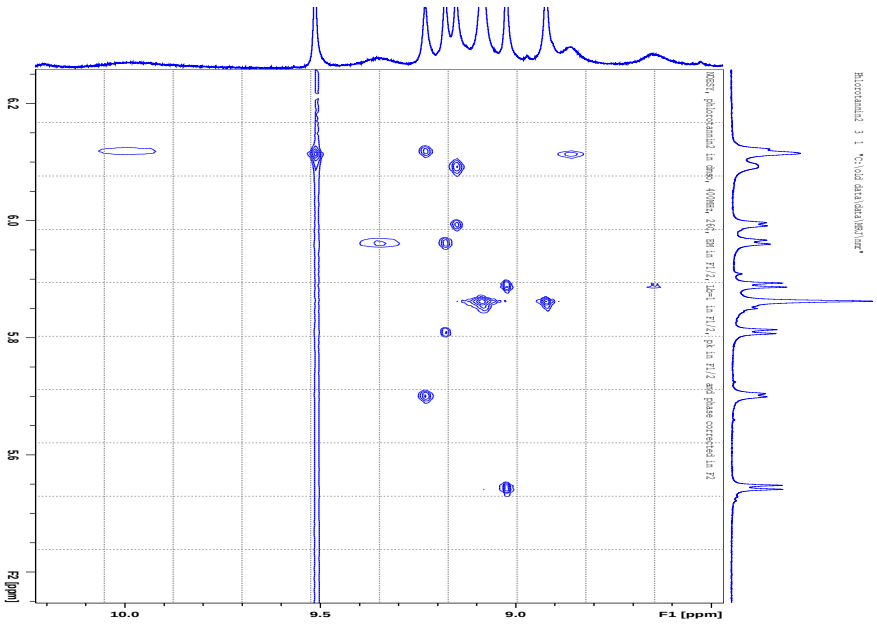

Figure S10. Positive ESI mode of dibenzodioxin-fucodiphloroethol

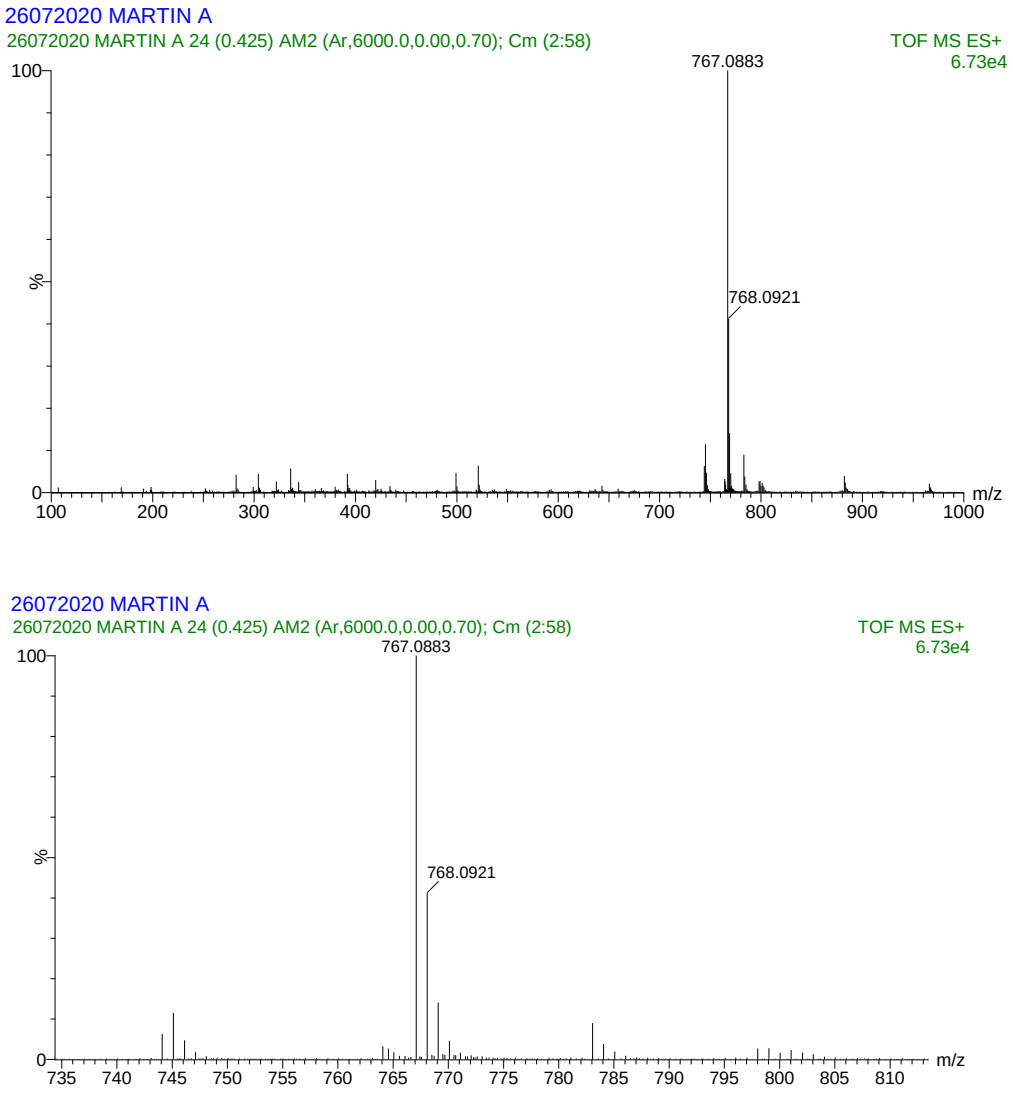

Statement of Authorship

Title of Paper	Neuroprotective activity of macroalgal fucofuroeckols against amyloid β peptide-induced cell death and oxidative stress.
Publication Status	☑ Published ☐ Accepted for Publication ☐ Submitted for Publication ☐ Unpublished and Unsubmitted work written in manuscript style
Publication Details	Shrestha, S., Choi, J.S., Zhang W., Smid, S.D. (2022) Neuroprotective activity of macroalgal fucofuroeckols against amyloid β peptide-induced cell death and oxidative stress. International Journal of Food Science & Technology.

Principal Author

Name of Principal Author (Candidate)	Srijan Shrestha		
Contribution to the Paper	Conceptualization; Data curation; Formal analysis; Investigation; Methodology; Software; Writing – original draft; Writing – review & editing		
Overall percentage (%)	80%		
Certification:	This paper reports on original research I conducted during the period of my Higher Degree by Research candidature and is not subject to any obligations or contractual agreements with a third party that would constrain its inclusion in this thesis. I am the primary author of this paper.		
Signature		Date	17/05/2022

Co-Author Contributions

By signing the Statement of Authorship, each author certifies that:

i. the candidate's stated contribution to the publication is accurate (as detailed above);

ii. permission is granted for the candidate in include the publication in the thesis; and

iii. the sum of all co-author contributions is equal to 100% less the candidate's stated contribution.

Name of Co-Author	Dr. Jae Sue Choi		
Contribution to the Paper	Methodology, Resources		
Signature		Date	19/05/2022

Name of Co-Author	Dr. Wei Zhang		
Contribution to the Paper	Conceptualization, Resources, Methodology, Supervision		
Signature		Date	31/05/2022

Name of Co-Author	Dr. Scott Smid		
Contribution to the Paper	Conceptualization, Funding acquisition, Formal analysis, Resources, Supervision, Writing-review, and editing.		
Signature		Date	21-06-22

Chapter 4: Neuroprotective activity of macroalgal fucofuroeckols against amyloid β peptide-induced cell death and oxidative stress

Srijan Shrestha[1*], Jae Sue Choi[2], Wei Zhang[3,4] and Scott D. Smid[1]

[1]Discipline of Pharmacology, School of Biomedicine, Faculty of Health Sciences, The University of Adelaide, South Australia, Australia

[2]Institute of Fisheries Sciences, Pukyong National University, Busan, 46041, Republic of Korea

[3]Centre for Marine Bioproducts Development (CMBD) and [4]Dept. of Medical Biotechnology, College of Medicine and Public Health, Flinders University, South Australia, Australia

International Journal of Food Science and Technology., 2022; DOI: 10.1111/ijfs.15753

Abstract

Phlorotannins are polyphenolic compounds predominantly found in brown seaweeds tentatively identified as having neuroprotective bioactivity, however the effects of individual constituent phlorotannins against amyloid β neurotoxicity, the main hallmark neurotoxic protein in Alzheimer's disease, is yet to be fully characterized. In the present study four phlorotannins, namely eckol, dieckol, phlorofucofuroeckol-A (PFFA) and 974-A sourced from the brown seaweed *Ecklonia* species were assessed for their ability to protect against the toxic effects of H_2O_2, lipid peroxidation via tert-butyl hydroperoxide (*t*-BHP) and $A\beta_{1-42}$ in neuronal PC-12 cells. All compounds significantly scavenged reactive oxygen species (ROS). However, only PFFA and 974-A protected PC-12 cells from oxidative stress-evoked neurotoxicity, providing significant increases in cell viability in response to both cytosolic (H_2O_2) and lipid peroxidation-evoked (*t*-BHP) cell stress. None of the phlorotannins tested inhibited $A\beta_{1-42}$ aggregate morphology, which suggested that their neuroprotective activity was unrelated to direct interactions with $A\beta_{1-42}$ protein. Our results indicate that while all phlorotannins tested exhibited ROS scavenging activity, only fucofuroeckol-type phlorotannins such as PFFA and 974-A afforded broader neuroprotective activity in response to both oxidative stress and amyloid β exposure. The additional amyloid-protective capacity of fucofuroeckols reveals the potential importance of the benzofuran moiety in neuroprotection and further studies are encouraged to investigate the chemico-biological basis of this distinction in the search for neuroprotective therapies in dementia and other neurodegenerative conditions.

Keywords: Fucofuroeckols, Eckols, Phlorotannin, β amyloid, Antioxidant, Neuroprotection

Introduction

Alzheimer's disease (AD) is an age-dependent progressive and irreversible neurodegenerative disorder characterized by extracellular deposition of the amyloid β peptide, occurring as senile plaques in addition to abnormal hyperphosphorylation of tau protein resulting in accumulation of intracellular neurofibrillary tangles (Francis *et al,*. 2005, Francis *et al,*. 1999). The various and complex interactions amongst several contributing factors including genetics, oxidative stress, inflammatory and environmental factors are believed to be the underlying cause of neurodegeneration in AD. Studies reveal that the presence of excessive misfolding amyloid β (Aβ) protein leads to oxidative stress that induces neuroinflammation and apoptotic neurodegeneration, which ultimately leads to cognitive decline and clinical progression (Li *et al,*. 2014, Ahmad *et al,*. 2017). Reactive oxygen species (ROS), including superoxide radical anions and hydroxyl radicals are known to cause oxidative stress and this represents an early event in the pathogenesis of AD (Nunomura *et al,*. 2001). Current treatments such as cholinesterase inhibitors and memantine are limiting and not considered disease-modifying (Vaz and Silvestre 2020), while the recently approved IgG1 anti-amyloid-β antibody targeting Aβ aggregates, Aducanumab, has questionable efficacy regarding clinical improvement in patients receiving treatment (Hooker 2021). Recently, sodium oligomannate, a brown seaweed derived (*Ecklonia kurome*) oral oligosaccharide has been approved in China for the treatment of mild to moderate AD (Lu *et al,*. 2021). While further clinical evidence of its efficacy as a dementia treatment awaits, this discovery has revealed potential opportunities for the development of a therapeutic drug from marine natural products for the treatment of AD.

Brown seaweed are considered versatile and can be sustainably used as a potential source for various applications worldwide including biomass feedstock, conversion into green biofuels,

animal and aqua feed, active ingredients in pharmaceutical and nutraceutical products along with integration in the human food chain (Chia *et al,*. 2018, Ong *et al,*. 2019, Biris-Dorhoi *et al,*. 2020). Brown seaweed has been used as a dietary and functional food for centuries, especially in Asian countries where consumption can reach 1 kg of dry weight per person annually (Tamama 2021). These brown algae (Phaeophyta) synthesize a variety of phloroglucinol-based polyphenols as phlorotannins. Phlorotannins have been previously demonstrated to have neuroprotective activity via various modes of action including inhibition of acetylcholinesterase, butyrylcholinesterase, monoamine oxidase and beta-site amyloid precursor protein cleaving enzyme 1 (BACE-1) activity (Barbosa *et al,*. 2020). Phlorotannins can also modulate neuronal receptors and regulate signalling pathways linked to neuroinflammation, oxidative stress and neuronal cell death (Shrestha *et al,*. 2021b, Barbosa *et al,*. 2020). Previous studies have shown that eckol, dieckol and phlorofucofuroeckol A (PFFA) decreased Aβ-induced cell death, inhibited intracellular ROS generation and calcium generation (Ahn *et al,*. 2012), while Lee et al. (2019) demonstrated that eckol and dieckol were ascribed anti-neuroinflammatory properties in $A\beta_{25-35}$ treated neuronal PC-12 cells mediated by the downregulation of NF-κB and pro-inflammatory enzymes iNOS and COX-2. (Lee *et al,*. 2019). Additionally, we also recently reported the neuroprotective actions of dibenzodioxin-fucodiphloroethol (Shrestha *et al,*. 2021a), thus collectively demonstrating support for a neuroprotective role for phlorotannins through multiple pathways. However, more research is needed to clarify the contributions of specific phlorotannin classes towards this neuroprotection and some of its potentially operant protective pathways, such as antioxidant capacity and direct modulation of amyloid-aggregating properties.

In the present study $A\beta_{1-42}$, H_2O_2 and the lipid peroxidant *tert*-butyl hydroperoxide (*t*-BHP) were used to induce oxidative stress and toxicity in neuronal PC-12 cells. Two eckol-type phlorotannins

(eckol and dieckol) and two fucofuroeckol-type phlorotannins (PFFA and 974-A) (Figure 1) were then investigated for their neuroprotective capacity in these settings. In addition, we investigated the direct interaction of these phlorotannins with ROS scavenging activity and anti-aggregatory effects against $A\beta_{1-42}$ fibrillisation, in order to further explore their potential neuroprotective mechanisms.

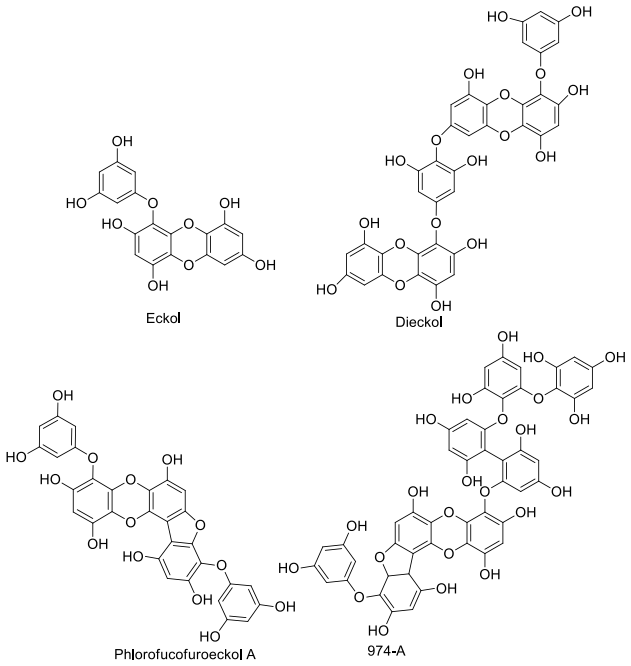

Figure 1. Structure of phlorotannins used in this study; eckol, dieckol, PFFA, and 974-A

Materials and methods

Reagents and chemicals

Eckol was obtained as mentioned previously (Shrestha *et al,.* 2020). Briefly, ethyl acetate fraction of the ethanolic extract of *Ecklonia radiata* was subjected to centrifugal partition chromatography with varying ratios of solvents. The fractions were collected and pooled to give four sub-fractions and eckol was found in subfraction-3. Dieckol, phlorofucofuroeckol-A (PFFA) and 974-A isolated from *Ecklonia* species were kindly provided by Prof. Jae Sue Choi (Pukyong National University, Republic of Korea). All other chemicals and reagents were purchased from Sigma-Aldrich (NSW,

Australia) unless otherwise stated. Hydrogen peroxide was obtained from Thermo Fisher (Australia) and the DCFDA/H2DCFDA kit for ROS quantitation was purchased from Abcam (Victoria, Australia). Human amyloid β protein ($A\beta_{1–42}$) was obtained from rPeptide (Bogart, Georgia, USA).

Preparation of $A\beta_{1-42}$ and phlorotannins

Lyophilized $A\beta_{1–42}$ was dissolved in dimethyl sulfoxide (DMSO) to prepare a concentration of 3.8 mM and diluted to 100 μM with sterile phosphate buffered saline (PBS). The aliquots were stored at -70°C. The phlorotannins were dissolved in DMSO to prepare 20 mM stock.

Cell culture

Rat pheochromocytoma PC-12 (Ordway) cells displaying a semi-differentiated neuronal phenotype with neuronal projections donated by Prof. Jacqueline Phillips (Macquarie University, NSW, Australia) were maintained in complete RPMI-1640 media (10% FBS, 1% penicillin/streptomycin and 1% NEAA) at 37°C with 5% CO_2.

Cytotoxicity of phlorotannins in PC-12 cells

Neuronal cell viability was measured as described previously (Shrestha *et al,*. 2020). Initially, the potential toxicity of each phlorotannin was assessed. PC-12 cells were seeded at 2×10^4 cells per well in 100 μL media into 96 well tissue culture plates and incubated for 24 h at 37°C with 5% CO_2. The cells were each treated with eckol, dieckol, PFFA and 974-A from 0-100 μM and incubated for 24 h. The media was replaced with 3-(4,5-dimethylthiazol-2-yl)-2,5-diphenyl tetrazolium bromide (MTT) dissolved in serum free media and incubated for 2 h. The solution was then replaced with DMSO and was measured at 570 nm using a Synergy MX microplate reader (Bio-Tek, Bedfordshire, UK).

Neuroprotective activity of phlorotannins against $A\beta_{1–42}$

In order to determine the neuroprotective activity of compounds against $A\beta_{1–42}$, PC-12 cells were pre-treated with a non-toxic concentration of each phlorotannin (12.5 μM) as determined in the concentration-response profiles for 15 min prior to incubation with $A\beta_{1-42}$ (0-1.5 μM) for 48h at 37°C with 5% CO_2. MTT absorbance was measured at 570 nm as described earlier.

Neuroprotective activity of phlorotannins against H_2O_2 and *t*-BHP-evoked toxicity

PC-12 cells were seeded at 3×10^4 cells per well into 96 well tissue culture plates and incubated for 24 h at 37°C with 5% CO_2. The cells were pre-treated with 12.5 μM of compounds prior to treatment with 150 μM and 200 μM of H_2O_2 and *t*-BHP followed by incubation for 6 h and 4 h, respectively. MTT absorbance was measured at 570 nm as described earlier

Measurement of ROS generation from lipid peroxidation: effects of phlorotannins

A 2′,7′-dichlorofluorescin diacetate (DCFDA) assay was used for the measurement of ROS generation according to the manufacturer's instructions. Briefly, 1×10^5 cells per well in 100 μL phenol red-free media were seeded and stained with DCFDA (20 μM) for 30 min at 37°C with 5% CO_2. DCFDA was washed out and 100 μL phenol red-free media added. Cells were pre-treated with 12.5 μM of phlorotannins followed by *t*-BHP (50 μM) for 4 h. The fluorescence intensity was measured using a Synergy MX microplate reader (Bio-Tek, Bedfordshire, UK) with excitation and emission wavelengths at 485 nm and 535 nm, respectively.

Transmission electron microscopy of $A\beta_{1–42}$ aggregate morphology

$A\beta_{1–42}$ (10 μM) was incubated alone or with 12.5 μM of each phlorotannin for 48h at 37°C in PBS. The interaction was visualised using a FEI Tecnai G2 Spirit Transmission electron microscope

(FEI, Milton, QLD, Australia) and representative images were taken at 18500×magnification as described previously (Shrestha *et al*,. 2020).

Statistical analysis

All experiments were performed in quadruplicate with at least 3-4 independent experiments and data expressed as mean±SD. GraphPad Prism 8 (GraphPad Software, San Diego, USA) was used for data analysis and graph presentation. Two-way analysis of variance (ANOVA) with a Bonferroni's post-hoc test was used to determine statistical significance between treatments, with a significance level set at $p < 0.05$.

Results

Effects of phlorotannins on PC-12 cell viability

Initially, phlorotannins were tested for their cytotoxicity in PC-12 cells up to the concentration of 100 µM as shown in Figure 2. Each phlorotannin was non-toxic up to the concentration of 12.5 µM. However, when cells were incubated with each phlorotannin from 25-100 µM, viability was significantly reduced versus control (*** $p < 0.001$ *vs* control). Of the four phlorotannins, dieckol was the most toxic, with 50% cell viability at 50 µM. All phlorotannins reduced cell viability by less than 32% at 100 µM. Therefore, a non-toxic test concentration of 12.5 µM for all compounds was used for all other interventions.

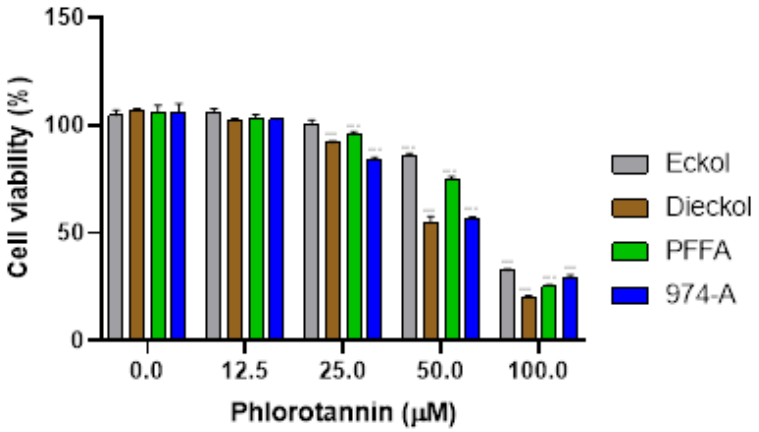

Figure 2. Cell viability following incubation with each of the phlorotannins; eckol, dieckol, PFFA and 974-A (each at 0-100 µM) in PC-12 cells. *** $p < 0.001$ vs control (no treatment).

Effect of phlorotannins on hydrogen peroxide-induced PC-12 cell viability

As shown in Figure 3, PC-12 cells treated with 150 µM and 200 µM of H_2O_2 demonstrated concentration-dependent loss of cell viability, with 56% and 32% of cell viability compared to control (no H_2O_2). Interestingly, a slight increase in cell viability was observed when cells were treated with PFFA and 974-A only. Pre-treatment of PC-12 cells with eckol and dieckol prior to incubation with H_2O_2 did not significantly protect PC-12 cells. However, pre-treatment of cells with PFFA and 974-A (12.5 µM each) significantly (*** $p < 0.001$ *vs* control) inhibited the H_2O_2-induced loss of cell viability compared with vehicle (H_2O_2 only).

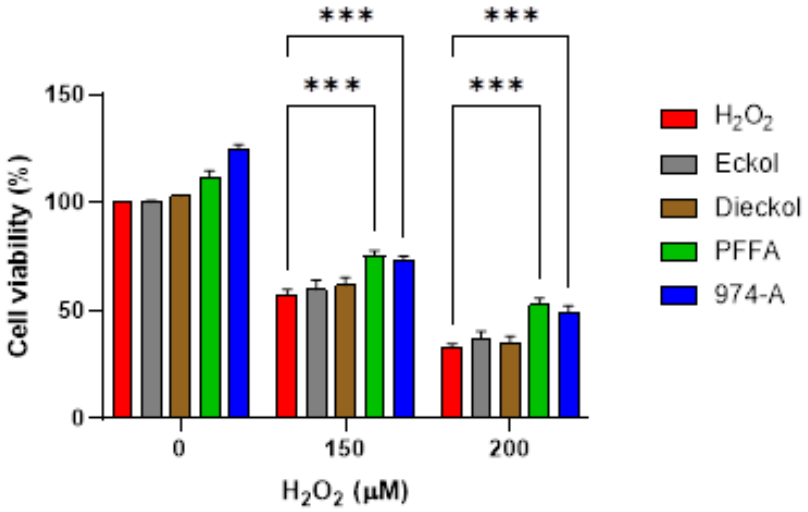

Figure 3. Neuroprotective activity of phlorotannins in H_2O_2 exposed PC-12 cells. Cells were pretreated with 12.5 µM of each phlorotannin for 30 minutes prior to exposure with H_2O_2 (0-200 µM) for 6h. *** $p < 0.001$ vs control (n=4).

Effect of phlorotannins on *t*-BHP-induced PC-12 cell viability

As shown in Figure 4, when PC-12 cells were treated with individual phlorotannins (12.5 µM) in the absence of *t*-BHP, the viability of cells was not affected for eckol and dieckol but a slight increase in cell viability was observed for PFFA and 974-A. However, when PC-12 cells were treated with 150 µM and 200 µM of *t*-BHP, cell viability was reduced to 63% and 59% compared to control (no *t*-BHP), respectively. Two phlorotannins, PFFA and 974-A were able to protect PC-12 cells significantly compared with the vehicle (*t*-BHP only). PFFA significantly (*** $p < 0.001$) increased cell viability at 150 µM and 200 µM of *t*-BHP to 94% and 92%, respectively. Similarly, 974-A increased cell viability to 86% and 81% versus *t*-BHP only. Conversely, eckol and dieckol demonstrated no protective activity in response to cytosolic oxidative stress evoked by *t*-BHP.

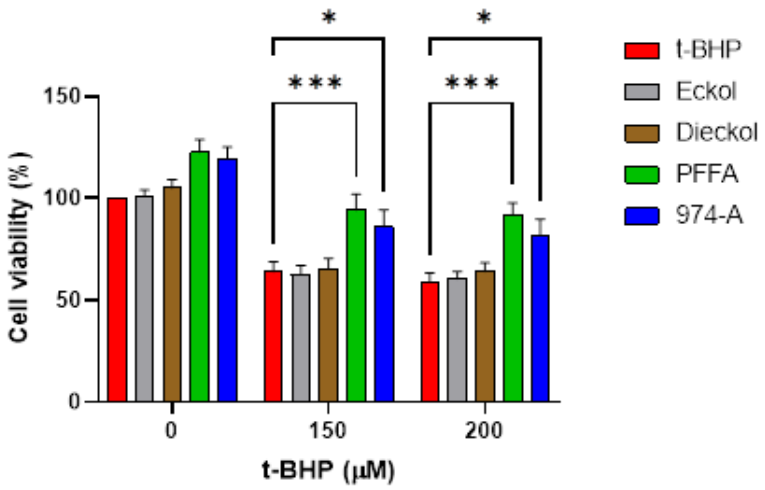

Figure 4. Neuroprotective activity of phlorotannins in *t*-BHP exposed PC-12 cells. Cells were pretreated with 12.5 µM of each phlorotannin for 15 minutes prior to exposure with *t*-BHP (0-200 µM) for 4 h. *** $p < 0.001$; * $p < 0.05$ vs control (n=5).

Phlorotannins reduce reactive oxygen species levels from *t*-BHP in PC-12 cells

To evaluate the effect of phlorotannins on oxidative stress induced by *t*-BHP in PC-12 cells, the level of ROS was measured through the DCFDA fluorescence assay. As shown in Figure 5, *t*-BHP (50 µM) significantly (*** $p < 0.001$) increased ROS levels more than two-fold compared with the untreated control. When PC-12 cells were pre-treated with 12.5 µM of phlorotannins before *t*-BHP treatment, the level of ROS was reduced significantly (*** $p < 0.001$) and equally (approx. 150 %) in all phlorotannin-treated groups.

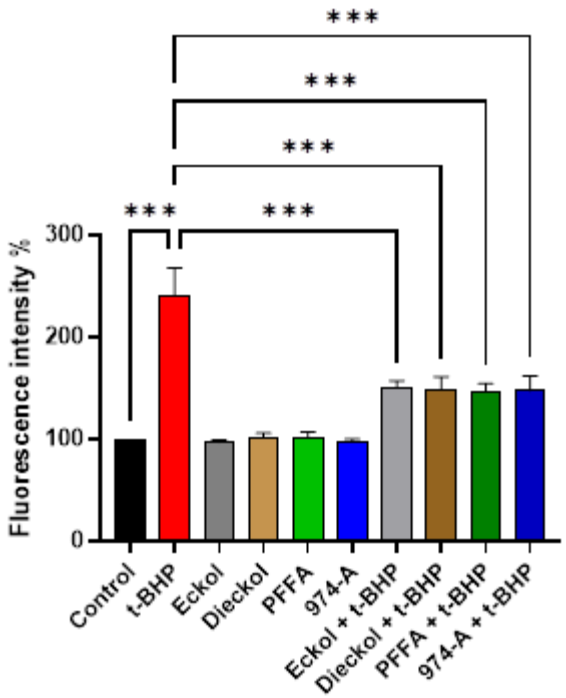

Figure 5. Intracellular radical scavenging activities of phlorotannins in PC-12 cells (as % ROS formation). Cells were labeled with fluorescent dye DCFH-DA (20 µM) and pretreated with 12.5 µM of each phlorotannin followed by *t*-BHP incubation (50 µM) for 4 h. *** $p < 0.001$ vs *t*-BHP (n=4).

Effect of phlorotannins on Aβ$_{1–42}$-induced PC-12 cells

As shown in Figure 6, incubation of PC-12 cells with Aβ$_{1–42}$ over 48 h elicited a concentration-dependent decrease in cell viability to 85%, 79% and 70% at 0.5, 1.0, and 1.5 µM respectively. Interestingly, only PFFA and 974-A demonstrated a protective effect across all concentrations of Aβ. Specifically, pre-treatment of cells with PFFA and 974-A (12.5 µM) significantly increased cell viability up to 100 % (*** $p < 0.001$ vs Aβ-treated cells). In contrast, eckol and dieckol provided no significant neuroprotection.

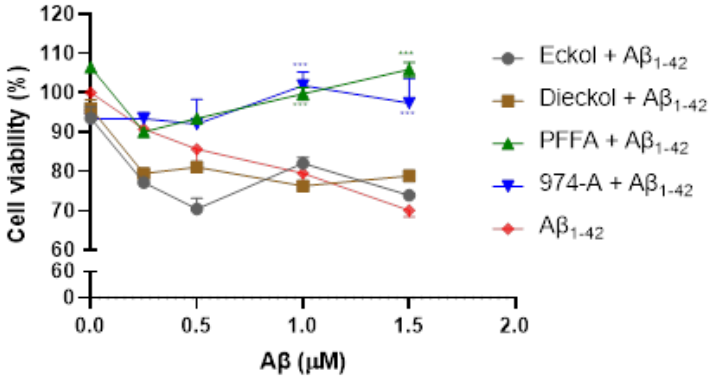

Figure 6. Neuroprotective activity of eckol, dieckol, PFFA and 974-A in $A\beta_{1-42}$ exposed PC-12 cells. Cells were pre-treated with 12.5 µM of each phlorotannin for 15 minutes prior to exposure with $A\beta_{1-42}$ (0-2.0 µM) for 48 h. *** $p < 0.001$ vs $A\beta_{1-42}$ (n=3).

Effect of phlorotannins on $A\beta_{1–42}$ fibrillisation and aggregate formation

Transmission electron microscopy was used to assess the effects of phlorotannins on Aβ fibril formation and aggregation. $A\beta_{1–42}$ (10 µM) was incubated with each of the four phlorotannins at a concentration of 12.5 µM each for 48 h at 37°C to enable aggregate formation over an equivalent period to match the cell incubation studies (48 h). Although, PFFA and 974-A provided protection against oxidative stress and Aβ toxicity, none of the four phlorotannins tested altered or diminished the density or morphology of Aβ aggregates (Figure 7).

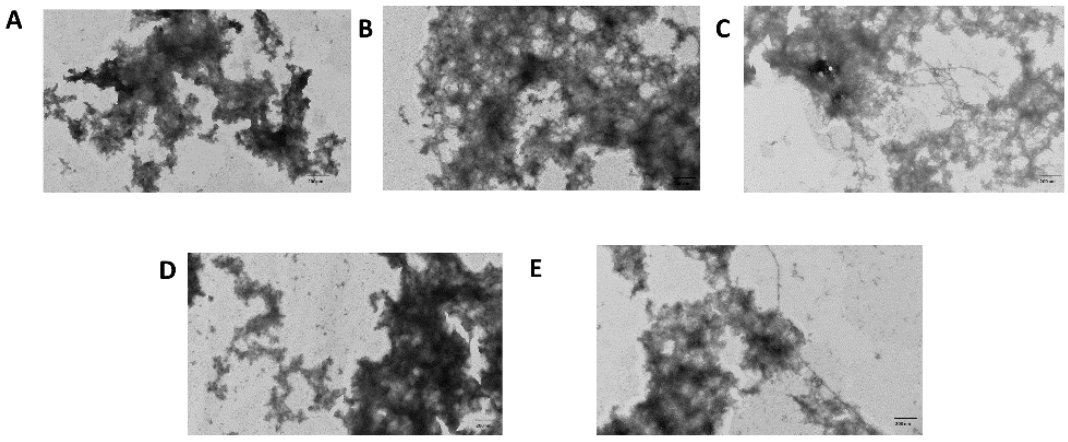

Figure 7. Representative transmission electron microscopic images of $A\beta_{1-42}$ fibril and aggregate formation alone (A) and following 48 h incubation with eckol (B), dieckol (C), PFFA (D), and 974-A (E). Each 12.5 µM concentration was used. Scale bar = 200 nm.

Discussion

A growing number of studies have indicated the bioactive potential of phlorotannins in regard to neuroprotection via antioxidant and anti-neuroinflammatory properties, in addition to reported anti-aggregatory activity versus amyloid β (Shrestha *et al,*. 2021b, Lee *et al,*. 2019, Ahn *et al,*. 2012, Wang *et al,*. 2018, Barbosa *et al,*. 2020). Overall, the present study suggests that while diverse phlorotannins more broadly share free radical scavenging and antioxidant neuroprotective properties, not all phlorotannin classes provide discreet protection against amyloid β-evoked neurotoxicity. Notably though, selected fucofuroeckols such as PFFA and 974-A have pronounced neuroprotective properties against oxidative stress and amyloid β, despite limited direct influence on amyloid β aggregation.

The brain is more vulnerable than other organs to oxidative stress due to the high consumption of oxygen, relatively low levels of endogenous antioxidant capacity and generation of superoxides by the action of various oxidases and nitric oxide synthase (Yavin *et al,*. 2002). Oxidative stress can impair redox homeostasis and induce mitochondrial dysfunction, leading to damage in neuronal cells (Li *et al,*. 2020) and H_2O_2 has previously been used to effectively generate cytosolic oxidative stress (Cai *et al,*. 2008, Shin *et al,*. 2021). Our results demonstrated that the fucofuroeckols PFFA and 974-A were able to prevent H_2O_2-induced death in PC-12 cells, while no protective effects were observed with eckol and dieckol (Figure 3). Our results also demonstrated that the phlorotannins were cytotoxic beyond 12.5 µM, which was consistent with previous studies (Ahn *et al,*. 2012, Kim *et al,*. 2016). By contrast, Lee et al. (2019) reported that eckol and dieckol were not toxic up to a concentration of 100 µM. Additionally, Shin et al. (2021) reported that dieckol at a concentration of 50 µg/ml (approx. 67 µM) protected PC-12 cells against H_2O_2 (200 µM) (Shin *et al,*. 2021). This variability could be due to the difference in phlorotannin

concentrations and/or the PC-12 cells, where PC-12 cells displaying a semi-differentiated phenotype with neuronal projections (Ordway subclone) (Dixon *et al,*. 2005) were used in the present study, whereas these previous studies used undifferentiated cells (Shin *et al,*. 2021, Lee *et al,*. 2019).

T-BHP is a short-chain, cell permeant lipid hydroperoxide analogue commonly used to generate lipid peroxidation (Hibaoui *et al,*. 2009, Kučera *et al,*. 2014). *T*-BHP-induced oxidative stress was reported to exert deleterious effects on mitochondria involving ferroptosis and dysfunction leading to cell death (Wu *et al,*. 2018). When PC-12 cells were pre-treated with phlorotannins and exposed to *t*-BHP, a similar profile of protective effects was observed as in response to H_2O_2. The two fucofuroeckols, PFFA and 974-A significantly protected PC-12 cells exposed to 150 µM and 200 µM of *t*-BHP, while no protection was observed with eckol and dieckol. Interestingly, all tested phlorotannins significantly scavenged intracellular ROS when measured via the DCFDA assay. Previously, Manandhar et al. (2019) reported a similar scavenging activity of eckol, PFFA and 974-A in B16F10 melanoma cells treated with 400 µM of *t*-BHP (Manandhar *et al,*. 2019). The author points out that the effect is likely related to their phenol rings, which act as electron traps to scavenge peroxynitrite and superoxide anions as well as hydroxyl radicals.

Phlorotannins were then tested for their ability to protect PC-12 cells against $A\beta_{1\text{-}42}$. A similar pattern (as seen in H_2O_2 and *t*-BHP stimulated cells) was observed when PC-12 cells where pre-treated with phlorotannins prior to exposure to $A\beta_{1\text{-}42}$. PFFA and 974-A protected PC-12 cells against $A\beta_{1\text{-}42.}$ However, eckol and dieckol were not able to similarly rescue cells. Previously, eckol and dieckol were reported to have protected PC-12 cells against $A\beta_{25\text{-}35}$, which contrasts with our results (Ahn *et al,*. 2012, Lee *et al,*. 2019). However, in this study we used $A\beta_{1\text{-}42}$, which is more pathologically relevant than $A\beta_{25\text{-}35}$. Previous studies demonstrated that $A\beta_{25\text{-}35}$ did not

induce hippocampal damage and neurotoxicity (Stein-Behrens *et al,*. 1992, Malouf 1992) and lacks key neurotoxic residues limiting its comparative use for studies seeking insights into neurotoxicity mechanisms related to $A\beta_{1-42}$ (Butterfield and Sultana 2011).

We previously reported the neuroprotective activity of an ethyl acetate fraction of *E. radiata* and suggested that eckol and eckol-type phlorotannins might be the predominant bioactive agents (Shrestha *et al,*. 2020). However, the findings of the present study underscore the potential contribution of varying phlorotannin types present in *Ecklonia* species. Previous studies also reported a similar pattern in LPS-induced RAW 264.7 cells (Kim *et al,*. 2009). When dieckol and PFFA were assessed for their antioxidant and anti-inflammatory properties, both compounds were able to scavenge intracellular ROS significantly. By contrast, only PFFA was able to significantly reduce the production of nitric oxide and PGE_2 and suppress the expression of iNOS and COX-2 proteins. Additionally, fucofuroeckol-A isolated from *Eisenia bicyclis* was reported to have prevented $A\beta_{1-42}$-induced damage in SH-SY5Y cells (Lee and Byun 2018a). Our results aligned with this study, and it can be suggested that the selective activity might be related to the structure-activity relationship (SAR) of these phlorotannins to $A\beta_{1-42}$ oligomers, notably to the fucofuroeckols containing the additional benzofuran ring compared with eckols. This is supported by previous studies demonstrating that benzofuran derivatives have neuroprotective properties against Aβ (González-Ramírez *et al,*. 2018, Rizzo *et al,*. 2008, Cabrera-Pardo *et al,*. 2020, Lee and Byun 2018b). González-Ramírez et al. (2018) reported a natural fungal-derived benzofuran with potent neuroprotective activity and suggested the direct effect on neuronal function without interfering with the Aβ aggregation process (González-Ramírez *et al,*. 2018), which is consistent with the findings of the present study. Additionally, Cabrera-Pardo et al. (2020) explored the multi-target neuroprotective potential of benzofuran scaffolds and suggested that privileged oxygen-

containing heterocycles such as benzofurans exert neuroprotection by inhibiting several important events involved in the AD process including cholinesterase, ROS stress and Aβ-cell membrane binding (Cabrera-Pardo *et al,*. 2020, Rizzo *et al,*. 2012, Rizzo *et al,*. 2008). However, further in-depth investigations with individual phlorotannins are required to confirm neuroprotective specificity and the chemico-biological basis conferring neuroprotection.

Transmission electron microscopy revealed no difference in amyloid β aggregate density or morphology between any of the phlorotannin treatments compared with control (Figure 7). Previously, Seong et al. (2019) reported that eckol, dieckol, and PFFA inhibited $A\beta_{25-35}$ self-aggregation via the thioflavin-T (ThT) fluorescence assay (Seong *et al,*. 2019). However, polyphenolic compounds may inhibit ThT fluorescence without necessarily inhibiting fibril formation, directly quenching fluorophores and generating false positives (Das *et al,*. 2016, Coelho-Cerqueira *et al,*. 2014, Hudson *et al,*. 2009). In such cases, transmission electron microscopy can therefore provide qualitative but arguably more definitive evidence of any anti-aggregatory effect of polyphenols, and in the present study we observed no direct anti-fibrillar effect of the selected phlorotannins.

In term of food safety and dosing, several human studies have confirmed that the phlorotannins are safe for consumption as a food supplement (Oh *et al,*. 2010, Lee *et al,*. 2012, Choi *et al,*. 2015). Additionally, the European Food Safety Authority (EFSA) Panel on Dietetic Products recommends an intake level of 3.75 mg/kg body weight per day (163 mg/day for adolescents from 12 to 14 years of age, 230 mg/day for adolescents above 14 years of age and 263 mg/day for adults) (EFSA Panel on Dietetic Products *et al,*. 2017).

In terms of the bioavailability of phlorotannins for use as functional food or nutraceutical supplements, various studies indicate that phlorotannins exhibit similar bioavailability to that of

plant polyphenols, which are absorbed and metabolized predominantly in the large intestine via gut microbial metabolism (Crozier *et al,*. 2010, Li *et al,*. 2017, Corona *et al,*. 2016, Baldrick *et al,*. 2018). Analysis of human plasma and urine after phlorotannin-rich brown seaweed consumption indicate levels of various phlorotannin metabolites such as hydroxytrifuhalol A, 7-hydroxyeckol and phloroglucinol dimers with levels of individual phlorotannins attained up to 8 μg/mL in human plasma (Corona, 2016). This would accord to a plasma concentration of approximately 20μM for a small (< 400 g/mol) phlorotannin such as eckol and hence the concentrations used in our present study (12.5 μM) would be reasonably expected to be attainable in vivo.

While polyphenol bioavailability is generally considered low in the gastrointestinal tract, much attention has been recently focused on prebiotic effects of polyphenols and their beneficial attribution towards the gut microbiome as it impacts neurodegenerative disorders. This is exemplified by the mechanism of oligomannate derived from brown seaweed as a clinically approved treatment for Alzheimer's disease in China, whereby improvements in gut dysbiosis are believed to be the underlying mechanism behind its clinical benefit (Wang *et al,*. 2019). Phlorotannin-rich fractions from brown seaweed also modulate human enteric bacterial populations in vitro, suggesting changes in both microbial population and their host-beneficial mediators such as short-chain fatty acids (Catarino *et al,*. 2021, Charoensiddhi *et al,*. 2017). This recognition of the importance of the gut-brain axis and microbiome health has important implications for dietary interventions that until now were often considered as limited based on low gastrointestinal bioavailability. This also now underscores the importance of further research in dietary polyphenols, including seaweed-derived phlorotannins, in the normalisation of dysbiosis that occurs in neurodegenerative conditions and its applications for brain health.

Conclusions

Specific phlorotannins, in particular the fucofuroeckols PFFA and 974-A, possess protective effects against oxidative stress-induced neuronal cell damage through antioxidant mechanisms as well as preventing $A\beta_{1-42}$-induced neurotoxicity. These results highlight fucofuroeckols as a class of phlorotannin from brown seaweed that can effectively mitigate both oxidative stress and amyloid-evoked toxicity of relevance to neurodegenerative pathways in Alzheimer's disease. Future studies are required to differentiate the mechanistic basis for the protection conferred by fucofuroeckols, as well as additional in vivo studies to further establish preclinical efficacy as a guide to informing further clinical trials in nutraceutical or pharmaceutical settings.

Conflict of interest

The authors have no conflict of interest to declare

Acknowledgments

Srijan Shrestha is supported by Australian Government Research Training Program (RTP) Scholarship. Wei Zhang acknowledges the support of ARC Industry Transformation and Training Centre for Green Chemistry in Manufacturing, Qingdao Gather Great Ocean Algae Industry Group Co, Ltd and Australian Kelp Products Pty Ltd.

References

Ahmad, A., Ali, T., Park, H. Y., Badshah, H., Rehman, S. U. & Kim, M. O. (2017). Neuroprotective effect of fisetin against amyloid-beta-induced cognitive/synaptic dysfunction, neuroinflammation, and neurodegeneration in adult mice. *Molecular Neurobiology,* **54,** 2269-2285.

Ahn, B. R., Moon, H. E., Kim, H. R., Jung, H. A. & Choi, J. S. (2012). Neuroprotective effect of edible brown alga *Eisenia bicyclis* on amyloid beta peptide-induced toxicity in PC12 cells. *Archives of Pharmacal Research,* **35,** 1989-98.

Baldrick, F. R., McFadden, K., Ibars, M., Sung, C., Moffatt, T., Megarry, K., Thomas, K., Mitchell, P., Wallace, J. M. W., Pourshahidi, L. K., Ternan, N. G., Corona, G., Spencer, J., Yaqoob, P., Hotchkiss, S., Campbell, R., Moreno-Rojas, J. M., Cuevas, F. J., Pereira-Caro, G., Rowland, I. & Gill, C. I. R. (2018). Impact of a (poly)phenol-rich extract from the brown algae *Ascophyllum nodosum* on DNA damage and antioxidant activity in an overweight or obese population: a randomized controlled trial. *The American Journal of Clinical Nutrition,* **108,** 688-700.

Barbosa, M., Valentão, P. & Andrade, P. B. (2020). Polyphenols from brown seaweeds (Ochrophyta, Phaeophyceae): Phlorotannins in the pursuit of natural alternatives to tackle neurodegeneration. *Marine Drugs,* **18,** 654.

Biris-Dorhoi, E. S., Michiu, D., Pop, C. R., Rotar, A. M., Tofana, M., Pop, O. L., Socaci, S. A. & Farcas, A. C. (2020). Macroalgae—A sustainable source of chemical compounds with biological activities. *Nutrients,* **12,** 3085.

Butterfield, D. A. & Sultana, R. (2011). Methionine-35 of $A\beta_{(1-42)}$: Importance for oxidative stress in Alzheimer disease. *Journal of Amino Acids,* **2011,** 198430-198430.

Cabrera-Pardo, J. R., Fuentealba, J., Gavilán, J., Cajas, D., Becerra, J. & Napiórkowska, M. (2020). Exploring the multi-target neuroprotective chemical space of benzofuran scaffolds: a new strategy in drug development for Alzheimer's disease. *Frontiers in Pharmacology,* **10,** 1679-1679.

Cai, L., Wang, H., Li, Q., Qian, Y. & Yao, W. (2008). Salidroside inhibits H_2O_2-induced apoptosis in PC12 cells by preventing cytochrome c release and inactivating of caspase cascade. *Acta Biochimica et Biophysica Sinica,* **40,** 796-802.

Catarino, M. D., Marçal, C., Bonifácio-Lopes, T., Campos, D., Mateus, N., Silva, A. M. S., Pintado, M. M. & Cardoso, S. M. (2021). Impact of phlorotannin extracts from *Fucus vesiculosus* on human gut microbiota. *Marine Drugs,* **19,** 375.

Charoensiddhi, S., Conlon, M. A., Vuaran, M. S., Franco, C. M. M. & Zhang, W. (2017). Polysaccharide and phlorotannin-enriched extracts of the brown seaweed *Ecklonia radiata* influence human gut microbiota and fermentation in vitro. *Journal of Applied Phycology,* **29,** 2407-2416.

Chia, S. R., Show, P. L., Phang, S. M., Ling, T. C. & Ong, H. C. (2018). Sustainable approach in phlorotannin recovery from macroalgae. *Journal of Bioscience and Bioengineering,* **126,** 220-225.

Choi, E. K., Park, S. H., Ha, K. C., Noh, S. O., Jung, S. J., Chae, H. J., Chae, S. W. & Park, T. S. (2015). Clinical trial of the hypolipidemic effects of a brown alga *Ecklonia cava* extract in patients with hypercholesterolemia. *International Journal of Pharmacology,* **11,** 798-805.

Coelho-Cerqueira, E., Pinheiro, A. S. & Follmer, C. (2014). Pitfalls associated with the use of Thioflavin-T to monitor anti-fibrillogenic activity. *Bioorganic & Medicinal Chemistry Letters,* **24,** 3194-3198.

Corona, G., Ji, Y., Anegboonlap, P., Hotchkiss, S., Gill, C., Yaqoob, P., Spencer, J. P. & Rowland, I. (2016). Gastrointestinal modifications and bioavailability of brown seaweed phlorotannins and effects on inflammatory markers. *British Journal of Nutrition,* **115,** 1240-1253.

Crozier, A., Del Rio, D. & Clifford, M. N. (2010). Bioavailability of dietary flavonoids and phenolic compounds. *Molecular Aspects of Medicine,* **31,** 446-467.

Das, S., Stark, L., Musgrave, I. F., Pukala, T. & Smid, S. D. (2016). Bioactive polyphenol interactions with β amyloid: a comparison of binding modelling, effects on fibril and aggregate formation and neuroprotective capacity. *Food & Function,* **7,** 1138-1146.

Dixon, D. N., Loxley, R. A., Barron, A., Cleary, S. & Phillips, J. K. (2005). Comparative studies of PC12 and mouse pheochromocytoma-derived rodent cell lines as models for the study of neuroendocrine systems. *In Vitro Cellular & Developmental Biology,* **41,** 197-206.

EFSA Panel on Dietetic Products, N., Allergies, Turck, D., Bresson, J.L., Burlingame, B., Dean, T., Fairweather-Tait, S., Heinonen, M., Hirsch-Ernst, K. I., Mangelsdorf, I., McArdle, H. J., Naska, A., Neuhäuser-Berthold, M., Nowicka, G., Pentieva, K., Sanz, Y., Siani, A.,

Sjödin, A., Stern, M., Tomé, D., Vinceti, M., Willatts, P., Engel, K.H., Marchelli, R., Pöting, A., Poulsen, M., Schlatter, J. R., Ackerl, R. & van Loveren, H. (2017). Safety of *Ecklonia cava* phlorotannins as a novel food pursuant to Regulation (EC) No 258/97. *European Food Safety Authority Journal,* **15,** e05003.

Francis, P. T., Nordberg, A. & Arnold, S. E. (2005). A preclinical view of cholinesterase inhibitors in neuroprotection: do they provide more than symptomatic benefits in Alzheimer's disease? *Trends in Pharmacological Sciences,* **26,** 104-111.

Francis, P. T., Palmer, A. M., Snape, M. & Wilcock, G. K. (1999). The cholinergic hypothesis of Alzheimer's disease: a review of progress. *Journal of Neurology, Neurosurgery, and Psychiatryy,* **66,** 137-147.

González-Ramírez, M., Gavilán, J., Silva-Grecchi, T., Cajas-Madriaga, D., Triviño, S., Becerra, J., Saez-Orellana, F., Pérez, C. & Fuentealba, J. (2018). A natural benzofuran from the patagonic *Aleurodiscus vitellinus* fungus has potent neuroprotective properties on a cellular model of amyloid-β peptide toxicity. *Journal of Alzheimer's Disease,* **61,** 1463-1475.

Hibaoui, Y., Roulet, E. & Ruegg, U. T. (2009). Melatonin prevents oxidative stress-mediated mitochondrial permeability transition and death in skeletal muscle cells. *Journal of Pineal Research,* **47,** 238-252.

Hooker, J. M. (2021). FDA approval of aducanumab divided the community but also connected and united it. *ACS Chemical Neuroscience,* **12**, 2716-2717.

Hudson, S. A., Ecroyd, H., Kee, T. W. & Carver, J. A. (2009). The thioflavin T fluorescence assay for amyloid fibril detection can be biased by the presence of exogenous compounds. *The FEBS Journal,* **276,** 5960-5972.

Kim, A. R., Shin, T. S., Lee, M. S., Park, J. Y., Park, K. E., Yoon, N. Y., Kim, J. S., Choi, J. S., Jang, B. C. & Byun, D. S. (2009). Isolation and identification of phlorotannins from *Ecklonia stolonifera* with antioxidant and anti-inflammatory properties. *Journal of Agricultural and Food Chemistry,* **57,** 3483-3489.

Kim, J. J., Kang, Y. J., Shin, S. A., Bak, D. H., Lee, J. W., Lee, K. B., Yoo, Y. C., Kim, D.K., Lee, B. H., Kim, D. W., Lee, J., Jo, E.K. & Yuk, J.M. (2016). Phlorofucofuroeckol improves glutamate-induced neurotoxicity through modulation of oxidative stress-mediated mitochondrial dysfunction in PC12 cells. *PLoS One,* **11,** e0163433-e0163433.

Kučera, O., Endlicher, R., Roušar, T., Lotková, H., Garnol, T., Drahota, Z. & Cervinková, Z. (2014). The effect of tert-butyl hydroperoxide-induced oxidative stress on lean and steatotic rat hepatocytes in vitro. *Oxidative Medicine and Cellular Longevity,* **2014,** 752506.

Lee, D. H., Park, M. Y., Shim, B. J., Youn, H. J., Hwang, H. J., Shin, H. C. & Jeon, H. K. (2012). Effects of *Ecklonia cava* polyphenol in individuals with hypercholesterolemia: A pilot study. *Journal of Medicinal Food,* **15,** 1038-1044.

Lee, J. K. & Byun, H.G. (2018). A novel BACE inhibitor isolated from *Eisenia bicyclis* exhibits neuroprotective activity against β-amyloid toxicity. *Fisheries and Aquatic Sciences,* **21,** 38.

Lee, S., Youn, K., Kim, D., Ahn, M. R., Yoon, E., Kim, O. Y. & Jun, M. (2019). Anti-neuroinflammatory property of phlorotannins from *Ecklonia cava* on $A\beta_{25-35}$-induced damage in PC12 cells. *Marine Drugs,* **17,** 7.

Li, X., Zhao, X., Xu, X., Mao, X., Liu, Z., Li, H., Guo, L., Bi, K. & Jia, Y. (2014). Schisantherin A recovers Aβ-induced neurodegeneration with cognitive decline in mice. *Physiology & Behavior,* **132,** 10-16.

Li, X. Q., Wang, R. T., Wang, Q. H., Tang, X. L., Lu, C. T., Gong, H. G. & Wen, A. D. (2017). Determination of phloroglucinol by HPLC-MS/MS and its application to a bioequivalence study in healthy volunteers. *European Review for Medical and Pharmacological Sciences,* **21,** 1990-1998.

Li, Z., Jiang, T., Lu, Q., Xu, K., He, J., Xie, L., Chen, Z., Zheng, Z., Ye, L., Xu, K., Zhang, H. & Hu, A. (2020). Berberine attenuated the cytotoxicity induced by t-BHP via inhibiting oxidative stress and mitochondria dysfunction in PC-12 cells. *Cellular and Molecular Neurobiology,* **40,** 587-602.

Lu, J., Pan, Q., Zhou, J., Weng, Y., Chen, K., Shi, L., Zhu, G., Chen, C., Li, L., Geng, M. & Zhang, Z. (2022). Pharmacokinetics, distribution, and excretion of sodium oligomannate, a recently approved anti-Alzheimer's disease drug in China. *Journal of Pharmaceutical Analysis,* **12,** 145-155.

Malouf, A. T. (1992). Effect of beta amyloid peptides on neurons in hippocampal slice cultures. *Neurobiology of Aging,* **13,** 543-551.

Manandhar, B., Wagle, A., Seong, S. H., Paudel, P., Kim, H.R., Jung, H. A. & Choi, J. S. (2019). Phlorotannins with potential anti-tyrosinase and antioxidant activity isolated from the marine seaweed *Ecklonia stolonifera*. *Antioxidants,* **8,** 240.

Nunomura, A., Perry, G., Aliev, G., Hirai, K., Takeda, A., Balraj, E. K., Jones, P. K., Ghanbari, H., Wataya, T., Shimohama, S., Chiba, S., Atwood, C. S., Petersen, R. B. & Smith, M. A. (2001). Oxidative damage is the earliest event in Alzheimer disease. *Journal of Neuropathology & Experimental Neurology,* **60,** 759-767.

Oh, J. K., Shin, Y. O., Yoon, J. H., Kim, S. H., Shin, H. C. & Hwang, H. J. (2010). Effect of supplementation with *Ecklonia cava* polyphenol on endurance performance of college students. *International Journal of Sport Nutrition and Exercise Metabolism,* **20,** 72-79.

Ong, M. Y., Syahira Abdul Latif, N. I., Leong, H. Y., Salman, B., Show, P. L. & Nomanbhay, S. (2019). Characterization and analysis of Malaysian macroalgae biomass as potential feedstock for bio-oil production. *Energies,* **12,** 3509.

Rizzo, S., Rivière, C., Piazzi, L., Bisi, A., Gobbi, S., Bartolini, M., Andrisano, V., Morroni, F., Tarozzi, A., Monti, J.-P. & Rampa, A. (2008). Benzofuran-based hybrid compounds for the inhibition of cholinesterase activity, β amyloid aggregation, and Aβ neurotoxicity. *Journal of Medicinal Chemistry,* **51,** 2883-2886.

Rizzo, S., Tarozzi, A., Bartolini, M., Da Costa, G., Bisi, A., Gobbi, S., Belluti, F., Ligresti, A., Allarà, M., Monti, J. P., Andrisano, V., Di Marzo, V., Hrelia, P. & Rampa, A. (2012). 2-Arylbenzofuran-based molecules as multipotent Alzheimer's disease modifying agents. *European Journal of Medicinal Chemistry,* **58,** 519-532.

Seong, S. H., Paudel, P., Jung, H. A. & Choi, J. S. (2019). Identifying phlorofucofuroeckol-A as a dual inhibitor of amyloid-β_{25-35} self-aggregation and insulin glycation: Elucidation of the molecular mechanism of action. *Marine Drugs,* **17,** 600.

Shin, Y. S., Kim, K. J., Park, H., Lee, M. G., Cho, S., Choi, S. I., Heo, H. J., Kim, D. O. & Kim, G. H. (2021). Effects of *Ecklonia cava* extract on neuronal damage and apoptosis in PC-12 cells against oxidative stress. *Journal of Microbiology and Biotechnology,* **31,** 584-591.

Shrestha, S., Johnston, M. R., Zhang, W. & Smid, S. D. (2021a). A phlorotannin isolated from *Ecklonia radiata*, Dibenzodioxin-fucodiphloroethol, inhibits neurotoxicity and aggregation of β-amyloid. *Phytomedicine Plus,* **1,** 100125.

Shrestha, S., Zhang, W., Begbie, A. J., Pukala, T. L. & Smid, S. D. (2020). *Ecklonia radiata* extract containing eckol protects neuronal cells against $A\beta_{(1-42)}$ evoked toxicity and reduces aggregate density. *Food & Function,* **11,** 6509-6516.

Shrestha, S., Zhang, W. & Smid, S. (2021b). Phlorotannins: a review on biosynthesis, chemistry and bioactivity. *Food Bioscience,* **39,** 100832.

Stein-Behrens, B., Adams, K., Yeh, M. & Sapolsky, R. (1992). Failure of beta-amyloid protein fragment 25-35 to cause hippocampal damage in the rat. *Neurobiology of Aging,* **13,** 577-579.

Tamama, K. (2021). Potential benefits of dietary seaweeds as protection against COVID-19. *Nutrition Reviews,* **79,** 814-823.

Vaz, M. & Silvestre, S. (2020). Alzheimer's disease: Recent treatment strategies. *European Journal of Pharmacology,* **887,** 173554.

Wang, J., Zheng, J., Huang, C., Zhao, J., Lin, J., Zhou, X., Naman, C. B., Wang, N., Gerwick, W. H., Wang, Q., Yan, X., Cui, W. & He, S. (2018). Eckmaxol, a phlorotannin extracted from *Ecklonia maxima*, produces anti-beta-amyloid oligomer neuroprotective effects possibly via directly acting on glycogen synthase kinase 3beta. *ACS Chemical Neuroscience,* **9,** 1349-1356.

Wang, X., Sun, G., Feng, T., Zhang, J., Huang, X., Wang, T., Xie, Z., Chu, X., Yang, J., Wang, H., Chang, S., Gong, Y., Ruan, L., Zhang, G., Yan, S., Lian, W., Du, C., Yang, D., Zhang, Q., Lin, F., Liu, J., Zhang, H., Ge, C., Xiao, S., Ding, J. & Geng, M. (2019). Sodium oligomannate therapeutically remodels gut microbiota and suppresses gut bacterial amino acids-shaped neuroinflammation to inhibit Alzheimer's disease progression. *Cell Research s,* **29,** 787-803.

Wu, C., Zhao, W., Yu, J., Li, S., Lin, L. & Chen, X. (2018). Induction of ferroptosis and mitochondrial dysfunction by oxidative stress in PC12 cells. *Scientific Reports,* **8,** 574.

Yavin, E., Brand, A. & Green, P. (2002). Docosahexaenoic acid abundance in the brain: a biodevice to combat oxidative stress. *Nutritional Neuroscience,* **5,** 149-157.

Statement of Authorship

Title of Paper	Protective effects of phlorotannins on cytokine-induced intestinal epithelial barrier damage
Publication Status	☐ Published ☐ Accepted for Publication ☐ Submitted for Publication ☑ Unpublished and Unsubmitted work written in manuscript style
Publication Details	The chapter is formatted for submission to Journal of Medicinal Food

Principal Author

Name of Principal Author (Candidate)	Srijan Shrestha		
Contribution to the Paper	Conceptualization; Data curation; Formal analysis; Investigation; Methodology; Software; Writing – original draft; Writing – review & editing		
Overall percentage (%)	80%		
Certification:	This paper reports on original research I conducted during the period of my Higher Degree by Research candidature and is not subject to any obligations or contractual agreements with a third party that would constrain its inclusion in this thesis. I am the primary author of this paper.		
Signature		Date	17/05/2022

Co-Author Contributions

By signing the Statement of Authorship, each author certifies that:

i. the candidate's stated contribution to the publication is accurate (as detailed above);
ii. permission is granted for the candidate in include the publication in the thesis; and
iii. the sum of all co-author contributions is equal to 100% less the candidate's stated contribution.

Name of Co-Author	Dr. Jae Sue Choi		
Contribution to the Paper	Methodology, Resources		
Signature		Date	17/05/2022

Name of Co-Author	Dr. Wei Zhang		
Contribution to the Paper	Conceptualization, Resources, Methodology, Supervision		
Signature		Date	31/05/2022

Name of Co-Author	Dr. Scott Smid		
Contribution to the Paper	Conceptualization, Funding acquisition, Formal analysis, Resources, Supervision, Writing-review, and editing.		
Signature		Date	21-06-22

Chapter 5: Protective effects of phlorotannins on cytokine-induced intestinal epithelial barrier damage

Srijan Shrestha[1], Jae Sue Choi[2], Wei Zhang[3,4] and Scott D. Smid[1*]

[1]Discipline of Pharmacology, School of Biomedicine, Faculty of Health Sciences, The University of Adelaide, South Australia, Australia

[2]Institute of Fisheries Sciences, Pukyong National University, Busan 46041, Korea

[3]Centre for Marine Bioproducts Development (CMBD) and [4]Dept. of Medical Biotechnology, College of Medicine and Public Health, Flinders University, South Australia, Australia

*Corresponding Author
Scott Smid
Discipline of Pharmacology
School of Biomedicine, Faculty of Health Sciences
The University of Adelaide
Adelaide SA 5005 Australia
Tel: 61 8 83135287
Fax: 61 8 82240685
Email: scott.smid@adelaide.edu.au

Abstract

Increased intestinal permeability and systemic inflammation linked to gastrointestinal dysbiosis may contribute to the development of Alzheimer's disease (AD) pathologies and cognitive impairment via neuronal, immunological, endocrine, and metabolic pathways. Sodium oligomannate derived from brown seaweed has been approved for the treatment of Alzheimer's disease in China, whereby improvements in gastrointestinal function linked to dysbiosis are believed to be the underlying mechanism behind its clinical benefit. While phlorotannins have direct neuroprotective bioactivity applicable to neurodegenerative conditions, effects on gastrointestinal barrier function have not been extensively explored. In this Chapter, the effect of phlorotannins eckol, dieckol, phlorofucofuroeckol-A (PFFA), and 974-A on cytokine-evoked trans-epithelial electrical resistance (TEER) reductions in Caco-2 intestinal epithelial monolayers, as a measure of paracellular permeability and barrier integrity were investigated. Caco-2 monolayers were incubated with TNF-α and IL-1β (100 ng/ml each) in the presence or absence of phlorotannins. Significant improvements in epithelial barrier function at 48 h occurred with eckol, dieckol and PFFA but not 974-A. This indicates a broader capacity of the phlorotannins to support intestinal epithelial barrier function against deleterious proinflammatory cytokines. All phlorotannins were also excellent scavengers of lipid peroxidation-generated free radicals as indicated by DCFDA assay, which may be linked to the observed barrier function improvement.

Keywords: TEER, phlorotannins, Epithelial barrier function, cytokines, Caco-2 cell line

1. Introduction

Alzheimer's disease (AD) is a progressive neurodegenerative disorder characterized by gradual cognitive decline. The pathological hallmarks of AD include amyloid beta (Aβ) deposition, hyperphosphorylated tau-protein and neurofibrillary tangles (NFTs) in brain tissue (Grill & Cummings, 2010). Significant interventional efforts have been made targeting such pathological hallmarks, however no disease-modifying treatment for AD has been clinically approved in two decades (Cummings, Lee, Ritter, & Zhong, 2018). Nevertheless, the recent approval of sodium oligommante derived from brown seaweed in China has opened a new horizon to explore novel target-related AD therapeutics (Lu et al., 2022). Wang et al. demonstrated that sodium oligomannate was able to suppress intestinal dysbiosis, reducing the accumulation of phenylalanine and isoleucine leading to cognitive improvement in AD mouse models (Wang et al., 2019). Intestinal microbiota interface with, and are important in regulating gut mucosal function, particularly epithelial barrier integrity and overall intestinal permeability, with implications in the onset and progression of neurodegenerative disease (Ceppa et al., 2020). Gut dysbiosis, intestinal epithelial barrier dysfunction and vascular Aβ deposition in the gut were reported to occur in a transgenic mouse model of AD and in intestinal autopsies of AD-afflicted patients before the onset of cerebral Aβ deposition (Honarpisheh et al., 2020). Furthermore, an increased concentration of lipopolysaccharides in the brain responsible for inflammation and induction of accumulation of Aβ may be due to damaged tight junctions and increased intestinal permeability (Asti & Gioglio, 2014; González, Elgueta, Montoya, & Pacheco, 2014; Marizzoni et al., 2020). A 'leaky' gut may also allow lipopolysaccharide (LPS) to penetrate the enteric nervous system stimulating CCAAT/enhancer binding protein β (C/EBPβ) activation and upregulating asparagine endopeptidase (AEP), resulting in aggregation of amyloid beta and neurofibrillary tangles in the

myenteric and submucosal nervous system, which may be distributed into the brain via vagal nerve pathways in AD patients (Chen et al., 2020). Furthermore, enteric Aβ oligomers were found to induce an alteration in gastric function, affect amyloidosis in the CNS and AD-like dementia in ICR (Institute of Cancer Research, USA) mice via the vagal nerve with the Aβ load originating in the GI tract and translocating to the brain (Sun et al., 2020). Therefore, gut inflammation and dysbiosis are directly associated with gut barrier dysfunction and increased intestinal permeability ("leaky gut") and therein may contribute to the process of neurodegeneration leading to AD.

Phlorotannins, the polyphenolic compounds from brown seaweed have been reported to have a diverse range of biological activities such as neuroprotective, antioxidant and anti-inflammatory effects (Shrestha, Johnston, Zhang, & Smid, 2021; Shrestha, Zhang, Begbie, Pukala, & Smid, 2020; Shrestha, Zhang, & Smid, 2021). However, very little is known about the effects of phlorotannins on intestinal permeability and there is no study investigating the effects of these phlorotannins on cytokine-induced epithelial permeability in Caco-2 monolayers to our knowledge, which are commonly used as a model of intestinal permeability and barrier integrity. Therefore, the influence of four phlorotannins, namely eckol, dieckol, phlorofucofuroeckol-A (PFFA) and 974-A on intestinal permeability was investigated in the present study using proinflammatory cytokines to induce barrier deficits.

2. Materials and methods

2.1. Chemicals and reagents

3-(4,5-Dimethylthiazol-2-yl)-2,5-diphenyltetrazolium bromide (MTT), DMEM, trypan blue, non-essential amino acids (NEAA), penicillin/streptomycin, trypsin EDTA, foetal bovine serum (FBS), phosphate buffered saline (PBS), TNF-α and IL-1β were purchased from Sigma-Aldrich (NSW, Australia). Eckol was obtained as mentioned previously (Shrestha et al., 2020). Dieckol,

phlorofucofuroeckol-A (PFFA), and 974-A were kindly provided by Prof. Jae Sue Choi (Pukyong National University, Republic of Korea). The structure of the phlorotannins is illustrated in Fig. 1.

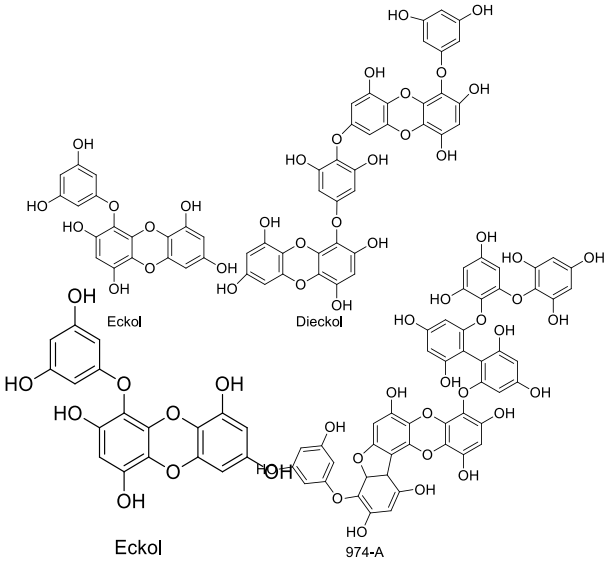

Figure 1. Phlorotannin structures (eckol, dieckol, PFFA, and 974-A) used in this study

2.2. Caco-2 epithelial cell culture

Caco-2 cells derived from human colorectal carcinoma were obtained from the American Type Culture Collection (ATCC) (Manassas, VA, USA) and were maintained in 75cm^2 tissue culture flasks (Corning Life Sciences, Lowell, MA, USA) at 37 °C with 5% CO_2 in DMEM supplemented with 10% foetal calf serum and 1% penicillin/streptomycin solution. The cells were passaged every 3-4 days until reaching 80 % confluence.

2.3. Assessment of Caco-2 cytotoxicity and treatment

The measurement of cell viability was performed using the established MTT assay. Caco-2 cells were seeded at 2×10^4 cells per well in 100 µL media into 96 well tissue culture plates. The cells were incubated for 48 hours at 37 °C with 5% CO_2 and treated with different concentrations (0-100 µM) of eckol, dieckol, PFFA, and 974-A and incubated for 24 h. MTT absorbance was measured at 570 nm.

2.4. TEER measurements of epithelial permeability

Trans-epithelial electrical resistance (TEER) experiments were conducted in confluent Caco-2 monolayers using Nunc™ Polycarbonate Cell Culture Inserts in Multi-Well Plates (culture area 0.47 cm^2, 0.4 μm pore size, tissue culture treated polycarbonate membrane) (ThermoFisher Scientific, MA, USA). The basolateral compartment was filled with 1 mL of complete DMEM containing 1% amphotericin B. All subsequent media used in the Transwell plate was supplemented with 1% amphotericin B to avoid fungal contamination. Caco-2 cells were seeded at a density of 23,500 cells per insert in 0.3 mL of media in the apical compartment. An insert was labelled as blank containing media only. The transwell plate was then incubated at 37 °C with 5% CO_2 for 28 days to enable differentiation and monolayer formation. Media in apical and basolateral wells was replaced every 2-3 days. TEER readings of the monolayer were constantly monitored via an EVOM2 epithelial volt/ohm meter with chopstick electrodes (World Precision Instruments, Sarasota, FL, USA) as an indicator of epithelial integrity. TEER was calculated according to the following formula.

$$\text{TEER } (\Omega \text{cm}^2) = [TEER\ total\ (\Omega) - TEER\ blank\ (\Omega)] \times A(\text{cm}^2)$$

where A is the area of the insert

Only inserts with a threshold of more than 500 Ω cm^2 were used in the experiments. On the day of treatment, media was replaced with complete media without amphotericin B. The measurements were taken after allowing the plate to equilibrate to room temperature for 5 minutes.

2.5. Cytokine and phlorotannin treatments

Caco-2 monolayers in Transwell plates were treated as established previously in our laboratory (Harvey, Nicotra, Vu, & Smid, 2013). Human recombinant TNF-α and IL-1β produced significant

TEER reductions in preliminary studies at 100 ng/ml, and this concentration was subsequently used for the study. Cells were pretreated with eckol, dieckol, PFFA and 974-A at 50 μM each applied apically and incubated for 15 minutes followed by combined treatment with or without cytokines (TNF-α and IL-1β) at 100 ng/ml each applied to the basolateral compartment. The TEER of each well was measured at the time points of 0, 2, 6, 24, and 48 h.

2.6. Measurement of ROS generation from lipid peroxidation

A 2′,7′-dichlorofluorescin diacetate (DCFDA) assay was used for the measurement of ROS generation in Caco-2 cells according to the manufacturer's instructions. Briefly, 1×10^5 cells per well in 100 μL phenol red-free media were seeded and stained with DCFDA (20 μM) for 30 min at 37°C with 5% CO_2. DCFDA was removed and 100μL phenol red-free media was added. Cells were pre-treated with 50 μM of each phlorotannin followed by the lipid peroxidant *t*-BHP (50 μM) for 4 h. The fluorescence intensity was measured using a Synergy MX microplate reader (Bio-Tek, Bedfordshire, UK) with excitation and emission wavelengths at 485 nm and 535 nm, respectively.

3. Results and Discussions

3.1. Effects of phlorotannins on Caco-2 cell viability

Caco-2 cells were treated with different concentrations (0-100 μM) of phlorotannins (eckol, dieckol, PFFA and 974-A) as shown in Figure 2. Phlorotannins did not demonstrate cytotoxicity in Caco-2 cells even in the highest tested concentration (100 μM). Murata et al. also observed similar results when Caco-2 cells were treated with various concentrations (0-500 μg/ml) of phlorotannins (Murata, Keitoku, Miyake, Tanaka, & Shibata, 2022), whereby neither eckol, dieckol or PFFA had any impact on cell viability up to the concentration of 500 μg/ml, which is approximately 1343, 673, and 829 μM, respectively (Murata et al., 2022).

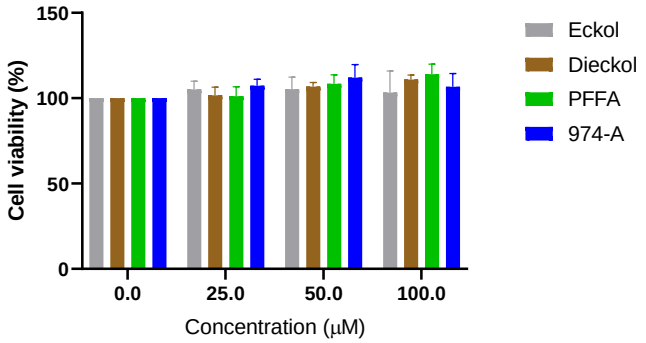

Figure 2. Cell viability of phlorotannins (eckol, dieckol, PFFA, and 974-A each 0-100 µM) in Caco-2 cells via the MTT assay.

3.2. Influence of phlorotannins on epithelial permeability in Caco-2 cells

Caco-2 cells form confluent monolayers and express a range of transporters, tight junctions, and enzymes similar to the intestinal enterocytes (Hidalgo, Raub, & Borchardt, 1989). Thus, Caco-2 cells are considered a suitable model for our study and have been previously used successfully to characterize novel bioactive interventions supporting intestinal barrier function (Harvey et al., 2013; Harvey, Sia, Wattchow, & Smid, 2014). The influence of phlorotannins on intestinal epithelial barrier function disruption in response to proinflammatory cytokines in differentiated Caco-2 cell monolayers was evaluated functionally by measuring TEER (Fig. 3). Our preliminary data indicated that treatment with cytokines (TNF-α and IL-1β) each at 100 ng/ml evoked a time-dependent increase in Caco-2 monolayer permeability, as demonstrated by a significant decrease in transepithelial electrical resistance (TEER) over 48 h (Fig. 3). Values were expressed as percentages compared with the control group. When the monolayer was treated with TNF-α and IL-1β, TEER values fell to approx. 70 % over the period of 6 hours, increased slightly to approx. 82 % at 24 h and then declined to approx. 80 % at 48 h. These were consistent with our previous studies where a combination of these cytokines evoked a time-dependent increase in Caco-2 cell monolayer permeability (Harvey et al., 2013). Treatment of each of the phlorotannins in Caco-2

cell monolayers did not have any significant effect on permeability. However, when the monolayer was pretreated with 50 µM of phlorotannins followed by cytokines (TNF-α and IL-1β; 100 ng/ml each), all phlorotannins, eckol, dieckol, and PFFA demonstrated significant protection as indicated by increased TEER values, with the exception of 974-A.

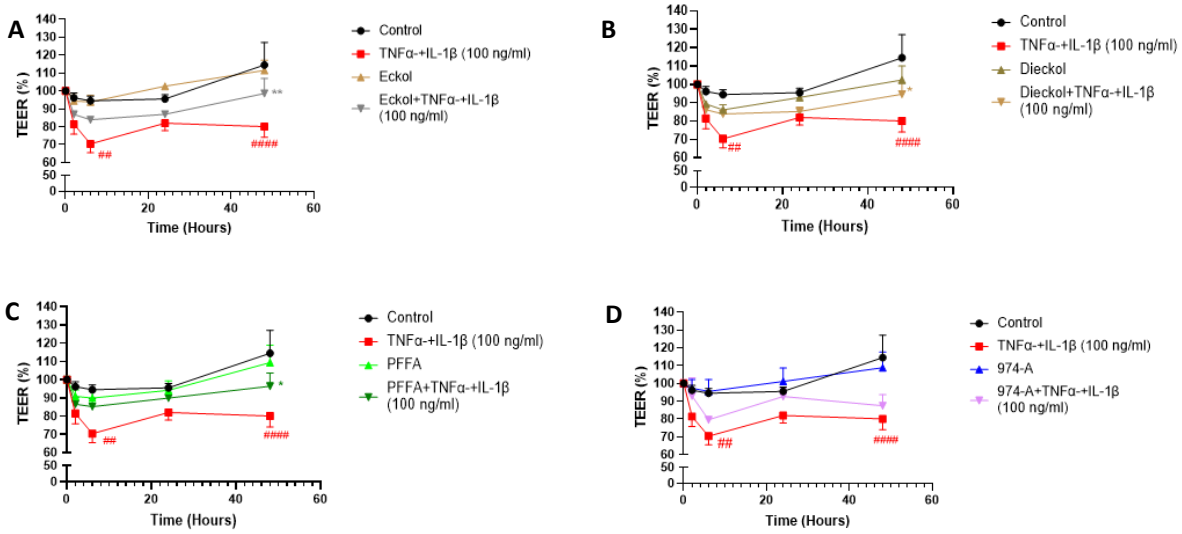

Figure 3. Effect of phlorotannins on cytokine (TNF-α + IL-1β)-evoked trans-epithelial electrical resistance (TEER) reductions as a measure of Caco-2 paracellular permeability over 48 h (∗ vs TNF-α + IL-1β; ### vs control). Significant (*) improvements in epithelial barrier function at 48 h occur with all phlorotannins except 974-A.

Eckol demonstrated a superior protective activity against cytokines, followed by PFFA and dieckol. When the monolayer was pretreated with 50 µM of eckol followed by cytokines, TEER values increased to ~100% at 48 h compared with control (~ 80%) (**$p < 0.01$ *vs* TNF-α + IL-1β). Furthermore, TEER values were also restored to 95% and 96 %, respectively, after pretreatment with dieckol and PFFA followed by cytokines at 48 h (*$p < 0.1$ *vs* control). Similar findings were reported when IPEC-J2 cells (an intestinal porcine enterocyte cell line) were treated with eckol, dieckol and PFFA, where eckol was able to recover TEER values and intestinal permeability compared to untreated cells by upregulating AKT phosphorylation and ZO-1 expression (Lee & Kim, 2020). Eckol was also previously shown to induce pancreatic and duodenal homeobox-1

(PDX-1) expression, which itself regulates heparin-binding epidermal growth factor (HBEGF) expression involved in intestinal barrier function integrity and wound healing, through PI3K/AKT and P38 signaling (Lee & Kim, 2020).

3.3. Phlorotannins reduce reactive oxygen species levels from *t*-BHP in Caco-2 cells

Our preliminary assessment of *t*-BHP exposure in Caco-2 cells demonstrated that *t*-BHP was nontoxic up to the concentration of 200 µM. Therefore, 200 µM of *t*-BHP was used to evaluate the effects of phlorotannins on oxidative stress in Caco-2 cells and ROS formation as measured through the DCFDA assay. As shown in Fig 4, *t*-BHP significantly (**** $p < 0.001$) increased ROS levels by more than 500 % compared with the control (untreated cells). However, when Caco-2 cells were pre-treated with phlorotannins followed by *t*-BHP treatment, the level of ROS was reduced significantly (*** $p < 0.001$) by all phlorotannins. Each phlorotannin alone did not have any impact on ROS formation in Caco-2 cells. Previously, we reported similar findings using neuronal PC-12 cells (Shrestha, Choi, Zhang, & Smid, 2022), where each tested phlorotannin reduced ROS generation significantly in PC-12 cells when induced by *t*-BHP. Furthermore, eckol was also able to alleviate H_2O_2-induced oxidative stress through PI3K/AKT signaling in a previous study (Lee & Kim, 2020).

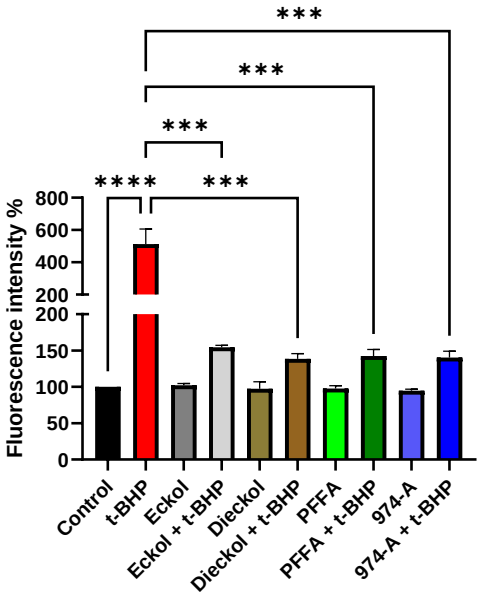

Figure 4. Intracellular radical scavenging activities of phlorotannins in Caco-2 cells. Cells were labelled with fluorescence dye DCFH-DA (20 µM) and pretreated with 50 µM of phlorotannins followed by *t*-BHP (200 µM) for 4 hrs. **** $p < 0.0001$, *** $p < 0.001$ vs *t*-BHP (n=3). The results are shown as % ROS formation. All phlorotannins were excellent scavengers of lipid peroxidation-generated free radicals.

A leaky gut due to increased intestinal permeability leads to a compromised barrier, allowing gut contents such as immune cells and microbiota to enter the bloodstream enabling systemic inflammation (El-Hakim, Bake, Mani, & Sohrabji, 2022). An increased level of pro-inflammatory cytokines has the potential to impact both systemic organs and the brain. The blood brain barrier, which protects the brain, is likely to be disrupted by the chain of events leading to the neuroinflammation associated with neurogenerative diseases like AD, Parkinson's disease, multiple sclerosis, and neuropsychiatric disorders. In addition, increased intestinal permeability may have local multiple consequences, facilitating the onset of a variety of gastrointestinal diseases including inflammatory bowel diseases, celiac disease and some metabolic disorders (Bischoff et al., 2014).

Phlorotannins have been consumed as a functional food in Asian countries for generations in the form of seaweeds (Tamama, 2020). Furthermore, various clinical trials and human research have shown that phlorotannins are safe to consume (Choi et al., 2015; Lee et al., 2012; Oh et al., 2010). Previously, these phlorotannins were also reported to have protective effects on radiation-induced intestinal injury in mice and oxidative stress-induced mitochondrial dysfunction (Kim et al., 2014; Moon et al., 2008). Yuan et al. (2019) also reported the beneficial effect of phlorotannins on regulating altered microbial ecology in diabetic rats (Yuan et al., 2019). The intestinal epithelium serves as an important first line of defense and oxidative stress is considered a major cause of barrier disruption and failure to regenerate (Vergauwen et al., 2015). Previous reports have claimed that exposure of Caco-2 intestinal cells to pro-oxidants resulted in reduced barrier integrity via disrupted tight junction protein expression and localization (Kitts, 2021). In terms of the operant radical scavenging chemistry applicable to phlorotannins, Vergauwen et al. argued that the presence of one or more aromatic rings and double bonds might be responsible for stabilising the free radical after donating a proton or receiving electrons through resonance (Vergauwen et al., 2016).

Conclusions

Phlorotannins such as eckol, dieckol and PFFA significantly recovered cytokine (TNF-α + IL-1β)-evoked trans-epithelial electrical resistance (TEER) reductions and exhibited significant radical scavenging activity in Caco-2 cells. Taken together, it can be suggested that macroalgal phlorotannins exhibit a multifaceted protective potential against a range of disorders associated with diminished intestinal permeability and oxidative stress. Consumption of brown seaweed may therefore have multifaceted actions in mitigating the underlying pathophysiology of neurodegeneration, notably here indirectly via actions as a functional bioactive to promote

intestinal health. Further in vivo animal investigations and clinical trials however are necessary to fully understand any protective role of phlorotannins within the complex interactions of the brain-gut-microbiome axis as it is currently posited towards the development or facilitation of neurodegenerative disease.

References

Asti, A., & Gioglio, L. (2014). Can a bacterial endotoxin be a key factor in the kinetics of amyloid fibril formation? *J Alzheimers Dis, 39*(1), 169-179.

Bischoff, S. C., Barbara, G., Buurman, W., Ockhuizen, T., Schulzke, J. D., Serino, M., . . . Wells, J. M. (2014). Intestinal permeability--a new target for disease prevention and therapy. *BMC Gastroenterol, 14*, 189.

Ceppa, F. A., Izzo, L., Sardelli, L., Raimondi, I., Tunesi, M., Albani, D., & Giordano, C. (2020). Human gut-microbiota interaction in neurodegenerative disorders and current engineered tools for its modeling. *Front Cell Infect Microbiol, 10*, 297.

Chen, C., Ahn, E. H., Kang, S. S., Liu, X., Alam, A., & Ye, K. (2020). Gut dysbiosis contributes to amyloid pathology, associated with C/EBPβ/AEP signaling activation in Alzheimer's disease mouse model. *Sci Adv, 6*(31), eaba0466.

Choi, E.-K., Park, S.-H., Ha, K.-C., Noh, S.-o., Jung, S.-J., Chae, H.-J., . . . Park, T.-S. (2015). Clinical trial of the hypolipidemic effects of a brown alga *Ecklonia cava* extract in patients with hypercholesterolemia. *Int J Pharmacol, 11*(7), 798-805.

Cummings, J., Lee, G., Ritter, A., & Zhong, K. (2018). Alzheimer's disease drug development pipeline: 2018. *Alzheimers Dement (NY), 4*, 195-214.

El-Hakim, Y., Bake, S., Mani, K. K., & Sohrabji, F. (2022). Impact of intestinal disorders on central and peripheral nervous system diseases. *Neurobiol Dis, 165*, 105627.

González, H., Elgueta, D., Montoya, A., & Pacheco, R. (2014). Neuroimmune regulation of microglial activity involved in neuroinflammation and neurodegenerative diseases. *J Neuroimmunol, 274*(1), 1-13.

Grill, J. D., & Cummings, J. L. (2010). Novel targets for Alzheimer's disease treatment. *Expert Rev of Neurother, 10*(5), 711.

Harvey, B. S., Nicotra, L. L., Vu, M., & Smid, S. D. (2013). Cannabinoid CB2 receptor activation attenuates cytokine-evoked mucosal damage in a human colonic explant model without changing epithelial permeability. *Cytokine, 63*(2), 209-217.

Harvey, B. S., Sia, T. C., Wattchow, D. A., & Smid, S. D. (2014). Interleukin 17A evoked mucosal damage is attenuated by cannabidiol and anandamide in a human colonic explant model. *Cytokine, 65*(2), 236-244.

Hidalgo, I. J., Raub, T. J., & Borchardt, R. T. (1989). Characterization of the human colon carcinoma cell line (Caco-2) as a model system for intestinal epithelial permeability. *Gastroenterology, 96*(3), 736-749.

Honarpisheh, P., Reynolds, C. R., Blasco Conesa, M. P., Moruno Manchon, J. F., Putluri, N., Bhattacharjee, M. B., . . . Ganesh, B. P. (2020). Dysregulated gut homeostasis observed prior to the accumulation of the brain amyloid-β in Tg2576 Mice. *Int J Mol Sci, 21*(5), 1711.

Kim, A. D., Kang, K. A., Piao, M. J., Kim, K. C., Zheng, J., Yao, C. W., . . . Hyun, J. W. (2014). Cytoprotective effect of eckol against oxidative stress-induced mitochondrial dysfunction: involvement of the FoxO3a/AMPK pathway. *J Cell Biochem, 115*(8), 1403-1411.

Kitts, D. D. (2021). Antioxidant and functional activities of MRPs derived from different sugar-amino acid combinations and reaction conditions. *Antioxidants (Basel), 10*(11), 1840.

Lee, D. H., Park, M. Y., Shim, B. J., Youn, H. J., Hwang, H. J., Shin, H. C., & Jeon, H. K. (2012). Effects of *Ecklonia cava* polyphenol in individuals with hypercholesterolemia: a pilot study. *J Med Food, 15*(11), 1038-1044.

Lee, S. I., & Kim, I. H. (2020). Eckol alleviates intestinal dysfunction during suckling-to-weaning transition via modulation of PDX1 and HBEGF. *Int J Mol Sci, 21*(13), 4755.

Lu, J., Pan, Q., Zhou, J., Weng, Y., Chen, K., Shi, L., . . . Zhang, Z. (2022). Pharmacokinetics, distribution, and excretion of sodium oligomannate, a recently approved anti-Alzheimer's disease drug in China. *J Pharm Anal, 12*(1), 145-155.

Marizzoni, M., Cattaneo, A., Mirabelli, P., Festari, C., Lopizzo, N., Nicolosi, V., . . . Frisoni, G. B. (2020). Short-chain fatty acids and lipopolysaccharide as mediators between gut dysbiosis and amyloid pathology in Alzheimer's disease. *J Alzheimers Dis, 78*(2), 683-697.

Moon, C., Kim, S. H., Kim, J. C., Hyun, J. W., Lee, N. H., Park, J. W., & Shin, T. (2008). Protective effect of phlorotannin components phloroglucinol and eckol on radiation-induced intestinal injury in mice. *Phytother Res, 22*(2), 238-242.

Murata, N., Keitoku, S., Miyake, H., Tanaka, R., & Shibata, T. (2022). Evaluation on intestinal permeability of phlorotannins using Caco-2 cell monolayers. *Nat Prod Commun, 17*(1), 1-7.

Oh, J. K., Shin, Y. O., Yoon, J. H., Kim, S. H., Shin, H. C., & Hwang, H. J. (2010). Effect of supplementation with *Ecklonia cava* polyphenol on endurance performance of college students. *Int J Sport Nutr Exerc Metab, 20*(1), 72-79.

Shrestha, S., Choi, J. S., Zhang, W., & Smid, S. D. (2022). Neuroprotective activity of macroalgal fucofuroeckols against amyloid β peptide-induced cell death and oxidative stress. *Int J Food Sci*, doi: 10.1111/ijfs.15753.

Shrestha, S., Johnston, M. R., Zhang, W., & Smid, S. D. (2021). A phlorotannin isolated from *Ecklonia radiata*, Dibenzodioxin-fucodiphloroethol, inhibits neurotoxicity and aggregation of β-amyloid. *Phytomed Plus, 1*(4), 100125.

Shrestha, S., Zhang, W., Begbie, A., Pukala, T. L., & Smid, S. D. (2020). *Ecklonia radiata* extract containing eckol protects neuronal cells against $A\beta_{1-42}$ evoked toxicity and reduces aggregate density. *Food Funct, 11,* 6509-6516.

Shrestha, S., Zhang, W., & Smid, S. (2021). Phlorotannins: a review on biosynthesis, chemistry and bioactivity. *Food Biosci, 39*, 100832.

Sun, Y., Sommerville, N. R., Liu, J. Y. H., Ngan, M. P., Poon, D., Ponomarev, E. D., . . . Rudd, J. A. (2020). Intra-gastrointestinal amyloid-β1-42 oligomers perturb enteric function and induce Alzheimer's disease pathology. *J Physiol, 598*(19), 4209-4223.

Tamama, K. (2020). Potential benefits of dietary seaweeds as protection against COVID-19. *Nutr Revs, 79*(7), 814-823.

Vergauwen, H., Prims, S., Degroote, J., Wang, W., Casteleyn, C., van Cruchten, S., . . . van Ginneken, C. (2016). In vitro investigation of six antioxidants for pig diets. *Antioxidants (Basel), 5*(4), 41.

Vergauwen, H., Tambuyzer, B., Jennes, K., Degroote, J., Wang, W., De Smet, S., . . . Van Ginneken, C. (2015). Trolox and ascorbic acid reduce direct and indirect oxidative stress in the IPEC-J2 cells, an in vitro model for the porcine gastrointestinal tract. *PLoS One, 10*(3), e0120485.

Wang, X., Sun, G., Feng, T., Zhang, J., Huang, X., Wang, T., . . . Wang, H. (2019). Sodium oligomannate therapeutically remodels gut microbiota and suppresses gut bacterial amino acids-shaped neuroinflammation to inhibit Alzheimer's disease progression. *Cell Res, 29*(10), 787-803.

Yuan, Y., Zheng, Y., Zhou, J., Geng, Y., Zou, P., Li, Y., & Zhang, C. (2019). Polyphenol-rich extracts from brown macroalgae *Lessonia trabeculate* attenuate hyperglycemia and modulate gut microbiota in high-fat diet and streptozotocin-induced diabetic rats. *J Agric Food Chem*, *67*(45), 12472-12480.

Statement of Authorship

Title of Paper	Macroalgal phlorotannins decrease both basal and cytokine-induced angiotensin converting enzyme 2 (ACE2) expression in human intestinal and respiratory epithelial cells
Publication Status	☐ Published ☐ Accepted for Publication ☐ Submitted for Publication ☑ Unpublished and Unsubmitted work written in manuscript style
Publication Details	The chapter is formatted for submission to International Journal of Food Science and Technology

Principal Author

Name of Principal Author (Candidate)	Srijan Shrestha		
Contribution to the Paper	Conceptualization; Data curation; Formal analysis; Investigation; Methodology; Software; Writing – original draft; Writing – review & editing		
Overall percentage (%)	80%		
Certification:	This paper reports on original research I conducted during the period of my Higher Degree by Research candidature and is not subject to any obligations or contractual agreements with a third party that would constrain its inclusion in this thesis. I am the primary author of this paper.		
Signature		Date	17/05/2022

Co-Author Contributions

By signing the Statement of Authorship, each author certifies that:

i. the candidate's stated contribution to the publication is accurate (as detailed above);

ii. permission is granted for the candidate in include the publication in the thesis; and

iii. the sum of all co-author contributions is equal to 100% less the candidate's stated contribution.

Name of Co-Author	Dr. Jae Sue Choi		
Contribution to the Paper	Methodology, Resources		
Signature		Date	17/05/2022

Name of Co-Author	Dr. Wei Zhang		
Contribution to the Paper	Conceptualization, Resources, Methodology, Supervision		
Signature		Date	31/05/2022

Name of Co-Author	Dr. Scott Smid		
Contribution to the Paper	Conceptualization, Funding acquisition, Formal analysis, Resources, Supervision, Writing-review, and editing.		
Signature		Date	21-06-22

Chapter 6: Macroalgal phlorotannins decrease both basal and cytokine-induced angiotensin converting enzyme 2 (ACE-2) expression in human intestinal and respiratory epithelial cells

Srijan Shrestha[1], Jae Sue Choi[2], Wei Zhang[3,4,] Scott D. Smid[1*]

[1]Discipline of Pharmacology, School of Biomedicine, Faculty of Health Sciences, The University of Adelaide, South Australia, Australia

[2]Institute of Fisheries Sciences, Pukyong National University, Busan 46041, Korea

[3]Centre for Marine Bioproducts Development (CMBD) and [4]Dept. of Medical Biotechnology, College of Medicine and Public Health, Flinders University, South Australia, Australia

*Corresponding Author
Dr. Scott D. Smid
Discipline of Pharmacology
School of Biomedicine, Faculty of Health Sciences
The University of Adelaide
Adelaide SA 5005 Australia
Tel: 61 8 83135287
Fax: 61 8 82240685
Email: scott.smid@adelaide.edu.au

Abstract

As angiotensin converting enzyme 2 (ACE-2) enzyme is exploited by SARS-CoV-2 to gain epithelial cell entry with subsequent viral replication and covid-19 disease pathology, ACE-2 has emerged as a potential target for the development of SARS-CoV-2 therapies. Macroalgal (seaweed) phlorotannins have been shown to exhibit a variety of biological actions and are well tolerated by humans. In the present study, the effects of two eckol-type (eckol and dieckol) and fucofuroeckol-type (phlorofucofuroeckol-A (PFFA) and 974-A) phlorotannins in modulating basal and cytokine-stimulated ACE-2 expression and activity in intestinal Caco-2 and respiratory A549 cells were investigated. Results indicated that phlorotannins were innocuous to both Caco-2 and A549 cells up to 100 μM. Proinflammatory cytokine (TNF-α and IL-1β) incubation increased ACE-2 expression in both Caco-2 and A549 cell lines. In Caco-2 cells, eckol and dieckol had negligible influence on either basal or cytokine-stimulated ACE-2 expression. In A549 cells, dieckol significantly reduced basal ACE-2 isoform A expression, while eckol and dieckol significantly reduced the cytokine-induced expression of ACE-2 isoform A. In the Caco-2 cell line, however, PFFA and 974-A significantly reduced ACE-2 expression. Additionally, both compounds downregulated the basal and cytokine-induced expression of both isoforms A and B, with the exception of isoform B in PFFA-treated A549 cells. Altered expression profiles were accompanied by substantial inhibition of cytokine-induced ACE-2 enzymatic activity in PFFA and 974-A- treated cells. Overall, our findings demonstrate that phlorotannins can variably modulate the expression and activity of ACE-2 in both basal and pro-inflammatory settings and suggest these macroalgal polyphenols may therefore inform further development of COVID-19 treatment strategies centred upon prophylaxis and virulence mitigation.

Keywords: Phlorotannins, ACE-2, SARS-CoV-2, Fucofuroeckols, eckols

1. Introduction

In the last two decades, three major pandemics were encountered caused by coronaviruses namely, severe acute respiratory syndrome-related coronavirus 1 (SARS-CoV-1), Middle East respiratory and syndrome-related coronavirus (MERS-CoV) and novel coronavirus (2019-nCoV or SARS-CoV-2) (Cui, Li, & Shi, 2019). These viruses belong to the beta-coronavirus genus, the type of positive-stranded RNA viruses that cause mild to severe respiratory disease (Ziegler et al., 2020). A coronavirus consists of four structural proteins namely envelope, membrane, nucleocapsid, and spike proteins (Beyerstedt, Casaro, & Rangel, 2021). The spike protein consists of subunits S1 and S2 and are responsible for attachment, membrane fusion and entry. The spike protein engages with human angiotensin-converting enzyme 2 (ACE-2) protein as their entry receptor, thus playing a crucial role in infectivity (Li et al., 2003) and it is believed that higher infectivity of evolving variants is related to an enhanced affinity of spike protein to ACE-2 (Kumar, Singh, Hasnain, & Sundar, 2021; Tai et al., 2020; Wrapp et al., 2020). ACE-2 is a type 1 membrane protein expressed in the lungs, heart, kidney, and intestines where enhanced expression in the lungs is particularly linked to a range of respiratory conditions. ACE-2 expression in human small airway epithelium was found to be elevated in SARS-CoV-1 and SARS-CoV-2 infected patients, smokers and chronic obstructive pulmonary disease patients and in a smoke inhalational rat model, which could be associated with higher COVID-19 infection propensity and disease severity (Hung et al., 2016; Leung et al., 2020; Yilin, Yandong, & Faguang, 2015; Zhuang et al., 2020). Therefore, downregulation of ACE-2 levels could be a viable strategy for mitigating infection vulnerability.

Phlorotannins are polyphenolic compounds synthesized especially by Class Phaeophyceae, or brown marine macroalgae (Shrestha, Zhang, & Smid, 2021). These compounds have been reported to have antiviral activities against influenza virus (Cho et al., 2019), HIV (Ahn et al., 2004; Artan

et al., 2008), porcine epidemic diarrhea virus (Kwon et al., 2013), murine norovirus (Eom et al., 2015), and SARS-CoV $3CL^{pro}$ (Park et al., 2013). Furthermore, Tamama (2020) argued that the lower number of deaths per 100,000 population in Southeast Asian countries like Japan and South Korea could be attributed to the consumption of dietary seaweed containing diverse bioactive components including phlorotannins (Tamama, 2020). These phlorotannins have also been reported to have antioxidant and anti-inflammatory activity, decreasing reactive oxygen species levels in infected cells, and targeting various signaling pathways for reducing viral load (Fedoreyev et al., 2018). Most notably, a recent clinical investigation found that such phlorotannins are well tolerated when used in Type II Diabetes mellitus patients with recent cardiovascular complications (ClinicalTrials.gov Identifier: NCT04141241).

In the present study, two eckol-type (eckol and dieckol) and two fucofuroeckol-type (PFFA and 974-A) phlorotannins (see Fig. 1) were selected for their influence on modulating ACE-2 expression and activity in human lung-derived epithelial cells (A549) and human intestinal epithelial cells (Caco-2) under basal and proinflammatory conditions using cytokines IL-1β and TNF-α. ACE-2 protein is expressed in both these cell lines (Chu et al., 2020; Jia et al., 2005; Xiao et al., 2021) and both IL-1β and TNF-α have been shown to increased ACE-2 mRNA levels in primary cultures (Chang et al., 2020; Coperchini et al., 2021; Potdar et al., 2021; Ziegler et al., 2020), providing an adaptable cell model system enabling screening of selected marine-derived bioactives for ACE-2 modulatory effects.

2. Materials and Methods

2.1. Reagents and chemicals

Eckol was obtained as described previously (Shrestha, Zhang, Begbie, Pukala, & Smid, 2020). Dieckol, phlorofucofuroeckol-A (PFFA) and 974-A were kindly provided by Prof. Jae Sue Choi (Pukyong National University, Republic of Korea). 3-(4,5-Dimethylthiazol-2-yl)-2,5-diphenyltetrazolium bromide (MTT), DMEM, trypan blue, non-essential amino acids (NEAA), penicillin/streptomycin, trypsin EDTA, foetal bovine serum (FBS), phosphate buffered saline (PBS), and *tert*-butyl hydroperoxide (*t*-BHP) were purchased from Sigma-Aldrich (NSW, Australia). Angiotensin II Converting Enzyme (ACE-2) Activity Assay Kit (Fluorometric), RIPA buffer, protease inhibitor cocktail, rabbit monoclonal β-actin antibody (ab115777) and rabbit polyclonal ACE-2 antibody (ab15348) were purchased from Abcam (Victoria, Australia). Goat anti-rabbit antibody (SA535571) was obtained from ThermoFisher Scientific (Victoria, Australia).

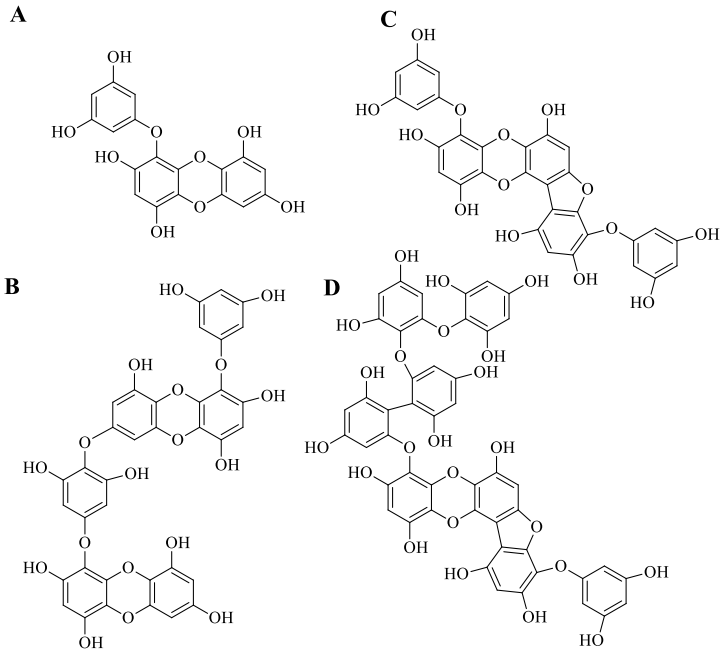

Fig 1. Structure of phlorotannins used in this study; eckol (**A**), dieckol (**B**), PFFA (**C**), and 974-A (**D**)

2.2. Cell culture

Caco-2 cells derived from human colorectal carcinoma were obtained from the American Type Culture Collection (ATCC) (Manassas, VA, USA). A549 cells were kindly donated by Prof. Philip C. Burcham (University of Western Australia, Australia). Both cell lines were maintained in 75cm^2 tissue culture flasks (Corning Life Sciences, Lowell, MA, USA) at 37 °C with 5% CO_2 in DMEM supplemented with 10% FBS and 1% penicillin/streptomycin solution. Cells were passaged every 3-4 days when at approximately 80% confluence.

2.3. Assessment of effects of phlorotannins on cell viability

The measurement of cell viability was determined using the MTT assay. Both cell lines were seeded at 2×10^4 cells per well in 100 µL media into 96 well tissue culture plates. The cells were incubated for 48 h at 37 °C with 5% CO_2 and treated with 0 to 100 µM concentrations of phlorotannins. The plate was then incubated for 24 h and MTT absorbance measured at 570 nm.

2.4. ACE-2 enzyme activity assay

A549 cells were seeded at 2×10^5 cells per ml in 25cm^2 tissue culture flasks (Corning Life Sciences, Lowell, MA, USA) and incubated for 48 hours at 37 °C with 5% CO_2. The cells were then pre-treated with phlorotannins (100 µM) followed by treatment with TNF-α (10 nM) and IL-1β (10 nM) and incubated for 24 hours. After treatment, A549 cells were harvested in ice-cold lysis buffer and the assay performed according to the manufacturer's protocol (Abcam # ab273297). Briefly, the amount of protein was measured by BCA assay and normalised accordingly. The samples (phlorotannins; positive and negative control) were mixed with 50 µL of a prepared substrate to make a final volume of 100 µL in 96 well black plates. The fluorescence was then monitored using a Synergy MX microplate reader (Bio-Tek, Bedfordshire, UK) with excitation and emission wavelengths of 320 nm and 420 nm, respectively, at 25 °C every 10

minutes for 2 hours. A methoxycoumarin (MCA) standard curve was obtained, and ACE-2 activity (mU/mg) was obtained as per the formula:

$$\text{ACE2 activity } \left(\frac{\text{mU}}{\text{mg}}\right) = (B \times D)/(\Delta T \times P)$$

where:

B = released MCA in the sample based on the standard curve slope (pmol)

ΔT = reaction time

P = sample used (in mg)

D = sample dilution

2.5. Western blotting for ACE-2 protein expression

Cell lysates were prepared as described earlier (in Section 2.4). The protein in each sample was measured via the BCA assay and normalised using lysis buffer. Approx. 31 µg of protein lysate was loaded in each well of a Mini Protein TGX precast (any kD) gel (Bio-Rad, Gladesville, NSW, Australia) and electrophoresis was performed at 80V for 15 min and 100V for 2 h in running buffer. After electrophoresis, proteins were transferred onto a PVDF membrane at 80V for 1 h in transfer buffer. The membrane was then blocked with 5% non-fat dry milk in 0.1% Tween 20 in Tris-buffered saline. Western blot analysis was performed using polyclonal ACE-2 antibody (Abcam #ab15348) and β-actin antibody (Abcam #ab115777) was used to normalize the data. The membrane was incubated with a primary antibody with recommended dilutions over 18 h at 4°C and incubated with an HRP-conjugated goat anti-rabbit antibody (Invitrogen #SA535571) for 1 h at room temperature. The membrane was then washed and air-dried before ACE-2 immunoreactive bands were detected using a Li-COR Odyssey infrared imaging system at 800 nm and 700 nm (Li-Cor Biosciences, Cambridge, UK). The density of the protein was quantified using ImageJ software and expressed relative to β-actin density.

2.6. Molecular docking studies

Molecular docking analysis of phlorotannins in the active site of ACE-2 was carried out using a previously reported procedure in CLC Drug Discovery Workbench (v2.4.1) (Shrestha, Johnston, Zhang, & Smid, 2021).The 3D structure of eckol, dieckol, and PFFA were obtained from PubChem (CID: 145937, 3008868, 130976) and the structure of 974-A was prepared and optimized in Chem3D Pro v12.0 and adjusted to pH 7.0 using MarvinSketch (ChemAxon, Budapest, Hungary). The X-ray crystallized structure of ACE-2 (PDB ID: 1R4L) was obtained from the RCSB protein data bank (rcsb.org/). The binding pockets of 1R4L were determined and the binding site was established around the ACE-2 inhibitor MLN-4760, defined to enclose residues located within 13 Å as documented previously (Tateyama Makino et al., 2021; Teralı, Baddal, & Gülcan, 2020). The protocol was validated by re-docking the co-crystallized ligand MLN-4760 and protein structure 1R4L, with the pose of the inhibitor reproduced well as demonstrated in the Results (Table 1). The results were exported and visualized via Discovery Studio 2021 Client (Accelrys, San Diego, USA).

2.7. Statistical analysis

All experiments were performed in quadruplicate with at least 3-4 independent experiments and expressed as mean±SD. GraphPad Prism 8 was used for data analysis and graph creation (GraphPad Software, San Diego, USA). Data obtained from MTT assays and Western blots were analysed via one-way analysis of variance (ANOVA) with a Bonferroni's post-hoc test to determine statistical significance between treatments, with a significance level set at $p < 0.05$.

3. Results

3.1. Effects of phlorotannins on cell viability in Caco-2 and A549 cell lines

No decrease in cell viability was observed up to a concentration of 100 µM of each phlorotannin as indicated by the MTT assay (Fig. 2A and 2 B).

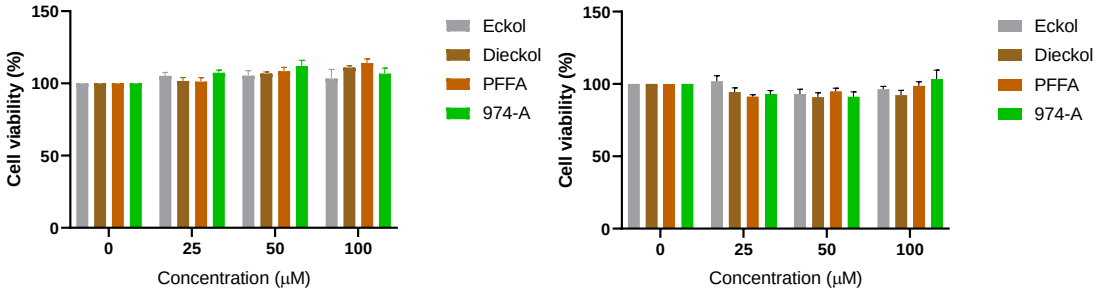

Fig. 2 Cell viability assay of phlorotannin in Caco-2 (**A**) and A549 (**B**) cells following 24 h incubation with different concentration of phlorotannins. Each bar is an average from at least four independent experiments

3.2. Influence of phlorotannins on basal ACE-2 expression in Caco-2 and A549 cell lines

As shown in Fig. 3, a single band corresponding to ACE-2 protein was observed at ~ 100 kDa in the Caco-2 cell line. Each phlorotannin demonstrated some intrinsic degree of influence on ACE-2 expression. Eckol and dieckol reduced ACE-2 expression marginally but not significantly, whereas PFFA and 974-A markedly reduced ACE-2 expression (**$p < 0.01$ *vs* control).

A549 cells were treated with 100 µM of each phlorotannin and ACE-2 expression was determined as shown in Fig 4(A, B, and C). In contrast to Caco-2 cells, two bands were observed between 150-100 kDa (A-isoform) and 100-75 kDa (B-isoform). As demonstrated in Fig 4(B), all phlorotannins were able to decrease ACE-2 isoform A expression significantly except for eckol-treated cells; ACE-2 expression was markedly reduced by both fucofuroeckols 974-A (**** $p < 0.0001$ *vs* control) and PFFA (*** $p < 0.001$ *vs* control), but also to a lesser extent by dieckol (**

$p < 0.01$ *vs* control). Only 974-A, however, was able to significantly reduce the expression of ACE-2 isoform B (Fig 4(C)).

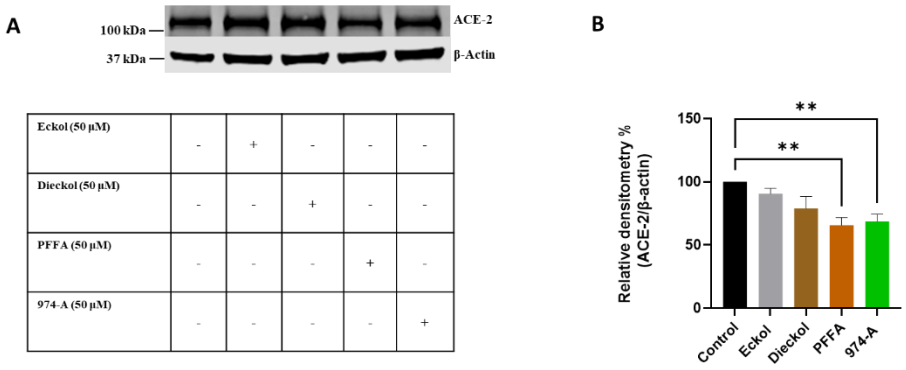

Fig 3. Influence of phlorotannins on basal ACE-2 expression in the Caco-2 cell line. Western blot analysis of ACE-2 protein. (**A**) A representative example of three similar blots from three separate experiments, with β-actin as control. (**B**) Relative densitometry of ACE-2 as determined using ImageJ. ** $p < 0.01$ *vs* control

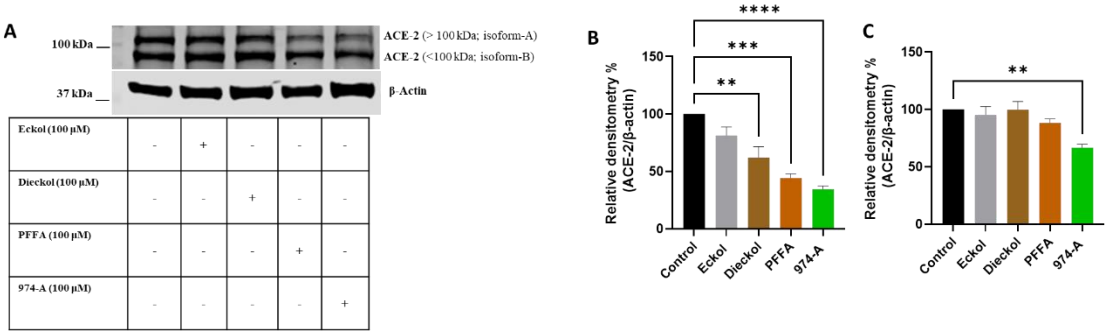

Fig 4. Influence of phlorotannins on basal ACE-2 expression in A549 cells. Western blot analysis of ACE-2, with β-Actin as control. (**A**) A representative example of three similar blots from three separate experiments. Relative densitometry of ACE-2 isoform A (**B**) and isoform B (**C**) as determined using ImageJ. **$p < 0.01$ *vs* control; *** $p < 0.001$ *vs* control; **** $p < 0.0001$ *vs* control.

3.3. Influence of phlorotannins on ACE-2 expression induced by cytokines in Caco-2 and A549 cells

Our preliminary findings revealed that intestinal Caco-2 cells pretreated with a combination of TNF-α and IL-1β (each at 10 ng/ml) expressed significantly higher ACE-2 levels than when incubated with each cytokine individually (data not shown), so these cytokines were used in combination in subsequent experiments. TNF-α and IL-1β (each at 10 ng/ml) induced a significant increase in ACE-2 expression in Caco-2 cells (Fig. 5; *$p < 0.1$ *vs* control). Caco-2 cells were then pretreated with 50 µM of each phlorotannin for 2 h followed by cytokine treatment. Eckol and dieckol did not alter the level of ACE-2 which appears at ~ 100 kDa by Western blot (Fig 5A). However, the level of ACE-2 was significantly decreased in PFFA and 974-A treated cells in the presence of TNF-α and IL-1β (Fig 5B; *** $p < 0.001$ *vs* cytokines).

TNF-α (10 ng/ml) + IL-1β (10 ng/ml)	-	+	+	+	+	+
Eckol (50 µM) + TNF-α (10 ng/ml) + IL-1β (10 ng/ml)	-	-	+	-	-	-
Dieckol (50 µM) TNF-α (10 ng/ml) + IL-1β (10 ng/ml)	-	-	-	+	-	-
PFFA (50 µM) TNF-α (10 ng/ml) + IL-1β (10 ng/ml)	-	-	-	-	+	-
974-A (50 µM) TNF-α (10 ng/ml) + IL-1β (10 ng/ml)	-	-	-	-	-	+

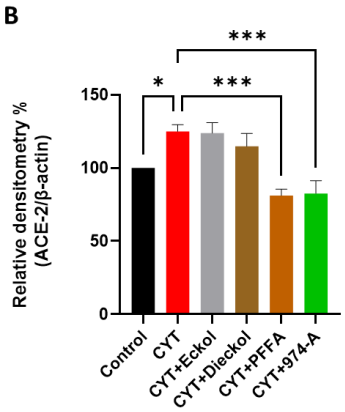

Fig 5. Influence of phlorotannins in ACE-2 expression induced by cytokines (CYT) in Caco-2 cell line. Western blot analysis of ACE-2 with β-Actin as a control. (**A**) A representative example of three similar blots from three separate experiments. (**B**) Relative densitometry as determined using ImageJ. *$p < 0.1$ *vs* control; *** $p < 0.001$ *vs* control.

Similar effects were demonstrated in respiratory epithelial A549 cells when treated with TNF-α and IL-1β (each at 10 ng/ml) as shown in Fig 6 (A). ACE-2 A isoform was upregulated significantly versus control (*** $p < 0.001$), while all of the four tested phlorotannins significantly downregulated ACE-2 isoform A expression compared with the cytokine-treated group (Fig. 6B; *** $p < 0.001$ *vs* cytokines). Notably again, the fucofuroeckols PFFA and 974-A were markedly effective in reducing ACE-2 expression compared with eckol and dieckol, with three- to five-fold reductions noted in isoform A (Fig 6B). By contrast, isoform B was less affected by prior phlorotannin exposure overall, where only PFFA and 974-A were able to downregulate the ACE-2 isoform B as demonstrated in Fig.6 (C) (** $p < 0.01$ *vs* cytokines).

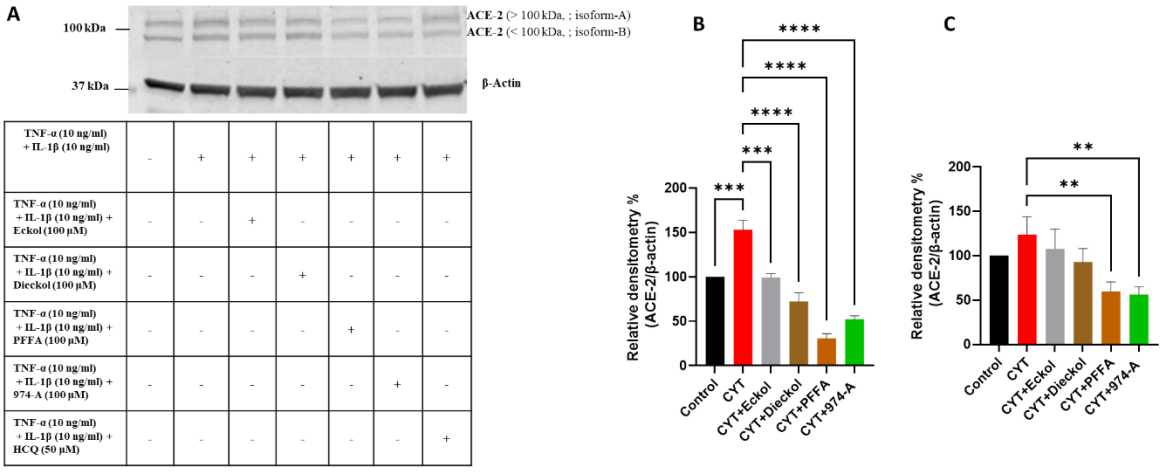

Fig 6. Influence of phlorotannins in ACE-2 expression induced by cytokines (CYT) in the A549 cell line. Western blot analysis of ACE-2 with β-Actin as a control. (**A**) A representative example of three similar blots from three separate experiments. Relative densitometry of ACE-2 isoform-A (**B**) and isoform-B (**C**) was determined using ImageJ. **$p < 0.01$ *vs* control; *** $p < 0.001$ *vs* control; **** $p < 0.0001$ *vs* control.

3.4. ACE-2 enzyme activity in A549 cells: effects of phlorotannins

An increment in ACE-2 enzymatic activity in cytokine-treated A549 cells was observed versus control (Fig 7; **$p < 0.01$ *vs* control) while ACE-2 enzymatic activity was unaltered by pretreatment of cells with eckol and dieckol. However, pretreatment with PFFA or 974-A

significantly reduced enzymatic activity by approximately 45% in PFFA-treated cells (**** $p <$ 0.0001 *vs* cytokines) and 22 % in 974-A treated cells (**$p < 0.01$ *vs* cytokines). ACE-2 activity was not measured in Caco-2 cells.

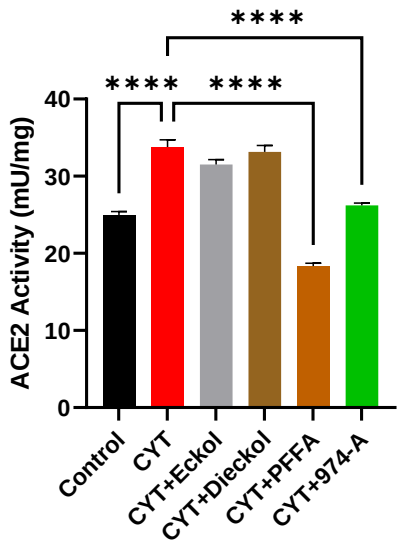

Fig 7. ACE-2 enzyme assay. A549 cells were pretreated with cytokines (TNF-α and IL-1β) and treated with 100 μM of different phlorotannins followed by 24 h incubation and were harvested for enzyme assay. Data are presented as the mean ± SEM of at least three cell cultures. **** $p <$ 0.0001 *vs* control

3.5. Interaction of phlorotannins in the active site of ACE-2 (Modelling/In silico studies)

Each phlorotannin was docked into the active site of ACE-2 (PDB:1R4L) as shown in Fig. 8 and the results illustrated in Table 1. Eckol has the lowest binding score of -65.67 along with the steric interaction score of -47.05 compared with the other phlorotannins as shown in Table 1. Eckol formed three hydrogen bonds with ARG273, GLU406, and THR445 with hydrogen bond score of -20.70. Furthermore, THR276, ASP269, THR371, GLU375, PRO346, SER 409, HIS505, TYR515, and ARG518 of 1R4L participated in Van der Waals interactions. PHE 274 and HIS374 participated in π-π stacked interactions and LEU370 and ASP367 were involved in π-alkyl and π-anion interactions, respectively as shown in Fig 8 (A and E).

Dieckol exhibited a binding score of -76.89 along with 62.29 steric interaction score. ARG273, ALA348, CYS361, and GLU402 engaged in hydrogen bond interaction with a hydrogen bond score of -21.16 and 4.00 metal interaction score. Further, LEU144, TYR127, SER128, GLU145, ASN149, TRP271, PHE274, THR347, TRP349, MET360, THR362, LYS363, ASP368, THR371, GLU375, ASP 382, HIS401, TYR510, ARG514, and ARG518 participated in Van der Waals interactions with dieckol. Two phenolic rings from each end were involved in π-π stacked interactions with CYS344 and HIS378, while HIS345, PRO346, HIS374, HIS505, and TYR515 engaged in π-alkyl interaction as shown in Fig 8 (B and F).

PFF-A had a binding score of -71.15 along with steric interaction score of -60.99. HIS345 and LYS363 participated in the formation of two hydrogen bonds with H-bond score of -18.23. TYR127, LEU144, GLU145, TRP271, ARG273, THR276, CYS 344, PRO346, CYS361, ASP367, HIS374, GLU406, SER409, THR445, ARG518 and PHE504 engaged in Van der Waals interactions with PFFA as shown in Fig 8(C and G). Additionally, PHE274 and LEU370 participated in π-π stacked and π-alkyl interactions, respectively.

974-A exhibited a docking score of -56.88 with a -50.60 steric interaction score. ASP269, HIS345, and ASP367 engaged in the formation of three H-bond with 974-A as shown in Fig. 8(D and H). TYR127, SER128, GLU145, GLY268, ARG273, ASN 277, CYS344, THR347, ALA348, CYS361, LYS363, THR365, ASP368, THR371, HIS374, GLU375, HIS378, GLU402, LEU503, PHE504, HIS505, and TYR515 residues were involved in the Van der Waals interactions with the phenolic rings of 974-A. Additionally, TRP271, PHE274, and TYR510 formed π-π stacked interactions while LEU144, ALA153, and PRO346 formed π-alkyl interactions with the 974-A.

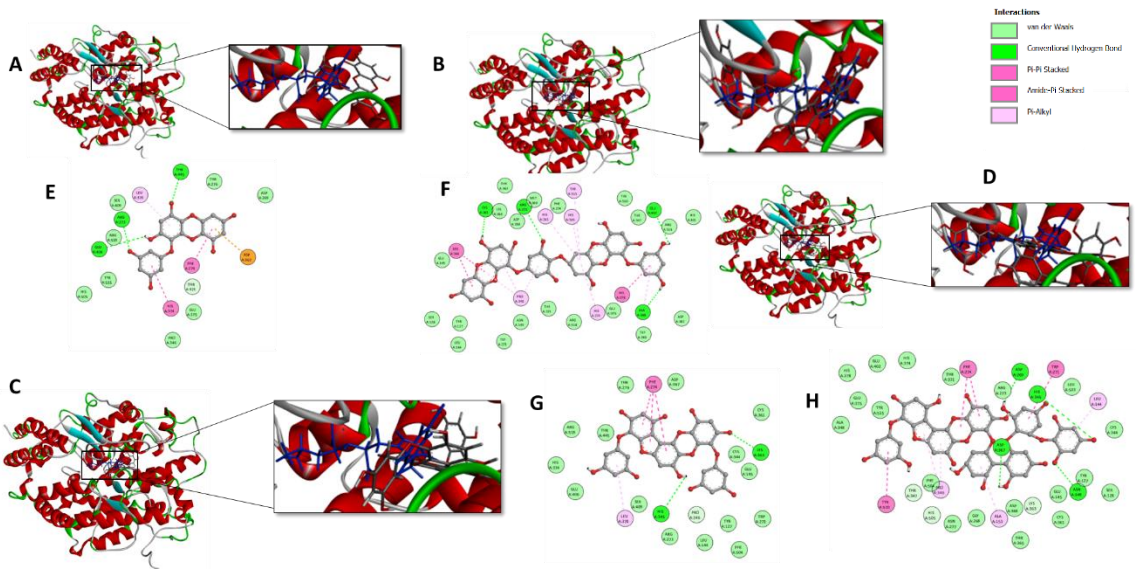

Fig 8. Binding sites of eckol (**A**), dieckol (**B**), PFFA (**C**), and 974-A (**D**) in active site of ACE-2. 2D ligand interaction diagram of active site with eckol (**E**), dieckol (**F**), PFFA (**G**), and 974-A (**H**). Discovery Studio R2 was used for visualization.

4. Discussion

ACE-2 is an integral membrane protein found in the lungs, intestine, liver, heart, kidney and endothelium (Donoghue et al., 2000; Li, Li, Zhang, & Wang, 2020). Unlike other corona viruses, SARS-CoV-2 only exploits ACE-2 protein for cell entry and subsequent viral replication (Guan et al., 2020; Huang et al., 2020). ACE-2 expression has been previously reported to be upregulated by proinflammatory cytokines such as TNF-α and IL-1β (Zhuang et al., 2020). Additionally, the regulation of ACE-2 expression has also been previously shown to be mediated by the interferons, including induction of ACE-2 expression in primary nasal epithelial cells (Chang et al., 2020; Ziegler et al., 2020). Comparable results were observed in our study when the combination of TNF-α and IL-1β was used in epithelial Caco-2 and A549 cells. Our findings demonstrated that eckol and dieckol have negligible overall effects on the regulation of ACE-2 expression in Caco-2 cells. It's worth noting that these are the most abundant compounds found in the extract of

Ecklonia species and Seapolynol^{TM} (commercially available *Ecklonia* extract from Botamedi, Jeju, Korea) (Choi, Jeon, Lee, & Lee, 2015; Shrestha et al., 2020). Two different ACE-2 isoforms were observed via western blot in A549 cells, but not Caco-2 cells. Previously, Xiao et al. also noted a similar isoform distribution in the A549 cell line (Xiao et al., 2021), while several other studies have reported the expression of similar isoforms (Uhal, Dang, et al., 2013; Uhal, Nguyen, et al., 2013; Wang, Li, Fiselier, Kovalchuk, & Kovalchuk, 2022). All phlorotannins except eckol significantly reduced basal ACE-2 isoform A expression in A549 respiratory epithelial cells, whereas basal ACE-2 isoform-B was reduced by 974-A only (Fig 4C). On the other hand, all phlorotannins diminished the cytokine-induced increase in ACE-2 isoform-A expression and only PFFA and 974-A decreased the ACE-2 isofrom-B (Fig 6B and 6C).

A similar pattern of changes in ACE-2 expression was observed in a previous study using medicinal cannabis extracts in EpiAirway (human 3D mucociliary tissue model that consists of normal, human-derived tracheal/bronchial epithelial cells) and EpiOral tissues (human-derived oral epithelial cells, where such cannabidiol-rich extracts significantly downregulated ACE-2 expression (Wang et al., 2020). Additionally, these cannabis extracts suppressed COX-2 expression and markedly attenuated TNFα/IFNγ triggered induction of proinflammatory factors IL-6 and IL-8 via the AKT pathway (Wang et al., 2022). As phlorotannins were also reported to have suppressed inflammatory responses in various cell lines by decreasing the expression of COX-2 and iNOS through blockade of NF-κB activation via inhibition of AKT pathways (A.-R. Kim et al., 2016; A.-R. Kim et al., 2009; A. R. Kim et al., 2011), it stands to reason that downregulation of ACE-2 by phlorotannins may be due to an AKT-mediated inhibition similar to that described for cannabidiol as the purported predominant phytocannabinoid in cannabis extracts (Wang et al., 2022).

Additionally, only PFFA and 974-A significantly inhibited the enzymatic activity of ACE-2 induced by cytokines, while eckol and dieckol had no impact (Fig 7). This difference between phlorotannin classes provides some insight into potential structure-activity relationships for bioactivity, where a similar profile of differential bioactivity between phlorotannin classes has been observed in a previous study comparing neuroprotective effects of these phlorotannins (Shrestha, Choi, Zhang, & Smid, 2022), with the most notable structural difference potentially attributable to the findings being the presence of benzofuran ring in the fucofuroeckols (PFFA and 974-A). Benzofuran-containing compounds have previously been reported to possess a spectrum of biological activities (Miao et al., 2019), however, no relevant information has been uncovered to date that ascribes a molecular or cellular basis of action conferring a selective benefit solely attributable to the benzofuran moiety.

Molecular modelling was also generated to provide some structural insights into the interactions of each phlorotannin with ACE-2. Molecular docking simulations revealed that all four phlorotannins were able to bind to the active site of ACE-2, potentially causing significant conformational rearrangements in the ACE-2 N-terminal peptidase domain to achieve a catalytic competent geometry and obstructing viral attachment to permissive cell surfaces (Teralı et al., 2020).

Phlorotannins are well documented for their antioxidant and anti-inflammatory properties (Sugiura et al., 2006). They are considered important sources of therapeutic agents and are capable of eliciting altered enzyme activities and modulating intracellular signaling due to their complex structures (Shrestha et al., 2021; Sugiura et al., 2006). Currently, there are several polyphenols in various clinical trials registered for prophylaxis and the treatment of COVID-19 (clinicalTrials.gov Identifier: NCT04377789, NCT04578158, NCT04536090, NCT04446065, NCT04861298,

NCT04851821, and NCT04799743). Therefore, more research into phlorotannins from brown seaweeds, particularly fucofuroeckols containing a benzofuran ring is needed as well as new synthetic or semi-synthetic compounds in order to determine structure-activity relationships.

However, it needs to be considered that apart from being the major receptor of SARS-Cov-2, ACE-2 is a putative regulator of the renin-angiotensin-aldosterone system (RAAS), converting angiotensin II to angiotensin (1–7) and playing a beneficial effect in lowering hypertension and activating anti-inflammatory pathways following tissue injury (Ahmad, Pawara, Surana, & Patel, 2021). Nonetheless, angiotensin-converting enzyme (ACE) inhibitory activity has also been reported for these phlorotannins (Jung, Hyun, Kim, & Choi, 2006; Wijesinghe, Ko, & Jeon, 2011), so the counterbalanced influence of phlorotannins on the RAAS system, inclusive of ACE-2 and associated hemodynamic and cardiovascular sequelae may be complex and merit further in vivo investigation. Notably though, phlorotannins have shown protective effects on proinflammatory responses and hypertensive nephropathy in vitro and in vivo (Kim et al., 2009; Moon et al., 2008; Son et al., 2021) suggesting potentially widespread benefits in multiple organ systems via modulation of inflammatory pathways more generally.

In conclusion, our results have demonstrated that phlorotannins have the potential to inform further drug development for the prophylaxis and mitigation of virulence of COVID-19 infection via downregulatory actions on constitutive and cytokine-induced ACE-2 enzyme expression and inhibition of functional catalytic activity.

Table 1. Hydrogen and hydrophobic interactions of phlorotannins with ACE-2 (1R4L)

Samples	Docking score	Steric interaction score	Hydrogen bond score	Metal interaction score	H-bond forming residues	Van der Waals residues	Others				
							π-π stacked	π-Alkyl	π-Sigma	Amide-π stacked	π-Anion
Eckol	-65.67	-47.05	-20.70	-	ARG273, GLU406, THR445	THR276, ASP269, THR371, GLU375, PRO346, SER 409, HIS505, TYR515, ARG518	PHE 274, HIS374	LEU370	-	-	ASP367
Dieckol	-76.89	-62.29	-21.16	4.00	ARG273, ALA348, CYS361, GLU402	LEU144, TYR127, SER128, GLU145, ASN149, TRP271, PHE274, THR347, TRP349, MET360, THR362, LYS363, ASP368, THR371, GLU375, ASP 382, HIS401, TYR510, ARG514, ARG518	CYS344, HIS378	HIS345, PRO346, HIS374, HIS505, TYR515	-	-	-
PFF-A	-71.15	-60.99	-18.23	-	HIS345, LYS363	TYR127, LEU144, GLU145, TRP271, ARG273, THR276, CYS 344, PRO346, CYS361, ASP367, HIS374, GLU406, SER409, THR445, ARG518, PHE504	PHE274	LEU370	-	-	-
974-A	-73.89	-61.87	-25.08	0.50	ASP269, HIS345, ASP367	TYR127, SER128, GLU145, GLY268, ARG273, ASN 277, CYS344, THR347, ALA348, CYS361, LYS363, THR365, ASP368, THR371, HIS374, GLU375, HIS378, GLU402, LEU503 PHE504, HIS505, TYR515	TRP271, PHE274, TYR510	LEU144, ALA153, PRO346	-	-	-
MLN-4760	-56.88	-50.60	-10.72	-4.00	HIS505, TYR515	GLU145, PHE274, THR347, ALA348, CYS361, ASP368, THR 371, HIS374, GLU375, HIS378, GLU402, PHE504, ARG514	-	LYS363, PRO346, TYR510	HIS345	CYS344	-

References

Ahmad, I., Pawara, R., Surana, S., & Patel, H. (2021). The repurposed ACE2 inhibitors: SARS-CoV-2 entry blockers of Covid-19. *Topics in Current Chemistry, 379*(6), 40.

Ahn, M. J., Yoon, K. D., Min, S. Y., Lee, J. S., Kim, J. H., Kim, T. G., . . . Kim, J. (2004). Inhibition of HIV-1 reverse transcriptase and protease by phlorotannins from the brown alga Ecklonia cava. *Biological and Pharmaceutical Bulletin, 27*(4), 544-547.

Artan, M., Li, Y., Karadeniz, F., Lee, S. H., Kim, M.-M., & Kim, S. K. (2008). Anti-HIV-1 activity of phloroglucinol derivative, 6, 6′-bieckol, from *Ecklonia cava*. *Bioorganic & Medicinal Chemistry, 16*(17), 7921-7926.

Beyerstedt, S., Casaro, E. B., & Rangel, É. B. (2021). COVID-19: angiotensin-converting enzyme 2 (ACE2) expression and tissue susceptibility to SARS-CoV-2 infection. *European Journal of Clinical Microbiology & Infectious Diseases, 40*(5), 905-919.

Chang, E. H., Willis, A. L., Romanoski, C. E., Cusanovich, D. A., Pouladi, N., Li, J., . . . Martinez, F. D. (2020). Rhinovirus infections in individuals with Asthma increase ACE2 expression and cytokine pathways implicated in COVID-19. *American Journal of Respiratory and Critical Care Medicine, 202*(5), 753-755.

Cho, H. M., Doan, T. P., Ha, T. K. Q., Kim, H. W., Lee, B. W., Pham, H. T. T., . . . Oh, W. K. (2019). Dereplication by high-performance liquid chromatography (HPLC) with quadrupole-time-of-flight mass spectroscopy (qTOF-MS) and antiviral activities of phlorotannins from *Ecklonia cava*. *Marine Drugs, 17*(3), 149.

Choi, H. S., Jeon, H. J., Lee, O. H., & Lee, B. Y. (2015). Dieckol, a major phlorotannin in *Ecklonia cava*, suppresses lipid accumulation in the adipocytes of high-fat diet-fed zebrafish and mice: Inhibition of early adipogenesis via cell-cycle arrest and AMPKα activation. *Molecular Nutrition & Food Research, 59*(8), 1458-1471.

Chu, H., Chan, J. F., Yuen, T. T., Shuai, H., Yuan, S., Wang, Y., . . . Yuen, K. Y. (2020). Comparative tropism, replication kinetics, and cell damage profiling of SARS-CoV-2 and SARS-CoV with implications for clinical manifestations, transmissibility, and laboratory studies of COVID-19: an observational study. *Lancet Microbe, 1*(1), e14-e23.

Coperchini, F., Ricci, G., Croce, L., Denegri, M., Ruggiero, R., Villani, L., . . . Rotondi, M. (2021). Modulation of ACE-2 mRNA by inflammatory cytokines in human thyroid cells: a pilot study. *Endocrine, 74*(3), 638-645.

Cui, J., Li, F., & Shi, Z.-L. (2019). Origin and evolution of pathogenic coronaviruses. *Nature Reviews Microbiology, 17*(3), 181-192.

Donoghue, M., Hsieh, F., Baronas, E., Godbout, K., Gosselin, M., Stagliano, N., . . . Acton, S. (2000). A novel angiotensin-converting enzyme-related carboxypeptidase (ACE2) converts angiotensin I to angiotensin 1-9. *Circulation Research, 87*(5), E1-9.

Eom, S. H., Moon, S. Y., Lee, D. S., Kim, H. J., Park, K., Lee, E. W., . . . Kim, Y. M. (2015). In vitro antiviral activity of dieckol and phlorofucofuroeckol-A isolated from edible brown alga *Eisenia bicyclis* against murine norovirus. *Algae, 30*(3), 241-246.

Fedoreyev, S. A., Krylova, N. V., Mishchenko, N. P., Vasileva, E. A., Pislyagin, E. A., Iunikhina, O. V., . . . Leonova, G. N. (2018). Antiviral and antioxidant properties of echinochrome A. *Marine Drugs, 16*(12), 509.

Guan, W.-J., Ni, Z.-Y., Hu, Y., Liang, W.-H., Ou, C.-Q., He, J.-X., . . . Zhong, N.-S. (2020). Clinical characteristics of coronavirus disease 2019 in China. *New England Journal of Medicine, 382*(18), 1708-1720.

Huang, C., Wang, Y., Li, X., Ren, L., Zhao, J., Hu, Y., . . . Cao, B. (2020). Clinical features of patients infected with 2019 novel coronavirus in Wuhan, China. *Lancet, 395*(10223), 497-506.

Hung, Y. H., Hsieh, W. Y., Hsieh, J. S., Liu, F. C., Tsai, C. H., Lu, L. C., . . . Lin, C. S. (2016). Alternative roles of STAT3 and MAPK signaling pathways in the MMPs activation and progression of lung injury induced by cigarette smoke exposure in ACE2 knockout mice. *International Journal of Biological Sciences, 12*(4), 454-465.

Jia, H. P., Look, D. C., Shi, L., Hickey, M., Pewe, L., Netland, J., . . . McCray, P. B., Jr. (2005). ACE2 receptor expression and severe acute respiratory syndrome coronavirus infection depend on differentiation of human airway epithelia. *Journal of Virology, 79*(23), 14614-14621.

Jung, H. A., Hyun, S. K., Kim, H. R., & Choi, J. S. (2006). Angiotensin-converting enzyme I inhibitory activity of phlorotannins from *Ecklonia stolonifera*. *Fisheries Science, 72*(6), 1292-1299.

Kim, A.-R., Lee, B., Joung, E. J., Gwon, W. G., Utsuki, T., Kim, N. G., & Kim, H. R. (2016). 6, 6′-Bieckol suppresses inflammatory responses by down-regulating nuclear factor-κB activation via Akt, JNK, and p38 MAPK in LPS-stimulated microglial cells. *Immunopharmacology and Immunotoxicology*, *38*(3), 244-252.

Kim, A.-R., Shin, T.-S., Lee, M.-S., Park, J.-Y., Park, K.-E., Yoon, N.-Y., . . . Byun, D.-S. (2009). Isolation and identification of phlorotannins from *Ecklonia stolonifera* with antioxidant and anti-inflammatory properties. *Journal of Agricultural and Food chemistry*, *57*(9), 3483-3489.

Kim, A. R., Lee, M. S., Shin, T. S., Hua, H., Jang, B. C., Choi, J. S., . . . Kim, H. R. (2011). Phlorofucofuroeckol A inhibits the LPS-stimulated iNOS and COX-2 expressions in macrophages via inhibition of NF-κB, Akt, and p38 MAPK. *Toxicology in Vitro*, *25*(8), 1789-1795.

Kumar, V., Singh, J., Hasnain, S. E., & Sundar, D. (2021). Possible link between higher transmissibility of Alpha, Kappa and Delta variants of SARS-CoV-2 and increased structural stability of its spike protein and hACE2 Affinity. *International Journal of Molecular Sciences*, *22*(17), 9131.

Kwon, H. J., Ryu, Y. B., Kim, Y. M., Song, N., Kim, C. Y., Rho, M. C., . . . Park, S. J. (2013). In vitro antiviral activity of phlorotannins isolated from *Ecklonia cava* against porcine epidemic diarrhea coronavirus infection and hemagglutination. *Bioorganic & Medicinal Chemistry*, *21*(15), 4706-4713.

Leung, J. M., Yang, C. X., Tam, A., Shaipanich, T., Hackett, T. L., Singhera, G. K., . . . Sin, D. D. (2020). ACE-2 expression in the small airway epithelia of smokers and COPD patients: implications for COVID-19. *European Respiratory Journal*, *55*(5).

Li, M. Y., Li, L., Zhang, Y., & Wang, X. S. (2020). Expression of the SARS-CoV-2 cell receptor gene ACE2 in a wide variety of human tissues. *Infectious Diseases of Poverty 9*(1), 45.

Li, W., Moore, M. J., Vasilieva, N., Sui, J., Wong, S. K., Berne, M. A., . . . Farzan, M. (2003). Angiotensin-converting enzyme 2 is a functional receptor for the SARS coronavirus. *Nature*, *426*(6965), 450-454.

Miao, Y. H., Hu, Y. H., Yang, J., Liu, T., Sun, J., & Wang, X. J. (2019). Natural source, bioactivity and synthesis of benzofuran derivatives. *RSC Advances*, *9*(47), 27510-27540.

Moon, C., Kim, S. H., Kim, J. C., Hyun, J. W., Lee, N. H., Park, J. W., & Shin, T. (2008). Protective effect of phlorotannin components phloroglucinol and eckol on radiation-induced intestinal injury in mice. *Phytotherapy Research, 22*(2), 238-242.

Park, J. Y., Kim, J. H., Kwon, J. M., Kwon, H. J., Jeong, H. J., Kim, Y. M., . . . Ryu, Y. B. (2013). Dieckol, a SARS-CoV 3CLpro inhibitor, isolated from the edible brown algae *Ecklonia cava*. *Bioorganic & Medicinal Chemistry, 21*(13), 3730.

Potdar, A. A., Dube, S., Naito, T., Li, K., Botwin, G., Haritunians, T., . . . McGovern, D. P. B. (2021). Altered intestinal ACE2 levels are associated with inflammation, severe disease, and response to anti-cytokine therapy in inflammatory bowel disease. *Gastroenterology, 160*(3), 809-822.e807.

Shrestha, S., Choi, J. S., Zhang, W., & Smid, S. D. (2022). Neuroprotective activity of macroalgal fucofuroeckols against amyloid β peptide-induced cell death and oxidative stress. *International Journal of Food Science & Technology*. DOI: 10.1111/ijfs.15753

Shrestha, S., Johnston, M. R., Zhang, W., & Smid, S. D. (2021). A phlorotannin isolated from *Ecklonia radiata*, Dibenzodioxin-fucodiphloroethol, inhibits neurotoxicity and aggregation of β-amyloid. *Phytomedicine Plus, 1*(4), 100125.

Shrestha, S., Zhang, W., Begbie, A. J., Pukala, T. L., & Smid, S. D. (2020). *Ecklonia radiata* extract containing eckol protects neuronal cells against $A\beta_{(1-42)}$ evoked toxicity and reduces aggregate density. *Food & Function, 11*(7), 6509-6516.

Shrestha, S., Zhang, W., & Smid, S. (2021). Phlorotannins: a review on biosynthesis, chemistry and bioactivity. *Food Bioscience, 39*, 100832.

Son, M., Oh, S., Choi, J., Jang, J. T., Son, K. H., & Byun, K. (2021). Attenuating effects of dieckol on hypertensive nephropathy in spontaneously hypertensive rats. *International Journal of Molecular Sciences, 22*(8), 4230.

Sugiura, Y., Matsuda, K., Yamada, Y., Nishikawa, M., Shioya, K., Katsuzaki, H., . . . Amano, H. (2006). Isolation of a new anti-allergic phlorotannin, phlorofucofuroeckol-B, from an edible brown alga, *Eisenia arborea*. *Bioscience, Biotechnology, and Biochemistry, 70*(11), 2807-2811.

Tai, W., He, L., Zhang, X., Pu, J., Voronin, D., Jiang, S., . . . Du, L. (2020). Characterization of the receptor-binding domain (RBD) of 2019 novel coronavirus: implication for

development of RBD protein as a viral attachment inhibitor and vaccine. *Cellular & Molecular Immunology, 17*(6), 613-620.

Tamama, K. (2020). Potential benefits of dietary seaweeds as protection against COVID-19. *Nutrition Reviews, 79*(7), 814-823.

Tateyama Makino, R., Abe Yutori, M., Iwamoto, T., Tsutsumi, K., Tsuji, M., Morishita, S., . . . Tsukinoki, K. (2021). The inhibitory effects of toothpaste and mouthwash ingredients on the interaction between the SARS-CoV-2 spike protein and ACE2, and the protease activity of TMPRSS2 in vitro. *PLoS One, 16*(9), e0257705.

Teralı, K., Baddal, B., & Gülcan, H. O. (2020). Prioritizing potential ACE2 inhibitors in the COVID-19 pandemic: Insights from a molecular mechanics-assisted structure-based virtual screening experiment. *Journal of Molecular Graphics and Modelling, 100*, 107697.

Uhal, B. D., Dang, M., Dang, V., Llatos, R., Cano, E., Abdul-Hafez, A., . . . Molina-Molina, M. (2013). Cell cycle dependence of ACE-2 explains downregulation in idiopathic pulmonary fibrosis. *European Respiratory Journal, 42*(1), 198-210.

Uhal, B. D., Nguyen, H., Dang, M., Gopallawa, I., Jiang, J., Dang, V., . . . Morimoto, K. (2013). Abrogation of ER stress-induced apoptosis of alveolar epithelial cells by angiotensin 1-7. *American Journal of Physiology - Lung Cellular and Molecular Physiology, 305*(1), L33-41.

Wang, B., Kovalchuk, A., Li, D., Rodriguez-Juarez, R., Ilnytskyy, Y., Kovalchuk, I., & Kovalchuk, O. (2020). In search of preventive strategies: novel high-CBD Cannabis sativa extracts modulate ACE2 expression in COVID-19 gateway tissues. *Aging (Albany NY), 12*(22), 22425-22444.

Wang, B., Li, D., Fiselier, A., Kovalchuk, I., & Kovalchuk, O. (2022). New AKT-dependent mechanisms of anti-COVID-19 action of high-CBD *Cannabis sativa* extracts. *Cell Death Discovery, 8*(1), 110.

Wijesinghe, W. A., Ko, S. C., & Jeon, Y. J. (2011). Effect of phlorotannins isolated from *Ecklonia cava* on angiotensin I-converting enzyme (ACE) inhibitory activity. *Nutrition Research and Practice, 5*(2), 93-100.

Wrapp, D., Wang, N., Corbett, K. S., Goldsmith, J. A., Hsieh, C.-L., Abiona, O., . . . McLellan, J. S. (2020). Cryo-EM structure of the 2019-nCoV spike in the prefusion conformation. *Science, 367*(6483), 1260-1263.

Xiao, K., Song, L., Bai, Y., Liu, P., Liu, Y., Xie, F., & Xie, L. (2021). Decipering the molecular mechanism of ACE2 regulating A549 Cells. *Frontiers in Genetics, 12*.

Yilin, Z., Yandong, N., & Faguang, J. (2015). Role of angiotensin-converting enzyme (ACE) and ACE2 in a rat model of smoke inhalation induced acute respiratory distress syndrome. *Journal of the International Society for Burn Injuries, 41*(7), 1468-1477.

Zhuang, M.-W., Cheng, Y., Zhang, J., Jiang, X.-M., Wang, L., Deng, J., & Wang, P.-H. (2020). Increasing host cellular receptor-angiotensin-converting enzyme 2 expression by coronavirus may facilitate 2019-nCoV (or SARS-CoV-2) infection. *Journal of Medical Virology, 92*(11), 2693-2701.

Ziegler, C. G. K., Allon, S. J., Nyquist, S. K., Mbano, I. M., Miao, V. N., Tzouanas, C. N., . . . Zhang, K. (2020). SARS-CoV-2 receptor ACE2 Is an Interferon-stimulated gene in human airway epithelial cells and is detected in specific cell subsets across tissues. *Cell, 181*(5), 1016-1035.e1019.

Chapter 7: Conclusion

The studies included in this thesis provide novel insights into the multifaced properties of phlorotannins including, but not limited to, neuroprotective, antioxidant, anti-inflammatory intestinal-protective and immune-modulatory actions via cell- and enzyme-based mechanisms, including using transmission electron microscopy (TEM) and molecular docking simulations for predictive and informative structural analysis. The following discussion highlights the significance of this study and makes some recommendations for future studies.

Significance

In this project, a thorough literature review on phlorotannins from brown seaweed was conducted with an emphasis on biosynthesis, chemistry and bioactivity. The accurate identification of phlorotannins is difficult due to their various chemical structures, complex chemical composition, isomers and relatively similar molecular weight and similar chemical characteristics (Li et al., 2017). In most cases, a combination of MS and NMR was used to accurately identify phlorotannin structures. However, a comprehensive library of NMR data of the isolated phlorotannins was lacking in the literature. Therefore, it was created to assist other researchers for accurate identification of these pure phlorotannins. Different techniques of phlorotannin profiling from the extract were also discussed in the first chapter. We have highlighted the existing evidence on antioxidant, anti-diabetic, anti-cancer, antiviral, antimicrobial, anti-inflammatory and neuroprotective activity, demonstrating promising potential in commercial applications in areas such as food, nutraceutical and some agricultural and pharmaceutical applications.

Ecklonia radiata is small kelp found abundantly in South Australia, however very few studies on chemical profiling and its biological activity, have been conducted (Wernberg et al., 2019). The

kelp forest is expected to provide more than $10 billion per year to Australia's gross domestic product through direct recreational and commercial fishing, as well as tourism (Wernberg et al., 2019). When the value of nutraceuticals, functional foods and animal feed is included, this figure may be much higher. Previous studies demonstrated superior neuroprotective activity among the selected brown algae (Alghazwi, Smid, & Zhang, 2018). However, no attempts were made to identify the particular chemical compounds responsible for this neuroprotective activity. We for the first time identified the ethyl acetate soluble (EA) fraction comprising 62% phlorotannins was responsible for the neuroprotection against amyloid β protein. Furthermore, the EA fraction demonstrated an amyloid β anti-aggregatory property as evidenced by TEM. Subsequently, ion mobility mass spectrometry (IMMS) and high-performance liquid chromatography quadrupole-time-of flight mass spectroscopy (HPLC-qTOF-MS) were used to characterize the major phlorotannins present in the EA fraction. Various phlorotannins were tentatively identified including eckol, dieckol, dibenzodioxin-fucodiphloroethol, eckmaxol, bieckol, fucodiphloroethol, phloroeckol, fucophloroethol, triphloroethol, phlorofucofuroeckol, and fucofuroeckol. Additionally, two compounds were isolated, purified and identified with the help of high-performance centrifugal partition chromatography (HPCPC). Nuclear magnetic resonance (NMR) including ^{1}H and ^{13}C and 2D COSY, HSQC, HMBC (broad and band selective) and NOESY along with mass spectroscopy enabled us to identify the major phlorotannins as eckol and dibenzodioxin-fucodiphloroethol (DFD). HPCPC offers a variety of operating modes and is very adaptable to various separation tasks (Skalicka-Woźniak & Garrard, 2014). It has various advantages over traditional liquid-solid separation methods such as requiring less solvent usage and 100% sample recovery. Additionally, large amounts of sample can be injected into the system and it has the capacity to accept particulates, which is essential for industrial commercialization (Skalicka-

Woźniak & Garrard, 2014). At present, there are no commercially available standards for phlorotannins except for the monomer phloroglucinol. The limited availability of these phlorotannins limits further preclinical and clinical therapeutic information in animal and human studies. We have successfully used this technique to isolate and purify phlorotannins that can be employed in commercial applications. Furthermore, four phlorotannins, eckol, dieckol, PFFA and 974-A demonstrated excellent ROS scavenging activity which could be attributed to their phenol rings and hydroxyl groups (Vergauwen et al., 2016). However, only PFFA and 974-A were able to protect PC-12 cells against $A\beta_{1\text{-}42}$, H_2O_2 and the lipid peroxidant tert-butyl hydroperoxide (*t*-BHP). This may be attributed to the presence of additional benzofuran rings in PFFA and 974-A compared with eckol and dieckol. The benzofuran scaffold has been associated with neuroprotection by inhibiting several important targets involved in neurodegeneration including cholinesterase, ROS stress and Aβ-cell membrane binding (Cabrera-Pardo et al., 2020; Lee & Byun, 2018; Rizzo et al., 2012).

Despite our knowledge of events involved in the pathophysiology of neurodegenerative diseases in the brain, growing evidence suggests that gut health might have greater implications for neurodegenerative disorders such as AD and Parkinson's disease through widespread immunomodulatory actions such as improving dysbiosis, barrier function and inflammatory signaling (Dinan & Cryan, 2017). Intestinal microbiota were reported to have a significant role in regulating the expression of gastrointestinal epithelial tight junctions and proinflammatory cytokines secreted by immune cells. Secreted cytokines such as TNF-α, IL-1β, and IL-6 act on tight junctions resulting in increased intestinal permeability (Al-Sadi & Ma, 2007; Capaldo & Nusrat, 2009), which leads to the translocation of various toxic secretions into the circulation including LPS, which can stimulate accumulation and aggregation of amyloid β and neurofibrillary

tangles in AD patients (Asti & Gioglio, 2014; Chen et al., 2020). We used the human intestinal epithelial Caco-2 cell line, which can spontaneously differentiate into a monolayer of cells containing absorptive enterocytes with a brush border layer similar to the small intestine, and express most receptors, transporters and drug metabolizing enzymes including aminopeptidase, esterase and sulfatase found in normal epithelium (Shimizu, 2010). Thus, it is considered a suitable cell line for using as an intestinal in vitro model of functional barrier integrity. Proinflammatory cytokines (TNF-α and IL-1β) were used to increase intestinal epithelial permeability and four phlorotannins (eckol, dieckol, PFFA, and 974-A) were subsequently investigated for their protective activity. All phlorotannins except 974-A protected and restored intestinal permeability disrupted by cytokines. Furthermore, phlorotannin-rich extracts and individual phlorotannins have been reported to have a positive impact on gut microbiota by stimulating their growth and production of metabolites for the maintenance of a healthy gastrointestinal environment and are considered a potential prebiotic candidate (Catarino et al., 2021; Charoensiddhi, Conlon, Vuaran, Franco, & Zhang, 2017; Vázquez-Rodríguez et al., 2021).

Lastly, these phlorotannins were able to modulate basal and cytokine-stimulated angiotensin-converting enzyme 2 (ACE-2) expression and activity in intestinal epithelial Caco-2 and respiratory epithelial A549 cells. ACE-2 is the negative regulator of the renin angiotensin system (RAS) that catalyzes the hydrolysis of angiotensin II to angiotensin (1-7) and so helps to maintain cardiovascular homeostasis by reducing blood pressure in a counterregulatory role. However, Corona viruses exploit ACE-2 as an entry receptor for cell invasion, which is critical for infectivity (Li et al., 2003). Therefore, Caco-2 and A549 cells expressing ACE-2 were selected for our study (Chang et al., 2020; Coperchini et al., 2021; Potdar et al., 2021; Ziegler et al., 2020), whereby we were able to firstly induce ACE-2 expression and activity using the proinflammatory cytokines IL-

1β and TNF-α, demonstrating an interesting and potentially important immunoregulatory augmentation of ACE-2 activity. In addition, macroalgal phlorotannins not only downregulated ACE-2 expression in these cell lines, but also inhibited the enzymatic activity of ACE-2, potentially by a direct interaction with the active site of ACE-2 as demonstrated by molecular docking simulations.

Recommended future work

1. Although we have tentatively identified the major phlorotannins from the ethyl acetate fraction of *E. radiata* using HPLC-qTOF-MS and IMMS, these phlorotannins need to be isolated and identified separately in order to confirm their presence in the extract in a similar way to that of eckol and dibenzodioxin-fucodiphloroethol.

2. Our studies demonstrated significant neuroprotective and antioxidant activity of these phlorotannins in various cell- and enzyme-based models. PFFA in particular was most effective at protecting neuronal cells against amyloid β toxicity via antioxidant and anti-aggregatory actions. We recommend investigating PFFA further to understand its mechanism of action, which may be related to properties conferred via the benzofuran moiety. Furthermore, other phlorotannins with additional benzofuran rings should be studied to understand and improve on any structure-activity relationships conferring anti-aggregatory and neuroprotective effects against Aβ.

3. Additional in vivo experiments are required to validate our findings from the cell-based and enzyme-based assays. We recommend using second and third generation transgenic mouse models containing humanized sequences and clinical mutations in endogenous mouse amyloid precursor protein and exploring the different signalling pathways associated with neuroprotection (Sasaguri et al., 2017; Sato et al., 2021). Such studies may

also enable a broader determination of the bioavailability of phlorotannins for further optimization as functional foods or pharmaceuticals.

4. The Caco-2 model lacks a mucus layer, which serves as physical and chemical barrier to food particles, chemicals, enzymes and host-secreted products. However, co-cultivation of HT-29 cells (goblet cells) which secrete mucin and form a layer over epithelial cells would be a better model to represent an in vitro intestinal epithelium. The use of probiotic bacterial strains such as *Lactobacillus* and *Bifidobacterium* is also warranted to study the interface and interaction of gut bacteria with phlorotannins and any ensuing influence on both barrier function and tight junction protein expression, such as ZO-1, occluding and E-cadherin.

5. In addition to ACE-2, the transmembrane serine protease 2 (TMPRSS2), which primes viral spike proteins and is crucial for SARS-CoV-2 entry into host cells should also be investigated. A549 and Caco-2 cells infected with the SARS-CoV-2 pseudo-virus may be employed in future studies to investigate the phlorotannin's role in COVID-19 prophylaxis and treatment.

Overall, this thesis investigated the potential use of macroalgal phlorotannins under various preclinical experimental therapeutic settings, demonstrating a widespread biological activity applied towards neurodegenerative, intestinal, and potentially infectious diseases. Our findings have broader implications informing further drug development and treatment of major global disease challenges using these novel marine polyphenols.

References

Al-Sadi, R. M., & Ma, T. Y. (2007). IL-1beta causes an increase in intestinal epithelial tight junction permeability. *J Immunol, 178*(7), 4641-4649. doi:10.4049/jimmunol.178.7.4641

Alghazwi, M., Smid, S., & Zhang, W. (2018). In vitro protective activity of South Australian marine sponge and macroalgae extracts against amyloid beta ($A\beta_{(1-42)}$) induced neurotoxicity in PC-12 cells. *Neurotoxicol Teratol, 68*, 72-83.

Asti, A., & Gioglio, L. (2014). Can a bacterial endotoxin be a key factor in the kinetics of amyloid fibril formation? *J Alzheimers Dis, 39*(1), 169-179.

Cabrera-Pardo, J. R., Fuentealba, J., Gavilán, J., Cajas, D., Becerra, J., & Napiórkowska, M. (2020). Exploring the multi-target neuroprotective chemical space of benzofuran scaffolds: a new strategy in drug development for Alzheimer's disease. *Front Pharmacol, 10*, 1679-1679.

Capaldo, C. T., & Nusrat, A. (2009). Cytokine regulation of tight junctions. *Biochim Biophys Acta, 1788*(4), 864-87.

Catarino, M. D., Marçal, C., Bonifácio-Lopes, T., Campos, D., Mateus, N., Silva, A. M. S., . . . Cardoso, S. M. (2021). Impact of phlorotannin extracts from *Fucus vesiculosus* on human gut microbiota. *Mar Drugs, 19*(7), 375.

Chang, E. H., Willis, A. L., Romanoski, C. E., Cusanovich, D. A., Pouladi, N., Li, J., . . . Martinez, F. D. (2020). Rhinovirus infections in individuals with Asthma increase ACE2 expression and cytokine pathways implicated in COVID-19. *Am J Respir Crit Care Med., 202*(5), 753-755.

Charoensiddhi, S., Conlon, M. A., Vuaran, M. S., Franco, C. M., & Zhang, W. (2017). Polysaccharide and phlorotannin-enriched extracts of the brown seaweed *Ecklonia radiata* influence human gut microbiota and fermentation in vitro. *J Appl Phycol, 29*(5), 2407-2416.

Chen, C., Ahn, E. H., Kang, S. S., Liu, X., Alam, A., & Ye, K. (2020). Gut dysbiosis contributes to amyloid pathology, associated with C/EBPβ/AEP signaling activation in Alzheimer's disease mouse model. *Sci Adv, 6*(31), eaba0466.

Coperchini, F., Ricci, G., Croce, L., Denegri, M., Ruggiero, R., Villani, L., . . . Rotondi, M. (2021). Modulation of ACE-2 mRNA by inflammatory cytokines in human thyroid cells: a pilot study. *Endocrine, 74*(3), 638-645.

Dinan, T. G., & Cryan, J. F. (2017). Gut instincts: microbiota as a key regulator of brain development, ageing and neurodegeneration. *J Physiol, 595*(2), 489-503.

Lee, J. K., & Byun, H. G. (2018). A novel BACE inhibitor isolated from *Eisenia bicyclis* exhibits neuroprotective activity against β-amyloid toxicity. *Fish Aquatic Sci, 21*(1), 38.

Li, W., Moore, M. J., Vasilieva, N., Sui, J., Wong, S. K., Berne, M. A., . . . Farzan, M. (2003). Angiotensin-converting enzyme 2 is a functional receptor for the SARS coronavirus. *Nature, 426*(6965), 450-454.

Li, Y., Fu, X., Duan, D., Liu, X., Xu, J., & Gao, X. (2017). Extraction and identification of phlorotannins from the brown alga, *Sargassum fusiforme* (Harvey) Setchell. *Mar Drugs, 15*(2), 49.

Potdar, A. A., Dube, S., Naito, T., Li, K., Botwin, G., Haritunians, T., . . . McGovern, D. P. B. (2021). Altered intestinal ACE2 levels are associated with inflammation, severe disease, and response to anti-cytokine therapy in inflammatory bowel disease. *Gastroenterology, 160*(3), 809-822.e807.

Rizzo, S., Tarozzi, A., Bartolini, M., Da Costa, G., Bisi, A., Gobbi, S., . . . Rampa, A. (2012). 2-Arylbenzofuran-based molecules as multipotent Alzheimer's disease modifying agents. *Eur J Med Chem, 58*, 519-532.

Sasaguri, H., Nilsson, P., Hashimoto, S., Nagata, K., Saito, T., De Strooper, B., . . . Saido, T. C. (2017). APP mouse models for Alzheimer's disease preclinical studies. *Embo J, 36*(17), 2473-2487.

Sato, K., Watamura, N., Fujioka, R., Mihira, N., Sekiguchi, M., Nagata, K., . . . Sasaguri, H. (2021). A third-generation mouse model of Alzheimer's disease shows early and increased cored plaque pathology composed of wild-type human amyloid β peptide. *J Biol Chem, 297*(3), 101004.

Shimizu, M. (2010). Interaction between food substances and the intestinal epithelium. *Biosci Biotechnol Biochem, 74*(2), 232-241.

Skalicka-Woźniak, K., & Garrard, I. (2014). Counter-current chromatography for the separation of terpenoids: a comprehensive review with respect to the solvent systems employed. *Phytochem Rev, 13*(2), 547-572.

Vázquez-Rodríguez, B., Santos-Zea, L., Heredia-Olea, E., Acevedo-Pacheco, L., Santacruz, A., Gutiérrez-Uribe, J. A., & Cruz-Suárez, L. E. (2021). Effects of phlorotannin and polysaccharide fractions of brown seaweed *Silvetia compressa* on human gut microbiota composition using an in vitro colonic model. *J Funct Foods, 84*, 104596.

Vergauwen, H., Prims, S., Degroote, J., Wang, W., Casteleyn, C., van Cruchten, S., . . . van Ginneken, C. (2016). In vitro investigation of six antioxidants for pig diets. *Antioxidants (Basel), 5*(4), 41.

Wernberg, T., Coleman, M. A., Babcock, R. C., Bell, S. Y., Bolton, J. J., Connell, S. D., . . . Shears, N. T. (2019). Biology and ecology of the globally significant kelp *Ecklonia radiata*. *Oceanography and marine biology*, 57.

Ziegler, C. G. K., Allon, S. J., Nyquist, S. K., Mbano, I. M., Miao, V. N., Tzouanas, C. N., . . . Zhang, K. (2020). SARS-CoV-2 receptor ACE2 Is an Interferon-stimulated gene in human airway epithelial cells and is detected in specific cell subsets across tissues. *Cell, 181*(5), 1016-1035.e1019.